FINAL REPORT

For the Florida Department of Transportation

ENGINEERING PROPERTIES OF FLORIDA CONCRETE MIXES FOR IMPLEMENTING THE AASHTO RECOMMENDED MECHANISTIC-EMPIRICAL RIGID PAVEMENT DESIGN GUIDE

FDOT Research Contract No.: BD-543-14
FSU Project No.: OMNI 018598

by

Principal Investigator: W. V. Ping, P.E.
Research Assistant: Raphael Kampmann

Department of Civil & Environmental Engineering
Florida A&M University – Florida State University
COLLEGE OF ENGINEERING
Tallahassee, FL 32310

December 2008

DISCLAIMER

The opinions, findings and conclusions expressed in this publication are those of the authors and not necessarily those of the State of Florida Department of Transportation or the U.S. Department of Transportation. This report is prepared in cooperation with the State of Florida Department of Transportation and the U.S. Department of Transportation.

METRIC CONVERSIONS

inches = 25.4 millimeters

feet = 0.305 meters

square inches = 645.1 millimeters squared

square feet = 0.093 meters squared

cubic feet = 0.028 meters cubed

pounds = 0.454 kilograms

poundforce = 4.45 newtons

poundforce per square inch = 6.89 kilopascals

pound per cubic inch = 16.02 kilograms per meters cubed

Technical Report Documentation Page

1. Report No. FL/DOT/RMC/BD-543-14	2. Government Accession No.	3. Recipient's Catalog No.
4. Title and Subtitle Engineering Properties of Florida Concrete Mixes for Implementing the AASHTO Recommended Mechanistic-Empirical Rigid Pavement Design Guide		5. Report Date August 2008 6. Performing Organization Code
7. Author(s) W. V. Ping and Raphael Kampmann		8. Performing Organization Report No. FSU C&G No. OMNI 018598
9. Performing Organization Name and Address FAMU-FSU College of Engineering Department of Civil & Environmental Engineering 2525 Pottsdamer Street Tallahassee, Florida 32310-6046		10. Work Unit No. (TRAIS) 11. Contract or Grant No. FDOT BD-543-14 13. Type of Report and Period Covered Final Report September 2006 - December 2008
12. Sponsoring Agency Name and Address Florida Department of Transportation Research Center, MS30 605 Suwannee Street Tallahassee, Florida 32399-0450		14. Sponsoring Agency Code
15. Supplementary Notes Prepared in cooperation with the Federal Highway Administration, U.S. Department of Transportation		

16. Abstract

The coefficient of thermal expansion (CTE) is a fundamental property of Portland cement concrete (PCC). The magnitude of temperature-related pavement deformations is directly proportional to the CTE during the pavement design life. Because of its critical effect on PCC performance, it is proposed to be considered for distress and smoothness prediction by the newly developed Mechanistic-Empirical Pavement Design Guide (M-E PDG).

To account for M-E PDG implementation in Florida, three typical Florida concrete mixtures were experimentally measured for compressive strength, flexural strength, splitting tensile strength, Young's modulus, Poisson's ratio, and CTE according to AASHTO TP-60. The test results revealed that PCC's CTE rapidly increases within the first week but stabilizes after 28 days. However, to accurately analyze the mix designs using the new mechanistic-empirical concept considering all three hierarchy levels, nine different JPCP models were generated. Their PCC layer thicknesses were iteratively determined before the resultant pavement structures were evaluated based on the predicted distresses (faulting and cracking) and smoothness (IRI). It was found, that cracking is the most critical pavement performance criterion for Florida JPCP. Moreover, top-down fatigue damage was isolated to be the controlling failure mechanism because of insignificant faulting and minor smoothness reduction.

Based on the thickness idealized JPCP models, a CTE sensitivity matrix was developed for adequate comparison of predicted pavement performance under interchanging CTE values. Despite wide ranging properties, clear patterns were exposed and distinctive performance envelopes arose for certain criteria. It was established that the new M-E PDG, is minimally CTE sensitive to faulting, CTE sensitive to bottom-up damage (for thin PCC layers), and extremely CTE sensitive to top-down damage, cracking, and smoothness.

17. Key Words cte sensitivity, mechanistic-empirical pavement design guide, pavement performance, rigid pavement, jpcp, coefficient of thermal expansion	18. Distribution Statement This document is available to the public through the National Technical Information Service, Springfield, Virginia, 22161		
19. Security Classif. (of this report) Unclassified	20. Security Classif. (of this page) Unclassified	21. No. of Pages 168	22. Price

ACKNOWLEDGEMENTS

Funding for this research was provided by the Florida Department of Transportation (FDOT) and Federal Highway Administration (FHWA) through the Research Center of the FDOT. This research was initiated by Bruce Dietrich, State Pavement Design Engineer, and managed by Emmanuel Uwaibi, Pavement Design Engineer with the FDOT.

The members of the FDOT supervisory group are: Tom Byron, Bruce Dietrich, Charles Ishee, Roger Schmitt, and Emmanuel Uwaibi (project manager). Charles Ishee with the FDOT Materials Office was extremely helpful throughout the experimental phase of the research.

The technical problems encountered during CTE measurement would not have been solved without the outstanding support of technical staff (Jussara Tanesi and Jagan Gudimettla) at the FHWA Turner-Fairbanks Research Laboratory.

Marc Ansley with the FDOT Structures Research Laboratory provided strong support to the testing program. The laboratory testing was carried out by Ed Mallory and Raphael Kampmann.

EXECUTIVE SUMMARY

Three typical Florida pavement PCC mix designs have been thoroughly evaluated throughout research phase one. To encompass a certain range of local concrete mixtures, attention was paid to the constituents and their proportion, with special focus on coarse aggregates. Two mixes contained dissimilar quantities of limestone while one mixture was based on granite. Considering the input parameters required for the mechanistic-empirical analysis procedure according to the new M-E PDG, the concrete engineering properties were laboratory measured for all essential maturity levels (7, 14, 28, and 90 days). To account for all three hierarchy levels, the characteristics under empirical evaluation included compressive strength, flexural strength, splitting tensile strength, Young's modulus, Poisson's ratio, (unit weight, air content, cement type, cement content, water-to-cement ratio), and coefficient of thermal expansion with an emphasis on concrete's thermal behavior. One sample per day was tested over a period of 130 days in accordance with AASHTO TP-60. Attributed to the proportion of constituent, the mix designs demonstrated distinctive results for all engineering properties with superior strength characteristics for one of the limestone mixes and beneficial thermal properties for the granite mixture. The two limestone mix designs showed comparable CTE values constantly with both mix designs 1 μm/m/°C lower than the granite mix. However, the test results revealed that PCC CTE rises over time. It was shown that the thermal behavior increases rapidly within the first week and stabilizes subsequently. After 28 days, the CTE swell was considered insignificant as the change in CTE was less than 1/10 μm/m/°C.

To accurately analyze the three typical Florida mix designs by means of the new M-E PDG, research phase two was initiated through proper generation of computer analysis models. Traffic loads, environmental conditions, structural parameters, and analysis criteria were defined on account of local requirements. Due to the introduced data input quality concept (three different hierarchy levels), nine diverse JPCP models were established, each reflecting a certain range of numerical results derived from research phase one to capture typical Florida PCC material properties. The remaining variable,

PCC layer thickness, was iteratively idealized and the outcomes demonstrated favorable use of hierarchy level one and a high sensitivity to input parameters for levels two and three. However, the resultant pavement structures were evaluated based on the predicted distresses (faulting and cracking) and smoothness (IRI). It was found that cracking is the critical performance criterion for Florida JPCP according to M-E PDG as the "% slabs cracked limit" was constantly attained before any other pavement performance became critical. Moreover, top-down fatigue damage was isolated to be the controlling failure mechanism because of insignificant faulting response and minor smoothness reduction.

The ensuing CTE sensitivity study was founded on the nine evaluated Florida pavement models (idealized for PCC layer thickness) and their original CTE values. A sensitivity matrix was developed to account for PCC's thermal behavior as a control variable over a ± 10 % CTE array comprising magnitudes typically expected in Florida. Although the sub-matrices differed considerably, a method was established to adequately compare the predicted performance criteria throughout alternating CTE values. Despite wide-ranging PCC, CTE, and thickness properties, clear resemblances were exposed for all scenarios under evaluation and distinctive performance envelopes arose for certain criteria. It was verified that the new Mechanistic-Empirical Rigid Pavement Design Guide is not CTE sensitive to load transfer efficiency, minimally CTE sensitive to faulting, CTE sensitive to bottom-up damage (for thin PCC layers), and extremely CTE sensitive to top-down damage, cracking, and smoothness. Overall, two out of three pavement performance criteria are highly susceptible to CTE in Florida JPCP structures.

TABLE OF CONTENTS

LIST OF TABLES

LIST OF FIGURES

CHAPTER 1: INTRODUCTION

1.1. Introduction

Starting in 1996, the American Association of State Highway and Transportation Officials (AASHTO) Joint Task Force on Pavements (JTFP) sponsored the development of mechanistic-empirical design methods for new and rehabilitated pavements. National Cooperative Highway Research Program (NCHRP) Project 1-37A, the largest project in the over 40-year history of the program, was recently concluded with the successful delivery of a recommended Mechanistic-Empirical Pavement Design Guide (M-E PDG). The proposed M-E Design Guide was designed to use state-of-the-art methods only. It predicts distresses (faulting and cracking) and smoothness (IRI) throughout the specified design life based on given traffic loads, local weather conditions, and the proposed layer assembly. The M-E PDG is a forward-looking approach in pavement design and an attractive tool for roadway engineers. If used correctly, it is assumed to prevent uneconomical pavement design, and therefore attracts the attention of transportation agencies across the country and explains the research interest developed after the anticipated software supported Guide was made public in 2004. In fact, the software was released for testing and evaluation to interested users in the public and private sectors of the U.S. and worldwide. Therefore, the M-E PDG is still under revision until adopted by AASHTO.

The M-E methodology introduces a new hierarchical concept to account for different data quality. Each input parameter has to be assigned using one of the three different hierarchy levels: level one for highest, level two for medium, and level three for lowest accuracy. Unlike earlier versions, the M-E Design Guide is not geared towards final pavement thickness, and it may be thought of as an analysis tool which predicts pavement performances for any layer arrangement suggested by the design engineer. Due to local calibration of the numerical mechanistic-empirical computation models and local traffic, climate, and material conditions, the analysis process and evaluation may differ significantly from district to district. Hence, the procedure according to the new M-E

PDG describes an iterative process that must be adjusted until the proposed structure complies with the performance limitations specified by the responsible agency.

1.2. Problem Statement

To properly activate the mechanistic-empirical analysis procedure, the Design Guide demands material properties which have never been critical to pavement design before. Numerous characteristics have been included, each affecting the predicted distresses and smoothness differently; in particular, the analysis of rigid pavement considers new Portland cement concrete (PCC) properties for three major levels of materials inputs:

- PCC inputs required for critical response computations
  - Static modulus of elasticity (E) adjusted with time
  - Poisson's ratio
  - Unit weight
  - Coefficient of thermal expansion

- Additional PCC inputs required for distress/transfer functions
  - Modulus of rupture, split tensile strength, compressive strength
  - Cement type, cement content, water-to-cement (w/c) ratio
  - Ultimate shrinkage, amount of reversible shrinkage

- Additional PCC inputs required for climatic modeling
  - Surface shortwave absorptivity
  - Thermal conductivity
  - Heat capacity of PCC

The aforementioned engineering properties of PCC are not generally required for the rigid pavement design procedures currently used in Florida, except the modulus of elasticity and the modulus of rupture. For future implementation of the new M-E Rigid

Pavement Design Guide in Florida, the required engineering properties of Florida PCC mixes will have to be further explored and evaluated for a better understanding of the materials behavior and the pavement design. Specifically, the coefficient of thermal expansion (CTE) describes an essential Portland cement concrete property as it is assumed to affect the performance of rigid pavement significantly [2], [3], [4], [and others]. Research is urgently needed to evaluate the thermal engineering properties of typical Florida PCC mixes.

To properly implement the new M-E analysis approach in Florida and to identify the importance of data quality, the above-mentioned Florida representative material properties have to be thoroughly examined by means of the proposed M-E PDG. Research is required to evaluate the performance of Florida PCC in typical local pavement structures with special focus on the pavement performance due to CTE.

1.3. Research Objectives

The primary objective of this research is the evaluation of thermal engineering properties for typical Florida PCC mixtures to study the CTE sensitivity of the new M-E PDG.

The goal is to determine and evaluate the required PCC material properties on three different quality levels (empirically, calculative, and through literature/database), with a major focus on experimental measurements in favor of level one, for satisfying the aforementioned PCC material inputs at all hierarchy levels to fulfill the M-E analysis requirements.

The research is targeted at typical Florida PCC materials and particularly their performance in Florida representative pavement structures under local climate conditions and traffic loads. The intention is to assess the predicted distresses and smoothness according to the new M-E PDG for the empirically analyzed PCC mixtures.

The CTE sensitivity of the new mechanistic-empirical concept represents the major purpose of the research. The aim is to study the consequence of interchanging PCC thermal properties throughout a typical Florida CTE array and the significance for the predicted distresses and smoothness models.

1.4. Research Scope

The scope of the study will be divided into two interrelated research segments and an extensive, preceding literature review to ensure a proper approach throughout the evaluation. Research phase one will exclusively be aimed at the PCC material properties whereas, research phase two will be designated to study the mechanistic-empirical concept.

The literature review will address each research phase separately. To ensure a proper understanding of the newly introduced design property, the physical meaning of CTE will be reviewed and its effect on PCC materials and pavement design summarized. This initiates the review of the recently developed mechanistic-empirical analysis approach. The concept will be outlined and the M-E PDG rigid pavement section addressed before the need for implementation will be discussed. The state of the art report will be concluded by the review of different sensitivity studies completed by other research groups.

Research phase one will be accomplished on account of M-E PDG required input data considering all hierarchy levels. The essential PCC engineering properties will be studied to evaluate their specified standard test procedures or protocols in order to properly conduct the experimental program. Three different Florida PCC mix designs have to be assigned to measure and identify their engineering properties. An extensive analysis follows before the experimental results can be utilized for research phase two.

In research phase two, the software supported M-E Pavement Design Guide will be thoroughly studied and applied to rigid pavement structures exposed to typical Florida conditions. On account of research phase one and the introduced hierarchy level concept, nine different pavement models will be generated to evaluate the three local PCC mixtures for each input data quality. After the models are examined and analyzed, the CTE sensitivity study will commence on top of those models. A proper CTE array will be defined capturing the local range for thermal expansion values to initiate the sensitivity analysis. Depending on the findings, conclusions will be drawn and recommendations for the implementation of the new M-E PDG in Florida presented.

1.5. Report Organization

This report follows the chronological order provided by the research scope. It outlines the preceding literature review before research phases one and two are addressed subsequently. The report is designated to review the conducted research, present the chosen methodologies, and summarize the findings and conclusions.

The introduction to the research is given in Chapter 1, followed by Chapter 2 addressing the literature review. Thereafter, Chapter 3 initiates the empirical research as it outlines the methodology of the study. Chapter 4 is exclusively concerned with the material research, describing the experimental program conducted in the laboratory. Chapter 5 is designated to present the achieved numerical results of material properties. The analysis of test results will be summarized in Chapter 6. The following chapter, Chapter 7, specifically discusses the modeling of the pavement structures and the M-E PDG experimental program. The results of thickness analysis will be found in Chapter 8, prior to Chapter 9 which outlines the CTE sensitivity study. Final conclusions and recommendations will be summarized in Chapter 10.

To account for additional information beyond the scope of the research, two appendices have been annexed to the main report. Appendix A elucidates the M-E Software Guide

and specifically outlines every required input parameter (and its common range). In addition, Appendix B briefly summarizes all input parameters (comprehensive list view) that have been necessary to conduct the M-E PDG research.

CHAPTER 2: STATE OF THE ART

2.1. Introduction

This chapter presents an overview of selected literature addressing the topics in question. The following publications discussed were chosen based on their quality, relevance, content, and information related to the research at hand. The discussion builds the foundation for this study, as it generates basic and in-depth understanding of the subjects. The objective is to guide the reader through the material under consideration and to provide comprehensive knowledge for the research that follows. A successive organization of the information was chosen which takes the reader from basic to essential details.

As explained previously, this research focuses on JPCP PCC design by means of the new AASHTO M-E PDG. Currently, it is believed that concrete's CTE has one of the most significant impacts on JPCP PCC performance [4], [6], [9], [11], thus, this chapter is broken up into two major parts – **2.2 Coefficient of Thermal Expansion** and **2.3 Mechanistic-Empirical Pavement Design Guide**. First, the material property CTE will be defined, and its characteristics in civil engineering applications as well as in Portland cement concrete will be explored in more detail. Afterwards, the new AASHTO TP 60 test procedure, which determines this property, will be outlined and discussed thoroughly to transit over to CTE in pavement design. This initiates the second major element of this literature review which outlines the new M-E PDG. Background information on earlier pavement design guides and the need for improvement are given. Furthermore, the Mechanistic-Empirical concept will be accentuated and discussed specifically, before the concrete modeling in the new design procedure will be addressed briefly. Afterwards, the hierarchy levels proposed by the M-E PDG will be contemplated and comprehensively explained by means of PCC's CTE. To be thorough, the M-E Software Design Guide will be addressed prior to the need for implementation. Finally, various sensitivity studies done by other researchers will be reviewed and a comparison will be delineated.

2.2. Coefficient of Thermal Expansion

2.2.1. Definition of Coefficient of Thermal Expansion

When temperature is changed in any (most) matter, the average amplitude of atoms' vibrating changes as well. Usually, additional heat causes higher amplitudes while lower temperatures slow vibration down[1]. This in turn changes the separation between individual atoms, causing the material to expand or contract. As the length change is similar for all atoms, the total volumetric change depends on the available atoms in each direction. This makes the length change proportional to length, the area change proportional to area, and the volumetric change proportional to volume [W 2], [W 5].

If a material does not go through a phase change, the expansion and contraction can proportionally be related to the change in temperature. The constant of proportionality is termed the coefficient of thermal expansion, in physics symbolized by the Greek letter alpha (α).

The coefficient of thermal expansion is defined as:

- linear thermal expansion $$\frac{\Delta L}{L_0 \Delta T} = \alpha_L \quad (2.1)$$
- area thermal expansion $$\frac{\Delta A}{A_0 \Delta T} = \alpha_A \quad (2.2)$$
- volumetric thermal expansion $$\frac{\Delta V}{V_0 \Delta T} = \alpha_V \quad (2.3)$$

where:

$\Delta L, \Delta A, \Delta V$ = change in length, area, and volume

A_0, A_0, V_0 = initial length, area, and volume

ΔT = change in temperature

[1] Some materials, like water, behave differently and expand in decreasing temperature. Such materials are indicated by a negative coefficient of thermal expansion.

The volumetric coefficient of thermal expansion can be measured for all substances of condensed matter (liquids and solid state). The linear thermal expansion can only be measured in the solid state [W 1].

The three characteristics are closely associated and can be related to each other. For exactly isotropic materials, the area coefficient of thermal expansion is approximated as twice the linear coefficient of thermal expansion and the volumetric behavior is nearly three times that of the linear one [W 3].

$$\frac{\Delta A}{A_0 \Delta T} = 2\alpha_L \tag{2.2a}$$

$$\frac{\Delta V}{V_0 \Delta T} = 3\alpha_L \tag{2.3a}$$

$$\alpha_V = \frac{1}{V}\frac{\partial V}{\partial T} = \frac{1}{L^3}\frac{\partial L^3}{\partial T} = \frac{1}{L^3}\left(\frac{\partial L^3}{\partial L}\frac{\partial L}{\partial T}\right) = \frac{1}{L^3}\left(3L^2\frac{\partial L}{\partial T}\right) = 3\frac{1}{L}\frac{\partial L}{\partial T} = 3\alpha_L \tag{2.4}$$

Equation 2.4 is a very close approximation for small differential changes. It is important to note that the differential change in volume is only valid for small changes in volume; therefore, the expression is not linear [W 1]. As the change in temperature increases and the value of linear coefficient of thermal expansion increases, the error in this formula increases as well. Thus, for non-negligible changes in volume, the reference volume has to be adjusted according to the following equation:

$$(L + \Delta L)^3 = L^3 + 3L^2\Delta L + 3L\Delta L^2 + \Delta L^3 \tag{2.5}$$

Equation 2.5 contains $3L^2$ as its main term, but also shows a secondary term that scales as $3L\Delta L^2 = 3L^3\alpha^2\Delta T^2$, and this portrays that a large change in temperature can overshadow a small value for the linear coefficient of thermal expansion. Although the coefficient of linear thermal expansion can be quite small, when combined with a large change in

temperature, the differential change in length can become large enough that this factor needs to be considered [W 1].

Considering the facts above, the coefficient of thermal expansion is generally defined as a fractional increase in measurement per unit change in temperature (parts-per notation). To describe thermal properties of materials, the linear coefficient of thermal expansion is mostly used in literature and databases [W 10]. In metric units, this is commonly expressed as micrometer per meter per degree Celsius or Kelvin (µm/m/°C or µm/m/°K). However, English expression typically uses millionths of an inch per inch per degree Fahrenheit (µin/in/°F or micro strain/°F). Other notations will be found throughout the literature, yet all notations will refer to a change in length per length per temperature change.

The exact definition of the coefficient of thermal expansion varies. It depends on whether it is specified at a precise temperature (termed; true coefficient of thermal expansion) or stipulated over a temperature range (named; mean coefficient of thermal expansion) [W 4]. The former is related to the slope of the tangent to the length at any point of the temperature vs. length change plot, while the latter is governed by the slope of the chord between two points on this curve. Due to the definition and temperature range used, considerable variations in values may occur as emphasized in Figure 2.1.

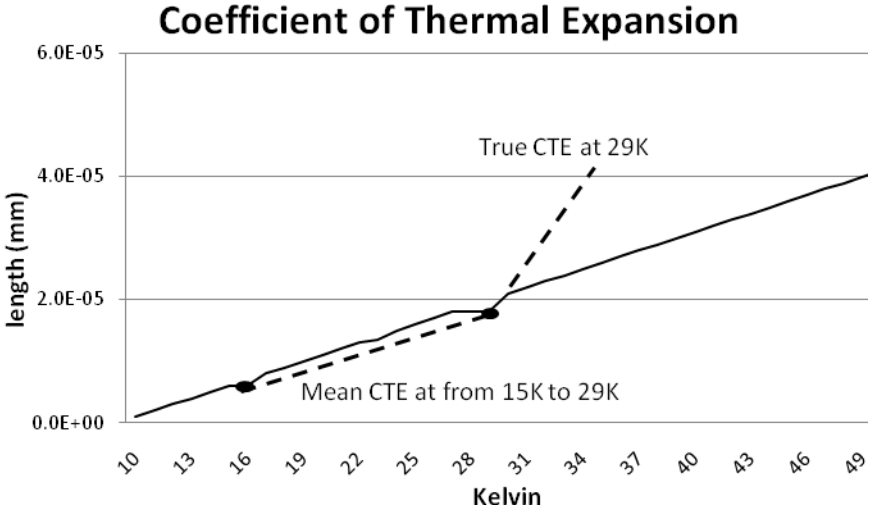

Figure 2.1: Temperature vs. length change

2.2.2. Coefficient of Thermal Expansion in Civil Engineering

The thermal behavior in civil engineering materials is mostly described via the more imprecise value – the mean coefficient of thermal expansion. Since relatively small temperature differences are expected throughout the design life of most structures, this value generally is sufficient enough. However, thermal expansion (or contraction) can be a dominant factor in design because tolerances due to dimension changes have to be guaranteed. It should be understood that thermal expansion can cause significant stress in a component if the design does not allow for expansion or contraction of components. The phenomena of thermal expansion can be challenging when designing bridges, buildings, pavements, and other structures, but it can be put to beneficial use.

The following table provides an overview of different materials used in construction to roughly outline the variation of coefficients of thermal expansion. Note that the values in Table 2.1 are not precise; they merely represent an average of common values.

Table 2.1: Coefficient of thermal expansion for common materials [W 1], [W 10]

Material	µm/m/°C	µin/in/°F
Lead	29.0	16.1
Aluminum	23.0	12.8
Brass	19.0	10.6
Stainless Steel	17.3	9.6
Copper	17.0	9.4
Nickel	13.0	7.2
Concrete	12.0	6.7
Steel	12.0	6.7
Iron	11.1	6.2
Carbon Steel	10.8	6.0
Platinum	9.0	5.0
Glass	8.5	4.7
Glass, Pyrex	3.3	1.8
Silicon	3.0	1.7
Invar	1.2	0.7
Diamond	1.0	0.6

In engineering the Greek letter alpha is rarely used; instead the coefficient of thermal expansion is mostly termed CTE – especially in concrete applications.

2.2.3. Coefficient of Thermal Expansion in Portland Cement Concrete Pavement

The coefficient of thermal expansion (CTE) is a fundamental property of Portland cement concrete (PCC). The magnitude of temperature-related pavement deformations is directly proportional to the CTE-value during pavement's design life. The property has long been known to have an effect on joint openings/closings, crack formations and openings/closings in continuously reinforced concrete pavement (CRCP), curling stresses, and thermal deformation in slabs [6]. For example, in pavement concrete the deformations, in combination with restraint offered by the base layer and slab weight, affect the resulting curling stress and axial stresses in the hardened slab. Consequently, PCC CTE is a very important factor in concrete pavement performance.

The CTE magnitude of PCC depends both on the composition of the mix and the hydrated state at the time of temperature change [1]. PCC CTE is highly affected by the constituents of the concrete mixture since the main elements (aggregates and hydrated cement paste) have dissimilar coefficients of thermal expansion and the CTE-value of the mixture is a resultant of those elements.

The CTE value of concrete aggregates ranges from 4 to 13 μm/m/°C [W 6] and is largely affected by its quartz content, whereas the linear CTE of hydrated cement paste varies between 11 and 20 μm/m/°C and is therefore higher than that of concrete aggregates [1]. Nevertheless, the CTE-value of aggregate has a much higher weight than the CTE of cement paste. This can be explained based on the fact that the CTE of concrete is a weighted average value of the constituents, and also that the aggregates form the bulk volume of the concrete since the aggregates account for about 60 to 80 % of the PCC volume.

CTE test results for PCC have been presented in various reports and textbooks for many years, despite the fact that there has not been a standardized test method available until fairly recently. Values in the range of about 6 to 13 μm/m/°C are reported in literature, and a value of 10 μm/m/°C is commonly used in pavement design so far [6]. The range of

CTE values of different concretes reflects the variation in CTE of concrete's component material.

It could be established that the coefficient of thermal expansion in PCC is largely affected by the type of aggregate [X 16], [1], [13]. There are many other factors influencing PCC properties, specifically the coefficient of thermal expansion (e.g. cement type, water-to-cement ratio, cement paste, surround temperature, maturity of the concrete, moisture condition, etc.). Nevertheless, it became obvious that the type of aggregate used in concrete plays the most significant role. This phenomenon can well be explained by the fact that the aggregates in plain concrete occupy the bulk of the volume. Mallela [6] reports that aggregate from igneous sources generally has a lower CTE than aggregate from sedimentary origin. Similar findings were also discovered by other researchers [X 16], [1], [4], [8], [X 18], [W 6]. Based on this knowledge, a follow-up evaluation was conducted by Mukhopadhyay [8]. The basic mineralogical properties of concrete constituents were studied and a new mineralogical approach to predict aggregate and concrete CTE was presented. An extensive study was done by the Portland Cement Association resulting in a summary table for CTE of aggregates used in concrete design across the US [X 16]. These values are illustrated in the following Table.

Table 2.2: CTE ranges for PCC components according to [X 16] and [W 6]

Aggregate Type	Coefficient of Thermal Expansion	
	µm/m/°C	µin/in/°F
Cement Paste	18 - 20	10 – 11
Quartzite	11 – 13	6.1 – 7.2
Sandstone	11 – 12	6.1 – 6.7
Dolomite	7 - 10	4 – 5.5
Granite	7 – 9	4 – 6
Basalt	6 - 8	3.3 – 4.4
Limestone	6	3.3
Marble	4 – 7	2.2 – 4

It should be noted that rocks with high quartz content, such as quartzite and sandstone, have the highest coefficient. Aggregates containing little or no quartz, such as limestone, have the lowest CTE. As previously mentioned, the most important influence on

concrete's CTE results from the utilized aggregate. This consequently leads to an estimation of CTE for PCC made from different types of aggregate. The Federal Highway Administration (FHWA) published the typical coefficient of thermal expansion range for common PCC components on their webpage [W 6]. The results as posted are congruent to those published by the Portland Cement Association (PCA) [X 16]. The results are summarized in Table 2.3.

Table 2.3: Concrete CTE depending on aggregate type according to [X 16]

Aggregate Type	Coefficient of Thermal Expansion	
	µm/m/°C	µin/in/°F
Quartz	11.9	6.6
Sandstone	11.7	6.5
Gravel	10.8	6.0
Granite	9.5	5.3
Basalt	8.6	4.8
Limestone	6.8	3.8

The CTE for concrete fluctuates because the coefficient of aggregate varies widely. However, it is generally agreed that the CTE increases as the quartz content increases. Since this holds true for aggregates, it also applies to concrete made of the aggregate with low or respectively high quartz percentage (subject to the condition that all other factors remain constant, which is theoretically impossible).

2.2.4. AASHTO TP 60 Procedure

Much research has been conducted in order to find a proper way to determine the magnitude of CTE in hydraulic cement concrete. Different approaches were developed throughout the past years; some of the developed procedures are more accurate than others and some are more complex and difficult to perform. However, by introducing the new Empirical-Mechanistic Pavement Design Guide (E-M PDG), a single procedure was finally adopted by the American Association of State Highway and Transportation Officials (AASHTO). The procedure was developed in the late 1990s, was adopted and

approved by AASHTO in 2000, and is now defined through test protocol AASHTO TP 60.

Since it is known that the degree of saturation of concrete influences its measured CTE, the moisture condition of the concrete specimens must be controlled. In this test procedure, (typically) cores or cylinders with a diameter of 4 inches are tested in their saturated condition. A rigid support frame provides the reference for an attached linear differential variable transformer (LDVT) during length change measurement of the specimen. The frame should be designed to have minimal influence on the length change measurements obtained during the test and also to support the specimen such that the specimen is permitted to freely adjust to any change in temperature. A suitable support frame and test setup according to AASHTO's TP 60 procedure is shown in Figure 2.2.

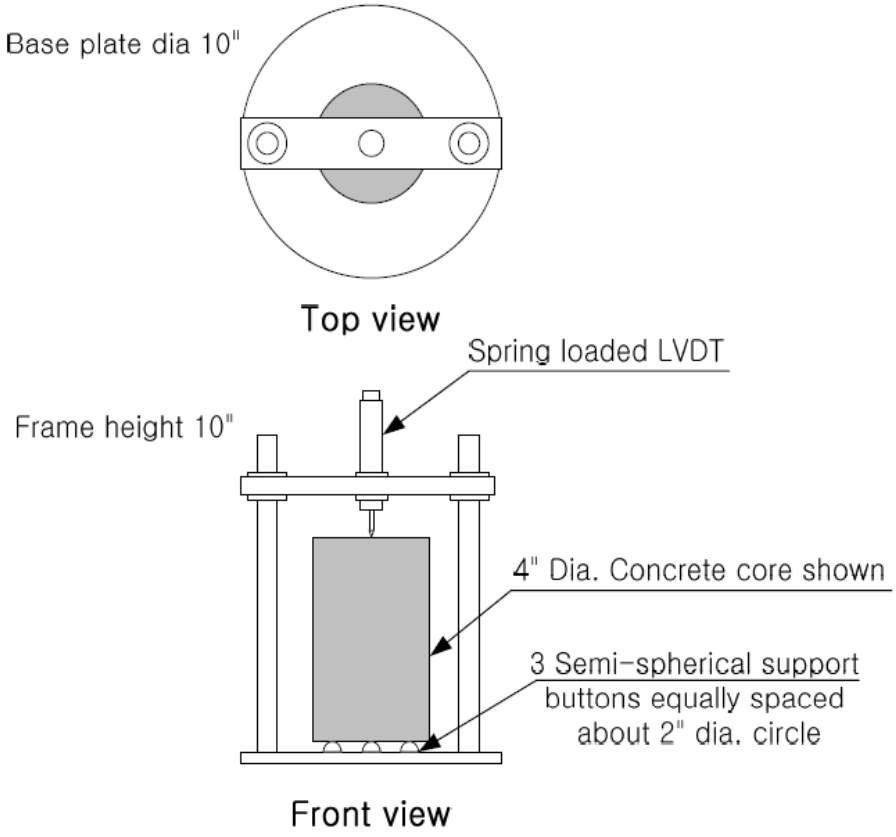

Figure 2.2: Test setup for test procedure TP 60 [X 14]

The frame containing the specimen is submerged in a temperature controlled water bath. After reaching a constant temperature, the test is conducted by changing the temperature of the water bath successively and recording the length change of the specimen. The unrestrained length change is typically calculated over a temperature range from 10°C to 50°C. The test is repeated until two successive measurements provide similar results. Depending on the size of the water bath and the effectiveness of the heaters and chillers, this may take a day or more.

Certainly, the LVDT measurement needs to be corrected as the supporting frame is affected by the same temperature gradient as the test specimen. TP 60 assumes linear length change of test frame with temperature and postulates a calibration specimen with a very well known CTE value. As a result, the measured length change (LVDT reading) can be subtracted from the known displacement of the calibration specimen to obtain the length change of measuring apparatus during temperature change. If frame and calibration specimen are made of the same material, this value represents the movement between LVDT mounting point and top surface of the calibration specimen. To obtain the calibration factor C_f, the length change of the frame is related to the initial length of the calibration specimen and the difference in temperature.

$$C_f = \frac{\Delta L_f}{L_{cs} \times \Delta T} = \frac{\Delta L_a - \Delta L_m}{L_{cs} \times \Delta T} = \frac{L_{cs} \times CTE_{cs} \times \Delta T - \Delta L_m}{L_{cs} \times \Delta T} \qquad (2.6)$$

where:

C_f = correction factor for frame movement

ΔL_f = length change of test frame

L_{cs} = measured length of calibration specimen

ΔT = temperature difference

ΔL_a = actual length change of calibration specimen

ΔL_m = measured length change (LVDT movement)

CTE_{cs} = CTE of calibration specimen

After the correction factor is defined, the frame can be used to measure the CTE of other materials. The linear coefficient of thermal expansion is determined according to equation II.1 by dividing the corrected length change by the product of the temperature gradient and the initial length of the specimen.

$$CTE = \frac{\Delta L_a}{L_0 \times \Delta T} = \frac{\Delta L_m + \Delta L_f}{L_0 \times \Delta T} = \frac{\Delta L_m + Cf \times L_0 \times \Delta T}{L_0 \times \Delta T} \quad (2.7)$$

where:

CTE = CTE of concrete specimen

ΔL_a = actual length change of calibration specimen

L_0 = measured length of concrete specimen

ΔT = temperature difference

ΔL_m = measured length change (LVDT movement)

ΔL_f = length change of test frame

C_f = correction factor for frame movement

The AASHTO TP 60 Procedure can be summarized as follows:

- Submerge the test frame, including the concrete specimen, in water for no less than 48 hours prior to the testing.
- Measure the length of the specimen to the nearest 0.1 mm and place the test frame in the water bath with the LVDT setup.
- Set the temperature of the water bath to 10 ± 1°C. Maintain this temperature until three successive readings of LVDT, taken every 10 minutes, are within 0.00025 mm (0.25 μm) of one another (initial reading).
- Set the temperature of the water bath to 50 ± 1°C. Maintain this temperature until three successive readings of LVDT, taken every 10 minutes, are within 0.00025 mm (0.25 μm) of one another. Record temperature to the nearest 0.1°C and LVDT readings to the nearest 0.00025 mm (0.25 μm) (second reading).
- Set the temperature of the water bath to 10 ± 1°C. Maintain this temperature until three consecutive readings of LVDT, taken every 10 minutes, are within 0.00025

mm (0.25 μm) of one another. Record temperature to the nearest 0.1°C and LVDT readings to the nearest 0.00025 mm (0.25 μm) (final reading).

- From the LVDT reading at 10°C and 50°C, compute CTE_i during heating (from initial to second reading) and CTE_f during cooling (from second to final reading). If the difference between these two values is less than 0.5 μm/m/°C, the average of these two values is the CTE. If this is not the case, complete one or more segments until the CTEs of two segments are within 0.5 μm/m/°C of one another and CTE computes.

It is evident that AASHTO TP 60 relates the length change in the material to two distinct temperature points. Consequently, it is the measurement of the *mean linear* coefficient of thermal expansion for hydraulic cement concrete.

2.2.5. Shortcomings of TP 60 Procedure

The method is theoretically sound; however, the accuracy and reliability of this test method depends to a great extent on the stability and accuracy of the displacement readings at 10°C and 50°C. Even though the test protocol TP 60 was recently adopted by AASHTO, it still has a few shortcomings. Some of these limitations were scientifically proven and have been evaluated [6], [13]. These deficiencies can be summarized as follows:

- CTE is sensitive to the moisture condition of the test specimen during testing. The thermal coefficient varies with internal relative humidity (RH). The value at 100 % RH is 20 to 25 % less than the maximum. However, the fully saturated condition was considered most practical from a testing standpoint. Furthermore, since pavement in the field has an internal RH of 80 % or more (except the region near the surface [1 to 2 top inches]) this may not be of great consequence.

- Temperature and displacement readings during the temperature change are not utilized for the evaluation of CTE – these do not yield the *true* coefficient of thermal expansion.
- Even if the temperature maintains a relatively constant value, the concrete displacement tends to vary. (The exact behavior of thermal expansion in concrete has not been completely described thus far.)
- The temperature distribution inside the specimen is not considered by the TP 60 test method.
- The tolerance between two successive CTEs of less than 0.5 micro strain/°C is not small enough for some DOTs to implement CTE requirements for actual paving projects [13].
- It was noted on several occasions that either the results of the TP 60 procedure could not be repeated or the procedure took too long to complete [13].

2.2.6. Coefficient of Thermal Expansion in Pavement Design

A large-scale research project was conducted in [6]. It presents CTE results from hundreds of cores taken from the Long Term Pavement Performance (LTPP) study throughout the United States and tested by FHWA's Turner Fairbanks Highway Research Center (TFHRC) Laboratory, using TP 60 procedure. The CTE, again, was found to vary widely depending on the predominant aggregate type used in the concrete. The test data were used to conduct a sensitivity analysis that showed the CTE to have a very significant effect on slab cracking and, to a lesser degree, on joint faulting. Its overall effect on smoothness (IRI) was also significant in this study (which is in contrast to [4]). The general range of CTE values was found to fall between 9 to 13 μm/m/°C, and is therefore in the range of values generally found in the literature. The analysis also agreed with the CTE values reported in the M-E PDG for level 3 use.

Besides the utilized aggregates, as mentioned above, the CTE magnitude is a function of other important PCC mixture factors and boundary conditions, such as cement type,

water-to-cement ratio, cement paste, surround temperature, maturity of the concrete, moisture condition, etc. An inappropriate choice of these parameters could lead to a highly variable pavement performance [6]. Some studies have already utilized the measured CTEs as input data for the newly developed E-M PDG (level 1). They build models based on determined concrete properties and assumed boundary conditions. In general, it is difficult to compare the different studies and their results because a high quantity of input data is needed and the studies differ significantly. Some research shows opposite findings and therefore makes contradictory recommendations. Nevertheless, the most important factors impacted by the CTE value could be narrowed down to the following [1],[4], [6], [9], and [X 18]:

- Early-age or premature random cracking.
- Higher mid-panel transverse and longitudinal fatigue cracking (i.e. cracking in perpendicular and parallel direction to traffic, respectively) due to higher curling stresses.
- Higher rate of faulting due to great loss of slab support at the time of construction (i.e., initial slab loft up during daytime construction), larger joint openings during adverse seasons, and greater corner deflection from curling.
- Joint spalling due to failures of joint sealant as a result of extensive joint movement.
- Crack spacing, and more importantly, crack width in continuously reinforced concrete pavements (CRCP) over the entire design life. This factor has a major effect on the crack load transfer efficiency and, hence, punchouts.

As such, the CTE has been recognized to be important and has been used for many years in finite element models (FEM) of concrete pavement to calculate those factors which are known to be critical to performance. In the previous AASHTO Design Guide, the CTE-value is used to calculate the opening/closing of transverse joints to proper sealant reservoir dimensions and also in the longitudinal reinforcement design. However, it is interesting to note that a factor so critical to concrete pavement performance has not been included as a direct input to structural design procedure for concrete pavements in the

past. The parameter has been overlooked for such a long time partly because (1) there is a general lack of guidance on the selection of PCC CTE based on components, (2) there is a lack of understanding of its impact on design, and (3) prior to TP-60 [X 14], there was a lack of standard protocol available to highway and airfield pavement designers to test for this property in a quick and practical manner [6]. But lately, the PCC CTE has been identified to be a critical parameter by the Mechanistic-Empirical Pavement Design Guide (M-E PDG). Due to its effect on critical PCC slab stresses and joint and crack openings as well as on some other factors, the CTE is included in the newly developed design procedure for the first time.

2.3. Mechanistic-Empirical Pavement Design Guide

2.3.1. Background

Since December 1914, pavement design in the United States is affiliated with rules and guidelines established by the American Association of State Highway Transportation Organizations (AASHTO). Numerous regulations have been released, improved, and adjusted ever since. Today, pavement design for practical applications is typically based on the *1993 AASHTO Guide for the Design of Pavement Structures* (1993 Guide) and its modifications for individual states[2]. The methods and calculations in the 1993 Guide were derived from empirical relationships established during the AASHTO Road Test conducted from 1958 to 1961 [3]. This Design Guide and its precedents served well for many decades, but serious limitations exist which can be listed according to [X 15]:

- **Traffic Loading:** Heavy truck traffic design volume levels have increased since 1960. The original interstate pavements were designed for 5 to 15 million trucks, whereas today these same pavements must be designed for 50 to 200 million

[2] e.g. pavement structures made of PCC and build in Florida are designed according to the *2004 Florida Rigid Pavement Design Manual* [X 17]

trucks and an even longer design life. The equations forming the basis of the earlier procedures were based on regression analyses of the AASHTO Road Test data. Thus, application of the procedure to modern traffic means the designer often must extrapolate the design methodology far beyond the data and experience providing the basis for the procedure.

- **Vehicle Characterization:** Vehicle suspension, axle configurations, tire types, and tire pressures were representative of the types used in the late 1950s. Many of these are outmoded (for example, tire pressures of 80 psi versus 120 psi today), resulting in pavement designs which are insufficient to carry these loadings.
- **Climatic Effects**: Because the AASHTO Road Test was conducted at one specific geographic location, it is impossible to address the effects of different climatic conditions on pavement performance. For example, at the Road Test a significant amount of distress occurred in the pavements during the spring thaw, a condition that almost does not exist in Florida.
- **Design Life:** Because of the short duration of the Road Test, the long-term effects of climate and aging of materials were not addressed. The Road Test was conducted over 2 years, while the design life for today's pavement is 20 to 50 years.
- **Surfacing Materials:** Only one hot mix asphalt mixture and one Portland cement concrete mixture were utilized at the Road Test. Today, many different hot mix asphalt concrete and PCC mixtures exist whose effects are not fully addressed.
- **Base Course:** Only two unbound dense granular base/subbase materials were included in the main flexible and rigid pavement sections of the AASHTO Road Test (limited testing of stabilized bases was included for flexible pavements). These base courses exhibited significant loss of modulus due to frost and erosion. Today, various stabilized types of higher quality are used routinely, especially for heavier traffic loadings.
- **Subgrade:** One type of subgrade was used for all test sections at the Road Test, but many types exist nationally that result in different performance of highway pavements.

- **Construction and Drainage:** Pavement designs, materials, and construction were representative of those used at the time of the Road Test. No subdrainage was included in the test sections, but positive subdrainage has become common in today's highways.
- **Rehabilitation:** Pavement rehabilitation design procedures were not considered at the AASHTO Road Test. Procedures in the 1993 Guide are completely empirical and very limited, especially in consideration of heavy traffic.
- **Performance:** Earlier AASHTO procedures relate the thickness of the pavement surface layers (asphalt layers or concrete slab) to serviceability. However, research and observations have shown that pavement needs rehabilitation for reasons that are not related directly to pavement thickness (e.g., rutting, thermal cracking, faulting).
- **Reliability:** The 1986 AASHTO Guide included a procedure for considering design reliability that has never been fully validated. This procedure resulted in a large multiplier of design traffic loadings to achieve a desired reliability level (e.g., a pavement designed for 50 million equivalent single axle loads [ESALs] was actually designed for 228 million).

The effectiveness of previous pavement design guides has been questioned by many researchers due to the factors listed above. Already in the 1980s, the 1986 AASTHO guide for pavement structures initially defined M-E design procedures as the calibration of mechanistic models with observations of performance. An example of this would be empirical correlations. Additionally, analytical methods in multi-layered pavement systems were delineated as numerical calculations of pavement responses when subject to external loads or the effect of temperature or moisture [2]. From 1987-1990, the National Cooperative Highway Research Program (NCHRP) Project 1-26 sought to consider mechanistic principles; however, only limited mechanistic principles were addressed in the 1993 Design Guide. The lack of applicability to present conditions is undeniable. Therefore, in March 1996, the AASHTO Joint Task Force on Pavements (JTFP) proposed a research program to develop a pavement design guide based on mechanistic-empirical principles with numerical models calibrated with pavement performance data

from the Long-term Pavement Performance (LTPP) program [X 15]. This study was sponsored by NCHRP and conducted as projects 1-37 and 1-37a (and 1-40d), resulting in the development of a mechanistic-empirical pavement analysis system [1], [3]. The need for such procedure was recognized by researchers much earlier [X 15]; however, practical use would require access to computers capable of handling the increased computational effort to perform the necessary calculations. The amount of computing power available on today's personal computers makes a mechanistic approach useful to pavement designers.

2.3.2. Mechanistic-Empirical Concept

The 2002 Mechanistic-Empirical Pavement Design Guide (M-E PDG) is anchored in a cumbersome iterative calculation approach based on numerous input variables which can be narrowed down into three major categories: traffic, climate, and structure. To account for this iterative process, the 2002 M-E PDG was accompanied by a software package capable of analyzing the entire pavement structure[3]. It must be understood that the proposed Design Guide does not provide a final thickness design (as older versions did); rather it should be thought of as an analysis tool for pavements. The results are highly dependent on the limitations and evaluations defined by the pavement engineer. Due to local conditions, the limitations and evaluations might differ significantly from state to state or even from district to district. Overall, the M-E PDG concept can be categorized into three major stages outlined in Figure 2.3.

The flowchart in Figure 2.3 is a simplified representation of the M-E PDG procedure. The Selection Stage incorporates three different input groups. Traffic and climate conditions can be considered constant for each individual project. The proposed pavement structure and its included materials are variable design values adjusted by the

[3] Until the guide will be adopted by AASHTO, the software (including a PDF version of the 2002 M-E PDG) will be available for anyone interested or revision purposes on TRB's website [W 7]

pavement engineer (using trail-and-error approach) depending on the third category, the analytical inputs.

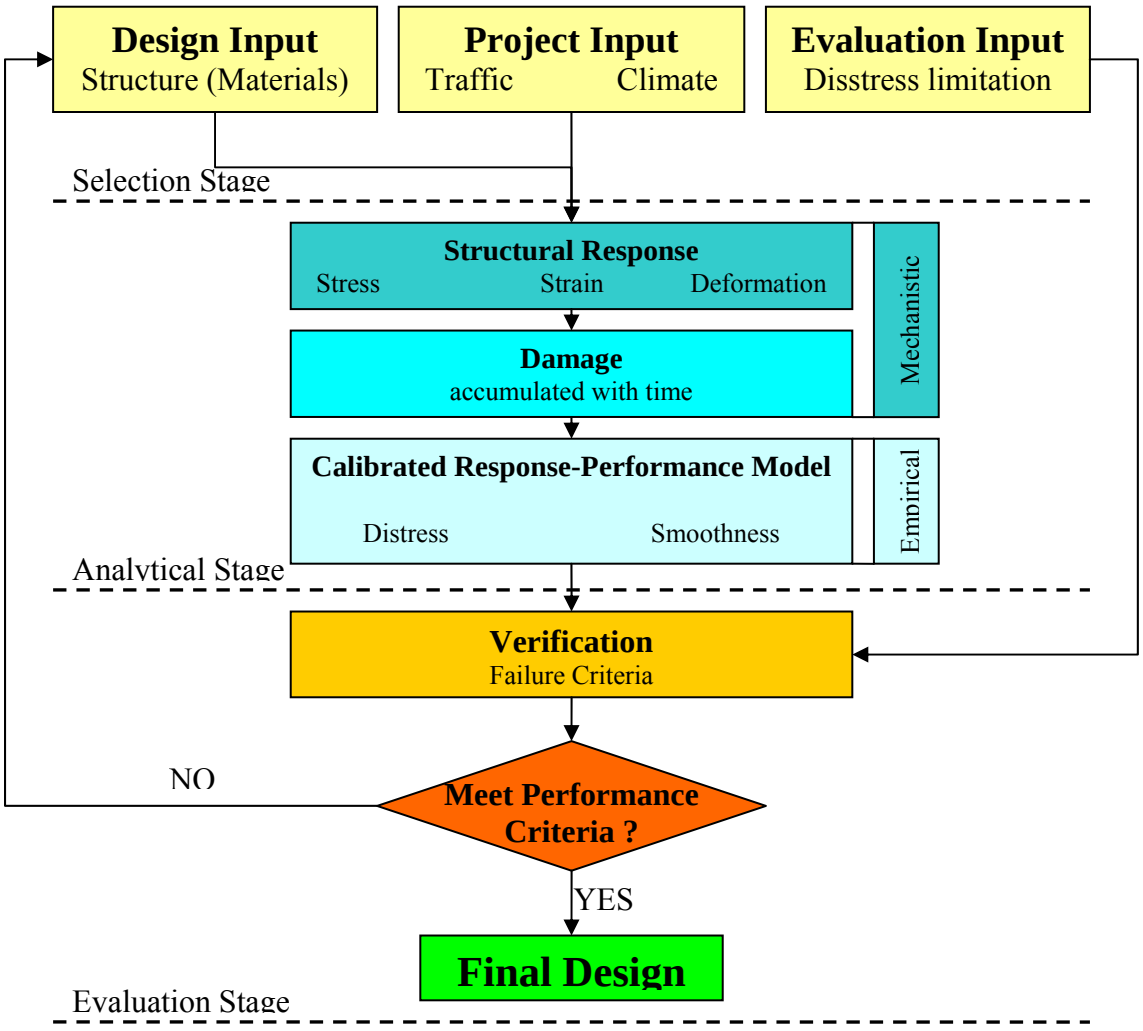

Figure 2.3: Three-stage M-E PDG concept

Initial trial designs can be created by the engineer, obtained from an existing design procedure, or selected from a general catalog. Certainly, local conditions significantly affect all input data. The analytical stage determines stress, strain, and deformation to estimate pavement distress and the accumulated pavement damage over time. This part forms the engineering mechanics basis used in the design procedure, which therefore labels the guide "mechanistic." Mechanistic procedures are referred to for their ability to translate the analytical calculation of the pavement response to physical distress such as cracking (pavement performance). However, pavement performance is subject to

numerous factors that cannot be exactly modeled by mechanistic methods. Therefore, the method also uses a series of models to define the input parameters and to develop distress predictions based on the mechanistic outputs (stress and strain) of the proposed pavement structure model. To ensure realistic predictions of pavement distress, the response-performance models require calibration, which explains the "Empirical" title [3]. In the evaluation stage, the results of the mechanistic-empirical design procedure are compared to the analysis inputs. Depending on the limitations defined by the agency, the proposed pavement structure will either be acceptable or not. If any criterion cannot be fulfilled, the pavement engineer has to reject the design and revise the structure until all performance criteria are satisfied.

The raw design inputs are processed by the software to obtain chronological increasing values for traffic, material, and climate. In particular, for PCC structures, the following sequences are undertaken during the M-E design process:

- **Environmental:** The temperature (hourly) and moisture (monthly) profiles are defined for 11 evenly spaced nodes throughout the PCC layer.
- **Traffic:** The traffic spectrum for the next time increment is defined (monthly).
- **Material:** The elastic properties and thicknesses of each layer are determined based on the age, temperature and moisture, materials, and traffic conditions.
- **Mechanistic:** Critical stresses and strains within the structure are determined due to the loading conditions in the given time interval.
- **Mechanistic:** Non-load-related stresses and strains (thermal/moisture gradients) are determined on a supplemental basis.
- **Empirical:** Incremental distresses (faulting, cracking, and roughness – IRI) are calculated based on the foregoing stress and strain determinations. They may result from calibrated deterministic empirical models.
- **Material:** Initial material parameters – if over-stressed or cracked – are adjusted, depending on the computed incremental damage.
- **Time:** To repeat the cycle, the time is incremented by $t = t_0 + \Delta t$

To simulate realistic pavement performance, for the first time, this design procedure includes the accumulation of monthly (or semi-monthly, depending on frost conditions) damage over the entire design life. The incremental, load by load, accumulating design approach over continuous time periods makes this design procedure very versatile and comprehensive [X 15].

2.3.3. Mechanistic-Empirical Concrete Model

The structural model for rigid pavement analysis is a 2-D finite element program, ISLAB2000. This FEA-based structural model was used as a basis for developing rapid solution neural networks (NN) because thousands of computations of responses are needed for any design. The neural networks were trained with the thousands of results from ISLAB2000. These NN provide accurate and virtually instantaneous solutions for critical responses and were developed so that the large numbers of computations needed could be accomplished rapidly. These structural response models require several monthly inputs, which were listed earlier. Given these inputs, the structural models produce stresses, strains, and displacements at critical locations in the pavement and subgrade layers.

2.3.4. Mechanistic-Empirical Hierarchical Levels

To account for project importance, M-E PDG introduces a new hierarchical concept based on data quality and project sensitivity. Each input variable and constant can be assigned using one of three different input levels. The actual identification of input information may differ depending on the category (Climate, Traffic, and Structure) but the concept remains throughout all inputs - level 1 from actual test data for highest accuracy; level 2 from less-than-optimal test situations and known relationships; and level 3 from agency database or local knowledge. In the following, the different levels and their qualities will be explained in terms of CTE input for PCC pavement structures.

At level 1, the PCC mixture used in design and construction should be laboratory tested in accordance with the previously mentioned AASHTO TP 60 protocol. Other common engineering properties (compressive strength, flexural strength, splitting tensile strength, Young's modulus, and Poisson's ratio) should be empirically tested as well. The measured values are the fundamental inputs used in the M-E PDG procedure.

Input level 2 is expected to be used in routine design [X 15], [1]. Level 2 inputs are typically user-selected, possibly from an agency database. The data can be derived from a less-than-optimum testing program or can be estimated empirically. At level 2, the PCC CTE can be predicted from a simple two-phase mixture rule that estimates PCC CTE as a weighted average of the constituent coefficient of thermal expansion. The weighted average is based on the relative volumetric proportion of constituents.

CTE estimation for input level 2 according to [1]:

$$CTE_{PCC} = CTE_{fine} \cdot V_{fine} + CTE_{agg} \cdot V_{agg} + CTE_{paste} \cdot V_{paste} \qquad (2.8.)$$

where:

CTE_{fine} = Coefficient of Thermal Expansion of fine aggregates
CTE_{agg} = Coefficient of Thermal Expansion of coarse aggregates
CTE_{paste} = Coefficient of Thermal Expansion of cement paste
V_{fine} = Volumetric proportion of fine aggregates in PCC mix
V_{agg} = Volumetric proportion of coarse aggregates in PCC mix
V_{paste} = Volumetric proportion of cement paste in PCC mix.

In [1] it was found that the calculated PCC CTE-value as a weighted average of the CTE of aggregates and hardened Portland cement paste is always higher than the measured value. Therefore, the use of input level 2 would result in a more conservative design than using level 1 in terms of PCC CTE.

For level 3, a default PCC CTE value is selected based on guidance provided in the M-E PDG tempered with local experience. Typically, it is the lowest class of design and should be used where there are minimal consequences.

Level 1 inputs require greater effort than level 2, which in turn involves even more than level 3. But it is obvious that the accuracy of CTE increases as the Input Level decreases; correspondingly, the testing effort expands.

2.3.5. Mechanistic-Empirical Software

To fully take advantage of the M-E design procedure notwithstanding its complexity, the Design Guide was accompanied by a software solution. While preparing this report, the software was available in its version 1.003 which was last built in May 2007 [W 7]. The software requires hundreds of input values with a minimum of thirty five PCC JPCP (material and structural) characteristics to analyze the pavement. Appendix A outlines all required parameters to analyze JPCP and presents the graphical user interface of the Design Guide.

2.3.6. Mechanistic-Empirical Implementation

It is unquestionable that the M-E PDG requires validation and calibration before it can be approved by DOTs across the country. The guide cannot possibly include all of the site-specific conditions that occur in each region of the United States. It is therefore necessary for the user to adapt local experience to the use of the guide. The default calibration built into the software is based on the LTPP data set which certainly provides a starting point. However, it does not consider specific Florida environmental conditions or local materials. These conditions can vary over an extremely wide range, even within each state [X 15].

To account for material importance the guide attempts to provide different methods and procedures (e.g., different hierarchy levels). While material requirements and construction specifications are not detailed at the moment, they still affect the overall design of the pavement structure immensely. The material exigencies and seasonal variation of characteristics should be evaluated thoroughly.

Initially, it might be tempting to take advantage of default traffic loading categories (level 3) [3]; nevertheless, in long-term implementation, it will be essential to accurately reflect local traffic. Traffic and traffic loading varies greatly throughout the country and it may differ seasonally as well. This also refers to traffic prediction; therefore, depending on different locations, traffic levels will either be stable or increase over time. The influence of traffic and the precision of its measurement has to be studied to fully implement the new Design Guide.

It is undeniable that, locally, one of the most influential parameters in pavement design is climate. Weather conditions vary widely throughout the United States. It is very unlikely that a pavement structure designed for Illinois will perform as well under Florida moisture and temperature conditions. The M-E PDG Software addresses this through climatic data collected from hundreds of weather stations throughout the country. These data can be downloaded for each state separately [W 7]. However, roadways are not always built next to or near weather stations. Although the Software Guide provides the possibility to interpolate between closely located weather stations, the effect has to be monitored on local bases.

The M-E PDG attempts to provide procedures to evaluate and estimate material, traffic, and environmental conditions; however, if the guide is at variance with proven and documented local experience, the demonstrated experience should prevail [X 15].

2.3.7. Mechanistic-Empirical Sensitivity

After the release of the M-E Software Design Guide, numerous studies were funded to initiate the implementation of the new design approach. These efforts were first made by Arkansas, Florida, Georgia, Indiana, Mississippi, Missouri, Montana, New York, Texas, Utah, and Virginia [W 8]. Initially, most researchers are interested in the issue of sensitivity, as the M-E methodology incorporates new input values and state-of-the-art procedures never used before. As outlined earlier in this text, several inputs are required to complete the iterative pavement performance prediction; certainly, every single input affects the final product differently. However, the remaining question is: Which input value affects which pavement performance criteria (IRI, cracking, faulting) and to what extent? For example, there might be a parameter extremely affecting JPCP faulting, while the effect of another input variable is insignificant. To analyze sensitivity, researchers created regionally representative pavement models and varied one input parameter (within its range [X 15]) while holding all other inputs constant [2], [3], [11]. Mostly, the results are comparative but it is interesting to note that different findings exist. Table 2.4 summarizes the most comprehensive results made by Hall, K. [2] and Guclu, A. [3].

While Salama, H. K. [11] defines performance threshold and age threshold for his evaluation, it is not known at this point which criteria Guclu, A. [3] used to determine sensitivity or insensitivity. In contrast, Hall, K. [2] invoked personal experience to define (1) faulting sensitivity greater than 0.1 inches for 20 years, (2) cracking to be sensitive if 25 % of concrete slab is cracked after 20 years, and (3) Smoothness (IRI) exceeding 30 inches per mile within 30 years. In all cases, results represent 90 % design reliability which simply reflects 50 % design reliability adjusted by a constant factor. As explained earlier, the Design Guide Software is a tool to analyze pavement structures which, in general, makes judgment of performance relative to (local) distress limitations. However, the findings in Table 2.4 are reference points and may help to guide future research towards important directions.

Although the findings made are not totally congruent, Table 2.4 indicates three structural characteristics and four PCC properties to dominate pavement performance. In agreement with other publications [4] [15], the major material parameters can be narrowed down to Curl/Warp Effective Temperature Difference and to the Coefficient of Thermal Expansion. Other sensitive inputs are Joint Spacing, PCC-Layer Thickness, Edge Support, Thermal Conductivity, and Unit Weight.

An interaction effect of input parameters is predicted [11] but only limited research on this topic has been done so far.

Table 2.4: Summary of input sensitivity

JPCP Material Characteristics	Performance Criteria					
	Faulting		Cracking		IRI	
	[2]	[3]	[2]	[3]	[2]	[3]
Curl/Warp Effective Temperature Difference	S	S	S	S	S	S
Joint Spacing	I	S	S	S	S/I	S
Sealant Type	I	I	I	I	I	I
Dowel Diameter	I	S	I	I	I	S
Dowel Spacing	I	I	I	I	I	I
Doweled Transverse Joints	S	*	I	*	S/I	*
Edge Support	I	S	S/I	S	I	S
PCC-Base Interface	I	I	I	I	I	I
Erodibility Index	I	I	I	I	I	I
Unbound Layer Modulus	S/I	*	I	*	S/I	*
Surface Shortwave Absorbtivity	I	I	S/I	S	S/I	I
Infiltration of Surface Water	I	I	I	I	I	I
Drainage Path Length	I	I	I	I	I	I
Pavement Cross Slope	I	I	I	I	I	I
PCC Layer Thickness	*	S	S	S	S/I	S
Unit Weight	I	S	S/I	S	I	S
Poisson's Ratio	I	I	S/I	S	S/I	I
Coefficient of Thermal Expansion	S/I	S	S	S	S	S
Thermal Conductivity	S/I	I	S	S	S	I
Heat Capacity	*	I	I	I	*	I
Cement Type	I	I	I	I	I	I
Cement Content	S/I	I	I	I	S/I	I
Water-to-Cement Ratio	S/I	I	I	I	S/I	I
Aggregate Type	I	I	I	I	I	I
PCC Set Temperature	I	I	I	I	I	I
Ultimate Shrinkage at 40% R.H.	I	I	I	I	I	I
Reversible Shrinkage	I	I	I	I	I	I
Time to Develop 50% of Ultimate Shrinkage	I	I	I	I	I	I
Curing Method	I	I	I	I	I	I
28-day PCC Modulus of Rupture	I	I	S	S	S/I	S
28-day PCC Compressive Strength	I	I	S	S	S/I	S
AADTT	S/I	*	S/I	*	S/I	*
Mean Wheel Location	S/I	*	S/I	*	S/I	*
Traffic Wander	I	*	I	*	I	*
Design Lane Width	I	*	I	*	I	*
Climate	I	*	S/I	*	I	*

S = extremely sensitive S/I = sensitive to insensitive I = insensitive * = no information provided

CHAPTER 3: RESEARCH APPROACH

3.1. Introduction

This section outlines the research approach implemented to strive for the goals of this study. Appropriate hypotheses are necessary to establish suitable methodologies leading the research approach. These initial assumptions are based on the objectives, research experiences, and the information obtained from the literature addressing state-of-the-art methods (see previous chapter).

The major objective is the verification/calibration of the new AASHTO M-E PDG and its applicability to certain Florida conditions. The M-E Design Guide is intended to serve as an analysis tool throughout the entire United States for new and rehabilitation design considering flexible and/or rigid pavement. Different materials and construction methods are addressed in the Software Guide; at this point in time this includes hot mix asphalt (HMA), joint plain concrete pavement (JPCP), and continuously reinforced concrete pavement (CRCP). Consequently, the new Design Guide is a comprehensive and wide-ranging analytical tool making it difficult to determine a single implementation plan within one research study. In the interest of Florida DOT, the scope was narrowed down to a specific material and its construction method. This research exclusively focuses on Portland cement concrete (PCC) structures (rigid pavement) designed for jointed plain concrete pavement (JPCP) because this is considered the most common construction method for PCC pavement in Florida. Keeping the major objective in mind, it was decided to conduct the research study in two successive and interrelated phases. The first phase of the research can be considered pure material research intended to determine specific engineering properties of different Florida DOT-approved PCC pavement mix designs suitable for utilization in the new M-E PDG. This directly ties into the second phase of the research focusing on the M-E Design Guide Software and its sensitivity. The experimental results from phase one will serve as input data to evaluate the Design Guide and its sensitivity for common Florida materials.

3.2. Material Research

To properly evaluate the chosen material type by means of the new M-E PDG, the important material characteristics have to be determined based on the literature review and the input requirements for the Design Guide Software. The required input properties partially depend on the chosen hierarchy level and the importance of design quality. Considering all possible key features for PCC analysis, the essential engineering properties can be outlined as follows:

- Cement type
- Cement content
- Water-to-cement ratio
- Aggregate type
- Unit weight
- Compressive strength
- Modulus of rupture
- Splitting tensile strength
- Young's modulus
- Poisson's ratio
- Coefficient of thermal expansion
- Thermal conductivity
- Heat capacity
- Set temperature (zero stress)
- Ultimate shrinkage at 40% R.H.
- Reversible shrinkage
- Time to develop 50% of ultimate shrinkage
- Curing method
- Layer thickness

Some of the above listed factors may require extensive research projects for realistic applications. As this is not the case for this study, and in order to maintain economical research proceedings, the left column of the above list comprises the properties to be evaluated throughout the material research phase.

All destructive (compressive strength, modulus of rupture, splitting tensile strength) and non-destructive (Young's modulus, Poisson's ratio, coefficient of thermal expansion) tests have to be determined based on state-of-the-art/practice test procedures and their related ASTM or AASHTO test protocols. To ensure statistically sound results, each test procedure will be conducted on a sufficient number of test samples. The test frequency

(sample maturity) results from the M-E PDG (Part II of Chapter II), and therefore it requires 7-day, 14-day, 28-day, and 90-day testing for almost all engineering properties. Additional characters and test ages might be added throughout the experimental program for better understanding of material behavior; nevertheless, the above incorporates the full data range required for PCC analysis using the new M-E PDG.

After definition of total data range for the individual material type, the material research methodology has to account for M-E PDG verification under common Florida conditions (material), as this is the final goal of this study. This will be accomplished through the evaluation of three different PCC materials. All mixtures have to be FDOT approved, mixed and batched under the same circumstances, tested in a similar environment, and statistically assessed in equivalent manners.

3.3. M-E PDG Software Research

The M-E PDG Software and its sensitivity to PCC materials is the key to this research. The different mix designs which will be evaluated throughout the material research have to be analyzed using the M-E Design Guide Software. Major focus will be the behavior of a specific mix design under interchanging hierarchy levels throughout a comparison study of the individual PCC mixtures to determine adequacy of each mixture. Afterwards, the CTE sensitivity of the new Design Guide can be evaluated within a typical CTE range expected for Florida conditions. Analysis parameter will be the provided distress and smoothness models which comprise faulting, cracking, and international roughness index (IRI).

3.3.1. Traffic Model

Although the traffic model will be fed into the Software Design Guide under hierarchy level three considerations, it will be important to ascertain a proper representation of interstate traffic occurring in Florida. The interstate condition is chosen on account of

material input level one. The new M-E PDG requires testing of material properties as used in construction for interstate design – it is expected to use material level one input in such projects only. Nevertheless, in this study, the same traffic pattern will be used for hierarchy level two and three evaluations. It is emphasized that in practical interstate application material inputs less than one should not be used in conjunction with the M-E PDG. However, from a research standpoint to ensure proper comparison, all material input levels will be studied considering the same (interstate) traffic pattern.

3.3.2. Climate Model

Florida environmental conditions (temperature and moisture) may challenge pavement design which turns the climatic model into an important feature for this research. A proper hypothetical location for the virtual paving project has to be identified. Ideally, this location will represent an average region in terms of moisture and temperature. The climatic input values will be constant throughout the entire research.

3.3.3. Pavement Structure Model

To ensure proper evaluation and valid comparisons of test results, an adequate pavement model, reflecting state-of-the-practice PCC structure in Florida, has to be developed. The structure model will be the groundwork for the sensitivity research as it forms the environment of material inputs other than PCC. Although, these values are not site-specific (like traffic or climate) and adjustable in real-world application, they will not be manipulated throughout research phase two and can be considered constant within this virtual paving project.

3.3.4. Comparison of Hierarchy Level

Research phase one will be designed to evaluate the entire data set of input values for all three hierarchy levels. Generally, the M-E PDG defines different hierarchy levels to accommodate diverse design qualities through alternating intensity of testing. Nevertheless, the material section will render all properties under level one consideration; even those inputs used in level two or three applications only (e.g., compressive strength) will be provided in a realistic manner (tested as used in construction). The explanation of this approach is justified through the research interest. The sensitivity of different hierarchy levels can be studied while the impact of real data under level two and three consideration can be assessed. Therefore, additional PCC property models will be generated for level two and three conditions to serve as an evaluation base. Level two data will be derived from less-than-optimal test situations and suitable computations, whereas level three PCC properties will be defined on account of default values taken from databases or literature. This approach will help to identify the sensitivity of the Design Guide Software to realistic data and reveal the difference (if any) and importance of chosen data quality.

3.3.5. CTE Sensitivity

Specifically, the coefficient of thermal expansion describes an essential Portland cement concrete property that is assumed to affect the performance of rigid pavement significantly [2], [3], [4], [and others]. Therefore, the CTE sensitivity of the new Mechanistic-Empirical concept represents a major purpose of this research. The aim is to study the consequence of interchanging PCC thermal properties throughout a typical Florida CTE array and the significance for the predicted distresses and smoothness models. A proper evaluation base has to be determined to establish suitable CTE sensitivity matrices guaranteeing a valid comparison study.

CHAPTER 4: MATERIALS RESEARCH - EXPERIMENTAL PROGRAM

4.1. Introduction

The material research focused mainly towards the coefficient of thermal expansion (CTE). However, to ensure proper concrete mixtures and to evaluate factors affecting CTE, other engineering properties had to be considered as well. The intention of this chapter is to outline all test sequences conducted in the laboratory; it describes each experimental setup on top of the related ASTM and AASHTO regulations. As necessary, this section summarizes important predicaments encountered during the empirical phase and explains how these difficulties were overcome.

The experiments accomplished for this research can be outlined as follows:

Fresh Properties
- Slump
- Temperature
- Air content

Hardened Properties
- Compressive strength
- Splitting tensile strength
- Flexural strength
- Modulus of elasticity
- Poisson's ratio
- Coefficient of thermal expansion

For adequate statistics, sufficient data points per test series were desirable. Consequently, seven specimens per maturity were found to be suitable for each engineering property. Due to lab capacity an exception had to be made in the case of flexural strength; 7-day flexural strength was tested on three specimens while 28-day and 90-day flexural strength were evaluated for five samples each.

The Gilson HM-251 was utilized to measure concretes' CTE. Throughout the entire research period, this unit was the one and only CTE test apparatus commercially

available following the AASTHO TP 60 protocol [X 14]. It mounts merely one cylindrical specimen (4/8) per test procedure while one test cycle may take 18 hours or more. Due to the given capacity, it was impossible to measure seven specimens within one day regarding CTE. Therefore, the decision was made to run one sample per day and base statistical values on seven specimens tested on subsequent days; e.g. the average 90-day CTE is the mean value of all specimens tested from day 90 to day 97.

The aforementioned facts required a suitable workflow to fully utilize the laboratory capacity without suffering any data points. A tide timetable was established and the decision was made to produce all specimens per mix design within one day while separating each batch by seven days. This ensured continual test flows during the experimental program – especially in terms of CTE testing – while the least amount of time was needed (considering the given capacity).

4.2. Mix Design

This research was initiated by Florida's Department of Transportation due to the newly developed M-E PDG. The new code requires supplementary material properties for the design of pavement and might be mandatory in the future. Consequently, it was important to study additionally requested characteristics of existing mixtures before these mix designs can be considered by the new design procedure.

A fundamental goal of this study is the implementation of local materials and their properties into the new M-E PDG – only FDOT approved mix designs were considered. For reasons of comparison, different compositions, engineering properties and ingredients were desirable. The local aggregates used in pavement mixtures are almost exclusively limestone and granite, whereas granite can be considered a rare constituent in Florida pavement applications.

The above-mentioned facts led to the choice of two concrete mixes based on limestone and one granite mix. The decision was narrowed down to the three concrete mixtures outlined in the table below.

Table 4.1: Mix design composition

	Unit	MIX-01	MIX-02	MIX-03
Mix Number	-	03-1419	A-22013	A-47AC
Cement	lb	511	415	470
Fly Ash	lb	132	105	-
Coarse Aggregates	lb	1750	1900	1921
Fine Aggregates	lb	1191	1278	1235
Air Entraining Admixture	oz	1.5	1.0	2.5
1st Admixture	oz	35.4	45	18
2nd Admixture	oz	-	-	-
Water	lb	279.1	258	267
Sum	lb	3863.1	3956	3893
Target Strength	psi	4500	3000	3000
Target Slump Range	in	1.5 to 4.5	2.0 to 4.0	3 to 5
Target Air Content	%	1.0 to 6.0	3.0 to 6.0	3.0 to 6.0
Target Unit Weight	pcf	143.1	146.6	144.2
Water-to-Cement Ratio	-	0.546	0.622	0.568
Water-to-Cementitious	-	0.43	0.50	0.57
Cement Paste	lb	790	673	737
Cementitious Paste	lb	922	778	737
Mortar	lb	2113	2678	1972
Mortar-to-Total	lb/lb	0.55	0.68	0.51

4.3. Materials

The different proportions of ingredients were outlined in Table 4.1. The specified concrete constituents (materials) and their properties are identical for all three mixtures. Moreover, only coarse aggregates differ. However, the next subcategories are designated to summarize the characteristics of materials used in this study.

4.3.1. Cement

Sulfate resistance makes Type I & Type II cement the most applied concrete adhesive in Florida. On account of local availability, an ASTM Type I cement was used. Its physical and chemical properties have been evaluated by Florida Rock Industries, Inc. Table 4.2 outlines the provided test results and describes the requirements according to ASTM C 150.

Table 4.2: Standard chemical requirements of cement and test results

Chemical Compounds	**Unit**	**Test Results**	**Specification ASTM C150**
Silicon Dioxide (SiO_2)	%	20.68	20.0 Min
Aluminum Oxide (Al_2O)	%	5.02	6.0 Max
Iron Oxide (Fe_3O_2)	%	3.69	6.0 Max
Calcium Oxide (CaO)	%	64.28	-
Magnesium Oxide (MgO)	%	0.72	6.0 Max
Sulfur Trioxide (SO_3)	%	3.02	3.0 Max
Lose on ignition	%	2.01	3.0 Max
Insoluble Residue	%	0.14	0.75 Max
Alkalies as (Na_2O)	%	0.34	0.60 Max
Tricalcium Silicate (C_3S)	%	64.5	
Dicalcium Silicate (C_2S)	%	7.8	
Tricalcium Aluminate (C_3A)	%	7.1	8.0 Max
Tetracalctium Aluminoferrite (C_4AF)	%	11.2	
$CaCo_3$ in Limestone, %	%	97.0	70.0 Min
Limestone, %	%	2.0	5.0 Max

From Table 4.2 it can be seen that the employed cement is suitable and in conformity with ASTM C 150. The specific gravity attains 3.15 for the employed cementious material.

4.3.2. Fly Ash

Fly ash is primarily silicate glass containing silica, alumina, iron, sulfur, sodium, potassium, carbon, and small amounts of crystalline compounds. The specific gravity of fly ash usually ranges between 2.2 and 2.8. ASTM C 168 Class F and C Fly ashes are commonly used as pozzolanic[4] admixture for concrete. The particle size in fly ash varies from less than 1 μm (micron = 1/1000 millimeter) to more than 100 μm with a typical particle size of 20 μm. Its ability to fill the gaps between the angular cement particles explains why fly ash is a desirable additive in concrete mixes. It increases the concrete density and results in a better matrix (enclosing fewer pores), leading to higher strength and advanced durability.

ASTM C 618 divides fly ash into two classes: low-lime fly ash (Type F) and high-lime fly ash (Type C). They differ significantly in their composition.

- **Type F, low-lime fly ash** (<10% lime), is produced by anthracite and bituminous coals. It has pozzolanic properties and needs an activator in order to undergo pozzolanic reaction.
- **Type C, high-lime fly ash** (≈10% lime), is produced of subbituminous and lignite coals. It possesses some cementitious (self-hardening) properties in addition to its pozzolanic properties. The disadvantage of this type is its high quality fluctuation.

[4] A pozzolan is a siliceous or aluminosiliceous material that in itself possesses little or no cementitious value but will, in finely divided form and in the presence of water, chemically react with the calcium hydroxide released by the hydration of Portland cement to form compounds possessing cementitious properties.

Type C fly ash is very rarely used in Florida and Type F (low-lime) fly ash is the common filler for local concrete projects. The fly ash for this research was supplied by Cemex, Inc and is labeled "Cemex Class F Fly Ash." This fly ash is constantly tested by Analytical Testing Service Laboratories, Inc. and their test results are presented in Table 4.3 below.

Table 4.3: Standard chemical requirements of fly ash and test results

Characteristics	Unit	Requirements		Test Results
		AASHTO-M295 Class "F"	ASTM C-618 Class "F"	
Fineness (+325 Mesh)	%	34 Max	34 Max	19.90
Moister Content	%	3 Max	3 Max	0.08
Loss on Ignition	%	5 Max	6 Max	2.14
Soundness	%	0.8 Max	0.8 Max	0.00
S.A.I., 7 Days	%	75 Min	75 Min	82.20
S.A.I., 28 Days	%	75 Min	75 Min	85.00
Water Req., of Control	%	105 Min	105 Min	97.90
Silica SiO2	%	-	-	45.98
Aluminum Oxide Al2O3	%	-	-	22.31
Ferric Oxide Fe2O3	%	-	-	18.59
Total	%	70 Min	70 Min	86.88
Sulfur Trioxide SO3	%	5 Max	5 Max	1.11
Calcium Oxide CaO	%	-	-	5.56
Magnesium Oxide MgO	%	-	-	1.06
Available Alkalies Na2O	%	1.5 Max	-	0.87

The Table proves the authenticity of Cemex Class F Fly Ash in accordance with ASTM C-618 and AASHTO M-295. Additionally, the specific gravity was measured to be 2.46.

4.3.3. Fine Aggregates

The fine aggregates are made of silica sand mined from Quarry Mine #47-314. Its properties are constantly controlled at the pit and Florida Rock, Inc. has made the test results available. Accordingly, the specific gravity of fine aggregates used in this evaluation amounts to 2.66. The specified grading ranges according to ASTM and sieve analysis results are outlined in Table 4.4.

Table 4.4: Gradation and specifications for concrete sand

Sieve Size			Retaining	Passing	Grading Range	
US	inch	mm	%	%	min %	max %
# 4	0.187	4.75	0	100	95	100
# 8	0.093	2.36	2	98	85	100
#16	0.046	1.18	14	84	65	97
#30	0.024	0.60	27	57	25	70
#50	0.012	0.30	34	23	5	35
#100	0.006	0.15	20	3	0	7
#200	0.030	0.75	3	0	0	4
Sum			100	365	275	413

Table 4.4 confirms ASTM standards for the utilized concrete sand which can be considered very fine based on its fineness modulus of 2.35 (concrete sand ranges from 2.3 to 3.1 – fine to coarse).

4.3.4. Coarse Aggregates

As mentioned earlier, the concrete mixtures employ identical ingredients but differ in terms of coarse aggregates. Three different compositions of coarse materials were used for this research; MIX-01 and MIX-02 are limestone-based using 67-stone and 57-stone respectively while MIX-03 employs a 67-stone made of granite.

The limestone material for MIX-01 and MIX-02 was mined from Quarry Mine #38-268 in Florida while the granite aggregates were imported from Plant 022-Barin in Georgia.

Sieve analysis and characterizations have been conducted at the mines and test results were obtained through Florida Rock Inc. The following tables present the findings:

Table 4.5: Gradation and specifications for limestone 67-stone

Sieve Size			Retaining	Passing	Grading Range	
US	inch	mm	%	%	min %	max %
	1.0	25.40	0	100	100	100
	3/4	19.05	14	86	90	100
	3/8	9.53	49	37	20	55
# 4	0.187	4.75	31	6	0	10
# 8	0.093	2.36	2	4	0	5
Sum			96	233	210	270

Slight discrepancies can be observed for 3/4 stones; nevertheless, the grading was found to be within acceptable ranges and harmless for this research. The fineness modulus of the limestone 67-stone was calculated to be 2.67 and its specific gravity was measured at 2.61.

Table 4.6: Gradation and specifications for limestone 57-stone

Sieve Size			Retaining	Passing	Grading Range	
US	inch	mm	%	%	min %	max %
	1.0	25.40	0	100	95	100
	1/2	12.70	42	58	25	60
# 4	0.187	4.75	48	10	0	10
# 8	0.093	2.36	5	5	0	5
Sum			95	173	120	175

Total ASTM authentication can be confirmed for the 57-stone made of limestone. The specific gravity was found to be 2.64 and the fineness modulus reached 2.27.

Table 4.7: Gradation and specifications for granite 67-stone

Sieve Size			Retaining	Passing	Grading Range	
US	inch	mm	%	%	min %	max %
	1.0	25.40	0	100	100	100
	3/4	19.05	0.7	99.3	90	100
	1/2	12.70	31.3	68	20	100
	3/8	9.53	36.5	31.5	20	55
# 4	0.187	4.75	29	2.5	0	10
# 8	0.093	2.36	1.5	1	0	5
Sum			99	302	230	370

The granite 67-stone verifies ASTM standards and is perfectly acceptable for this research. The fineness modulus amounts to 2.66 according to sieve analysis and its specific gravity is denoted by 2.70.

The following charts were created to provide a comprehensive overview of sieve analysis. They represent the results obtained from testing and display the limits according to ASTM.

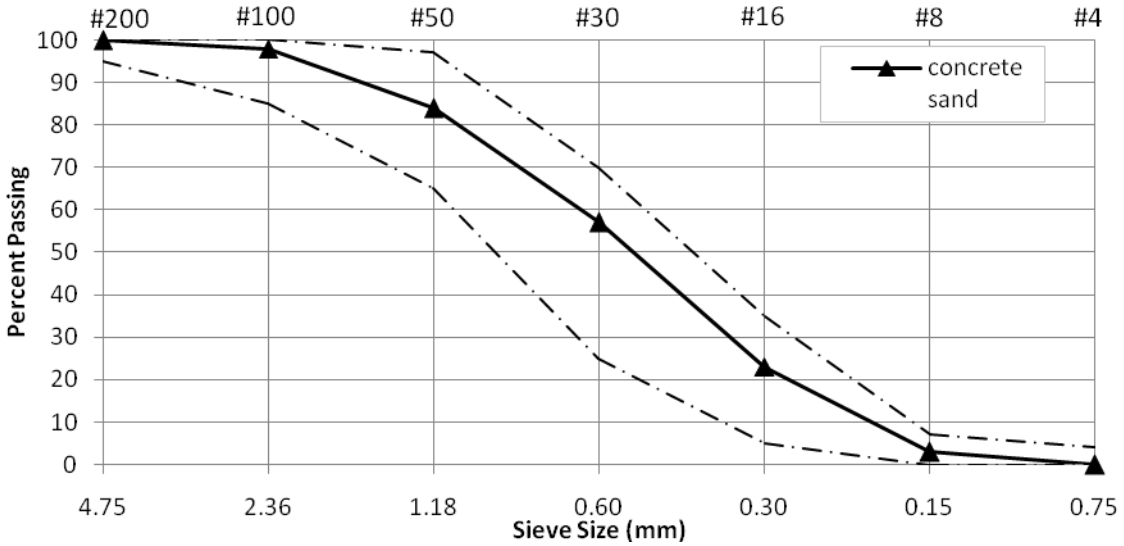

Figure 4.1: Gradation chart for concrete sand

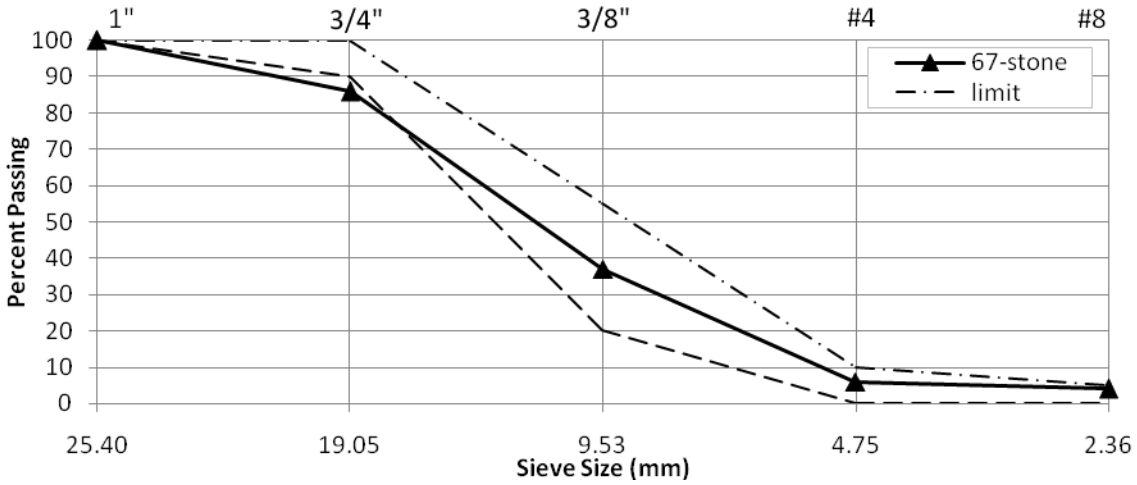

Figure 4.2: Gradation chart for limestone 67-stone

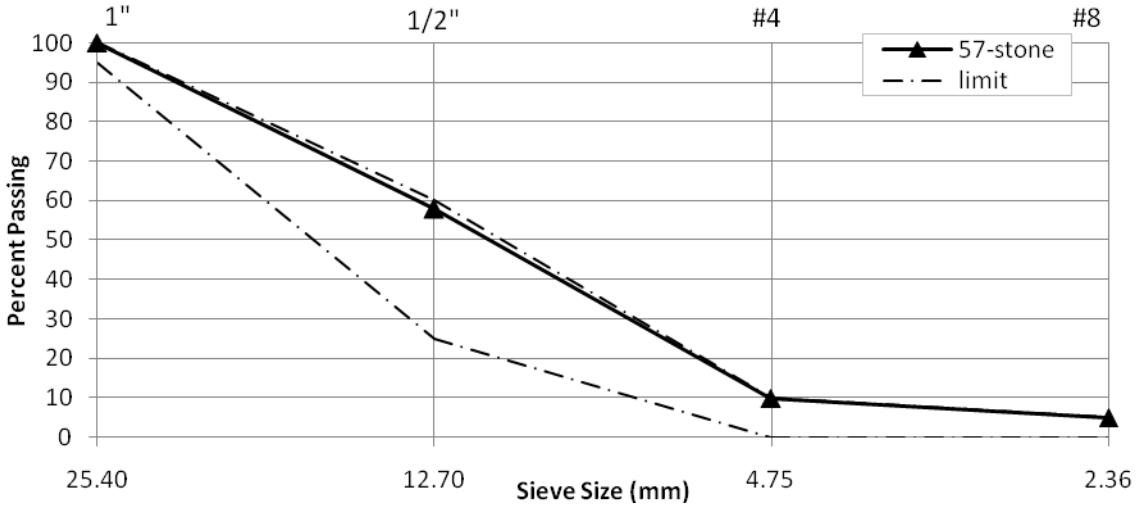

Figure 4.3: Gradation chart for limestone 57-stone

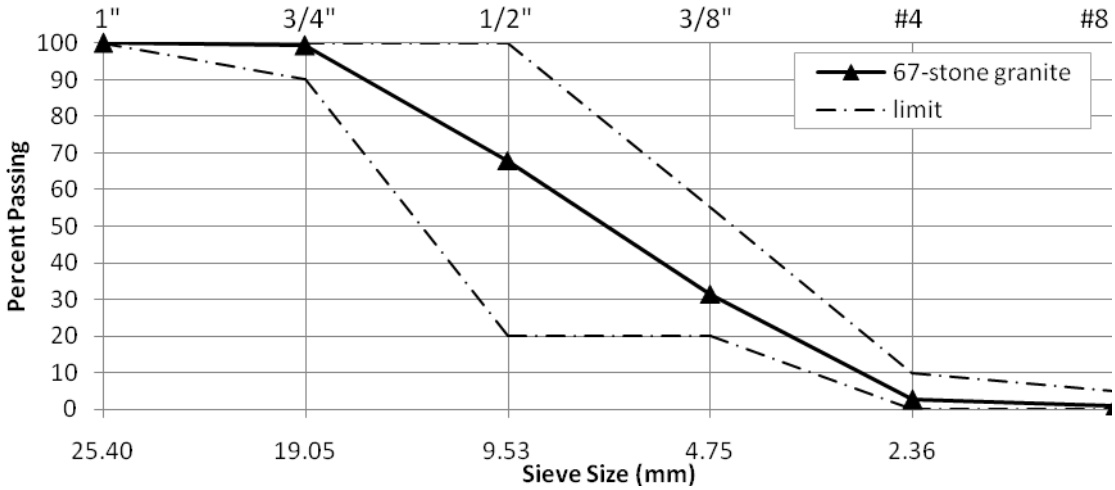

Figure 4.4: Gradation chart for granite 67-stone

4.4. Mixing and Batching

Since the Design Guide is intended for practical design application in the future, a lot of thought went into the process of concrete batching. In practical applications, the concrete ingredients are almost exclusively weighed and premixed at the plant before the concrete mixture is delivered to the jobsite by trucks. To account for mixtures as close as possible to real-world applications, the concrete was obtained from a local concrete supplier[5]. It was batched and pre-mixed at the concrete plant before drum mixing trucks delivered one cubic yard per mix design to the laboratory.

Table 4.8: Geometric properties of test specimens

Specimen	Depth	Width	Area	Length	Volume	
	in	in	in^2	in	in^3	ft^3
Beam	6	6	36	22	792	0.458
Cylinder 4/8			12.57	8	100.5	0.058
Cylinder 6/12			28.27	12	339.3	0.196

Table 4.9: Minimum specimen quantity per mix design

Specimen	Procedure	day						SUM	
		7	14	28	49	70	90		
Cylinder 4/8	Compressive	7	7	7			7	35	105
Cylinder 4/8	Tensile			7			7	14	
Cylinder 4/8	Poisson's	7	7	7	7	7	7	35	
Cylinder 4/8	Temperature	7		7			7	21	
Beam 6/6/21	Flexural	3		5			5	13	13

All concrete samples per mix design were cast on the same day for the reasons mentioned earlier. Combining Table 4.8 and Table 4.9, a minimum concrete volume of 8.7 cubic foot was necessary to create all specimens per mix design considering no waste or surplus material.

Immediately after truck arrival, slump tests were carried out according to ASTM C143 [X 1]. In cases in which the measured value exceeded the range stated in Florida DOT specifications or delivery slip, the concrete was discarded. If the value undercut the target

[5] Florida Rock Industries, Inc., 1005 Kissimmee St, Tallahassee, FL 32310

slump, additional water was added to the mixture. After sufficient mixing, the slump test was repeated until the slump was acceptable.

Only if slump results were acceptable, the air content was measured in concrete's fresh state. Since two out of three mix designs were using limestone aggregates (porous material), the pressure method according to ASTM C 231 or AASHTO T 152 was disregarded. Instead the volumetric method in line with ASTM C 173 [X 2] and AASHTO T 196 [X 9] was found to be suitable.

Figure 4.5: Volumetric air content test

The material was poured into the concrete reservoir in two equal layers while compaction was applied after each layer. Consolidation was attained in harmony with specimen preparation as explained later in the text. The excess material was struck off and the vessel was closed; one third of water and two thirds of alcohol were carefully added until the zero % mark was reached. Then, the vessel was closed and rolled in its forty-five degree position. Occasionally, the device was hammered up by hand or revolved to loosen the concrete, allowing the water-alcohol mixture to fill the pores. After sufficient mixing (all air pockets filled with liquid), the container was placed on a leveled surface for three to five minutes and the volumetric air content was read from the vertical scale.

Additionally, the temperature of the fresh concrete was measured every twenty minutes as well as the ambient temperature of the laboratory.

All specimens were prepared according to ASTM C192 [X 4] and AASHTO T126 [X 9] standard practice for making and curing concrete test specimens in the laboratory. The standard specimen size for this study was fixed to 4”/8” cylinders but additional 6”/12” cylinders were formed to validate test results if needed. However, since 120 specimens had to be prepared within 90 minutes, rodding was out of question and a mechanical vibration table was used instead. The material was funneled into the molds in at least two layers while vibration was applied after each layer. The required duration of vibration per layer depended upon the workability of the mix design. Sufficient vibration was applied as soon as the surface of the concrete was relatively smooth – vibration was continued only long enough to achieve proper consolidation. After vibration was finished, just enough concrete was added with a trowel to work it into the surface and then strike it off to even it out with the disposable plastic cylinder mold. The molds, then, were covered with plastic lids to anticipate vaporizing water. Finally, the freshly prepared specimens were stored on a leveled surface and twenty-four hours later the concrete was demolded to initiate curing.

4.5. Curing

Curing was accomplished as outlined in ASTM C192 [X 4] and AASHTO T 126 [X 9]. After breaking the cylinder molds and dismantling the beam formwork all specimens were moisture cured in a water tank. The lime water was concentrated at 10 grams of lime per 1 gallon of water while its temperature was maintained around 73.5 ± 3.5°F (23.0 ± 2.0°C).

4.6. Specimen Preparation

The identification of concretes CTE according to AASHTO TP 60 is based on small scale measurements, and therefore requires very well-prepared and parallel concrete surfaces. Specifically, for this purpose a concrete cylinder end grinder was purchased. The Gilson

HM 716A mounts four cylinders (4/8 or 6/12) at a time and needs roughly ten minutes to totally prepare the specimens for testing.

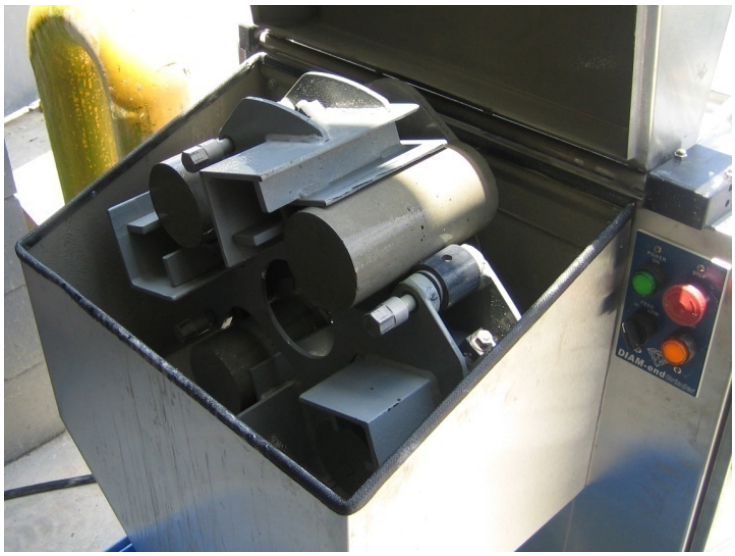

Figure 4.6: Concrete cylinder end grinder

All cylindrical concrete specimens were ground on both ends one day before testing and then placed back in the curing tank (room temperature) until testing. The end grinding process was performed flawlessly, and all strength tests were performed on surface dry specimens within about one hour after removal from the water tank – thanks to grinding, no capping was necessary. The samples used for the thermal expansion test were taken from the water tank, surface dried, measured, marked, and then immediately placed in the water bath of the thermal expansion unit for measurements.

4.7. Compressive Strength

To determine compressive strength, the experimental procedure was based on ASTM C 39 [X 5] and ASTM T 22 [X 11]. The tests have been carried out on cylindrical specimens using Testmarks CM-3000 Compression Testing Machine with digital load indicating system. The load was applied continuously and without chocking. Stress rates were adjusted to 35 ± 7 PSI/s. Neither capping compounds nor rubber pads were applied to the specimens, as they had been parallel end grinded before. Ultimate compressive

strength was calculated by dividing the maximum load carried by the specimen by the average cross-sectional area.

Figure 4.7: Compressive strength test (28-day MIX-04)

$$\sigma_C = \frac{P}{A_C} \; ; \qquad \sigma_C = \frac{P}{\pi \cdot r^2} \tag{4.1}$$

$$\sigma_C = \frac{P[lbs]}{28.274} \quad [\text{psi}]; \qquad \text{specimen 6”/12”} \tag{4.1a}$$

$$\sigma_C = \frac{P[lbs]}{12.566} \quad [\text{psi}]; \qquad \text{specimen 4”/8”} \tag{4.1b}$$

4.8. Flexural Strength

The flexural strength tests were completed according to ASTM C 78 [X 6] and AASHTO T 97 [X 12] by breaking beam shaped concrete specimens. Samples were formed by molds of 6 inches square in cross-section and 21 (18 + 2 (1.5)) inches in length. The specimens were tested 30 minutes after they were removed from the water tank. The ultimate load was achieved by dint of the third-point loading method as seen in Figure 4.8

and Figure 4.9. The specimen was loaded continuously and without shocking. The loading rate was fixed to 125 psi/min.

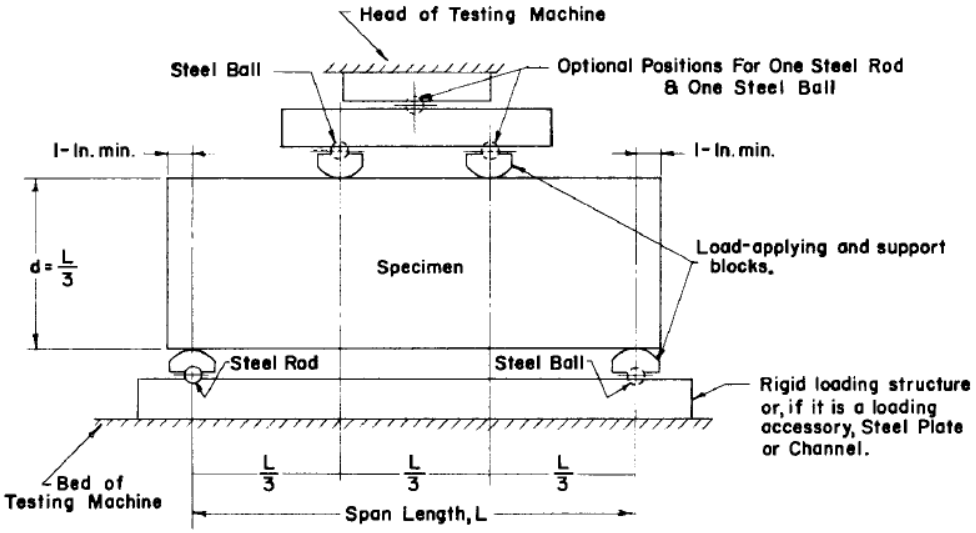

Figure 4.8: Flexural strength test using the third-point loading method [X 6]

Figure 4.9: Left: flexural strength test setup. Right: beam failure in bending

The ultimate strength is influenced by the introduced moment and the beam's section modulus. Therefore the flexural strength was computed as follows:

$$M = F/2 \cdot l/3 = \frac{P \cdot l}{2 \cdot 3} = \frac{P \cdot l}{6} \qquad (4.2)$$

$$S_{beam} = \frac{b \cdot d^2}{6} \tag{4.3}$$

$$\sigma_C = \frac{M}{S_{beam}} = \frac{\frac{F \cdot l}{6}}{\frac{b \cdot d^2}{6}} = \frac{P \cdot l \cdot 6}{6 \cdot b \cdot d^2} = \frac{P \cdot l}{b \cdot d^2} \tag{4.4}$$

$$= \frac{P \cdot l}{b \cdot d^2} = \frac{P \cdot 18}{6 \cdot 6^2} = \frac{P[lbs]}{12} \quad [psi] \quad \text{specimen 6”/6”/18”} \tag{4.4a}$$

4.9. Splitting Tensile Strength

The test documents applicable to the splitting tensile test are ASTM C 496 [X 7] and AASHTO T 198 [X 13]. To prevent load concentrations, two one-inch-wide plywood strips were applied between the specimen and the two bearing blocks.

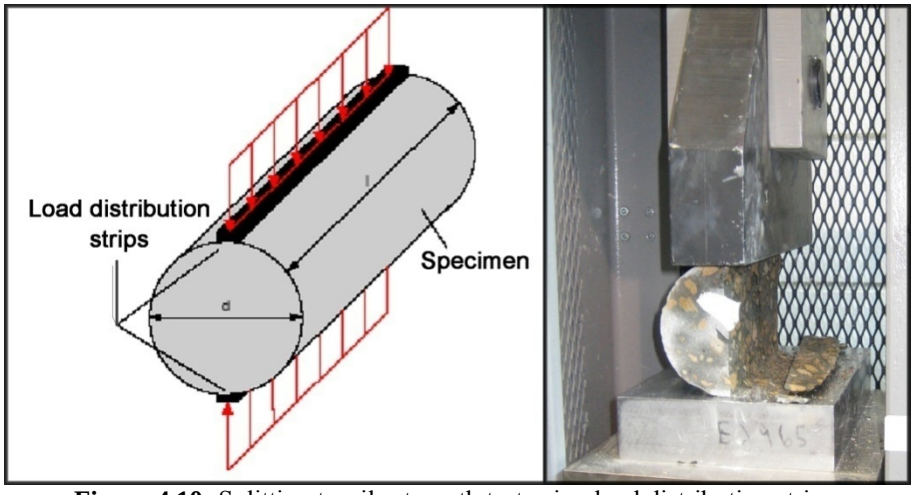

Figure 4.10: Splitting tensile strength test using load distribution strips

The test procedure was carried out 10 minutes after the specimens were taken from the curing tank. The load was applied constantly without shocking while loading rates were set to 150 PSI/min. The ultimate splitting tensile strength was (approximately) calculated using the maximum applied load and the cylindrical measurements.

$$T_C = \frac{2 \cdot P}{\pi \cdot l \cdot d} \qquad (4.5)$$

$$T_C = \frac{2 \cdot P}{\pi \cdot 8 \cdot 4} \quad = \frac{2 \cdot P}{\pi \cdot 32} = \frac{P}{\pi \cdot 16} = \frac{P[lbs]}{50.24} \quad \text{[psi]} \qquad (4.5a)$$

4.10. Young's Modulus and Poisson's Ratio

ASTM C 469 [X 8] covers determination of (1) chord modulus of elasticity (Young's) and (2) Poisson's ratio of molded concrete cylinders and diamond-drilled concrete cores when under longitudinal compressive stress. Both engineering properties can be measured at the same time within the same test procedure if suitable equipment is available. In this research the compressometer/extensometer method was chosen because numerous specimens had to be tested within one day.

Figure 4.11: Compressometer/Extensometer

For Young's modulus a compressometer (Figure 4.11) was used. It consists of two yokes, one of which is rigidly attached to the specimen (bottom yoke) and the other of which is attached at two diametrically opposite points (top yoke) so that the specimen is free to rotate. The yokes are connected through a pivot rod on the back whereas a vertical LVDT

measures the motion in front. Since the top yoke rotates freely about the center of the specimen (or half distance from front to back), the movement of the vertical LVDT is twice the specimen deformation. Therefore, the actual strain during testing was calculated based on the procedure shown in Figure 4.12.

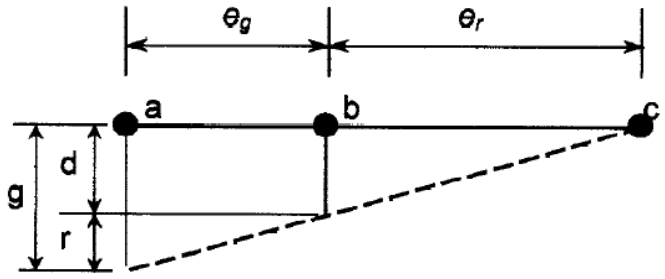

Figure 4.12: Diagram of displacement

Where:

a	location of gauge
b	support point of the rotating yoke
c	location of pivot rod
d	total deformation of the specimen throughout the effective gauge length
r	displacement due to rotation of the yoke about the pivot rod
g	gauge reading
e_r	perpendicular distance from the pivot rod to the vertical plane passing through the two support points of the rotating yoke
e_g	perpendicular distance from the gauge to the vertical plane passing through the two support points of the rotating yoke.

$$d = \frac{g e_r}{(e_r + e_g)} \qquad (4.6)$$

Young's modulus is characterized through the slope of a chord connecting two specified points on the stress-strain curve within the elastic range. In concrete, ASTM C 469 [X 8] defines the two points (1) corresponding to a strain of 50 millionths and (2) equivalent to

40 % of the ultimate compressive load. Thus, the E-modulus was calculated using the following equation.

$$E = \frac{S_2 - S_1}{\varepsilon_2 - \varepsilon_1} = \frac{S_2 - S_1}{\varepsilon_2 - 0.000050} \qquad (4.7)$$

where:
- E — chord modulus of elasticity
- S_1 — stress corresponding to a longitudinal strain, ε_1, of 50 millionths
- S_2 — stress corresponding to 40 % of ultimate load
- ε_1 — 50 millionths
- ε_2 — longitudinal strain produced by stress S2

Poisson's ratio is the ratio of the relative contraction strain or transverse strain normal to the applied load, divided by the relative extension strain or axial strain in the direction of the applied load.

$$\mu = \frac{\varepsilon_{t2} - \varepsilon_{t1}}{\varepsilon_2 - \varepsilon_1} = \frac{\varepsilon_{t2} - \varepsilon_{t1}}{\varepsilon_2 - 0.000050} \qquad (4.8)$$

where:
- μ — Poisson's ratio,
- e_{t1} — transverse strain at specimen midheight produced by stress S_1
- e_{t2} — transverse strain at specimen midheight produce by stress S_2
- ε_1 — 50 millionths
- ε_2 — longitudinal strain produced by stress S2

For Poisson's Ratio, the extensometer is attached horizontally to the specimen on two opposite points (distance = specimens diameter) to measure the change in diameter at mid-height. Similar to the compressometer, one LVDT measures twice the horizontal strain up front while the yoke rotates about its pivot point on the back side.

Compression was applied by the same machine as used for compressive strength test. Adjustments had to be made to account for data acquisition. This was achieved by

replacing the existing digital loading system with a three-channel TM-8000-02 MTESTwindows System. Therefore, the whole test procedure was computer controlled using the interface shown in Figure 4.13. The left window on the top shows the applied load while the window next to it applies the specimen measurements to represent the actual stress. The right windows indicate LVDT behaviors; the top window (Strain 1) outlines vertical displacements needed for Young's modulus while the bottom one (Strain 2) specifies the horizontal deformation to determine Poisson's Ratio. The Graph in the left bottom corner is adjustable but was configured for stress-strain1 relationship (E-modulus) in this research.

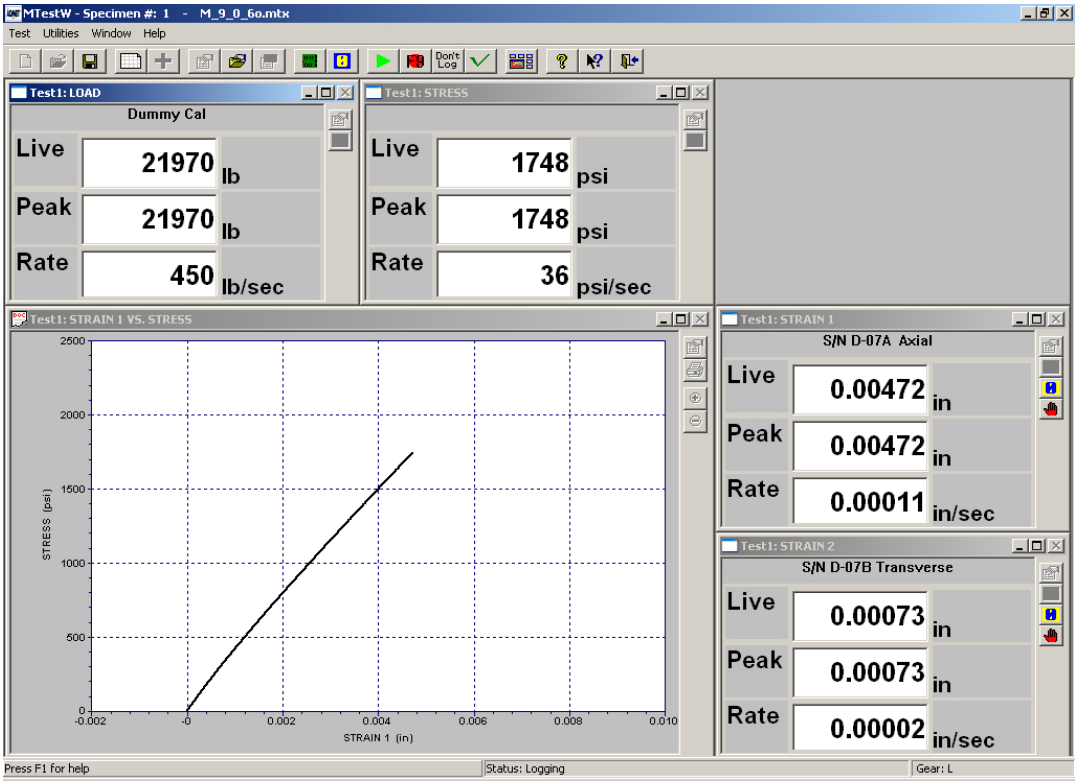

Figure 4.13: Young's modulus and Poisson's ratio run monitor (MIX-03 28-day)

All tests have been non-destructive since a compressometer/extensometer was used. The maximum applied load was slightly (approximately 1%) exceeding 40 % of the average ultimate compressive strength which was determined shortly before (7 different samples of same age and mix design). The loading rate was adjusted to 35 ± 7 PSI/s (0.25 ± 0.05 (N/mm²)/s). Each specimen was compressed and released five times after the compressometer/extensometer was applied. The first run was simply used for gauge

setting; hence, it was not considered in calculating Young's modulus or Poisson's Ratio. The actual value was determined as the mean value of the last four test sequences.

4.11. Coefficient of Thermal Expansion

AASHTO defines the method to determine the coefficient of thermal expansion of hydraulic cement concrete in protocol TP 60 [X 14]. The described test procedure is considered very new as it was developed in 2000 and, recently afterwards, adopted by AASHTO.

In this study the Gilson HM-251 was used to identify concrete's thermal properties. The unit is the first commercially available standalone solution following AASHTOs TP 60 protocol. As specified in the code, the instrument is equipped with a rigid support frame (Figure 4.14) which provides reference for the attached linear differential variable transformer (LDVT) during length change measurement of the specimen.

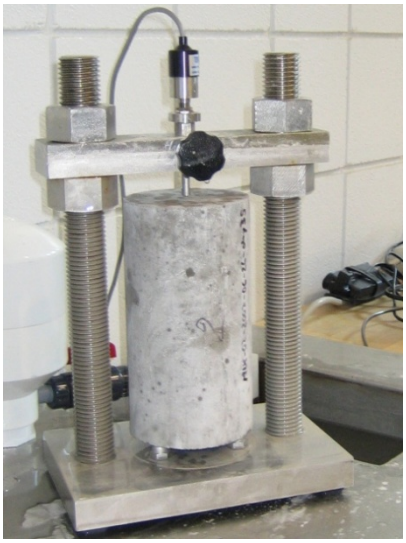

Figure 4.14: Support frame

The frame is made of 304 stainless steel (CTE = 17.3 µm/m/°C) which is the same material the calibration specimen is made of. For calibration, the reference length should be as close to the tested concrete specimens as possible, which results in a calibration rod length of ca. 200.3 mm (7.9 inches) at room temperature. Note that the picture shows a

typical concrete cylinder rather than the calibration rod. However, the calibration specimen looks like one of the two threaded rods (frame columns), but shorter in length.

Figure 4.15: Gilson HM-251 CTE test unit

The cabinet (Figure 4.15) provides room for a five-gallon water bath and the data acquisition equipment. The heater/chiller (Recirculator) is located to the left of the cabinet and connects to the water bath via two hoses. It is a self-contained water cycle system; one hose draws water into the Recirculator to heat it up and to cool it down, while the second hose introduces the temperature-changed water back into the tank. An additional temperature probe is located in the back left corner of the water bath, ensuring exact measurements as close to the specimen as possible. To keep the water level constant during testing and to compensate for vaporization of water at high temperatures, a PVC water reservoir is placed on top of the cabinet.

The LVDT, the Recirculator, and the thermometer are fed into the data acquisition system inside the cabinet. From the data acquisition hardware, a USB cable plugs into a laptop running "Challenge Technology Software HM-521." The software controls the heater/chiller based on the LVDT and temperature outputs following the rules described in Chapter 2 (Page 17).

Each specimen was taken from the curing tank 10 minutes prior to testing. The sample then was surface dried, marked, and measured to the nearest 0.1 mm (0.004 inches) at room temperature. Immediately afterwards, the specimens was placed on the three knobs at the base plate of the support frame. Since the software determines the range of LVDT placement, the software was started, the text file destination was chosen, and the lengths of the specimens was fed into the software before the LVDT was attached to the frame. Next, the whole frame including the concrete cylinder was positioned in the middle of the water tank. The water level was adjusted so that the entire sample was submerged in water but no water reached the electrical coil of the LVDT. Finally, the water reservoir was filled, the Recirculator deaerated, and the test initiated.

Since the water temperature at test launch was mostly found to be room temperature, the system hat to cool down the temperature to 10 degree C before actual CTE testing was initiated. After stabilization of water temperature and LVDT displacement, temperature was slowly increased to attain readings for expansion CTE, resulting in the decreasing line shown on the left in the black screen in Figure 4.16.

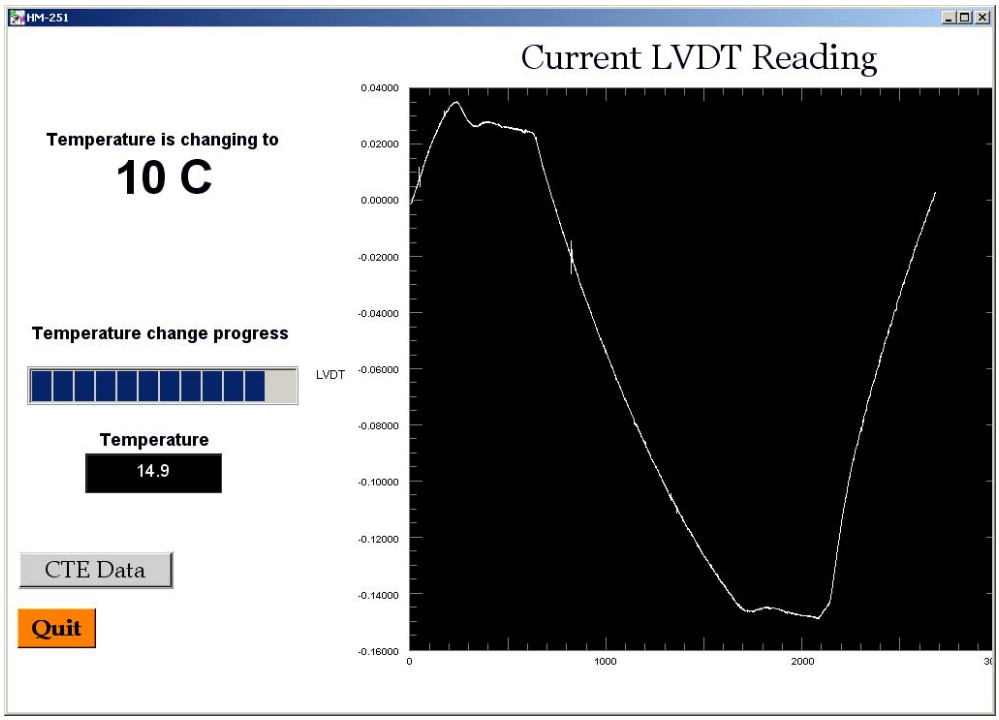

Figure 4.16: Run monitor displaying LVDT reading (MIX-01 day35)

At 50°C, the temperature and LVDT displacement were once again stabilized (almost horizontal line) and measurement of contraction CTE was started which caused the line to slope in Figure 4.16. Note that the run screen in Figure 4.16 is not displaying a total test cycle as the increasing line does not stabilize at 50°C. Rather it displays 5/6 of the test procedure. The complete test cycle may take 12 hours or more, depending on the ambient temperature, tested material, and the difference between two successive CTE measurements.

CHAPTER 5: MATERIAL RESEARCH - EXPERIMENTAL RESULTS

5.1. Introduction

This Chapter outlines all test results achieved throughout the experimental program. Attention was paid to the time of testing (maturity) and each result is displayed in conjunction with its failure time. All test results (except fresh properties) are presented in comparison to their equivalent of the other two mix designs. In case of destructive test methods, a note will be found describing the fracture type. For compressive strength, the failure patterns outlined in AASHTO T22 [X 11] were used according to Figure 5.1.

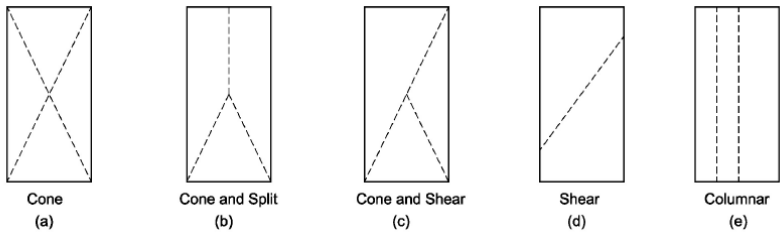

Figure 5.1: AASTHO compressive strength failure patterns

The third point loading method used to determine flexural strength may result in different failure patterns. The term “middle” in the following tables is used to describe cracking within the second (middle) third of the beam, whereas the expression “outside” would refer to a failure mechanism occurring in the outer third of beam.

In splitting tensile result tables, the fracture note “normal” describes the expected failure pattern due to the employed test procedure. Whenever the collapse differs from that, a note will be found describing the failure model.

Young’s modulus and Poisson’s ratio are based on six load cycles per specimen. However, the mean specimen value results from the average of the last five load cycles. Moreover, the age average is the outcome of seven sample results obtained by this method.

5.2. Fresh Properties

The fresh properties where tested according to their designated ASTM and AASHTO test protocols and the following tables outline the numerical results measured throughout the experimental program. All mix designs were mixed, batched, and tested in equal manners. The concrete and ambient air temperature was measured constantly.

Table 5.1: Fresh properties MIX-01

MIX-01				
5/22/2007				
	Time	Temperature		Value
		Air	Concrete	
		C	C	
Delivered	14:08	24.88	32.50	
1st Slump	14:11			3.2 "
2nd Slump				
Air Content	14:17			3.25%
	14:19	24.93	32.87	
	14:33	24.80	31.63	
	14:51	24.64	33.24	
	15:01	25.19	30.67	
Last Beam	14:55			
Last 4/8	14:59			
Last 6/12	15:08			

Table 5.2: Fresh properties MIX-02

MIX-02				
5/29/2007				
	Time	Temperature		Value
		Air	Concrete	
		C	C	
Delivered	14:55	26.50	36.89	
1st Slump	14:59			1.5 "
2nd Slump	15:01			2.5" [+5 gal]
Air Content	15:04			2.50%
	15:06	25.48	36.32	
	15:35	26.02	34.83	
	15:48	25.08	34.38	
	16:06	26.95	32.49	
Last Beam	15:48			
Last 4/8	15:58			
Last 6/12	16:06			

Table 5.3: Fresh properties MIX-03

MIX-03				
6/5/2007				
	Time	Temperature		Value
		Air	Concrete	
		C	C	
Delivered	14:42	26.72	31.69	
1st Slump	14:45			1"
2nd Slump	14:49			4.0" [+5 gal]
Air Content	14:55			3.00%
	14:58	26.50	31.86	
	15:17	26.40	31.52	
	15:31	26.65	31.62	
	15:39	26.80	31.73	
Last Beam	15:31			
Last 4/8	15:25			
Last 6/12	15:40			

5.3. Results of Compressive Strength

In general, the compressive strength was measured according to ASTM C 39 [X 5] and ASTM T 22 [X 11] for 4" by 8" cylinders. However, 28-day and 90-day compressive strength was tested for an additional 7 data points derived from 6 by 12 cylinders. The fracture patterns are described from a to e according to AASHTO T22 [X 11]

Table 5.4: 7-day compressive strength

7-day		MIX-01			MIX-02			MIX-03		
		5/29/2007			6/5/2007			6/12/2007		
NO	Type	Strength	Time	Fracture	Strength	Time	Fracture	Strength	Time	Fracture
	in/in	psi			psi			psi		
1	4/8	5387.4	11:13	e	5519.5	11:50	c	2899.4	12:22	d
2	4/8	5248.1	11:17	e	7228.0	11:56	a	3541.2	12:29	a
3	4/8	4794.5	11:22	e	6561.2	12:00	a	3520.1	12:38	a
4	4/8	5566.4	11:27	b	6242.1	12:06	c	3775.6	12:44	a
5	4/8	5677.1	11:32	e	5941.3	12:11	e	3193.4	12:52	a
6	4/8	1756.3	11:36	e	5980.2	12:15	a	3759.6	12:56	c
7	4/8	5391.4	11:41	not	5806.0	12:19	a	3733.0	13:02	d

Table 5.5: 14-day compressive strength

14-day		MIX-01			MIX-02			MIX-03		
		6/5/2007			6/12/2007			6/19/2007		
NO	Type	Strength	Time	Fracture	Strength	Time	Fracture	Strength	Time	Fracture
	in/in	psi			psi			psi		
1	4/8	6191.9	13:00	e	7147.3	13:11	c	4307.9	12:05	a
2	4/8	6479.2	13:06	a	7623.5	13:18	d	4333.8	12:13	c
3	4/8	6428.3	13:13	e	7490.2	13:24	a	4614.7	12:20	a
4	4/8	5811.5	13:20	e	7637.8	13:30	a	3961.0	12:25	c
5	4/8	6303.3	13:27	e	7418.2	13:37	c	3679.7	12:30	a
6	4/8	6090.1	13:33	e	7527.2	13:45	a	4570.9	12:35	c
7	4/8	5178.1	13:41	e	7249.1	13:50	c	4107.8	12:40	c

Table 5.6: 28-day compressive strength

28-day		MIX-01			MIX-02			MIX-03		
		6/19/2007			6/26/2007			7/3/2007		
NO	Type	Strength	Time	Fracture	Strength	Time	Fracture	Strength	Time	Fracture
	in/in	psi			psi			psi		
1	4/8	7451.2	11:12	e	8311.9	14:57	a	4300.8	12:37	c
2	4/8	7394.7	11:19	a	8280.0	15:05	a	4857.8	12:49	c
3	4/8	6835.7	11:26	e	8014.2	15:11	a	5083.8	12:54	a
4	4/8	7379.6	11:31	e	8552.2	15:17	a	5124.8	12:59	a
5	4/8	7309.6	11:36	e	8684.3	15:22	a	5033.7	13:04	d
6	4/8	6555.2	11:41	e	7974.5	15:28	a	4528.4	13:10	a
7	4/8	7167.5	11:46	e	7974.5	15:34	a	5256.9	13:15	d

Table 5.7: 28-day compressive strength (6/12)

28-day		MIX-01			MIX-02			MIX-03		
		6/19/2007			6/26/2007			7/3/2007		
NO	Type	Strength	Time	Fracture	Strength	Time	Fracture	Strength	Time	Fracture
	in/in	psi			psi			psi		
1	6/12	6212.0	16:21	a	7701.0	13:42	a	4187.5	17:05	d
2	6/12	6781.4	16:27	b	7421.9	13:49	a	4295.4	17:13	a
3	6/12	7021.6	16:35	a	8017.9	13:57	a	4458.1	17:17	a
4	6/12	7242.6	16:40	c	8017.2	14:12	a	4278.1	17:22	a
5	6/12	7133.3	16:47	a	7871.8	14:16	c	4355.9	17:25	a
6	6/12	6921.5	16:54	c	7894.8	14:23	a	4344.6	17:29	a
7	6/12	7045.3	17:00	c	7946.1	14:29	c	4411.8	17:33	a

Table 5.8: 90-day compressive strength

90-day		MIX-01			MIX-02			MIX-03		
		8/20/2007			8/27/2007			9/3/2007		
NO	Type	Strength	Time	Fracture	Strength	Time	Fracture	Strength	Time	Fracture
	in/in	psi			psi			psi		
1	4/8	7967.7	15:57	a	10133	11:15	a	6063.0	9:52	a
2	4/8	7649.4	16:04	a	9261.2	11:25	a	5591.1	9:56	a
3	4/8	7875.4	16:11	a	8791.7	11:31	a	5766.2	10:00	a
4	4/8	7601.6	16:16	a	9571.6	11:38	a	5882.4	10:05	a
5	4/8	7965.3	16:23	a	9050.3	11:45	a	5944.4	10:09	a
6	4/8	7967.7	16:29	a	8842.6	11:52	a	5845.8	10:13	a
7	4/8	7965.7	16:36	a	8666.0	11:57	a	5465.4	10:16	a

Table 5.9: 90-day compressive strength (6/12)

90-day		MIX-01			MIX-02			MIX-03		
		8/20/2007			8/27/2007			9/3/2007		
NO	Type	Strength	Time	Fracture	Strength	Time	Fracture	Strength	Time	Fracture
	in/in	psi			psi			psi		
1	6/12	7860.1	13:58	a	9178.6	18:06	a	4866.3	12:12	a
2	6/12	8590.5	14:04	a	9093.8	18:13	a	4921.8	12:16	a
3	6/12	8260.8	14:10	a	8467.4	18:20	a	4886.1	12:21	a
4	6/12	8056.4	14:17	a	9502.3	18:27	a	4999.9	12:26	a
5	6/12	8456.8	14:23	a	Machine failed			5003.1	12:33	a
6	6/12	8548.4	14:31	a				5002.1	12:36	a
7	6/12	8259.8	14:37	a				5244.3	12:40	a

5.4. Results of Flexural Strength

The flexural strength was measured for concrete beams according to ASTM C 78 [X 6] and AASHTO T 97 [X 12]. Due to laboratory capacity, the numerical results were derived for three data points at 7-day maturity and five data points at 28-day and 90-day maturity.

Table 5.10: 7-day flexural strength

7-day		MIX-01			MIX-02			MIX-03		
		5/29/2007			6/5/2007			6/12/2007		
NO	Type	Strength	Time	Fracture	Strength	Time	Fracture	Strength	Time	Fracture
	in/in/in	psi			psi			psi		
1	18/6/6	667.4	12:48	middle	761.4	12:55	middle	501.0	14:20	middle
2	18/6/6	716.9	12:49	middle	805.8	12:59	middle	529.0	14:28	middle
3	18/6/6	758.1	12:53	middle	764.6	13:05	middle	606.4	14:34	middle

Table 5.11: 28-day flexural strength

28-day		MIX-01			MIX-02			MIX-03		
		6/19/2007			6/26/2007			7/3/2007		
NO	Type	Strength	Time	Fracture	Strength	Time	Fracture	Strength	Time	Fracture
	in/in/in	psi			psi			psi		
1	18/6/6	758.1	15:45	middle	833.8	18:49	middle	667.4	18:00	middle
2	18/6/6	875.3	15:50	middle	955.8	18:57	middle	710.3	18:07	middle
3	18/6/6	784.4	15:55	middle	942.2	19:01	middle	618.0	18:15	middle
4	18/6/6	739.9	16:01	middle	812.4	19:11	middle	637.8	18:21	middle
5	18/6/6	726.7	16:07	middle	822.0	19:18	middle	677.3	18:27	middle

Table 5.12: 90-day flexural strength

90-day		MIX-01			MIX-02			MIX-03		
		8/20/2007			8/27/2007			9/3/2007		
NO	Type	Strength	Time	Fracture	Strength	Time	Fracture	Strength	Time	Fracture
	in/in/in	psi			psi			psi		
1	18/6/6	922.8	16:55	middle	855.3	17:23	middle	697.1	14:58	middle
2	18/6/6	893.2	17:02	middle	868.5	17:29	middle	669.1	15:09	middle
3	18/6/6	746.5	17:07	middle	838.8	17:36	middle	751.5	15:16	middle
4	18/6/6	772.9	17:15	middle	814.1	17:44	middle	713.6	15:24	middle
5	18/6/6	886.7	17:21	middle	779.5	17:50	middle	705.3	15:30	middle

5.5. Results of Splitting Tensile Strength

The tensile strength was evaluated using the splitting method according to ASTM C 496 [X 7] and AASHTO T 198 [X 13]. All results are based on full-size 4" by 8" cylinders. The normal fracture pattern splits the cylinder into two parts directly through its diameter.

Table 5.13: 28-day splitting tensile strength

28-day		MIX-01			MIX-02			MIX-03		
		6/19/2007			6/26/2007			7/3/2007		
NO	Type	Strength	Time	Fracture	Strength	Time	Fracture	Strength	Time	Fracture
	in/in	psi			psi			psi		
1	4/8	564.7	17:36	3 vertical	692.4	12:34	normal	322.4	16:16	normal
2	4/8	335.4	17:44	4 parts	599.9	12:40	normal	345.3	16:22	normal
3	4/8	526.0	17:52	normal	518.3	12:48	normal	406.4	16:31	normal
4	4/8	562.3	18:01	normal	559.5	12:57	normal	433.8	16:39	normal
5	4/8	546.7	18:09	normal	602.3	13:05	normal	504.1	16:45	normal
6	4/8	399.1	18:17	4 parts	618.7	13:11	normal	446.5	16:49	normal
7	4/8	502.9	18:21	normal	668.5	13:16	normal	351.1	16:52	normal

Table 5.14: 90-day splitting tensile strength

90-day		MIX-01			MIX-02			MIX-03		
		8/20/2007			8/27/2007			9/3/2007		
NO	Type	Strength	Time	Fracture	Strength	Time	Fracture	Strength	Time	Fracture
	in/in	psi			psi			psi		
1	4/8	619.4	14:56	normal	429.7	16:59	normal	355.2	18:23	normal
2	4/8	413.4	15:02	normal	592.8	17:04	3 parts	354.0	18:27	normal
3	4/8	607.7	15:06	normal	662.3	17:14	normal	403.5	18:32	normal
4	4/8	607.3	15:15	normal	532.9	17:21	normal	433.0	18:40	normal
5	4/8	536.4	15:19	normal	600.1	17:28	normal	401.6	18:44	normal
6	4/8	637.6	15:25	normal	598.7	17:36	normal	464.6	18:48	normal
7	4/8	509.5	15:31	normal	574.3	17:45	normal	403.9	18:55	normal

5.6. Results of Young's Modulus and Poisson's Ratio

The Young's modulus and Poisson's ratio (μ) was evaluated according to ASTM C 469 [X 8] for seven samples per mix design and maturity level. The numerical results are based on 4" by 8" cylinders compressed up to 40 % of their compressive strength – measured previously for each designated maturity level (outlined in section 5.3). Each specimen was compressed and unloaded seven times at the same loading rate. The following tables outline the numerical results achieved throughout the experimental program. However, the displayed average specimen results disregard the first measurements per sample because, as explained in section 4.10, the initial test run provides proper settlement of the test equipment (compressometer/extensometer) used in this research. Therefore, the average maturity results are based on the average sample results which are derived from six test runs.

Due to equipment and delivery problems, the Poisson's ratio test could not be conducted before 28-day testing. However, this was found to be acceptable, as the application of the new Mechanistic-Empirical Pavement Design Guide does not require a Poisson's ratio value for early concrete maturity levels.

Table 5.15: 7-day Young's modulus

7-day		MIX-01		MIX-02		MIX-03	
		5/29/2007		6/5/2007		6/12/2007	
Run	Type	E	Time	E	Time	E	Time
	in/in	psi		psi		psi	
Specimen-1							
1	4/8	5239782	9:48	4205570	11:17	2965999	9:35
2	4/8	x	9:48	4606480	11:17	NA	NA
3	4/8	4443705	10:09	4409479	11:38	3144571	9:57
4	4/8	4321583	10:09	4594549	11:38	NA	9:57
5	4/8	4425342	10:30	4416403	12:31	3161210	NA
6	4/8	4238648	10:30	4570272	12:31	NA	10:17
Average		4357319		4519437		3152890	
Specimen-2							
1	4/8	4039097	10:56	4322100	16:49	3126956	10:42
2	4/8	4277553	10:56	4535499	16:49	NA	NA
3	4/8	4037430	11:16	4250934	8:47	3242436	11:54
4	4/8	4365082	11:16	4486728	8:47	3523379	11:54
5	4/8	4138919	11:37	4319111	9:12	3317673	12:14
6	4/8	4211262	11:37	4528017	9:12	3523514	12:14
Average		4206049		4424058		3401750	
Specimen-3							
1	4/8	4113577	13:36	4394872	13:25	2715716	12:40
2	4/8	4491804	13:36	4854653	13:25	NA	NA
3	4/8	4340907	13:56	4576799	13:49	3020390	13:06
4	4/8	4533992	13:56	4786008	13:49	3239336	13:06
5	4/8	4347534	14:17	4614334	14:09	3033016	13:26
6	4/8	4488285	14:17	4825423	14:09	3213020	13:26
Average		4440505		4731443		3126440	
Specimen-4							
1	4/8	4005690	14:47	4202380	14:33	3174426	13:54
2	4/8	4604592	14:47	4735348	14:33	NA	NA
3	4/8	4265120	15:16	4492560	14:53	3519219	14:15
4	4/8	4554387	15:16	4630860	14:53	3759467	14:15
5	4/8	4327594	15:37	4460501	15:14	3526987	14:35
6	4/8	4562363	15:37	4681114	15:14	3742225	14:35
Average		4462811		4600077		3636975	

Table 5.15-Continued: 7-day Young's modulus

7-day		MIX-01		MIX-02		MIX-03	
		5/29/2007		6/5/2007		6/12/2007	
Run	Type	E	Time	E	Time	E	Time
	in/in	psi		psi		psi	
Specimen-5							
1	4/8	4569034	16:00	4142395	15:41	2860462	15:01
2	4/8	4601542	16:00	4454730	15:41	NA	NA
3	4/8	4638447	16:21	4262797	16:02	3172460	13:21
4	4/8	4564386	16:21	4419164	16:02	3400597	13:21
5	4/8	4427506	11:03	4248856	16:24	3185970	15:42
6	4/8	4628410	11:03	4401505	16:24	3377293	15:42
Average		4572058		4357410		3284080	
Specimen-6							
1	4/8	3755651	11:27	NA	NA	2686650	16:05
2	4/8	4175536	11:27	NA	NA	NA	NA
3	4/8	3907753	13:08	NA	NA	NA	NA
4	4/8	4166603	13:08	NA	NA	NA	NA
5	4/8	3943624	13:30	NA	NA	3077049	11:07
6	4/8	4156828	13:30	NA	NA	3351360	11:07
Average		4070069				3214205	
Specimen-7							
1	4/8	4258664	13:57	NA	NA	2792398	9:25
2	4/8	4547496	13:57	NA	NA	NA	NA
3	4/8	4430295	14:17	NA	NA	3135310	9:45
4	4/8	4533746	14:17	NA	NA	3381515	9:45
5	4/8	4361558	14:41	NA	NA	3108387	10:22
6	4/8	4529502	14:41	NA	NA	3348686	10:22
Average		4480519				3243474	
Average		4369904		4526485		3294259	

Table 5.16: 14-day Young's modulus and Poisson's ratio

14-day		MIX-01			MIX-02			MIX-03		
		6/6/2007			6/12/2007			6/19/2007		
Run	Type	E	μ	Time	E	μ	Time	E	μ	Time
	in/in	psi	-		psi	-		psi	-	
Specimen-1										
1	4/8	4502500	NA	10:44	4272216	NA	11:51	3400000	0.18	18:48
2	4/8	4873058	NA	10:44	4666021	NA	11:51	3600000	0.19	18:50
3	4/8	4656382	NA	11:04	4420843	NA	12:12	3600000	0.19	18:53
4	4/8	4826406	NA	11:04	4579998	NA	12:12	3500000	0.19	18:56
5	4/8	4667251	NA	11:25	4463382	NA	12:33	3500000	0.17	18:59
6	4/8	4803891	NA	11:25	4715592	NA	12:33	NA	NA	NA
Average		4765398			4569167			3550000	0.19	
Specimen-2										
1	4/8	4205570	NA	11:17	4381985	NA	13:04	3500000	0.17	19:05
2	4/8	4606480	NA	11:17	4806479	NA	13:04	3600000	0.18	19:07
3	4/8	4409479	NA	11:38	4562285	NA	13:24	3600000	0.18	19:09
4	4/8	4594549	NA	11:38	4751627	NA	13:24	3600000	0.18	19:12
5	4/8	4420161	NA	12:31	4592052	NA	14:07	3600000	0.18	19:13
6	4/8	4570272	NA	12:31	4753181	NA	14:07	NA	NA	NA
Average		4520188			4693125			3600000	0.18	
Specimen-3										
1	4/8	4501230	NA	1:00	4312428	NA	14:31	2900000	0.14	19:19
2	4/8	Failed	NA		4781966	NA	14:31	3000000	0.15	19:21
3	4/8	4250934	NA	8:47	4461584	NA	15:09	3000000	0.15	19:23
4	4/8	4486728	NA	8:47	4734591	NA	15:09	3000000	0.15	19:25
5	4/8	4322100	NA	4:49	4432377	NA	15:38	2900000	0.14	19:28
6	4/8	4535499	NA	4:49	4713335	NA	15:38	NA	NA	NA
Average		4398815			4624771			2975000	0.15	
Specimen-4										
1	4/8	4394872	NA	1:25	5092017	NA	16:12	3400000	0.17	19:34
2	4/8	4854643	NA	1:25	4392990	NA	16:12	3600000	0.18	19:36
3	4/8	4576799	NA	1:49	4375292	NA	8:42	3600000	0.19	19:38
4	4/8	4786008	NA	1:49	4616962	NA	8:42	3500000	0.19	19:40
5	4/8	4614224	NA	2:09	4458525	NA	9:03	3500000	0.19	19:42
6	4/8	4825423	NA	2:09	4606989	NA	9:03	NA	NA	NA
Average		4731419			4490152			3550000	0.19	

Table 5.16-Continued: 14-day Young's modulus and Poisson's ratio

14-day		MIX-01			MIX-02			MIX-03		
		6/6/2007			6/12/2007			6/19/2007		
Run	Type	E	μ	Time	E	μ	Time	E	μ	Time
	in/in	psi	-		psi	-		psi	-	
Specimen-5										
1	4/8	4202380	NA	2:33	4417793	NA	9:30	3600000	0.22	19:51
2	4/8	4735348	NA	2:33	4742569	NA	9:30	3600000	0.23	19:53
3	4/8	4492560	NA	2:53	4535123	NA	9:51	3600000	0.23	19:54
4	4/8	4630860	NA	2:53	4698059	NA	9:51	3600000	0.23	19:56
5	4/8	4460501	NA	3:14	4423513	NA	9:57	3600000	0.23	19:58
6	4/8	4684787	NA	3:14	4653044	NA	9:57	NA	NA	NA
Average		4600811			4610461			3600000	0.23	
Specimen-6										
1	4/8	4142395	NA	3:41	4601625	NA	10:23	3500000	0.19	20:04
2	4/8	4454730	NA	3:41	4668457	NA	10:23	3600000	0.19	20:06
3	4/8	4262797	NA	4:02	4546214	NA	10:44	3600000	0.19	20:08
4	4/8	4419164	NA	4:02	4691192	NA	10:44	3600000	0.19	20:09
5	4/8	4248856	NA	4:25	4583161	NA	11:05	3600000	0.19	20:11
6	4/8	4401505	NA	4:25	4675646	NA	11:05	NA	NA	NA
Average		4357410			4632934			3600000	0.19	
Specimen-7										
1	4/8	4470625	NA	9:37	4317396	NA	11:34	3200000	0.17	20:17
2	4/8	4835052	NA	9:37	4691379	NA	11:34	3400000	0.18	20:19
3	4/8	4665588	NA	9:58	4435606	NA	11:55	3400000	0.18	20:21
4	4/8	4862836	NA	9:58	4654398	NA	11:55	3400000	0.18	20:23
5	4/8	4693244	NA	10:18	4461520	NA	12:15	3400000	0.18	20:25
		4844050	NA	10:18	4677428	NA	12:15	NA	NA	NA
Average		4780154			4584066			3400000	0.18	
Average		4593457			4597535			3467857		

Table 5.17: 28-day Young's modulus and Poisson's ratio

28-day		MIX-01			MIX-02			MIX-03		
		6/19/2007			6/26/2007			7/3/2007		
Run	Type	E	μ	Time	E	μ	Time	E	μ	Time
	in/in	psi	-		psi	-		psi	-	
Specimen-1										
1	4/8	4500000	0.26	18:01	3700000	0.20	16:11	3750000	0.19	13:42
2	4/8	4600000	0.26	18:04	3750000	0.21	16:16	3900000	0.20	13:44
3	4/8	4500000	0.27	18:07	3800000	0.22	16:19	3850000	0.20	13:47
4	4/8	4500000	0.27	18:10	3800000	0.22	16:22	3900000	0.20	13:50
5	4/8	4600000	0.27	18:13	3750000	0.22	16:25	3850000	0.20	13:53
Average		4550000	0.27		3775000			3875000	0.20	
Specimen-2										
1	4/8	4500000	0.24	18:21	4150000	0.22	16:34	3700000	0.18	14:11
2	4/8	4600000	0.24	18:24	4100000	0.22	16:37	3750000	0.19	14:15
3	4/8	4500000	0.24	18:28	4050000	0.23	16:40	3750000	0.18	14:18
4	4/8	4500000	0.24	18:32	4050000	0.23	16:43	3750000	0.18	14:22
5	4/8	4500000	0.24	18:35	4050000	0.23	16:46	3750000	0.18	14:25
Average		4525000	0.24		4062500			3750000	0.18	
Specimen-3										
1	4/8	4000000	0.28	15:58	4100000	0.22	16:56	3750000	0.20	14:35
2	4/8	4100000	0.26	16:02	4150000	0.23	16:59	3950000	0.20	14:37
3	4/8	4100000	0.27	16:06	4100000	0.22	17:03	3950000	0.20	14:40
4	4/8	4100000	0.28	16:09	4150000	0.23	17:06	3900000	0.20	14:42
5	4/8	4100000	0.28	16:13	4150000	0.22	17:09	3900000	0.18	14:45
Average		4100000	0.27		4137500			3925000	0.20	
Specimen-4										
1	4/8	4200000	0.24	16:27	4300000	0.25	17:17	3600000	0.19	14:54
2	4/8	4200000	0.24	16:29	4400000	0.25	17:19	3800000	0.20	14:57
3	4/8	4200000	0.24	16:32	4400000	0.25	17:22	3800000	0.20	14:59
4	4/8	4200000	0.23	16:37	4400000	0.25	17:25	3800000	0.20	15:02
5	4/8	4100000	0.23	16:40	4400000	0.25	17:28	3750000	0.19	15:04
Average		4175000	0.24		4400000			3787500	0.20	

Table 5.17: 28-day Young's modulus and Poisson's ratio

28-day		MIX-01			MIX-02			MIX-03		
		6/19/2007			6/26/2007			7/3/2007		
Run	Type	E	μ	Time	E	μ	Time	E	μ	Time
	in/in	psi	-		psi	-		psi	-	
Specimen-5										
1	4/8	4700000	0.25	16:54	4300000	0.27	17:36	3550000	0.20	15:12
2	4/8	4800000	0.26	16:57	4450000	0.27	17:38	3650000	0.20	15:14
3	4/8	4600000	0.25	17:02	4450000	0.27	17:41	3650000	0.20	15:17
4	4/8	4700000	0.26	17:06	4450000	0.26	17:44	3650000	0.20	15:19
5	4/8	4600000	0.25	17:10	4500000	0.28	17:47	3600000	0.20	15:21
Average		4675000	0.26		4462500			3637500	0.20	
Specimen-6										
1	4/8	4300000	0.26	17:17	4700000	0.24	17:55	3500000	0.19	15:28
2	4/8	4400000	0.25	17:22	4800000	0.25	17:58	3650000	0.20	15:30
3	4/8	4400000	0.26	17:25	4850000	0.25	18:01	3650000	0.20	15:32
4	4/8	4400000	0.26	17:28	4850000	0.25	18:04	3650000	0.20	15:35
5	4/8	4400000	0.26	17:31	4850000	0.25	18:06	3650000	0.20	15:37
Average		4400000	0.26		4837500			3650000	0.20	
Specimen-7										
1	4/8	4400000	0.25	17:41	4850000	0.27	18:15	3050000	0.16	15:42
2	4/8	4500000	0.25	17:44	4850000	0.27	18:18	3150000	0.16	15:45
3	4/8	4500000	0.26	17:47	4850000	0.27	18:21	3150000	0.16	15:47
4	4/8	4600000	0.26	17:50	4850000	0.27	18:24	3100000	0.16	15:49
5	4/8	4500000	0.26	17:53	4850000	0.27	18:27	3100000	0.16	15:51
Average		4525000	0.26		4850000			3125000	0.16	
Average		4421429			4167500			3678571		

Table 5.18: 90-day Young's modulus and Poisson's ratio

90-day		MIX-01			MIX-02			MIX-03		
		8/20/2007			8/27/2007			9/3/2007		
Run	Type	E	μ	Time	E	μ	Time	E	μ	Time
	in/in	psi	-		psi	-		psi	-	
Specimen-1										
1	4/8	4000000	0.21	17:29	4650000	0.21	12:28	3850000	0.21	16:02
2	4/8	3900000	0.22	17:32	4400000	0.22	12:31	3900000	0.21	16:05
3	4/8	3950000	0.23	17:35	4550000	0.22	12:35	3900000	0.21	16:07
4	4/8	3950000	0.23	17:39	4500000	0.22	12:38	3850000	0.21	16:09
5	4/8	3800000	0.22	17:43	4450000	0.22	12:41	3850000	0.22	16:12
Average		3900000	0.23		4475000			3875000	0.21	
Specimen-2										
1	4/8	4600000	0.24	17:49	5500000	0.30	12:51	3750000	0.20	16:18
2	4/8	4700000	0.26	17:52	5400000	0.31	12:56	3950000	0.20	16:20
3	4/8	4650000	0.26	17:55	5300000	0.31	12:59	3900000	0.21	16:23
4	4/8	4600000	0.25	18:00	5400000	0.31	13:03	3900000	0.21	16:25
5	4/8	4550000	0.26	18:04	5350000	0.31	13:07	3900000	0.21	16:28
Average		4625000	0.26		5362500			3912500	0.21	
Specimen-3										
1	4/8	3700000	0.20	18:11	4150000	0.23	14:47	3900000	0.22	16:35
2	4/8	3750000	0.22	18:14	4250000	0.23	14:50	4100000	0.22	16:38
3	4/8	3750000	0.22	18:17	4250000	0.24	14:54	4150000	0.22	16:40
4	4/8	3700000	0.22	18:20	4250000	0.24	14:57	4150000	0.23	16:43
5	4/8	3700000	0.22	18:23	4250000	0.23	15:01	4100000	0.22	16:45
Average		3725000	0.22		4250000			4125000	0.22	
Specimen-4										
1	4/8	4150000	0.20	18:31	5050000	0.26	15:17	3900000	0.22	16:51
2	4/8	4100000	0.20	18:35	5100000	0.27	15:21	4100000	0.22	16:54
3	4/8	4100000	0.21	18:38	5100000	0.27	15:24	4100000	0.22	16:59
4	4/8	4100000	0.20	18:41	5050000	0.27	15:27	4050000	0.22	17:02
5	4/8	4100000	0.20	18:44	5050000	0.27	15:31	4050000	0.22	17:05
Average		4100000	0.20		5075000			4075000	0.22	

Table 5.18: 90-day Young's modulus and Poisson's ratio

90-day		MIX-01			MIX-02			MIX-03		
		8/20/2007			8/27/2007			9/3/2007		
Run	Type	E	μ	Time	E	μ	Time	E	μ	Time
	in/in	psi	-		psi	-		psi	-	
Specimen-5										
1	4/8	3800000	0.19	18:53	5150000	0.25	15:39	4150000	0.21	17:12
2	4/8	3850000	0.20	18:57	5250000	0.26	15:42	4250000	0.21	17:14
3	4/8	3800000	0.20	19:00	5200000	0.26	15:45	4250000	0.21	17:17
4	4/8	3800000	0.19	19:03	5200000	0.26	15:48	4250000	0.20	17:20
5	4/8	3800000	0.20	19:06	5200000	0.26	15:52	4250000	0.20	17:22
Average		3812500	0.20		5212500			4250000	0.21	
Specimen-6										
1	4/8	4200000	0.20	19:14	5100000	0.28	15:59	3650000	0.20	17:29
2	4/8	4100000	0.20	19:19	5200000	0.29	16:02	3850000	0.21	17:32
3	4/8	4100000	0.21	19:22	5150000	0.29	16:05	3950000	0.21	17:35
4	4/8	4100000	0.21	19:25	5150000	0.29	16:08	3900000	0.21	17:38
5	4/8	4050000	0.21	19:29	5150000	0.29	16:11	3900000	0.21	17:40
Average		4087500	0.21		5162500			3900000	0.21	
Specimen-7										
1	4/8	500000	0.29	19:41	4700000	0.28	16:19	3800000	0.22	17:47
2	4/8	5050000	0.29	19:45	4750000	0.28	16:22	4000000	0.22	17:50
3	4/8	4950000	0.29	19:48	4850000	0.27	16:25	4000000	0.22	17:52
4	4/8	5000000	0.29	19:51	4800000	0.28	16:29	4000000	0.22	17:54
5	4/8	4950000	0.29	19:54	4800000	0.28	16:32	4000000	0.22	17:57
Average		4987500	0.29		4800000			4000000	0.22	
Average		4176786			4875000			4019643		

5.7. Results of Coefficient of Thermal Expansion

The coefficient of thermal expansion was measured using a commercially available test unit designed to follow AASHTO TP 60 [X 14]. The following tables were created to present the numerical findings achieved throughout the experimental research. The outlined average values are based on seven concrete samples per mix design tested on seven successive days.

Table 5.19: 7-day coefficient of thermal expansion

7-day		CTE								
		MIX-01			Mix-02			Mix-03		
No.	Type	Date	Day	CTE	Date	Day	CTE	Date	Day	CTE
				µm/m/C			µm/m/C			µm/m/C
1	4/8	5/30/2007	8	10.52	6/9/2007	11	10.13	6/13/2007	8	9.30
2	4/8	5/31/2007	9	10.41	6/10/2007	12	10.10	6/14/2007	9	9.32
3	4/8	5/31/2007	9	10.47	6/11/2007	13	10.13	6/15/2007	10	9.35
4	4/8	6/3/2007	12	10.55	6/12/2007	14	10.12	6/16/2007	11	9.22
5	4/8	6/4/2007	13	10.36	6/14/2007	15	10.14	6/17/2007	12	9.30
6	4/8	6/5/2007	14	10.27	6/16/2007	17	10.16	6/18/2007	13	9.29
7	4/8	6/6/2007	14	10.51	6/18/2007	18	failed	6/19/2007	14	9.13
Average				10.44			10.13			9.27

Table 5.20: 28-day coefficient of thermal expansion

28-day		CTE								
		MIX-01			Mix-02			Mix-03		
No.	Type	Date	Day	CTE	Date	Day	CTE	Date	Day	CTE
				µm/m/C			µm/m/C			µm/m/C
1	4/8	6/20/2007	29	10.58	6/28/2007	30	11.70	7/4/2007	29	10.79
2	4/8	6/21/2007	30	10.74	6/29/2007	31	11.91	7/5/2007	30	10.84
3	4/8	6/22/2007	31	11.86	6/30/2007	32	11.83	7/6/2007	31	10.83
4	4/8	6/23/2007	32	12.11	6/30/2007	32	12.06	7/7/2007	32	10.64
5	4/8	6/24/2007	33	12.04	7/1/2007	33	11.87	7/8/2007	33	10.85
6	4/8	6/25/2007	34	12.07	7/2/2007	34	12.16	7/9/2007	34	failed
7	4/8	6/26/2007	35	12.20	7/3/2007	35	11.76	7/10/2007	35	failed
Average				11.66			11.90			10.79

Table 5.21: 49-day coefficient of thermal expansion (re-used specimens)

49-day		CTE								
		MIX-01			Mix-02			Mix-03		
No.	Type	Date	Day	CTE	Date	Day	CTE	Date	Day	CTE
				µm/m/C			µm/m/C			µm/m/C
1	4/8	7/11/2007	50	12.01	7/18/2007	50	failed	7/25/2007	50	10.62
2	4/8	7/12/2007	51	12.06	7/19/2007	51	failed	7/26/2007	51	10.68
3	4/8	7/13/2007	52	12.10	7/20/2007	52	failed	7/27/2007	52	10.77
4	4/8	7/14/2007	53	12.14	7/21/2007	53	failed	7/28/2007	53	10.74
5	4/8	7/15/2007	54	12.16	7/22/2007	54	failed	7/29/2007	54	10.58
6	4/8	7/16/2007	55	12.11	7/23/2007	55	failed	7/30/2007	55	10.72
7	4/8	7/18/2007	57	12.05	7/24/2007	56	12.09	7/31/2007	56	10.72
Average				12.09			12.09			10.69

Table 5.22: 70-day coefficient of thermal expansion (re-used specimens)

70-day		CTE								
		MIX-01			Mix-02			Mix-03		
No.	Type	Date	Day	CTE	Date	Day	CTE	Date	Day	CTE
				µm/m/C			µm/m/C			µm/m/C
1	4/8	8/1/2007	71	12.26	8/8/2007	71	11.96	8/15/2007	71	10.78
2	4/8	8/2/2007	72	12.27	8/10/2007	73	12.07	8/16/2007	72	10.70
3	4/8	8/3/2007	73	12.08	8/11/2007	74	12.07	8/17/2007	73	10.71
4	4/8	8/4/2007	74	11.95	8/11/2007	74	12.40	8/18/2007	74	10.70
5	4/8	8/5/2007	75	12.04	8/12/2007	75	12.20	8/19/2007	76	10.66
6	4/8	8/6/2007	76	12.11	8/13/2007	76	12.13	8/20/2007	77	10.54
7	4/8	8/7/2007	77	11.96	8/14/2007	77	12.13	8/21/2007	78	10.85
Average				12.10			12.14			10.71

Table 5.23: 90-day coefficient of thermal expansion

90-day		CTE								
		MIX-01			Mix-02			Mix-03		
No.	Type	Date	Day	CTE	Date	Day	CTE	Date	Day	CTE
				µm/m/C			µm/m/C			µm/m/C
1	4/8	8/23/2007	93	12.27	8/29/2007	92	12.26	9/5/2007	92	10.89
2	4/8	8/23/2007	93	12.14	8/30/2007	93	12.24	9/6/2007	93	10.53
3	4/8	8/24/2007	94	12.50	8/31/2007	94	12.35	9/7/2007	94	10.82
4	4/8	8/26/2007	96	12.21	9/1/2007	95	12.44	9/8/2007	95	10.71
5	4/8	8/27/2007	97	12.10	9/2/2007	96	12.26	9/9/2007	96	10.82
6	4/8	8/27/2007	97	12.16	9/3/2007	97	12.31	9/10/2007	97	10.72
7	4/8	8/28/2007	98	12.28	9/4/2007	98	12.24	9/11/2007	98	10.84
Average				12.24			12.30			10.76

Table 5.24: 111-day coefficient of thermal expansion (re-used specimens)

111-day		CTE								
		MIX-01			Mix-02			Mix-03		
No.	Type	Date	Day	CTE	Date	Day	CTE	Date	Day	CTE
				µm/m/C			µm/m/C			µm/m/C
1	4/8	9/12/2007	113	12.35	9/19/2007	113	12.25	9/27/2007	113	10.92
2	4/8	9/13/2007	114	12.28	9/21/2007	115	12.30	9/28/2007	114	10.88
3	4/8	9/14/2007	115	12.25	9/22/2007	116	12.55	9/29/2007	115	10.79
4	4/8	9/16/2007	117	12.08	9/23/2007	117	12.34	9/29/2007	115	10.77
5	4/8	9/17/2007	118	12.21	9/24/2007	118	12.26	9/30/2007	116	10.66
6	4/8	9/18/2007	119	12.23	9/25/2007	119	12.38	10/1/2007	117	10.82
7	4/8	9/18/2007	119	12.25	9/26/2007	120	12.29	10/2/2007	118	10.69
Average				12.24			12.34			10.79

CHAPTER 6: MATERIAL RESEARCH - ANALYSIS OF EXPERIMENTAL RESULTS

6.1. Introduction

Chapter VI aims to analyze the test results derived from experimental work. It interprets findings drawn from analytical graphs and figures to visualize and identify differences in material properties.

Firstly, each property will be studied independently to derive an individual understanding of that material characteristic. Charts will be developed to visualize (1) test results for each sample, (2) mean values of test range, and (3) standard deviation within the data series under observation. These mathematical properties will be determined based on the maturity (7-day, 14-day, 28-day, and 90-day) level of concrete. Single test results will be indicated through columns, while average values are represented by horizontal lines. The standard deviation is graphically displayed by vertical lines on top of each mix design's individual sample columns. After this has been done for each test date, a graphical comparison study will be initiated. Based on the mean values for each maturity level, a comprehensive growth rate curve will be generated for each mix design, representing an overall performance of the material property in question. After interpretation of single test results, a substantial analysis of mix design performance will follow. After all, the main goal is the implementation of the new Mechanistic-Empirical Pavement Design Guide. Therefore, the relevance of material properties and their numerical values have to be determined.

6.2. Analysis of Compressive Strength

This section aims to visualize the test results of compressive strength measurement to properly evaluate the three different Florida pavement concrete mix designs. The following four figures represent the four maturity levels (7, 14, 28, 90 days) requested by the new Mechanistic-Empirical Pavement Design Guide.

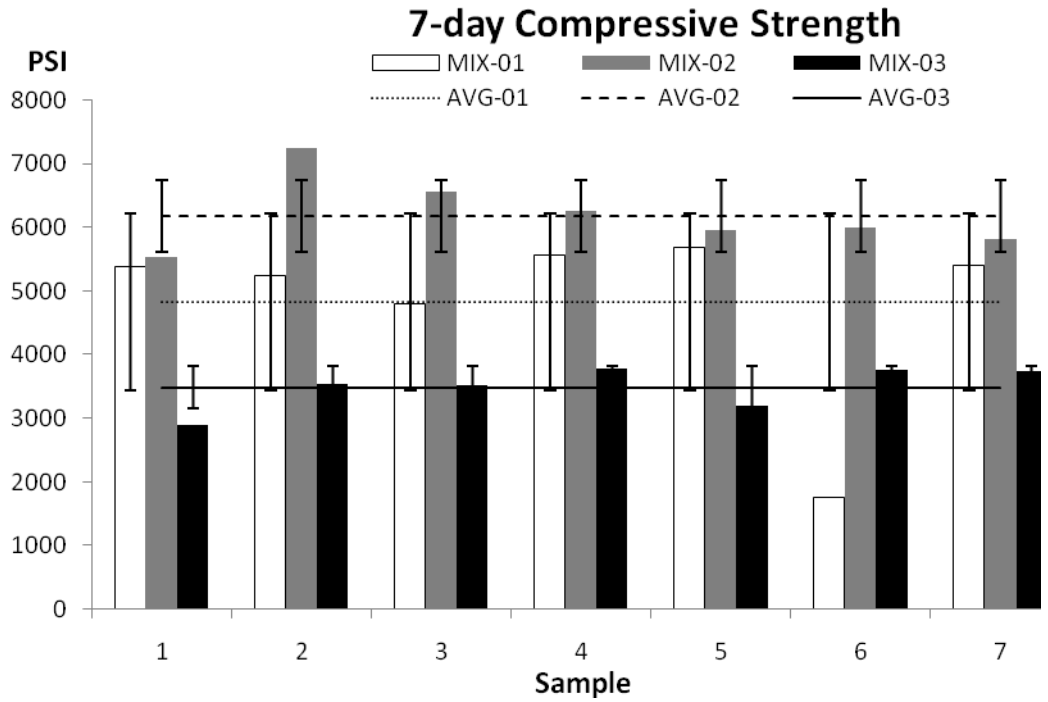

Figure 6.1: 7-day compressive strength

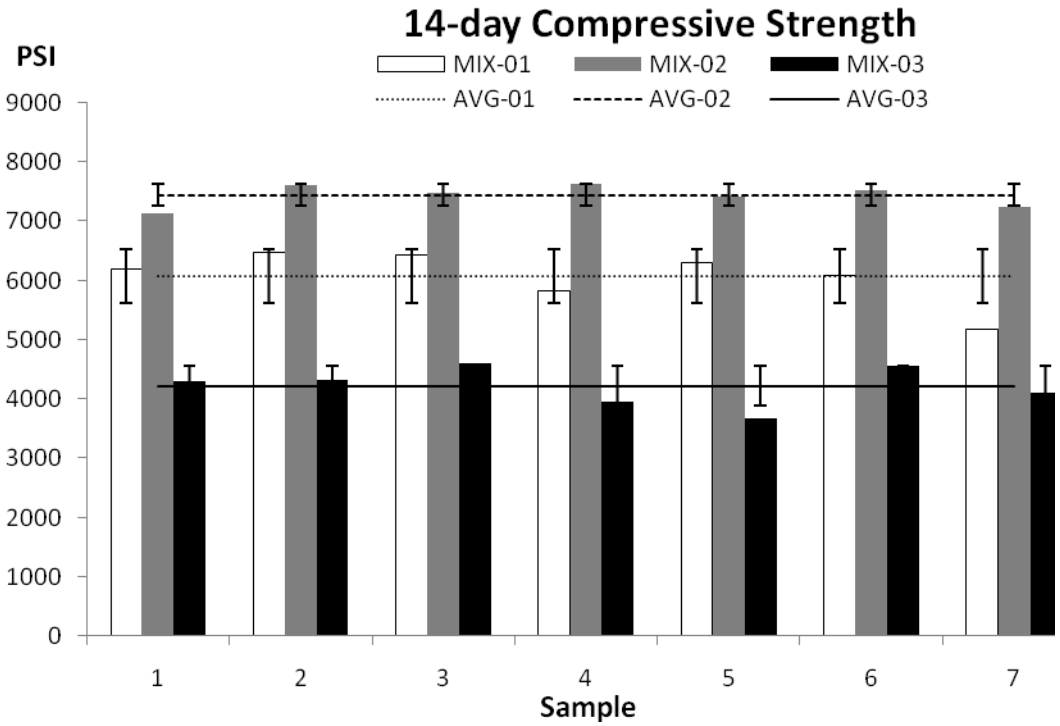

Figure 6.2: 14-day compressive strength

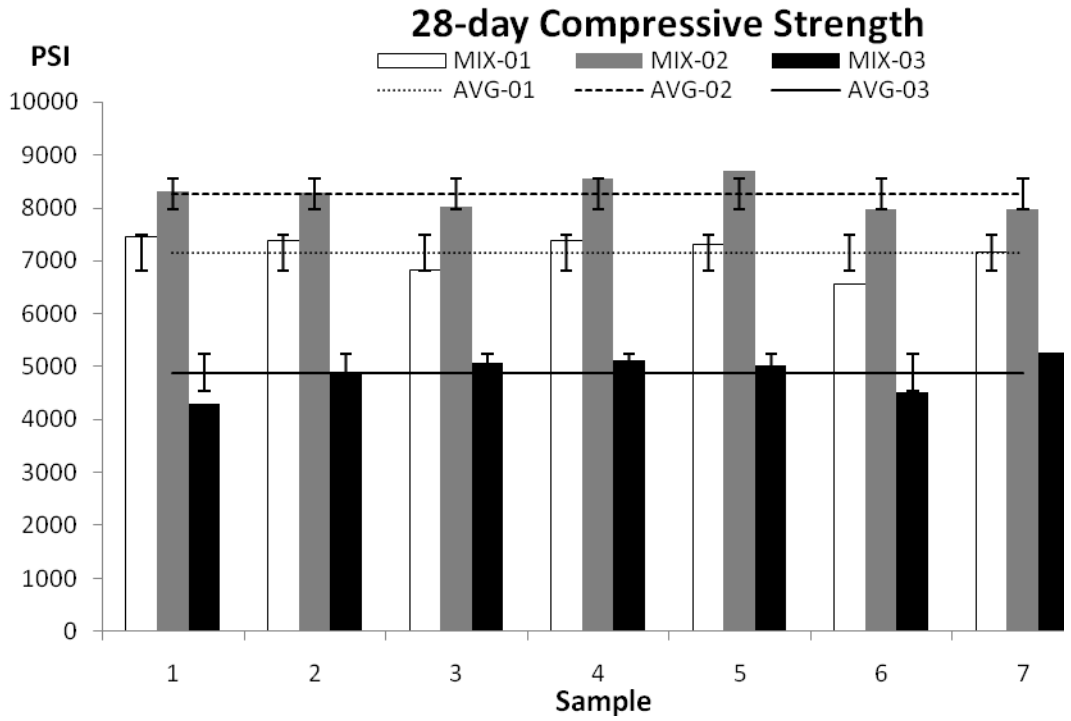

Figure 6.3: 28-day compressive strength

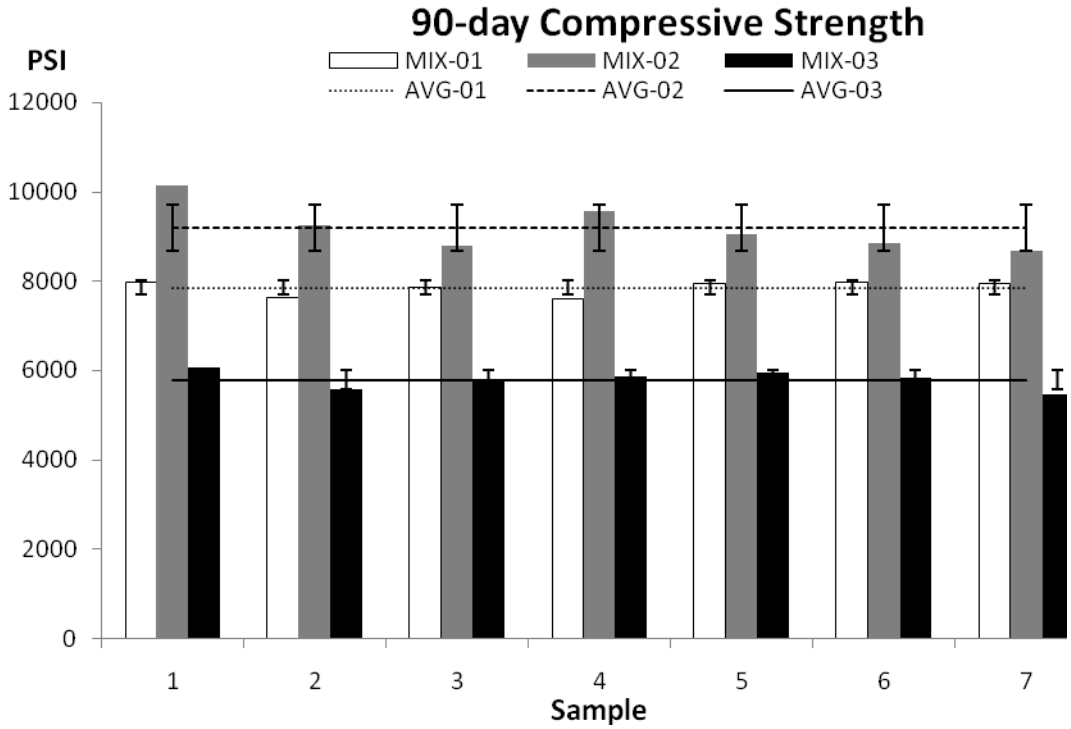

Figure 6.4: 90-day compressive strength

It can be seen that the highest 7-day compressive strength was measured for MIX-02 whereas the lowest strength was determined for MIX-03. However, the standard deviation at 7-day testing was calculated to be very high for MIX-01 (1385 psi) but very low for MIX-03.

After 14 days, MIX-02 shows highest compressive strength results and MIX-03 the lowest. The standard deviation at this maturity level presents very low values for MIX-02 (185 psi).

MIX-02 was measured with the highest results and MIX-03 with the lowest for concrete's reference maturity (28-day). The standard deviation for MIX-01 and MIX-03 are comparable showing values of 337psi and 348 psi, respectively. However, the lowest deviation at 28-day testing was derived for MIX-02.

For 90-day testing, MIX-02 attains the highest compressive strength (again) and MIX-03 shows the smallest values. The standard deviation shows a very low value for MIX-01 (161 psi) and a high significance for MIX-02 (518 psi).

In general, it can be observed that the test results within each maturity level are very consistent. The standard deviations ranging around the mean values of the mix design do not interfere with each other, and therefore show the reliability of test results. Notice that this is not the case for 7-day testing. However, it is emphasized that the deviation of test results constantly decreased with increasing concrete maturity. Consequently, the high standard deviation at 7-day testing is tracked back to the behavior of young concrete.

The following graph in Figure 6.5 represents the average values of compressive strength measurement derived from the horizontal lines shown in the diagrams above.

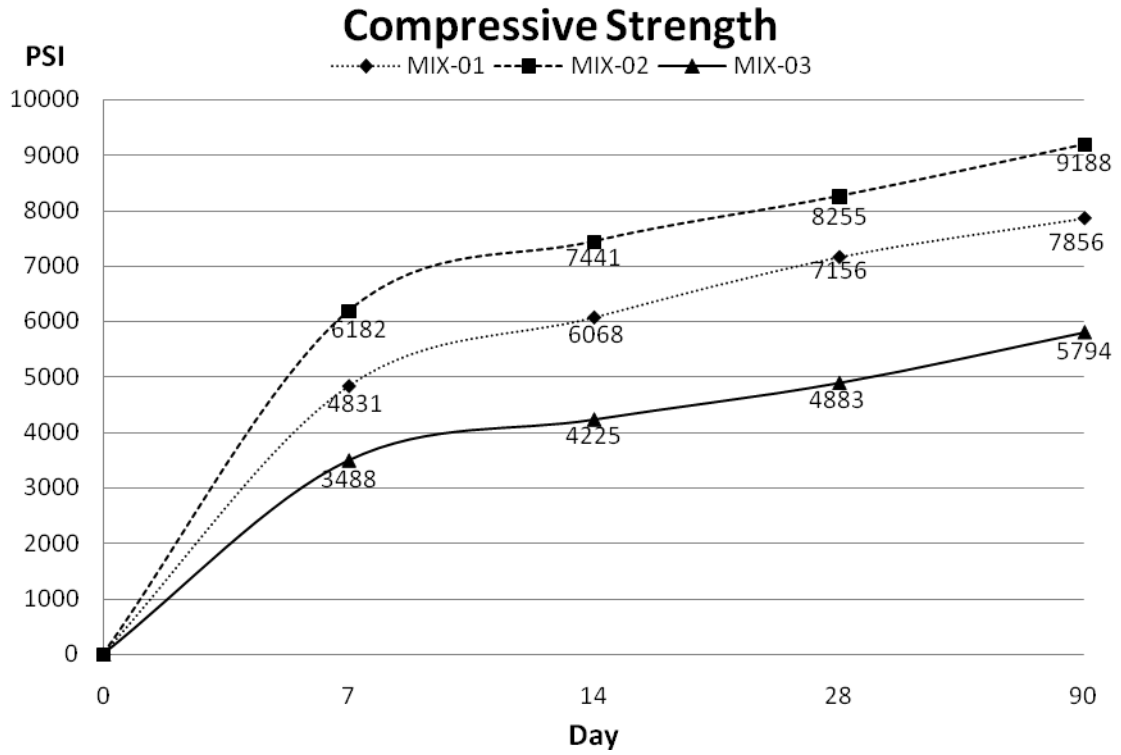

Figure 6.5: Compressive strength comparison

It can be seen that the compressive strength increases over time for all three mix designs with similar strength growth for MIX-01 and MIX-02, whereas MIX-03 gains compressive strength slower than the other mixes. In general, it can be stated that all concrete mixtures increase their target strength tremendously (starting at 7-day results); MIX-01 possesses 135 % of its predicted compressive strength, MIX-02 attains 248 %, and MIX-03 reaches 140 % of its designated target strength at 28-day testing. Overall, MIX-03 is the mix design with the lowest strength performance and MIX-02 is the concrete mixture that shows the highest compressive strength values within the scope of this study. MIX-02 may be considered high strength concrete.

6.3. Analysis of Flexural Strength

The following graphs depict the test results for flexural strength analysis. Figure 6.6 shows 7-day results for three data points and Figure 6.7 and Figure 6.8 display five test results for 28-day and 90-day testing, respectively.

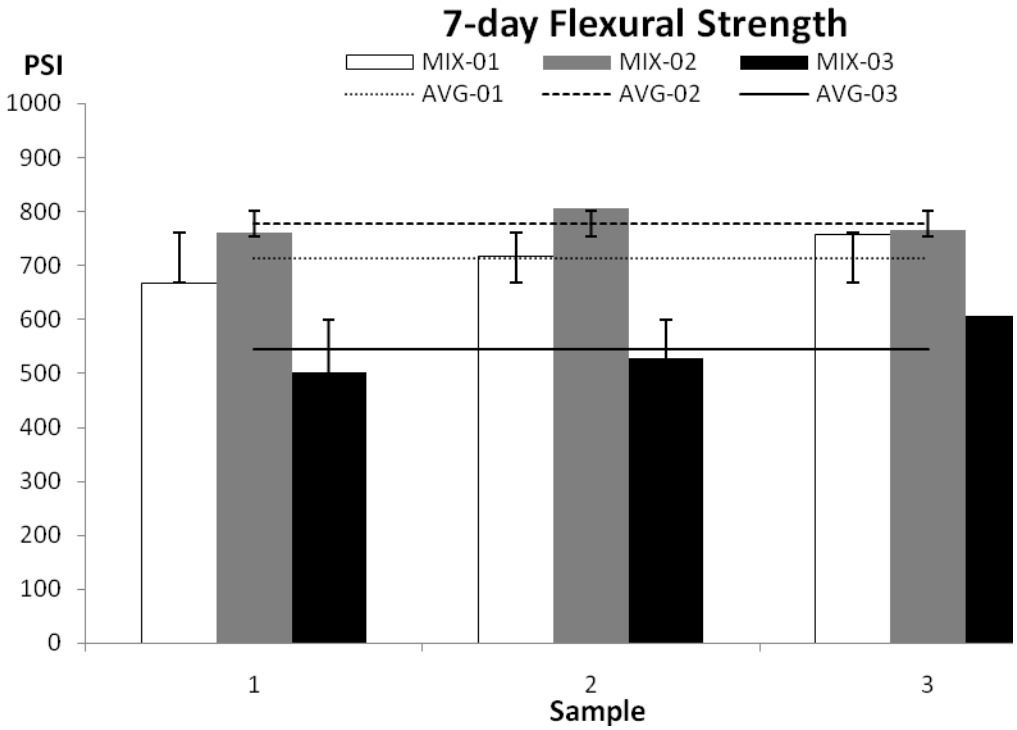

Figure 6.6: 7-day flexural strength

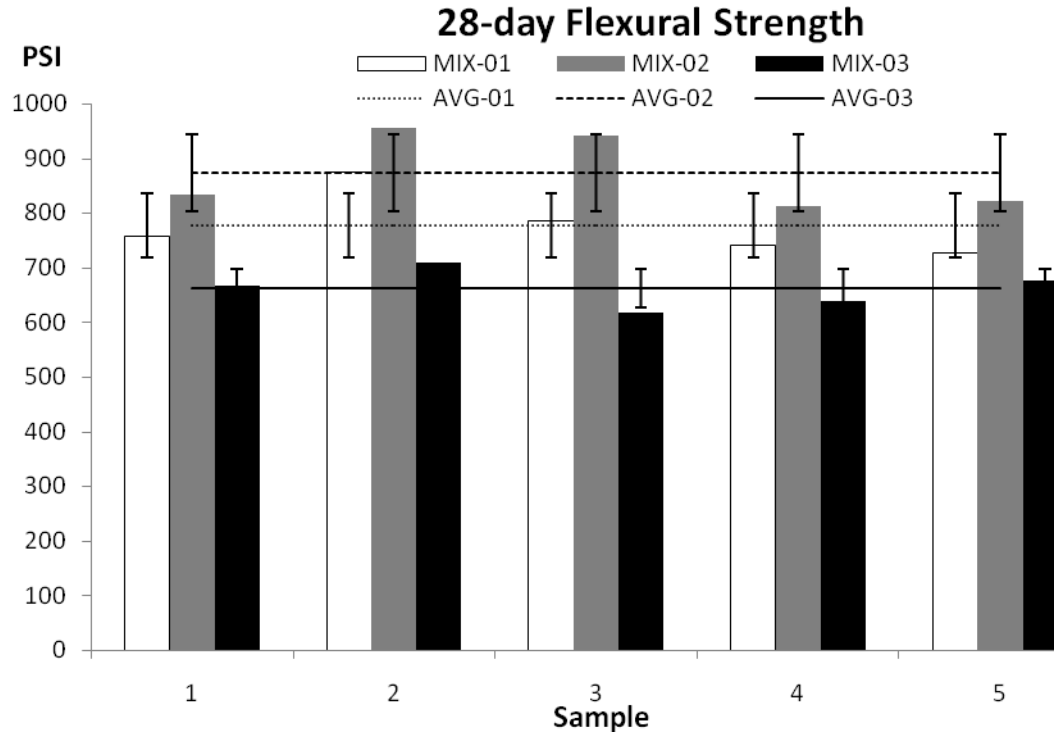

Figure 6.7: 28-day flexural strength

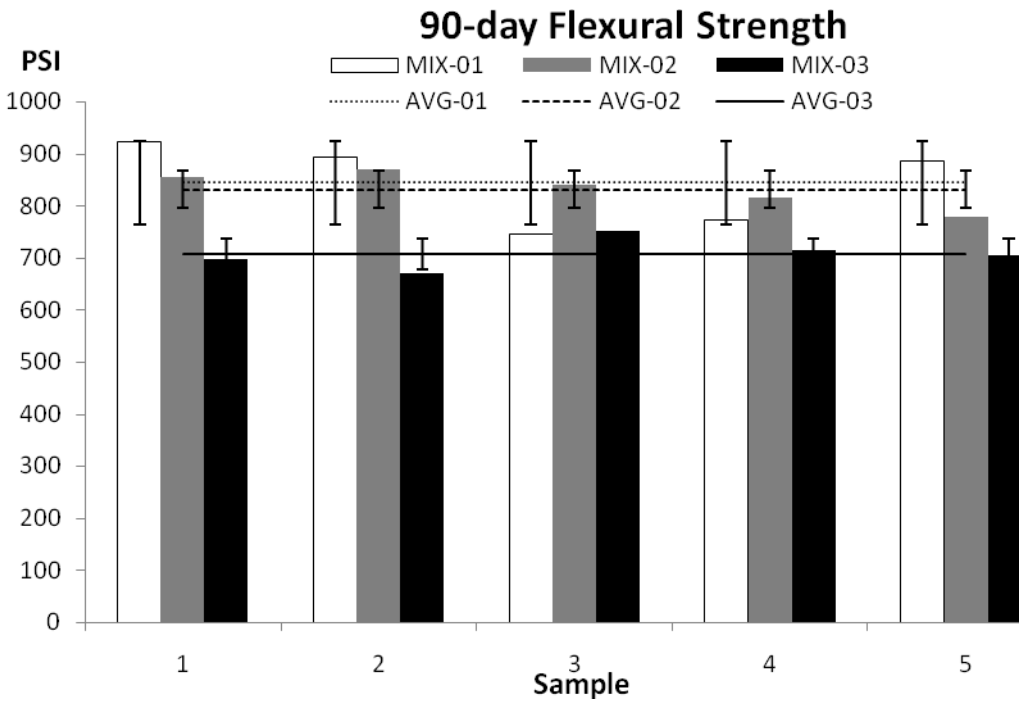

Figure 6.8: 90-day flexural strength

From Figure 6.6 it can be observed that the flexural strength at 7 days shows highest results for MIX-02 and lowest for MIX-03. The standard deviation of 25 psi is remarkably low for MIX-02.

At 28-day testing, MIX-02 possesses the highest flexural strength whereas MIX-03 consistently shows the lowest results. MIX-03 presents a low standard deviation with a numerical result of 35 psi.

The flexural strength at 90-day testing shows the lowest values for MIX-03 (again) and the highest results for MIX-01 while the average values of MIX-01 and MIX-02 are very comparable. Nevertheless, MIX-03 possesses the smallest standard deviation after 90 days with 29 psi.

In general, it can be observed that the deviation increases over time for MIX-01, fluctuates for MIX-02, and decreases over time for MIX-03.

The graph below displays the flexural strength derived from the average values outlined in the figures above to visualize the behavior of the property over time for each concrete mixture.

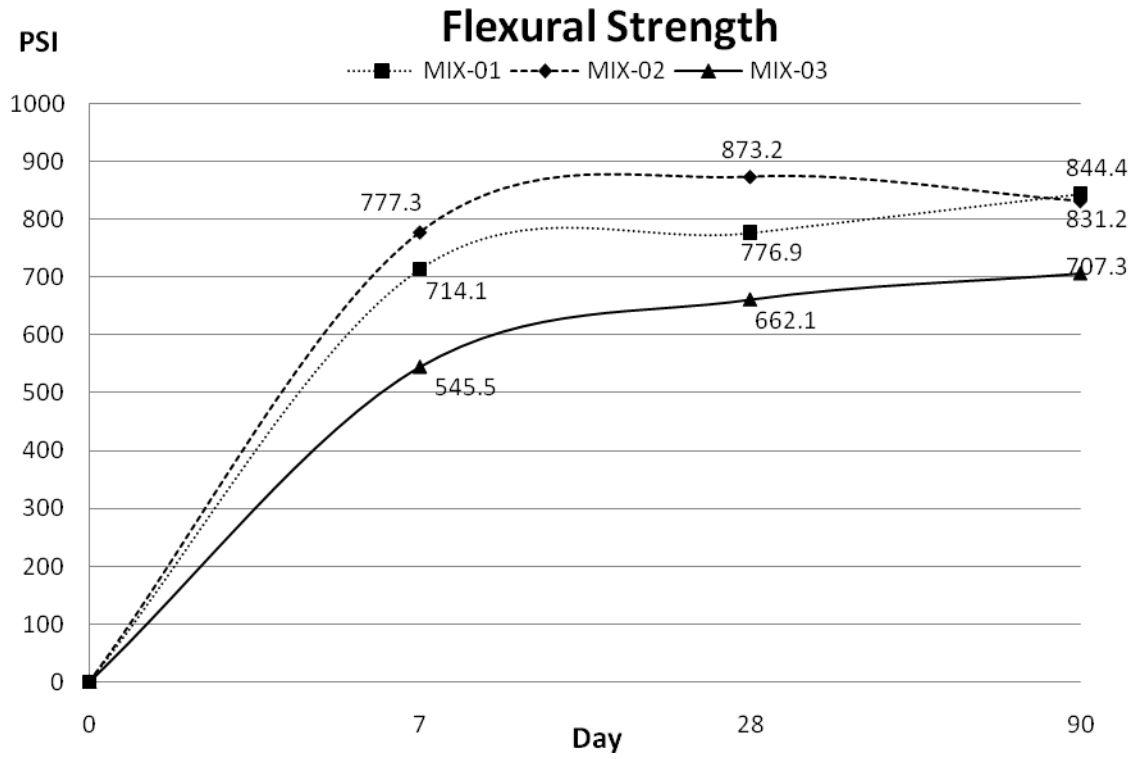

Figure 6.9: Flexural strength comparison

Although MIX-02 loses (average) flexural strength from 28-day to 90-day testing, the graph in Figure 6.9 closely follows the behavior of compressive strength outlined in Figure 6.5. Therefore, it can be stated that MIX-03 is the (relative) weakest mixture under comparison and MIX-02 the strongest.

According to ACI committee 435: $f_{fl} = f'_c \frac{3}{\sqrt{f'_c}}$ to $f'_c \frac{12}{\sqrt{f'_c}}$

$f'_{c\ target}$ = 3000 psi (MIX-02 and MIX-03)→ $f_{fl\ MIX\text{-}01}$ = 274 psi to 657 psi

$f'_{c\ target}$ = 4500 psi (MIX-01)→ $f_{fl\ MIX\text{-}02}$ = 335 psi to 805 psi

$f'_{c\ MIX-01}$ = 6068 psi → $f_{fl\ MIX-01}$ = 389 psi to 935 psi

$f'_{c\ MIX-02}$ = 7441 psi → $f_{fl\ MIX-02}$ = 432 psi to 1035 psi

$f'_{c\ MIX-03}$ = 4225 psi → $f_{fl\ MIX-03}$ = 325 psi to 780 psi

MIX-01 satisfactorily fulfills ACI expectation. MIX-02 exceeds ACI expectation for its target strength but conforms for the measured compressive strength; the same is true for MIX-03. Therefore, it can be noted that the ACI flexural strength prediction applies to the mix designs in this evaluation.

6.4. Analysis of Splitting Tensile Strength

This sub-section visualizes the numerical test results of splitting tensile strength for each maturity level and mix design. Figure 6.10 outlines 28-day test results and Figure 6.11 shows 90-day test data.

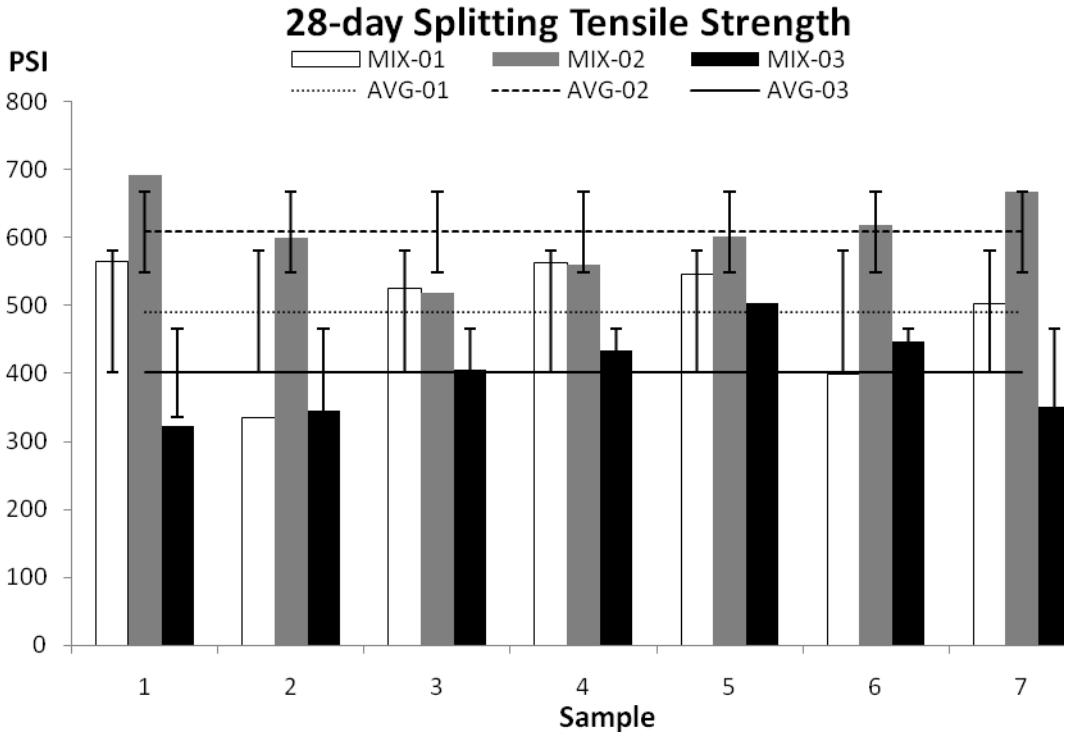

Figure 6.10: 28-day splitting tensile strength

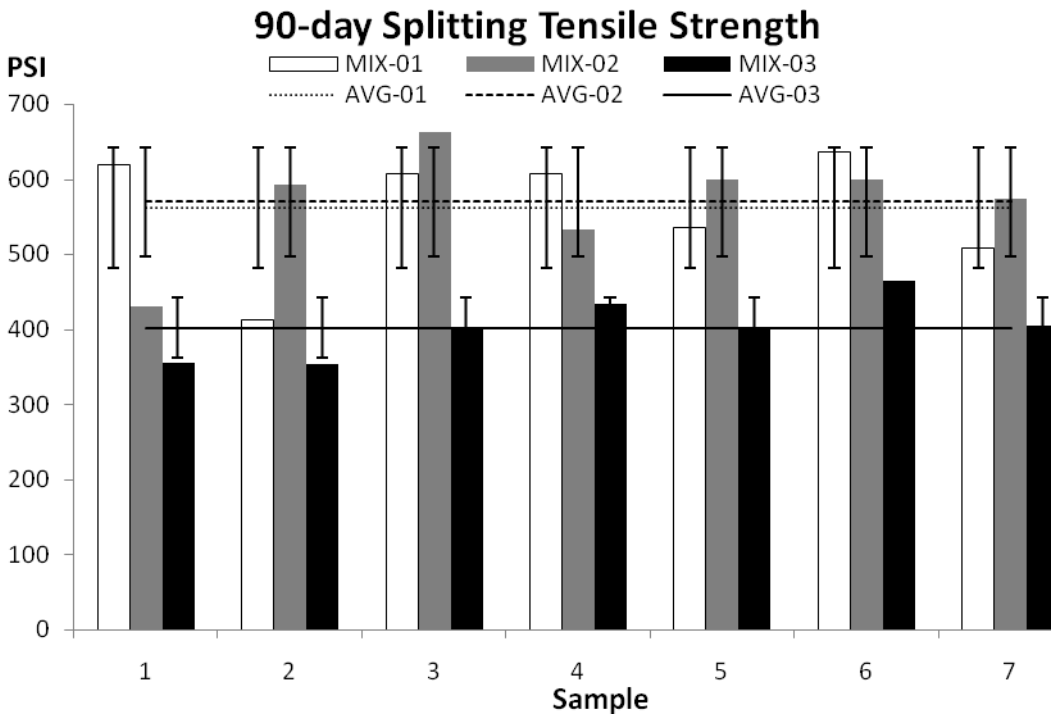

Figure 6.11: 90-day splitting tensile strength

The highest splitting tensile strength at 28-day testing is attained by MIX-02 whereas MIX-03 shows the lowest test results. In general, the standard deviation is very high but MIX-02 obtains the lowest divergence with 60 psi.

After 90 days, MIX-02 and MIX-01 show comparable test results with slightly higher tensile strength for MIX-02. However, MIX-03 displays the lowest splitting tensile strength at 90-day testing. Also, the standard deviation of MIX-01 and MIX-02 is comparable but relatively high (when compared to the average values), whereas MIX-03 shows a low deviation with 35 psi.

The following graph displays the splitting tensile strength of the tested concrete mixtures based on the average values which are outlined in Figure 6.10 and Figure 6.11. It is emphasized that Figure 6.12 would not represent the proper growth rate of splitting tensile strength if the data points were to be connected. Therefore, it was decided to merely outline the average values of each test date and mix design.

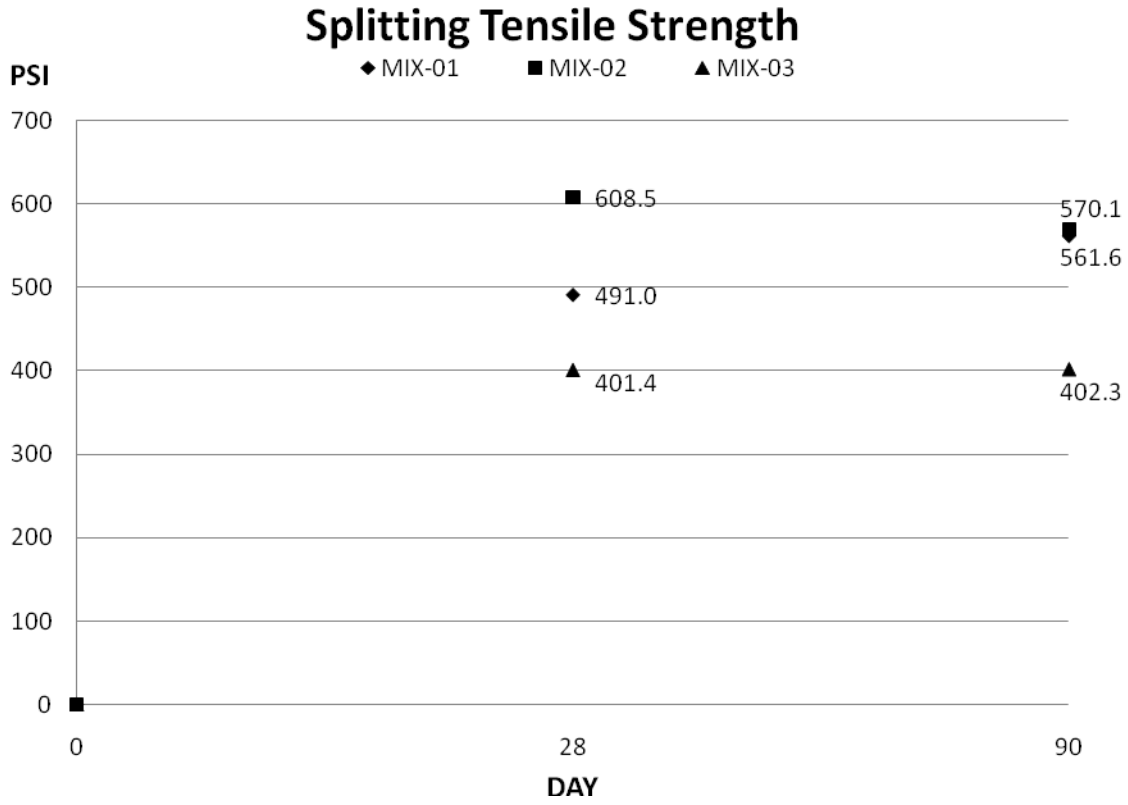

Figure 6.12: Splitting tensile strength comparison

Like flexural strength (Figure 6.9), MIX-02 loses (average) splitting tensile strength from day 28 to day 90 whereas MIX-03 does not gain (average) splitting tensile strength. In general, MIX-02 shows the highest and MIX-03 displays the lowest splitting tensile strength throughout the testing program.

6.5. Analysis of Young's Modulus

The determination of average sample results for the modulus of elasticity was explained earlier in section 5.6 and those results are visualized in the following diagrams. Additionally, the mean values and standard deviation for each mix design and maturity level are displayed.

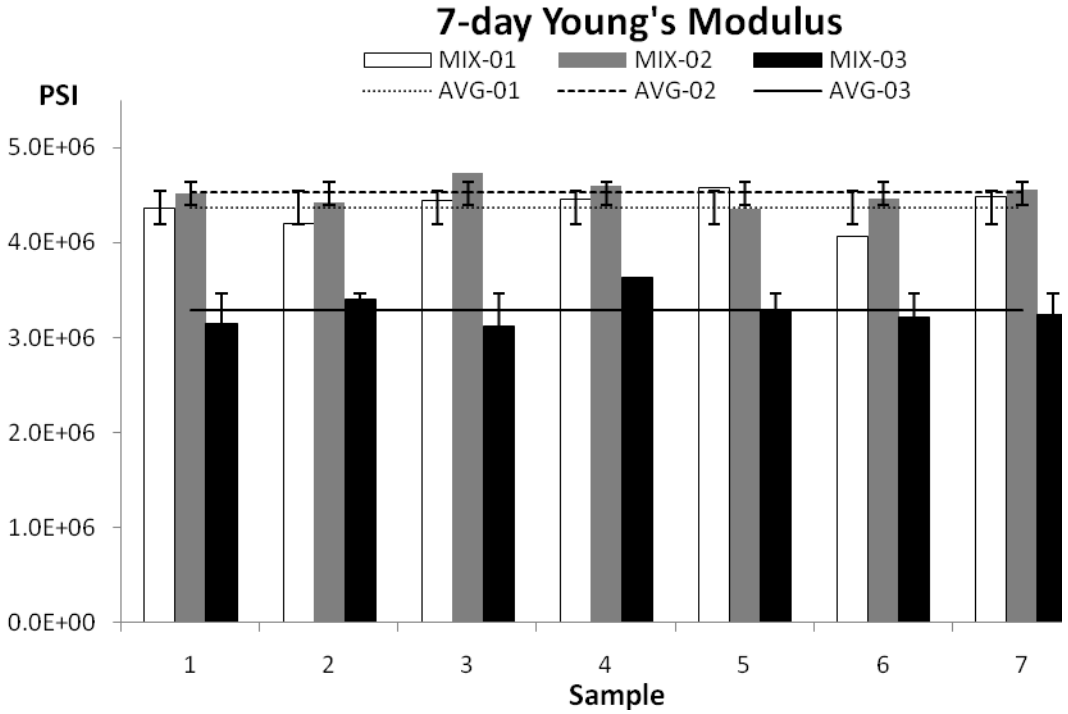

Figure 6.13: 7-day Young's modulus

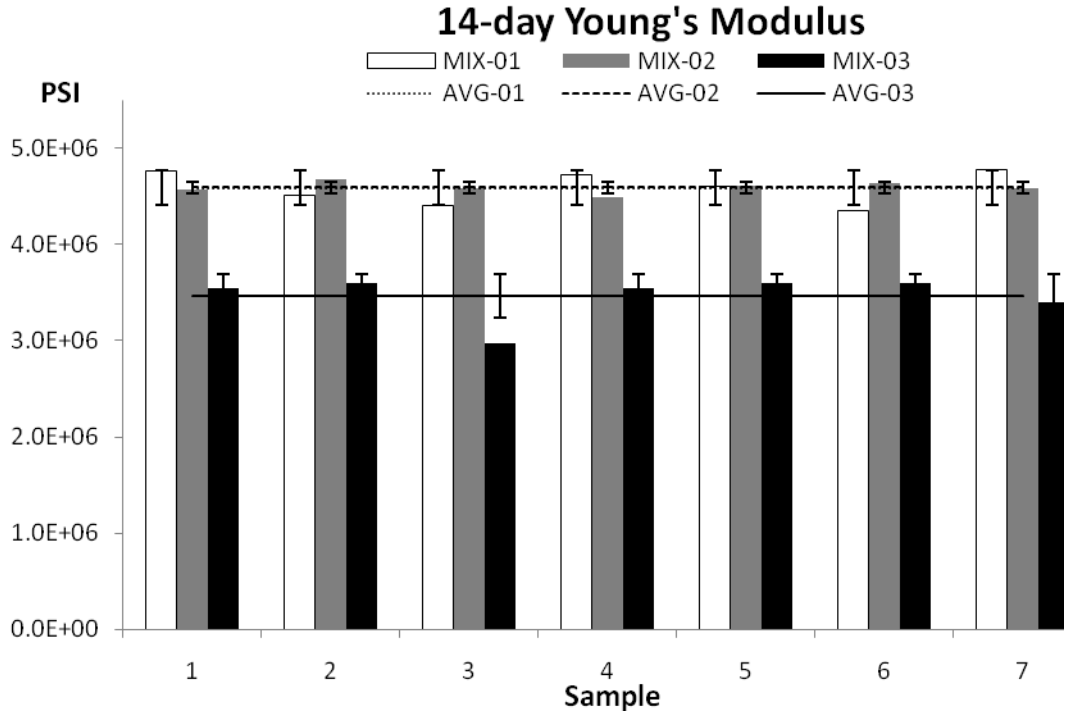

Figure 6.14: 14-day Young's modulus

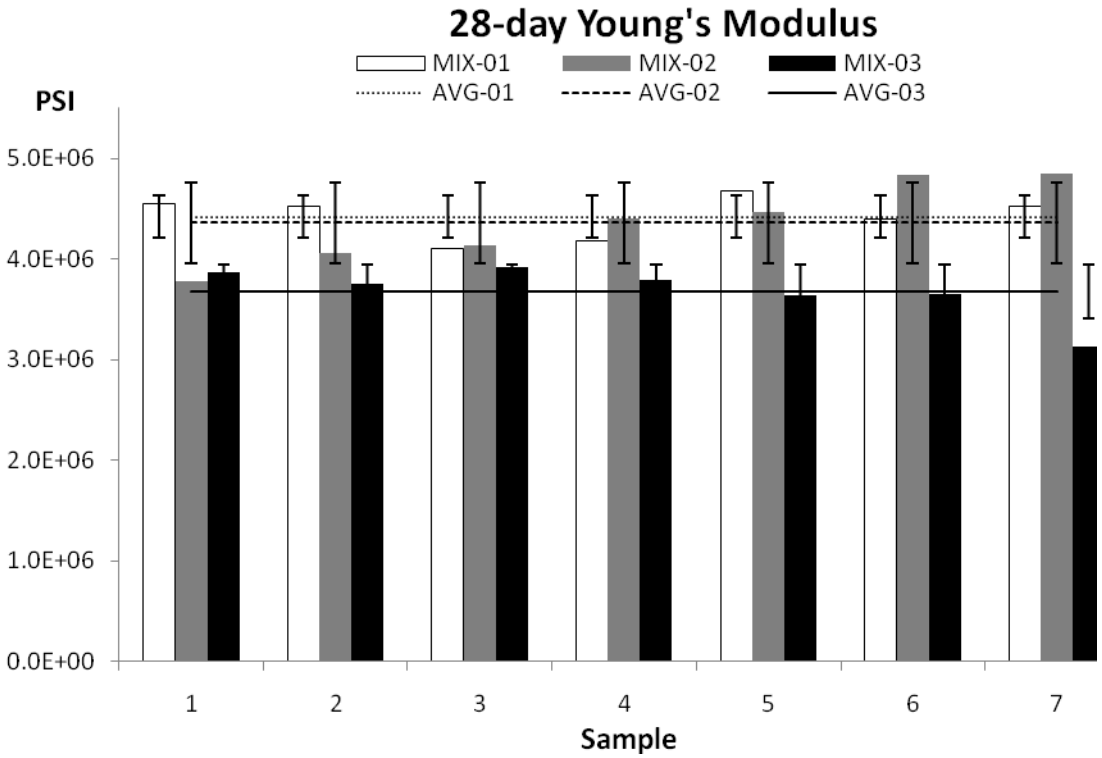

Figure 6.15: 28-day Young's modulus

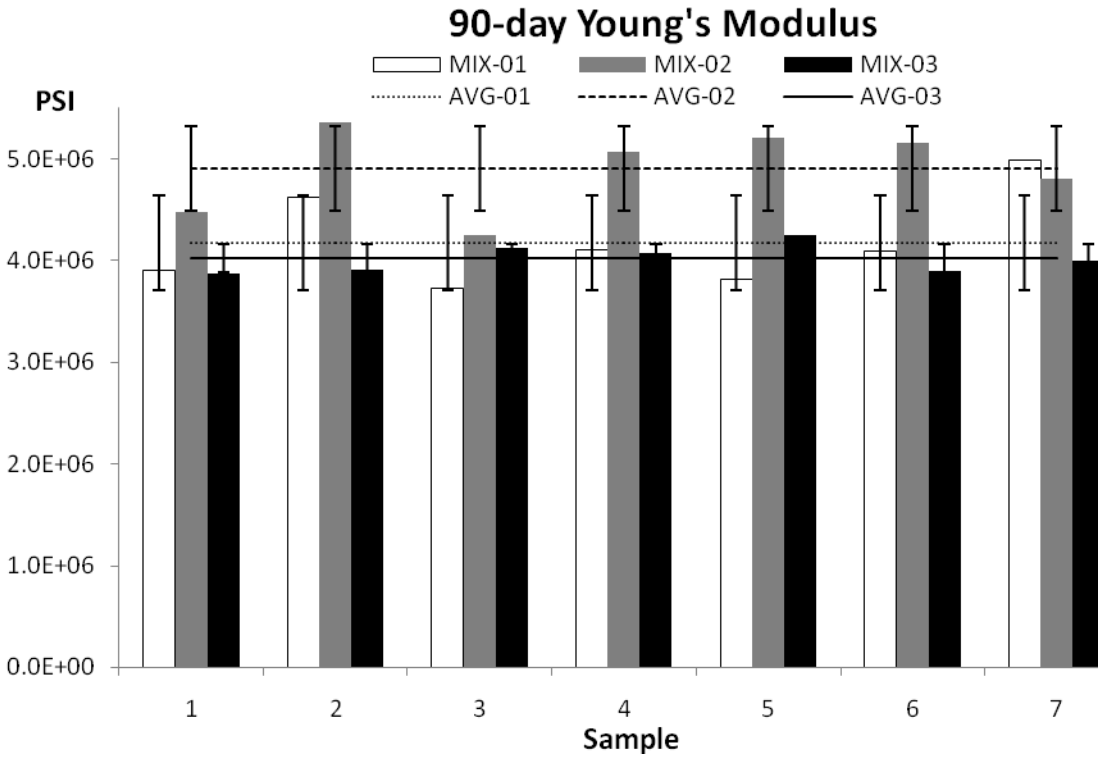

Figure 6.16: 90-day Young's modulus

At 7-day testing, MIX-02 appears to be the stiffest mixture while MIX-03 is the most elastic mix design. Numerically, MIX-01 and MIX-03 show similar standard deviation (but for dissimilar mean values) and MIX-02 presents the lowest divergence ($1.3 \cdot 10^5$ psi).

MIX-01 and MIX-02 show comparable stiffness at the maturity level of 14 days. MIX-03 presents the lowest results and is considered the most elastic mixture. MIX-02 possesses a very low standard deviation with $5.8 \cdot 10^4$ psi, far below MIX-03 which acquires the highest divergence after 14 days.

The highest modulus of elasticity after 28 days was measured for MIX-01. However, the results are very comparable to MIX-02 which attains the highest sample elasticity for specimens 6 and 7. MIX-03 consistently demonstrates the lowest modulus of elasticity for 28-day testing. The highest standard deviation of $4.0 \cdot 10^5$ psi was attained by MIX-02 whereas MIX-01 shows the lowest divergence.

According to Figure 6.16, MIX-02 consistently illustrates the highest modulus of elasticity for 90-day test results: the mixture is much stiffer than MIX-02 or MIX-03. However, consistent with the numerical results, MIX-03 is the most elastic mix design, and with $1.3 \cdot 10^5$ psi it also demonstrates the lowest standard deviation. MIX-01 and MIX-03 show similar (high) standard deviations with values ranging around $4.3 \cdot 10^5$ psi.

To compare the elasticity behavior of the three typical Florida pavement concrete mixtures, the following graph was created. It displays the average test results of each maturity level for the three concrete mixtures under evaluation in this research.

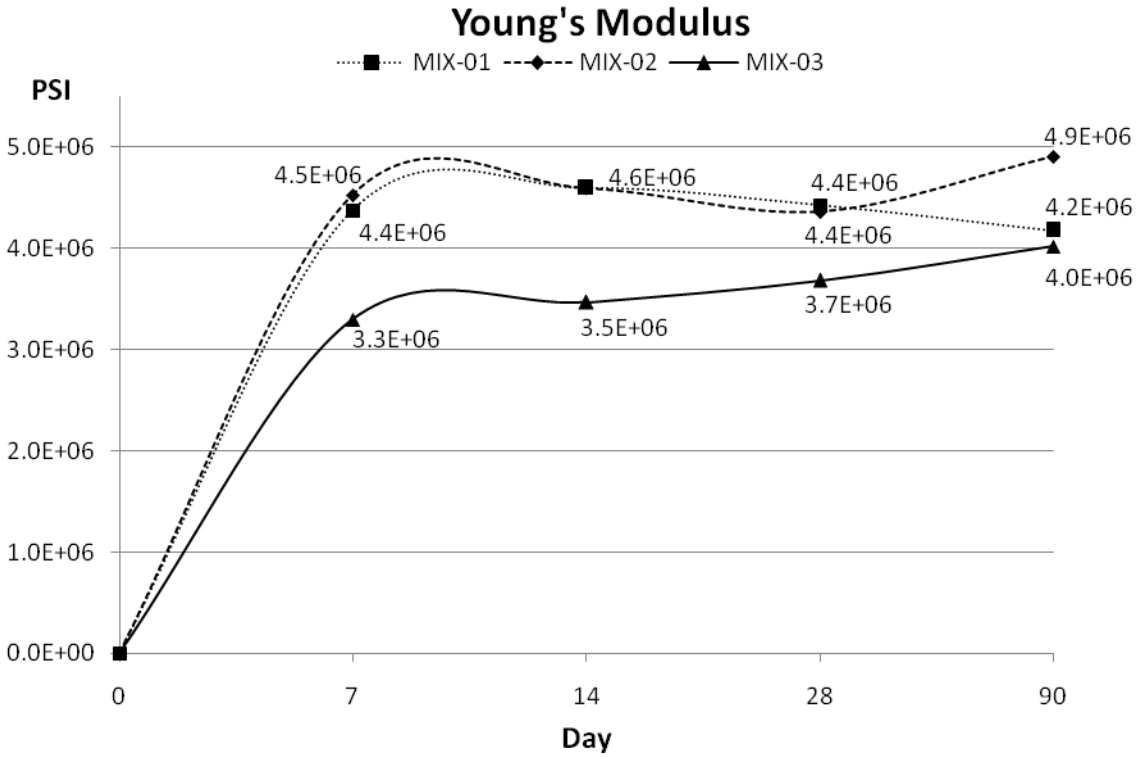

Figure 6.17: Young's modulus comparison

Throughout the duration of testing, MIX-03 possesses the highest elasticity (meaning numerical results are the lowest). MIX-02 shows slight fluctuations throughout the different maturity levels but in general it can be considered the stiffest concrete mixture under evaluation. On the 14th day of testing, MIX-01 and MIX-02 attain similar (average) stiffness. MIX-01 loses stiffness or respectively gains elasticity with increasing maturity (after 14-day testing). MIX-03 properly gains stiffness over time.

6.6. Analysis of Poisson's Ratio

The lateral strain of the concrete specimens was measured parallel with the measurement of Young's modulus, and the following results are derived from the same test samples. However, due to the reasons explained above (section 5.6.) Poison's ratio was mainly measured for 28 days and 90 days and only MIX-03 could be tested for 14-day Poisson's ratio.

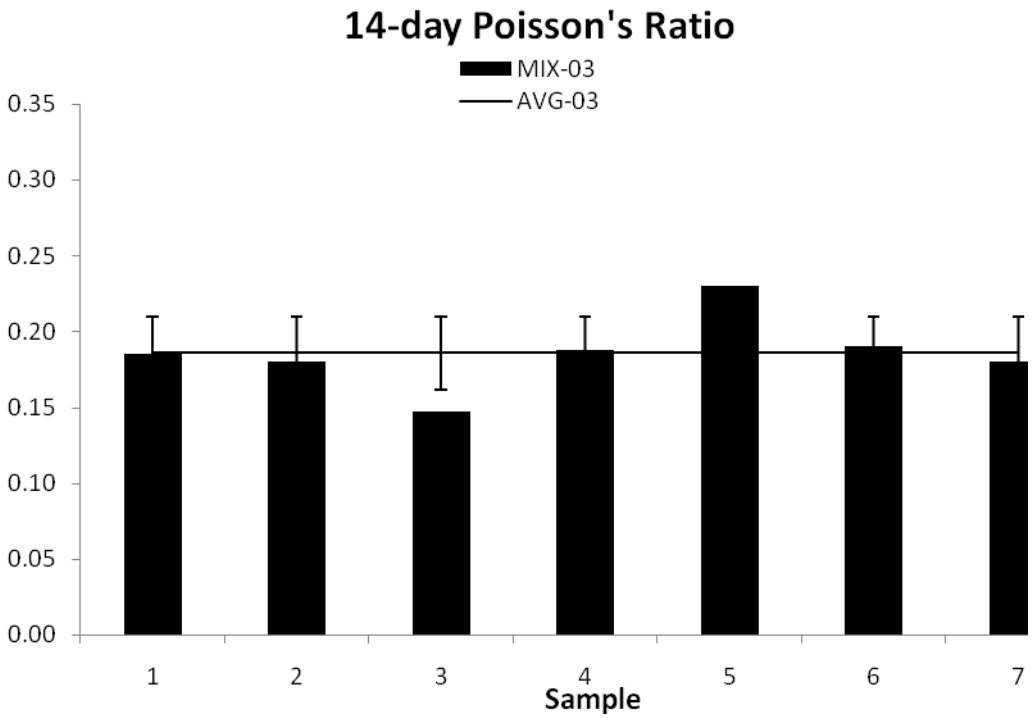

Figure 6.18: 14-day Poisson's ratio

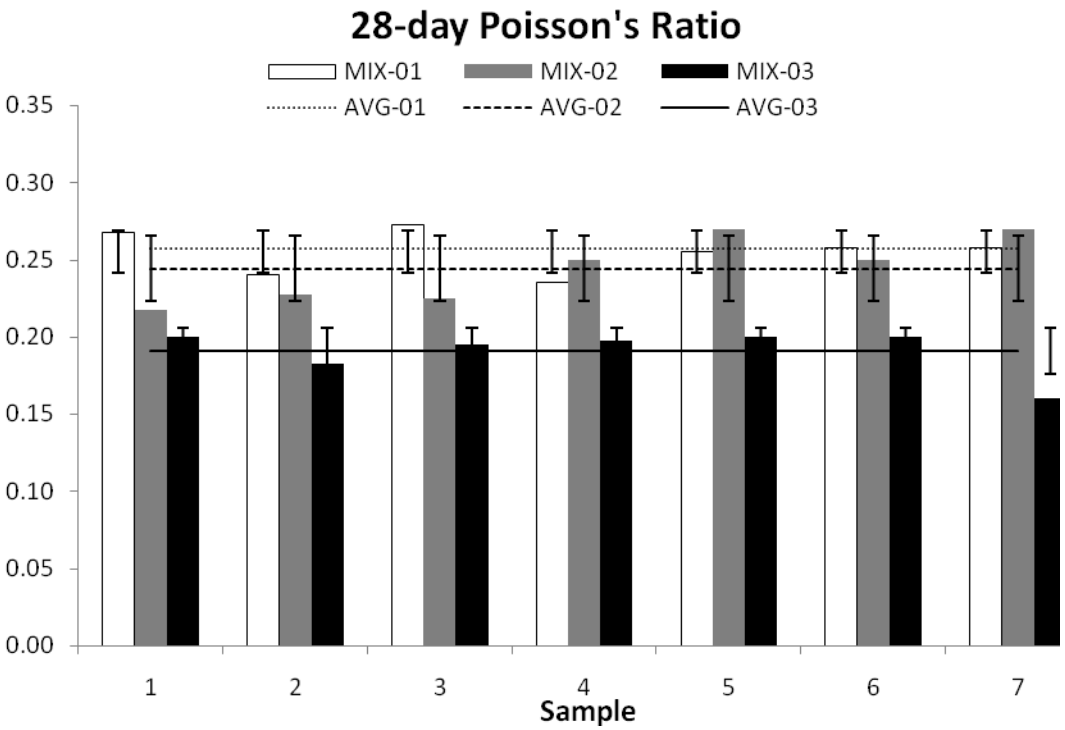

Figure 6.19: 28-day Poisson's ratio

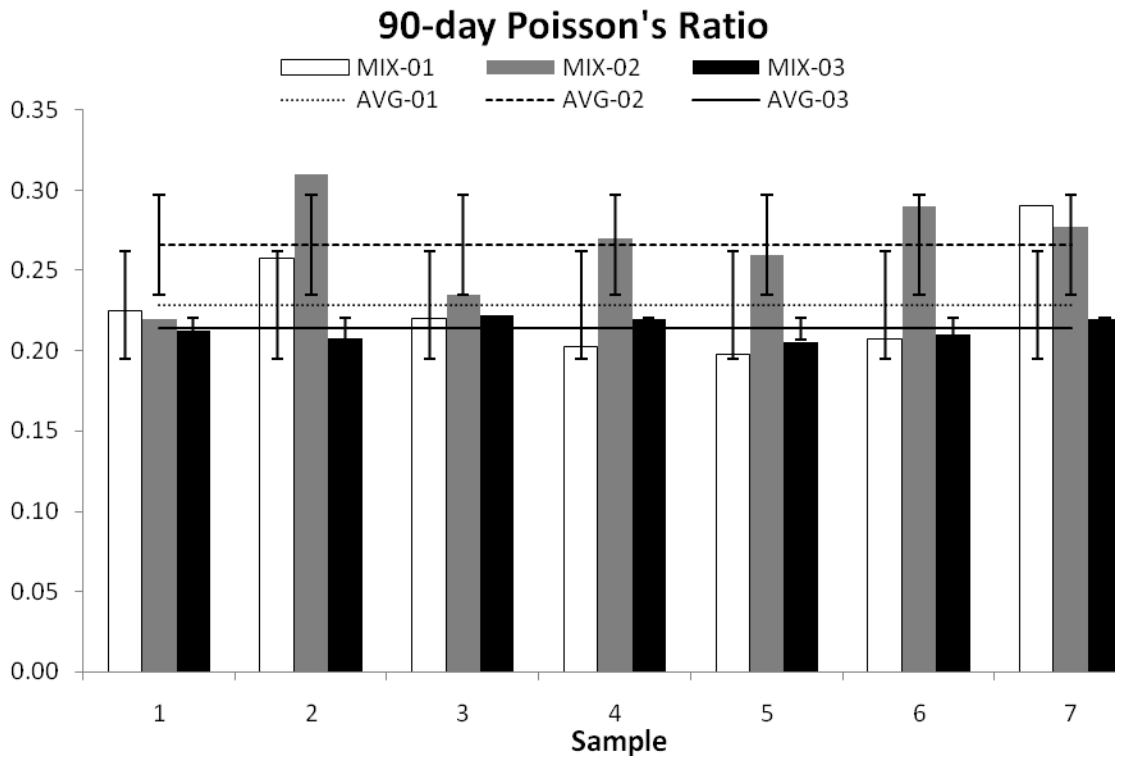

Figure 6.20: 90-day Poisson's ratio

Although after 14 days the Poisson's ratio was measured for MIX-03 only, it can be stated that the sample measurements vary within the normal numerical range which is usually expected for concrete (0.15 to 0.30 with a typical value of 025).

At 28-day measurement, the Poisson's ratio demonstrates very reliable test results for each mix design. MIX-03 numerically shows the lowest average value. It is emphasized that MIX-01 and MIX-02 attain similar highest sample values but due to standard deviation (0.02 for MIX-02), MIX-01 reaches the higher average Poisson's ratio.

After 90 days, Poisson's ratio shows highest values for MIX-02 and MIX-03 presents the mix design with the lowest Poisson's ratio. Standard deviation for 90-day measurement demonstrates similar high values for MIX-01 and MIX-02 (0.03), and a very low value for MIX-03 with 0.007.

The following graph in Figure 6.21 summarizes the average values for the measurement of Poisson's ratio. It is emphasized that the 14-day data point for MIX-01 and MIX-02 were not available, and therefore were estimated at 90 % of 28-day Poisson's ratio.

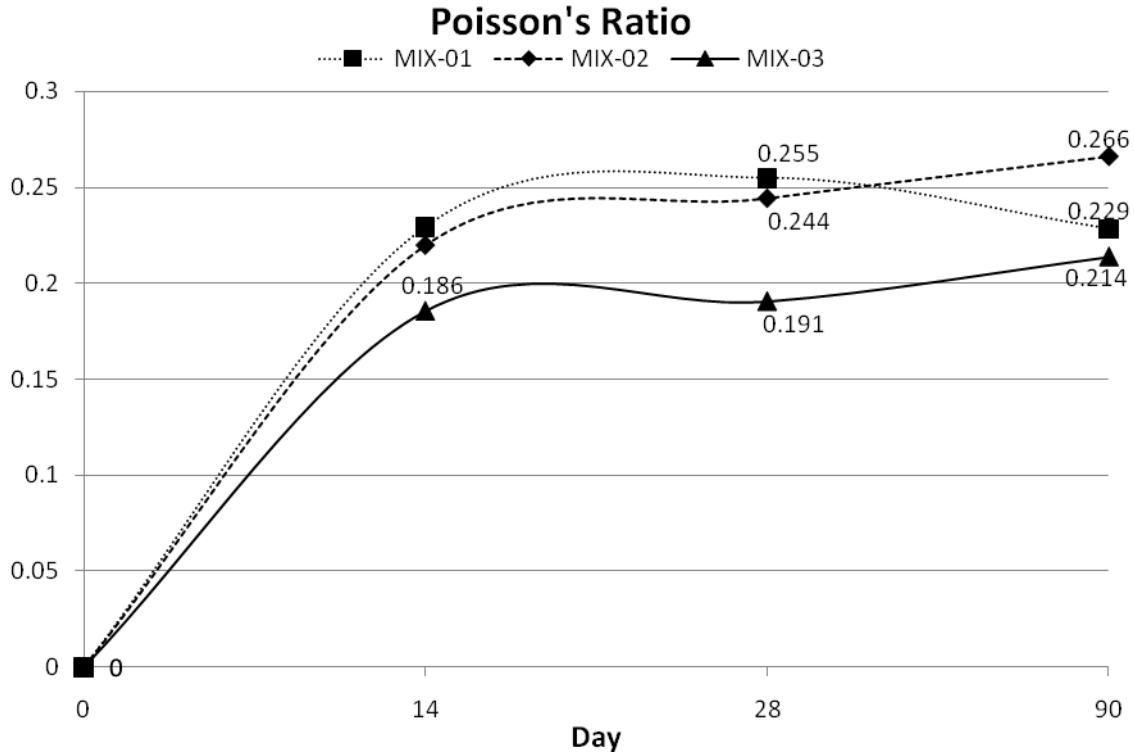

Figure 6.21: Poisson's ratio comparison

The Poisson's ratio increases over time for MIX-02 and MIX-03 but decreases from 28-day to 90-day measurement for MIX-01. The final Poisson's ratio (μ) for the three evaluated Florida pavement concrete mixtures is located between 0.21 and 0.27; this compares to the literature very well [7], [10] and is consequently acceptable.

6.7. Analysis of Coefficient of Thermal Expansion

This section is designated to outline the coefficient of thermal expansion for the three different concrete mixtures. The following graphs present the sample results, average values and standard deviation for each maturity level in question.

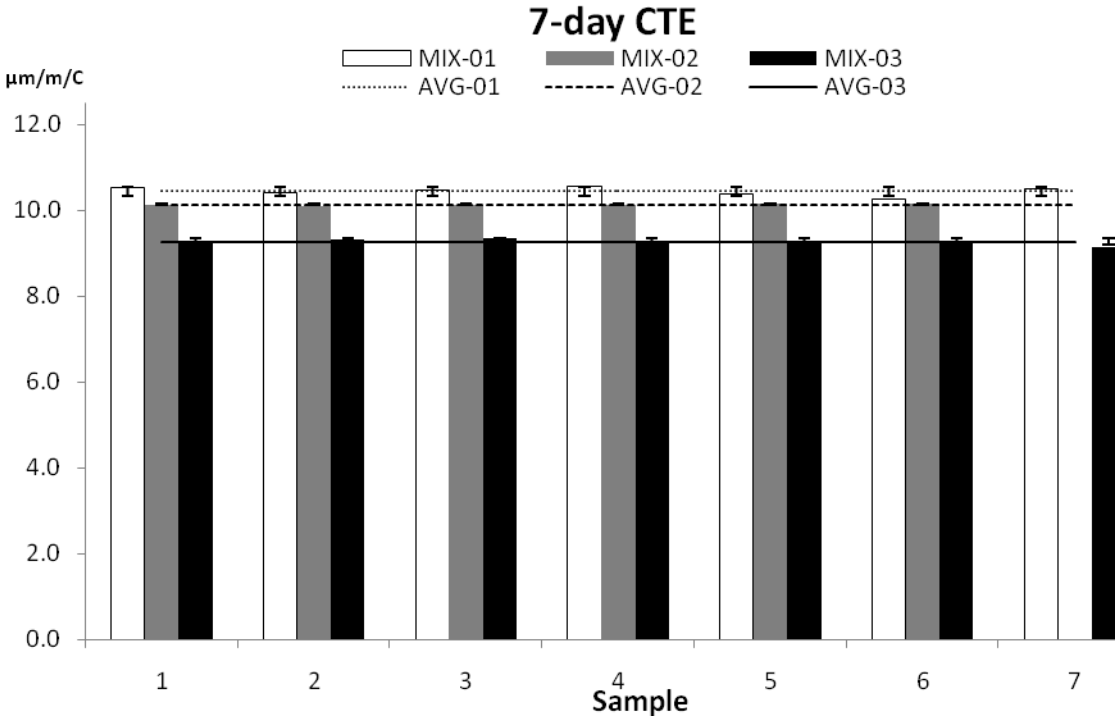

Figure 6.22: 7-day coefficient of thermal expansion

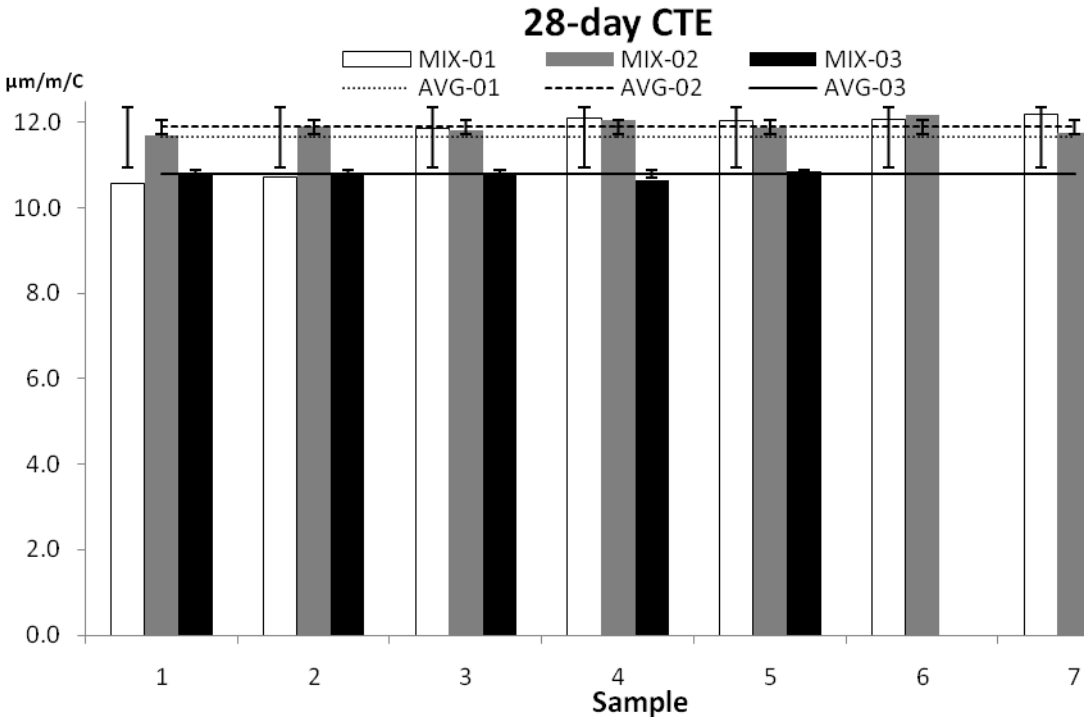

Figure 6.23: 28-day coefficient of thermal expansion

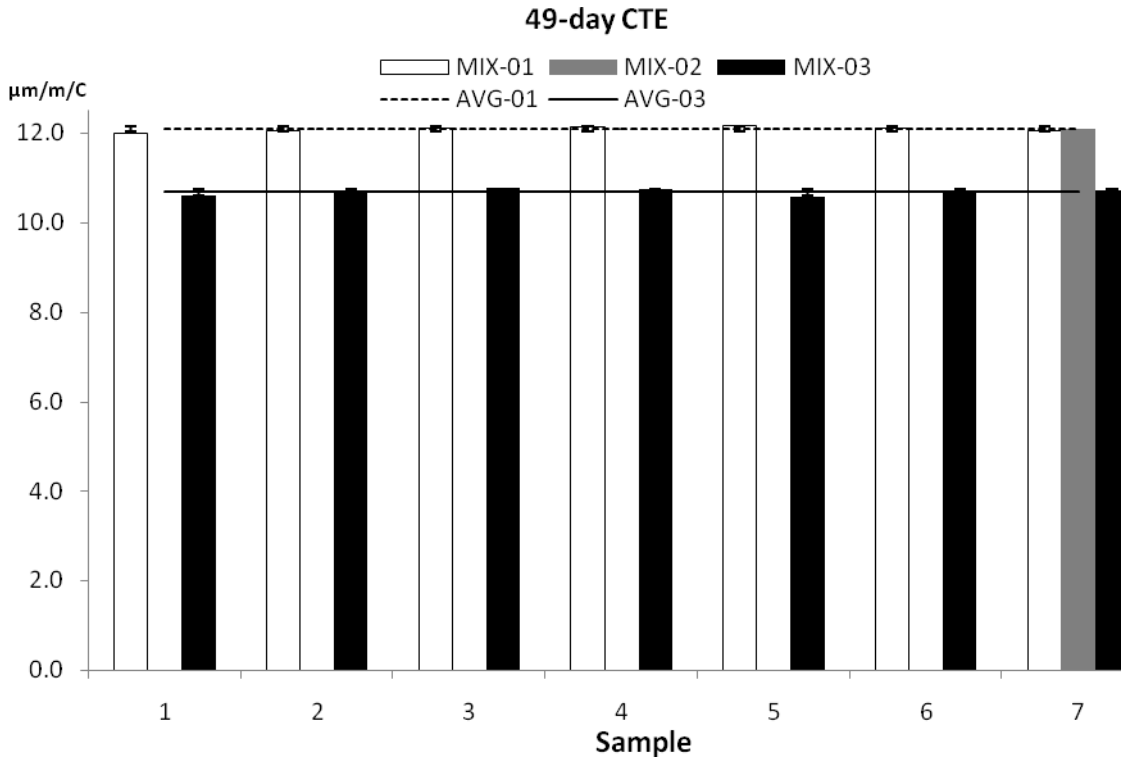

Figure 6.24: 49-day coefficient of thermal expansion (re-used specimen)

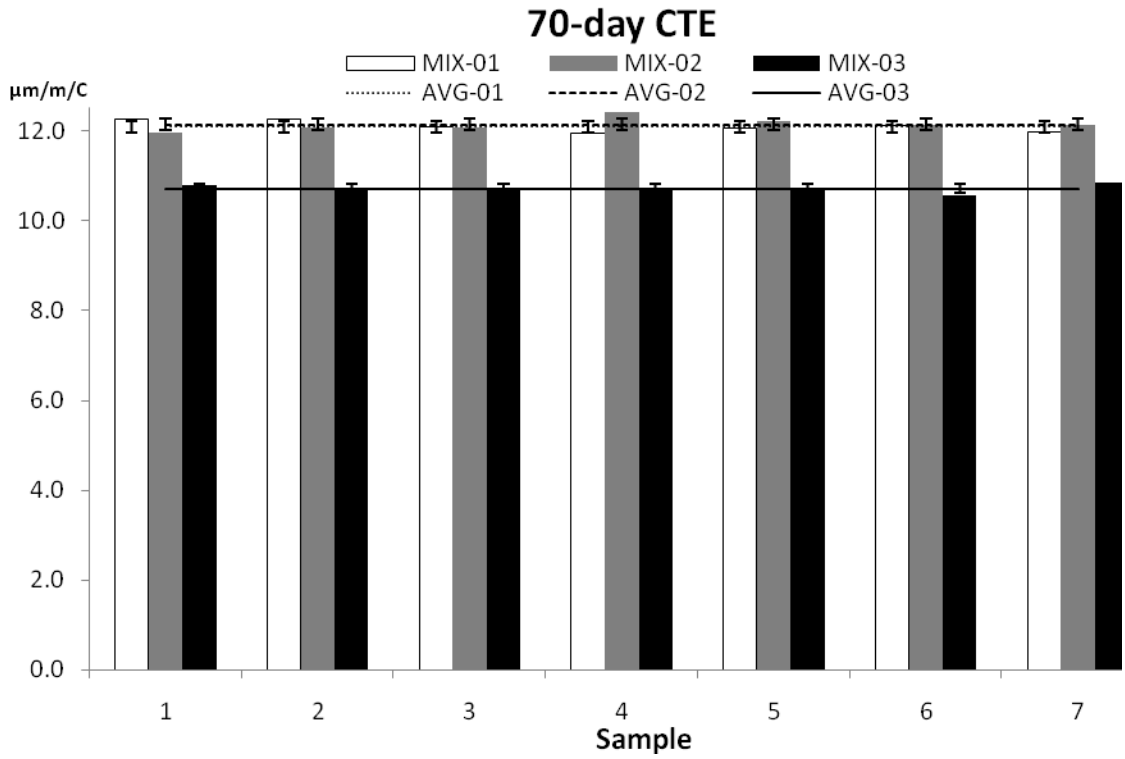

Figure 6.25: 70-day coefficient of thermal expansion (re-used specimen)

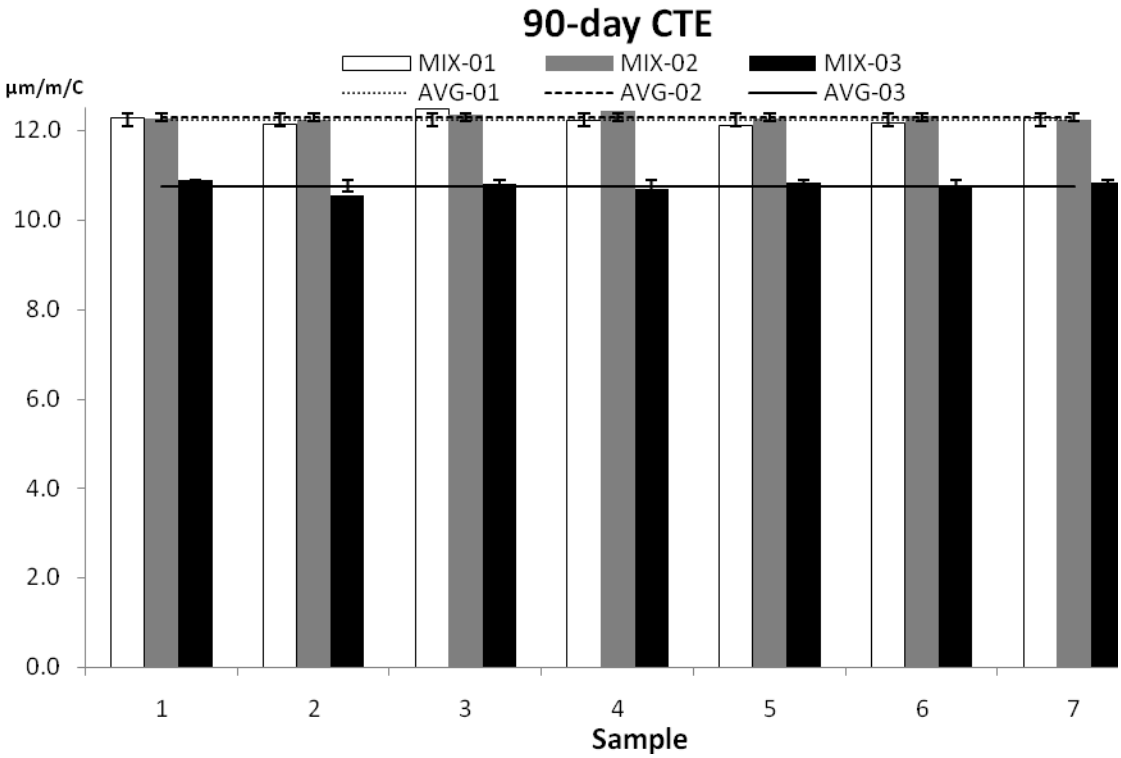

Figure 6.26: 90-day coefficient of thermal expansion

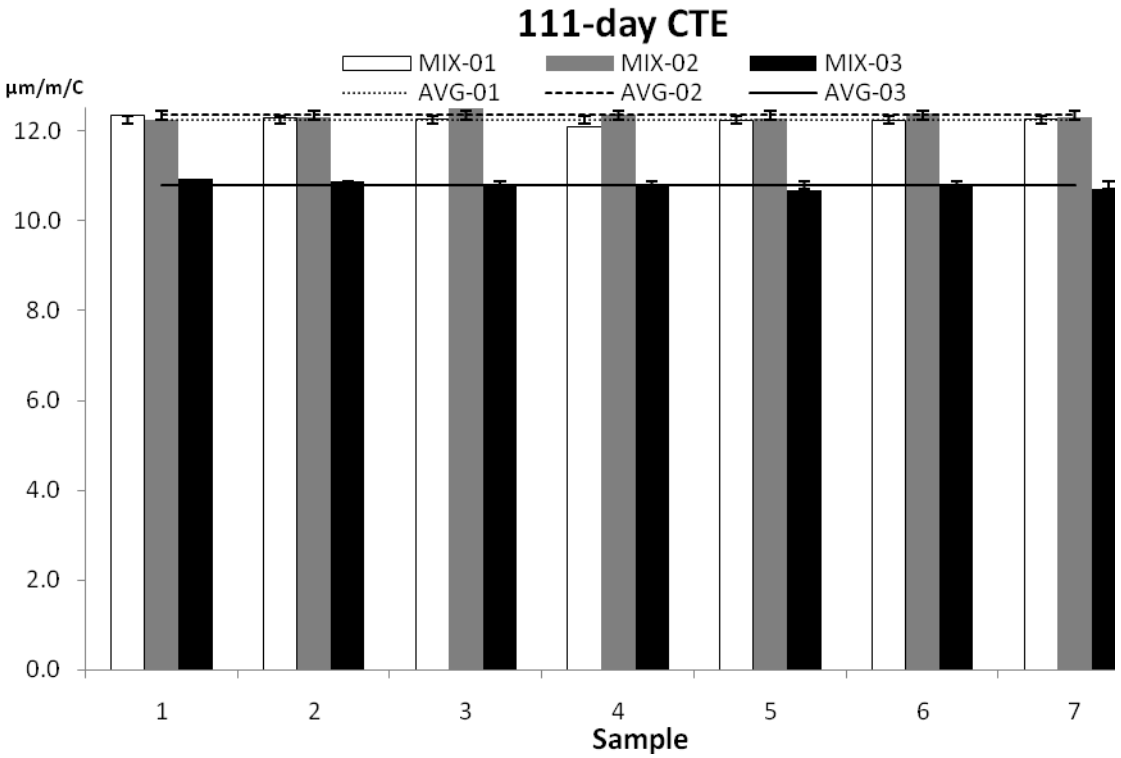

Figure 6.27: 111-day coefficient of thermal expansion

At 7-day testing, MIX-01 shows the highest and MIX-03 the lowest CTE values. Although the data points were taken on seven successive days, the standard deviation can be considered very low for all three mix designs.

After 28 days, MIX-02 possesses the highest CTE values. The lowest response to thermal influences was measured for MIX-03, which also shows a very small divergence from its mean value. However, the standard deviation is remarkably high for MIX-01 after the 28^{th} day.

The samples used for 7-day testing were re-used after 42 days for 49-day testing (sample 1 at 7-day = sample 1 at 49-day). Due to malfunctioning of the CTE test unit, only one single data point is available for MIX-02 at 49-day testing (statistically irrelevant). However, MIX-01 and MIX-02 demonstrate almost no standard deviation (0.05), and therefore the test results can be considered very reliable. According to Figure 6.24, MIX-02 is more susceptible to temperature than MIX-03.

The concrete specimens measured for 28-day CTE were re-used 49 days later (sample 1 at 28-day = sample 1 at 70-day). MIX-01 and MIX-02 show comparable CTE values ranging around 12 μm/m/°C. The standard deviation is similar for all three mix designs under evaluation and MIX-03 shows the lowest CTE results after 70 days.

MIX-01 and MIX-02 show comparable (high) reaction to thermal treatment after 90 days. In general, the standard deviation is very low throughout the data range for all three mix designs. MIX-03 shows the lowest CTE values after 90 days.

After 111 days, the highest CTE values were measured for MIX-02 which are only slightly higher than those of MIX-01. Again, MIX-03 undercuts its two competitors (by more than 1 μm/m/°C) and can be considered least susceptible to thermal gradients. The standard deviation is consistently small for all tested mix designs at the maturity level of 111 days.

In general, it has to be stated that the standard deviation remained very low in values throughout the testing program. This may be evidence of the coefficient of thermal expansion in concrete being a reliable property.

The following Figure 6.28. displays the average CTE values for the three tested concrete mixtures at all maturity levels. Notice that the numbers at 49-day, 70-day, and 111-day testing result from re-used specimens.

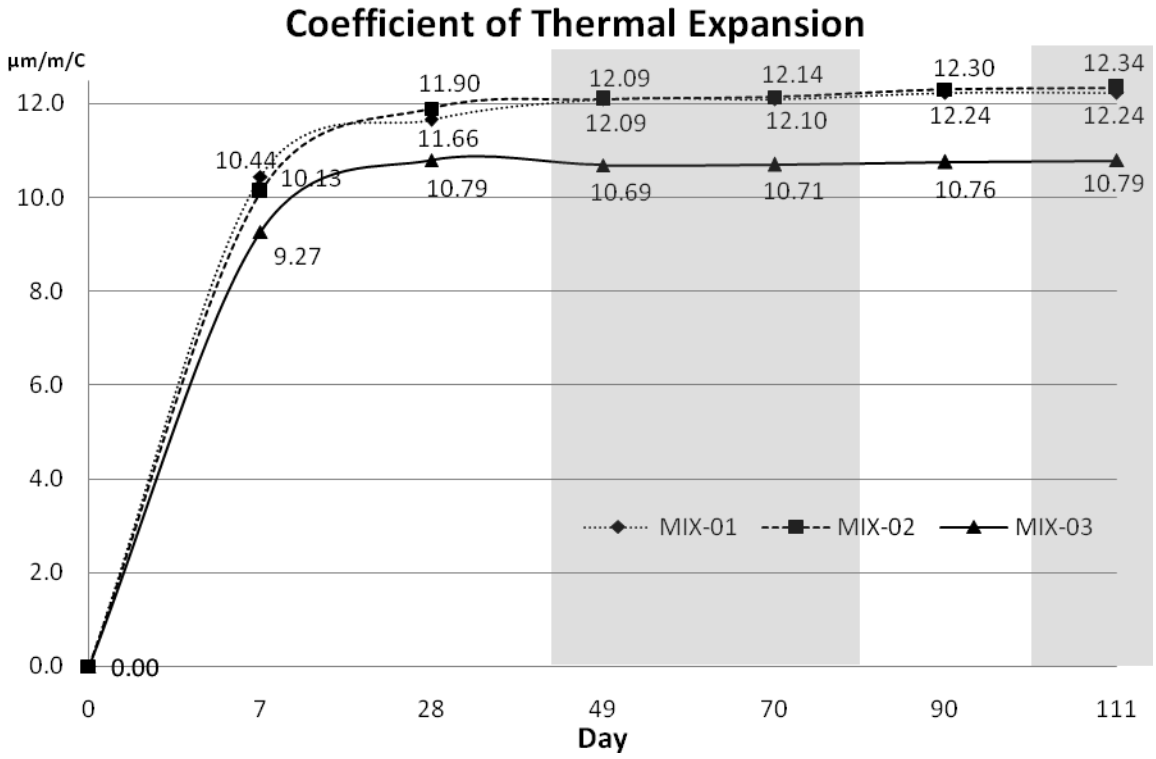

Figure 6.28: Coefficient of thermal expansion

With the exception of 7-day measurement, MIX-02 consistently demonstrates the highest CTE values throughout the testing program. However, MIX-02 and MIX-01 numerically are not far apart and are difficult to distinguish (same aggregates), whereas MIX-03 shows distinguished thermal behavior, undercutting its competitors by more than 1 µm/m/°C. In general, it can be stated that the coefficient of thermal expansion increases rapidly within the first weeks but stabilizes after the 28th day. The effect of re-using a specimen is not noticeable.

6.8. Summary of Mix Design Analysis

Mix design MIX-02 is the concrete composition which numerically achieved the highest values throughout all test procedures. It is therefore the highest strength mix design under evaluation. The opposite is true for MIX-03 in that this mixture obtains numerical values which constantly undercut the results of MIX-01 and MIX-02. MIX-03 can be considered the lowest strength mix design within this research project.

MIX-03 shows consistently increasing numerical test results throughout all evaluated engineering properties. As though it was retrieved from a text book, this mix design gains strength, elasticity, Poisson's effect, and CTE while its maturity level increases. Almost the same would be true for MIX-01 if Young's modulus and Poisson's ratio results were neglected. Nevertheless, MIX-01 gains strength and CTE with increasing concrete age. MIX-02 seems to fluctuate widely; although its behavior in compressive strength and Poisson's ratio follows the theoretical expectation, it varies throughout all other material characteristics.

Although MIX-03 contains the most durable and strongest aggregate type, it is not surprising that it is the weakest mix design within the three tested mixtures. With 470 lbs of cement, it contains more cement than MIX-02 but less than MIX-01, however, MIX-03 is the only concrete mixture relying exclusively on cement to develop adhesive properties and it contains no fly ash or any other cementitious material to support strength-gaining features. Also MIX-03 measures the highest water-to-cement ratio as well as the highest slump and lowest temperature during specimen preparation, three aspects which cause low strength concrete. Nevertheless, it is emphasized that MIX-03 meets all target criteria and is not a weak mix design in general; it is merely the least strong mixture within the research scope. The mix design fulfills Florida DOT regulations.

MIX-01 is targeted 1500 psi higher than MIX-02, a characteristic which cannot be validated through this research. Theoretically, the assumption makes perfect sense, as

MIX-01 not only contains a higher quantity of cement and cementitious materials, it also includes less aggregates (less fine and less coarse) and possesses a lower water-to-cement ratio. However, the experimental results clearly show higher strength for MIX-02 throughout all strength-related properties. This is traced back to the fresh properties of the concrete during specimen preparation. Note that the air content of 2.5 % undercuts the target range of 3 to 6 % which indicates a more dense concrete structure than assumed, especially in conjunction with a slump value of 2.5 inches (lowest of all three mix designs and at the lower end of the target slump) at a concrete temperature around 35°C (highest temperature of all three concretes) and an ambient temperature ranging around 26°C. Although the ingredient proportionality presumes more strength for MIX-01, it became evident that the variability of fresh properties greatly affects the final product and its strength-related characteristics.

The inconsistent stiffness and Poisson's behavior of MIX-01 and MIX-02 on and after the 28^{th} day is believed to be founded in concrete variance. Note the standard deviation for those two maturity levels; they show very high digression compared to earlier test results. The possibility of inaccurate measurement can be excluded as every single specimen was exposed five (5) times to stiffness/Poisson's effect testing and each specimen showed (very) consistent results. Consequently, it is assumed that the deviation of measurements results from naturally occurring variance in concrete products.

Numerically, the difference between MIX-01 and MIX-02 in terms of CTE measurement is very small while MIX-03 is more distinguishable with lower CTE results (more than 1.0 µm/m/°C) throughout the entire experimental phase. In general, the literature predicts lower CTE values for limestone-based concrete (MIX-01 and MIX-02) than for concrete made of granite aggregates (MIX-03), a behavior which could not be confirmed by this study. This is because it is not only the ingredient itself which plays a prominent role; the proportion of constituents determines thermal behavior as well. With 737 lbs/yd^3, MIX-03 contains the least amount of cementitious paste and this also results in the lowest quantity of mortar with 1972 lbs/yd^3. As outlined in Chapter 2, it is well known that cement paste possesses a much higher CTE value than most concrete aggregates do.

Especially since concrete's CTE is a resultant of three (3) different CTE values (coarse aggregates, fines aggregates, and mortar) and their volumetric proportion (see 2.3.4). The CTE results determined by the rule of mixture (as recommended for input level two) based on the volumetric proportions are not outlined here since it is a derived property rather than a measured one. However, those results will be presented later in the text (section 7.5.4.2 and table 7.3) to account for hierarchy level two input data as appropriate for pavement structure modeling according to the new M-E PDG.

The slightly higher propensity to thermal expansion of MIX-02 compared to MIX-01 may be explained through an analogous approach. MIX-02 contains a very high amount of fine aggregates, which results in a higher quantity of mortar (67 % by weight of total concrete mixture). Both mix designs rely on the same type of aggregates, turning the proportion of constituents into the governing factor for CTE. Therefore, MIX-02 is theoretically and empirically the mix design most affected by thermal impacts. However, the test results revealed that concrete's CTE value increases over time. It was shown that the thermal behavior increases rapidly within the first week and stabilizes subsequently. After 28 days, the CTE swell can be considered insignificant as the change was mostly less than 1/10 µm/m/°C.

To complete research phase one, the above-listed test results and analysis have to be converted into parameters suitable as input data for the M-E PDG. Since all test results showed very stable and consistent values, the decision was made to use the determined average values for each maturity level. No adjustments will be necessary. In cases where only one value – instead of several different values for different ages – is requested (e.g. Poisson's ratio), it was decided to utilize the 90-day average value. One can argue that usually, in concrete applications, the 28th day determines the design properties. However, as those characteristics are still rising for all three different mix designs, the 90-day property will be a conservative assumption for this research.

6.9. Improving TP 60 (Test Unit)

AASHTO TP 60 outlines a technique to measure the coefficient of thermal expansion for hydraulic cement concrete; it describes the test setup to achieve raw data and provides calculation procedures to convert the collected raw data into CTE values. However, certain problems had to be encountered during CTE measurement using a commercially available test unit. In consequence, an intensive study was initiated to fathom the sources. The evaluation revealed test machine dilemmas which were partially attributed to inconsistencies of the designated test protocol. Important findings were made, and certainly a lesson was learned.

Modest discrepancies were first recognized (June 2007) when comparing 7-day test data to PCC CTE values provided by the literature, as the numerical results slightly increased upper limits for concrete (7 μin/in/°F) already. Since TP-60 describes a new approach to determine CTE for concrete, aberrance of literature had to be considered. However, assuming the literature to be correct, the failure would have to be found in data measurement (LVDT/temperature) or data processing. Moreover, since each mix design showed consistent values for all tested specimens, the flaw must have been systematic.

The software used to determine the thermal expansion is commercially distributed, and can be considered a black-box to the laboratory technician. Although it is known that the software is based on the AASHTO TP-60 protocol, an inside view or manipulation of computations is impossible. Consequently, after the first suspicious values surfaced, the manufacturer was informed. It was revealed that some testing units were delivered with LVDT calibration flaws. A new program was written by the developer to compensate for the problem in future testing and to determine an adjustment factor for previously conducted tests. It was found that the correction factor for the LVDT used in this research was as small as 0.98, and thus it would not cancel the suspected divergence.

For further verification, 15 concrete samples (5 per mix design) were sent to Florida DOT Material Laboratory in Gainesville. Nine cylinders were cross-checked for CTE using FDOT's in-house built CTE unit. The measured test results differed up to 23 % but

compared to the literature satisfactorily. This was considered to verify the flaw in the test unit used in this research, especially as FDOT CTE results compares to Texas Transportation Institute (TTI) CTE results successfully. Again, the manufacturer was consulted but no action was taken.

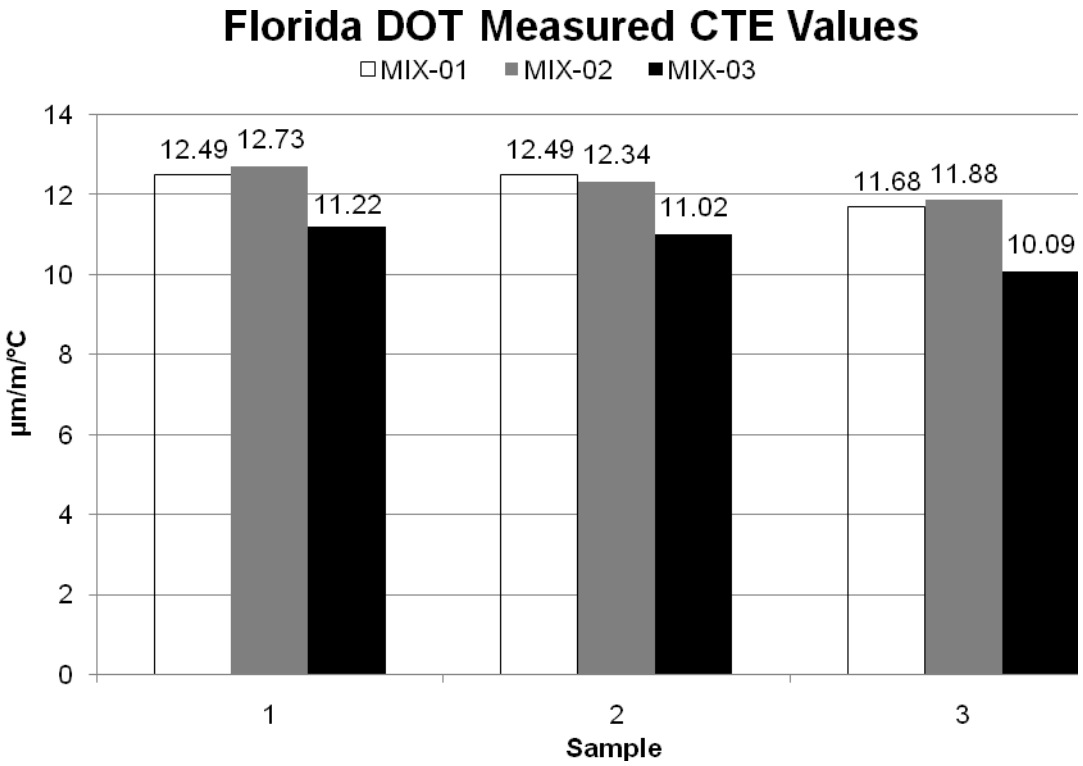

Figure 6.29: Florida DOT measured CTE values

Further research revealed that Federal Highway Administration (FHWA) was facing similar problems, since they possess several test devices to measure CTE including two units fabricated by the same manufacturer: one unit in stationary use at the laboratory in Washington D.C. and one that is built into the FHWA mobile laboratory. Initially, both the stationary and the mobile machines determined incorrect CTE values. To narrow down the problem without the manufacturer, who abstained from the problem, a cooperative effort was launched. FHWA agreed to test identical specimens made of aluminum, stainless steel, and concrete in both units (local and mobile laboratory) after CTE for those specimens was identified by the unit used for this research. Additionally, the specimens were tested in FHWA manually built units.

The results revealed fallacy of the commercially distributed software. For example, CTE for aluminum usually ranges around 25 µm/m/°C, a result that could not be confirmed by any of the three units (same model) under comparison. In fact, the software calculated values around 12 µm/m/°C. However, when using raw data, more correct values were achieved. Therefore, it was assumed that data processing was not done correctly by the software. Due to its black-box nature and the hesitation of the software developer, it was decided to calibrate the acquired results to FDOT measurement because (1) FDOT compares properly to other DOTs and is assumed to be correct, (2) the FDOT results compared to the literature, and (3) the problem must have been systematic as the daily CTE measurement showed high reliability for each mix design.

Although final calibration was determined, many obstacles had to be overcome to finally present proper CTE results. The exchange of specimens and particularly the establishment of valid comparisons between different test units caused major troubles. From a research standpoint, these dilemmas are unacceptable as they mostly arose from imprecisely defined test equipment. To prevent similar problems in future testing, less leeway has to be given to manufacturers when fabricating CTE test devices. The lesson learned during this research may be beneficial to further improve AASHTO TP-60 protocol and to truly standardize the equipment. The following refinements are proposed:

Specimen height: The current TP-60 protocol refers to a suitable length, but does not stipulate it. Since this property determines many other characteristics (Support frame, water-level, etc.), it is suggested to fix this value to 7.5 inches. The value is found to be suitable because specimens for this test method are molded into 4” by 8” cylinders, and 0.5 inches guarantees enough room for parallel end grinding. Also, when cores have to be taken in the field, 7.5 inches still is a suitable height undercutting most PCC top layer pavement thicknesses. It seems trivial, but in fact this property caused the most trouble when comparing different test units (note that the same model was compared) as the support frame of one unit was unable to mount the specimens designated for another one - either the specimen was to high and did not fit or it was too short and the LVDT did not touch the specimen sufficiently.

Specimen tolerance: In agreement with the previous paragraph, it is recommended to limit the specimen tolerance to ± 0.2 inches. This is an essential factor in terms of frame calibration and the resultant calibration factor C_f. It is emphasized that the calibration factor according to AASHTO TP-60 is a direct resultant of the calibration specimen material and its height. For the actual test run, this strictly means that the frame calibration factor C_f is theoretically correct, only if the test and calibration specimens are (exactly) identical in height – even small variations between those two heights would result in incorrect CTE values.

Reference point: To prevent pivoting, the specimen shall be placed on three semi-spherical support buttons 120 degrees apart on a 3-in diameter. The height of the support buttons characterizes the zero point for measurement and calibration which is essential for the next paragraph.

Calibration specimen: The height and diameter of the calibration specimen should be prescribed to eliminate inconsistencies between frame calibration and CTE measurement. This calls for a height of 7.5 ± 0.1 inches (at room temperature) and a diameter of more than 3 inches. It was found that commercially distributed test equipment was delivered with calibration samples of different heights and diameters as small as 3/4 in. As explained earlier, the height differences may cause trouble when comparing diverse test units; however, the real discrepancy originates from the small diameter. Any calibration specimen smaller than 3 inches in diameter would not be located on the semi-spherical support buttons, and therefore, causes different reference points for frame calibration and CTE testing. Sensitivity studies have shown that this affects the results significantly – especially if the support buttons are made of a different material than the calibration specimen, or vice versa. Best results were registered by using dimensions similar to actual test samples (diameter = 4 inches).

Frame height: The distance between the reference and LVDT mounting point should be nonadjustable (8.5 inches) to avoid high differences in calibration factors and to ensure proper comparison of test units.

Frame material: Diverse materials have been used to build the frame (even 304 stainless steel) but in order to ensure proper comparison, thought might be given to a specified frame material. Invar[6] would be the most logical choice as it reduces the frame movement due to temperature to a minimum.

Water coverage: The water coverage above the specimen defines the amount of support frame exposed to the thermal gradient. This is a sensitive factor, and it is critical that this be similar for calibration and testing. It was found that submerging depths differed (even for identical models). A fixed cover of 0.5 inches is suggested to define the water level during calibration and testing.

Stability: AASHTO TP-60 defines measurement accuracy at three repeatable temperature/LVDT readings. Although this is a valid definition, it was found that commercially distributed software compares successive numbers rather than three consistent results. It requires the acquisition of four similar numbers to obtain three consistent readings. A note should be provided in section 7 (AASHTO TP-60).

Reference length L_o: The measured length of specimen at room temperature provides the reference length for CTE calculation according to AASHTO TP-60. Physically, this is incorrect since L_o refers to the length at initiation of thermal gradient. The specimen experiences thermal contraction when temperature is lowered from room temperature to 10°C causing a new reference length (the same is true for expansion). Sensitivity studies

6 Invar (FeNi36) is a nickel steel alloy notable for its uniquely small coefficient of thermal expansion obtaining values as low as 0.62 um/m/C. It was invented in 1896 by Swiss scientist Charles Édouard Guillaume who was awarded with the Nobel Prize in Physics in 1920 for the discovery of Invar as this alloy was found to be indispensable for scientific instruments.

have proven this factor to be insignificant and acceptable from an engineering standpoint; however, a footnote should address the issue to declare adequacy and avoid confusion.

The suggestions above are outlined to further improve AASHTO TP 60. The recommendations should be considered to establish adequate test equipment following accurate standards; it will ensure proper comparison between test results obtained from different test units at different agencies. Manufacturers must be obligated to obey these standards when (mass) producing test equipment.

In general, it might be worthwhile to reconsider the approach outlined in TP-60. Although accounted for by the correction factor, the submerged test frame causes physical inconsistencies as the theoretical soundness of C_f is only valid for precisely equal heights of calibration and concrete sample. The LVDT mounting point should be uncoupled from the thermal gradient.

CHAPTER 7: M-E PDG RESEARCH - EXPERIMENTAL PROGRAM

7.1. Introduction

After identification of concrete material input values, the evaluation base for the M-E PDG sensitivity study has to be developed. The main focus in this study will be on the PCC layer and its response to interchanging hierarchy levels. To properly evaluate input level susceptibility, a virtual paving project will be generated to form the basic framework of this study. Traffic loads, environmental inputs, structural parameters, and analysis criteria have to be modeled based on state-of-the-art/state-of-the-practice methods to reflect real-world applications. This chapter is designated to summarize the virtual paving project and to substantiate the chosen steps towards the research goals in phase two.

The following paragraphs will summarize the most significant input factors and elucidate the values which have not been empirically determined. In certain cases (mostly hierarchy level three) explicit clarifications will be neglected as they go beyond the text. However, generally, more detailed information will be found in the Appendices. Specifically, Appendix A was created to provide an extensive overview of the Design Guide Software. It takes the reader step-by-step through all parameters necessary to successfully run the software. A brief instruction on each input value is made available before the adjacent interface is presented. If necessary, further references and information are provided as well. Although most input values are constant throughout research phase two, it is emphasized that the figures in Appendix A reflect input values for MIX-01 only.

7.2. General and Project Information

At this point, it is indisputable that this study examines rigid pavement only. However, different design methods for PCC pavement are provided by the new M-E Design

Software. Nevertheless, this virtual project considers newly designed Joint Plain Concrete Pavement (JPCP) only, as it is the most common construction method in Florida when using PCC materials. The typical design life ranges between 20 and 50 years for such objects, mostly dependent on the analysis parameters (explained later in this text) chosen by the agency. The design life cycle was fixed to 25 years.

The pavement construction month and pavement open month are very important project parameters which greatly affect PCC pavement distresses as they determine the zero-stress temperature and the concrete maturity at first traffic load appliance. Due to extreme-weather months in Florida, the pavement construction month plays a prominent role. To account for an average temperature, extremely hot months (June through September) and particularly cold months (December through February) were neglected. Also, it was important to create a future construction date since the virtual project reflects new design of JPCP. In such cases the software estimates the weather situation based on historical data, which in real-world application will always be the case. Consequently, the construction month was chosen to reflect the future at the time of report preparation. The pavement construction month was defined as October 2008 and open to traffic November in 2008.

The project location determines the climatic exposure and reflects, therefore, one of the most important project parameters. Certainly, this value will always be postulated by the actual road location; however, this research aims to cover an “average” Floridian location. This becomes very important in terms of ambient moisture conditions which at this point are believed to be found middling in Orlando. Consequently, Interstate 4 ranging from mile post 61.747 to 68.102 (Disney World) was chosen for the virtual paving project.

7.3. Traffic Model

The M-E Software Design Guide provides a very complex Traffic model using measured site-specific traffic data. Interestingly, only hierarchy levels one and three are available for traffic input – no intermediate data quality. When using level one, more than 4500 data points are necessary to accurately represent the traffic pattern. These traffic details go far beyond the scope of this study, which is why it was decided to use hierarchy level three. This may not abbreviate the required data but it reduces most inputs to default values provided by the software. However, it is emphasized that theoretically the M-E PDG exclusively requires hierarchy level one use for interstate design.

Certainly, traffic exposure is closely related to the location of the roadway. Based on the position, the traffic data were taken from the Florida Traffic Information CD-ROM [X 19]. The database provides an Annual Average Daily Truck Traffic (AADTT) of approximately 7,000 trucks for Interstate 4 in and around Orlando. The number of lanes in the design direction was determined to be 2, with 50 % of trucks in the design direction and 95 % of trucks using the design lane. Operational speed on Interstate 4 in this area might differ but was fixed to 70 mph for this research. The growth rate in this location is estimated to increase linearly by 2 %. Since the virtual paving project falls into the general category: "Principal Arterials – Interstates and Defense Routes," the AADTT load distribution of vehicle classes was chosen to be "mixed truck traffic with a higher percentage of single-trailer trucks," (LTT = 11).

All traffic values not mentioned in the paragraph above are based on default values offered by the Design Guide Software. The interested reader is referred to section A.6 in Appendix A as it outlines all values reflecting the default traffic data generated by the inputs listed above.

The traffic model will be held constant throughout the whole course of research and no adjustments will be made. It is a base factor necessary to evaluate the sensitivity of M-E PDG in terms of CTE.

7.4. Climate Model

The climatic model is based on Florida weather data available as software plug-in on TRB's webpage [W 7]. The section under evaluation is located at 28° 19' 35.54" latitudinal and -81° 33' 3.38" longitudinal with an average elevation of 90 ft (Exit 64). Based on this information, the software plug-in locates different weather stations surrounding the site in question. Multiple weather stations can be chosen to generate interpolated weather data. Best results occur by selecting stations that are geographically close and distributed in different directions.

Three different stations have been chosen to interpolate weather data for this research: (1) Leesburg Regional Airport which is located 19.0 miles north-east, (2) Winter Haven's Gilsberg Airport which is positioned 34.5 miles south, and (3) Executive Airport can be found 35.5 miles east in respect to the virtual paving project.

The climatic model remains untouched throughout research phase two as it is another fundamental input serving as an evaluation base for the study.

7.5. Pavement Structure Model

The rigid pavement design procedure allows a wide variety of PCC, base (layer directly underneath the PCC slab), and subbase material properties and layer thicknesses. The Design Guide Software can be used to analyze a maximum of 20 layers. However, because of automatic sublayering of certain layers, a maximum of 10 actual input layers is recommended, comprising the pavement structure and subgrade/bedrock [X 15] (Figure 7.1)

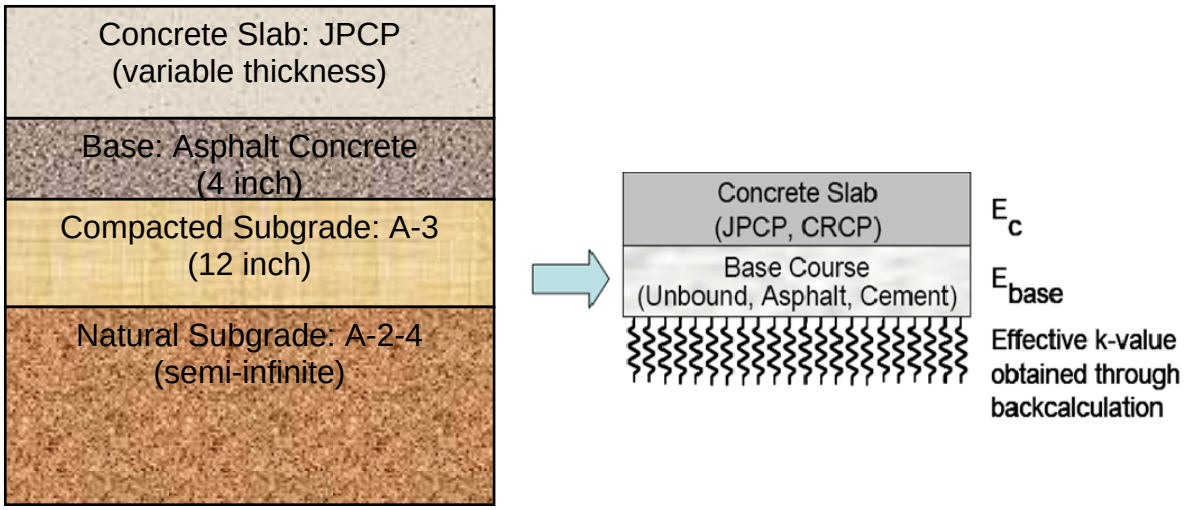

Figure 7.1: Structural research model and response model according to [X 15]

Depending on the selected trial design, sublayering may be necessary to satisfy the layering requirements of the analysis procedures. Specifying a trial design involves defining all pavement layers and material properties for each individual layer, including subgrade/bedrock. The following rules or constraints need to be satisfied in defining a rigid pavement structure for design [X 15]:

- The surface layer in rigid pavement design is always a PCC layer
- Slab-on-grade (two layers) is the minimum structure that can be analyzed
- Only one unbound granular layer can be placed between two stabilized layers
- The last two layers in the pavement structure must be unbound layers. To satisfy this constraint, the Design Guide Software automatically sublayers the subgrade into two identical layers for slab-on-grade pavements and for pavements where a bound layer rests directly on the subgrade

According to [X 15], pavement structures usually have four to six layers. However, the Design Guide Software may internally subdivide the pavement structure into 12 to 15 sublayers for the modeling of temperature and moisture variations. Only the unbound base layers thicker than 6 inches and unbound subbase layer thicker than 8 inches are sublayered. For the base layer (first unbound layer), the first sublayer is always 2 inches. The remaining thickness of the base layer and any subbase layers that are sublayered are

divided into sublayers with a minimum thickness of 4 inches. For compacted and natural subgrades, the minimum sublayer thickness is 12 inches. A pavement structure is sublayered only to a depth of 8 feet from the surface. Any remaining subgrade is treated as an infinite layer. If bedrock is present, the remaining subgrade is treated as one layer beyond 8 feet. Bedrock is not sublayered and is always treated as an infinite layer.

The following subparagraphs deliberate the selected pavement structure and the incorporated material characteristics. In this text, only key data will be presented but detailed information can be found in Appendix A, section A.8. Although the Design Guide Software requests the data from top to bottom, for the report it was decided to build the structure model from bottom up. The assembly was developed in collaboration with the Florida DOT Office of Roadway Design and its pavement management section based on locally available material (Region 5).

7.5.1. Layer # 4: Bedrock

Bedrock material is the soil assumed to be found at the location of the virtual paving project or roadway. It is the last layer the Design Guide Software includes for calculating distresses and smoothness models. Consequently, it must be considered semi-infinite, without any thickness value. Material properties for this layer are fed into the Design Guide Software on level three base – hierarchy level one and two do not apply for bedrock [X 15]. According to AASHTO classifications, the unbound soil is assumed to be A-2-4 material with a maximum dry unit weight of 115 pcf. Depending on those characteristics, a Poisson's ratio of 0.35, and the coefficient of lateral earth pressure K_o, which is estimated at 0.5, the software determines the layers' resilient modulus, necessary for the analysis process. Detailed information of soil properties, index properties, and results from sieve analysis for A-2-4 material can be found in Appendix A

7.5.2. Layer # 3: Subgrade Layer

For rigid pavement analysis, level one input is not available for base, subbase and subgrade. Moreover, since level two requires soil sample testing already, it was decided to use level three input which requires estimation using a correlation from soil classification such as AASHTO or UCS. Therefore, the subgrade in this study is defined as unbound material A-3 according to AASHTO classification, 12 inches in thickness. Its Poisson's ratio value is 0.35 while 0.5 represents the coefficient of lateral earth pressure K_o. Maximum dry unit weight shows a value of 101.3 pcf at a specific gravity of 2.70. Appendix A outlines additional information which was necessary to define the subgrade layer used in this research.

7.5.3. Layer # 2: Base Layer

The base course for this research is asphalt-stabilized as is mostly the case for rigid pavement applications in Florida. No sublayering is done within the asphalt-stabilized base layer for rigid design and analyses purposes within the Design Guide Software [X 15]. The material inputs required for this layer are grouped under two broad categories – general materials inputs and inputs required to construct E* master curve.

The primary material property of interest for asphalt-stabilized layers is its dynamic modulus, E*. A master curve of E* versus reduced time needs to be derived that defines the behavior of this layer under loading and at various climatic conditions. For input Levels two and three, the dynamic modulus prediction equation (outlined in Part 2 Chapter 2 in [X 15]) is used to construct the master curve. Figure 7.2 shows the master curve developed for the base layer derived from the material characteristics below.

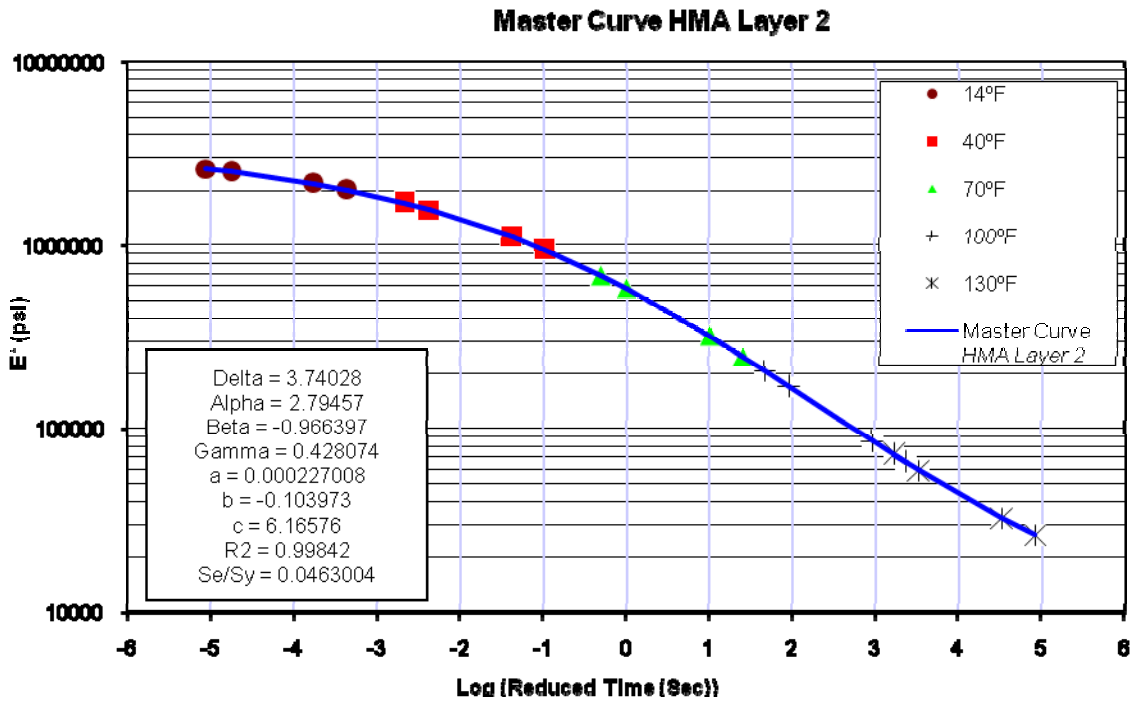

Figure 7.2: Master curve for stabilized base layer (asphalt bounded)

The base layer is made of asphalt concrete with a designated thickness of 4 inches. Aggregate gradation is specified at 0 % retaining on sieve 3/4, 15 % on sieve 3/8, and 35 % on sieve #4, while 5.7 % passes sieve #200. The employed asphalt binder is classified as PG70-22 using superpave binder grading at a reference temperature of 70°F for master curve development. Total unit weight shows a value of 148 pcf with an air void content of 7 % and an effective binder content of 11 %.

7.5.4. Layer # 1: Surface Layer

The layers listed above will serve as research framework and remain untouched throughout the entire study. Layers 4, 3, and 2 are the underlying sub-structure constantly supporting the interchanging PCC surface layers, outlined next. The goal is to evaluate the total pavement response in consequence of interchanging concrete materials (three different Florida concrete pavement mix designs) and their input precision (three different hierarchy levels). Based on the results obtained from research phase one, three different data categories will be developed regarding each mix design.

The M-E Design Guide Software explicitly accounts for different PCC layer hierarchy levels for strength related properties only. Nevertheless, a few input parameters might be determined on different quality levels as well (e.g. Poisson's Ratio, CTE, etc). They may be laboratory-measured, calculated based on raw material properties, or taken from data bases and default values. These values define this research and will be unambiguously outlined under the next three subheadings for all mix designs. However, prior to that, the constant PCC parameters will be presented in Table 7.1. These data are not necessarily independent of hierarchy levels (e.g. thermal conductivity, heat capacity, etc.) but they are outside of the research scope. Therefore, the table outlines the permanent PCC properties used in this study.

Table 7.1: General input parameters for PCC layer

	Unit	MIX-01	MIX-02	MIX-03
General and Thermal				
Layer thickness	in	variable		
Unit weight	pcf	143.1	146.6	144.2
Thermal conductivity •	BTU/hr-ft-°F	1.25		
Heat capacity •	BTU/lb-°F	0.28		
Mix				
Cement Type	-	Type I		
Cementitious material content	lb/yd3	643	520	470
Water/cement ratio	-	0.546	0.622	0.568
Aggregate type	-	limestone		granite
Zero-stress temperature •	°F	110	103	100
Ultimate shrinkage at 40% R.H. •	µin/in	903	780	680
Reversible shrinkage	%	50		
Time to develop 50% shrinkage	days	35		
Curing method	-	Curing compound		

• non-empirical value (suggested by ME-PDG)

7.5.4.1. Layer # 1 Under Hierarchy Level One Consideration

Hierarchy level one is considered most precise as it requires laboratory-tested results for all properties necessary. In this research, level one numbers will be exclusively based on data obtained from research phase one. As deviation was found to be within normal ranges, the employed numbers were derived from averaging all sample results within the

data series under consideration. Where the Design Guide Software requires only one single input, it was decided to use 90-day average data. Although 28-day properties are normally used in concrete (pavement) design, it was found to be more conservative to use 90-day data for Poisson's ratio and CTE as they kept growing after the 28th day.

Table 7.2: Level one input parameters for PCC layer

	Unit	MIX-01	MIX-02	MIX-03
General and Thermal				
Coefficient of thermal expansion	µin/in/°F	6.79	6.84	5.99
Poisson's ratio	-	0.23	0.27	0.21
Strength (level 1)				
E-modulus (7-day)	psi	4370000	4530000	3290000
E-modulus (14-day)	psi	4590000*	4590000*	3470000
E-modulus (28-day)	psi	4420000*	4360000*	3680000
E-modulus (90-day)	psi	4180000*	4905000	4020000
20 year/28 day ratio •	-	1.2		
Modulus of rupture (7-day)	psi	714	777	545
Modulus of rupture (14-day)	psi	745♦	825♦	603.5♦
Modulus of rupture (28-day)	psi	776	873	662
Modulus of rupture (90-day)	psi	844	831*	707
20 year/28 day ratio •	-	1.2		

* measured values not increasing as expected by theory
♦ non-empirical value (linearly interpolated)
• non-empirical value (suggested by ME-PDG)

7.5.4.2. Layer # 1 Under Hierarchy Level Two Consideration

Hierarchy Level two is referred to as intermediate design level using input data from less-than-optimal testing conditions. Although strength-related data is available under level one consideration, the required level two parameters can be isolated. However, the essential property to this research is the thermal behavior of the PCC layer. Section 2.3.4 outlines the principle to determine CTE based on volumetric proportion of ingredients (rule of mixture) – the proposed technique to compute CTE under hierarchy level two deliberation. Table 7.3 displays the volumetric proportions of ingredients and their CTE ranges for the materials used in this research.

Table 7.3: CTE values for hierarchy level two

Property	Unit	MIX-01	MIX-02	MIX-03
Cement Paste	% (V)	30.7	26.5	26.1
Coarse Aggregate	% (V)	41.6	29.7	44.8
Fine Aggregate	% (V)	27.8	43.8	29.1
CTE Cement Paste (min)	µin/in/°F	10.0	10.0	10.0
CTE Cement Paste (max)	µin/in/°F	11.0	11.0	11.0
CTE Coarse Aggregate (min)	µin/in/°F	3.3	3.3	4.0
CTE Coarse Aggregate (max)	µin/in/°F	3.3	3.3	6.0
CTE Fine Aggregate (min)	µin/in/°F	6.1	6.1	6.1
CTE Fine Aggregate (max)	µin/in/°F	7.2	7.2	7.2
CTE Concrete Calculated (min)	µin/in/°F	6.13	6.30	6.18
CTE Concrete Calculated (max)	µin/in/°F	6.75	7.05	7.65
CTE Concrete Calculated (mean)	µin/in/°F	6.44	6.68	6.92

The M-E Design Guide Software processes data much different for level two. For level one calculations, every property is available from direct inputs and certain estimations have to be made when using level two data. The Design Guide predicts Young's modulus and modulus of rupture (flexural strength) based on compressive strength data only. This property has to be made available to the software for 7, 14, 28, and 90 days. These parameters were achieved during research phase one, and proper values are presented in Table 7.4. It is emphasized that Poisson's ratio for hierarchy level two will not differ from level one consideration as there is no different definition available at this time.

Table 7.4: Level two input parameters for PCC layer

	Unit	MIX-01	MIX-02	MIX-03
General and Thermal				
Coefficient of thermal expansion	µin/in/°F	6.44	6.67	6.92
Poisson's ratio	-	0.23	0.27	0.21
Strength (level 2)				
Compressive Strength (7-day)	Psi	4832	6183	3489
Compressive Strength (14-day)	Psi	6067	7442	4225
Compressive Strength (28-day)	Psi	6908	8256	4883
Compressive Strength (90-day)	Psi	7856	9188	5794
20 year/28 day ratio •	-	1.2		

• non-empirical value (suggested by ME-PDG)

7.5.4.3. Layer # 1 Under Hierarchy Level Three Consideration

Hierarchy level three is the lowest design level relaying on default database values or local experience. Again, the used strength data was obtained from level one testing. Nevertheless, Poisson's ratios as well as the different CTE values are obtained from databases or default values suggested by the literature.

Table 7.5: Level two input parameters for PCC layer

	Unit	MIX-01	MIX-02	MIX-03
General and Thermal				
Coefficient of thermal expansion	µin/in/°F	7		
Poisson's ratio	-	0.25		
Strength (level 3)				
Modulus of rupture (28-day)	psi	776	873	662
E-Modulus (28-day)	psi	4420000*	4360000*	3680000

* measured values not increasing as expected by theory

7.5.5. Design Features

Besides thickness inputs for each layer, the pavement structure model is exclusively concerned with material properties. However, to determine distresses and smoothness, structural details – e.g. joint spacing, slab width, etc. – have to be made available to the Software Design Guide. These construction details are referred to as design features by the new M-E PDG. The JPCP design features selected for this research are outlined below.

The aspect ratio of PCC slab is fixed at 0.86 which results from a joint spacing of 15 feet for a slab width of 13 feet (widened slab). Transverse joints are liquid-sealed and doweled using 1.5 inches diameter dowel bars spaced at 12 inches. Tied PCC shoulders are assumed with 40 % of long-term load transfer efficiency (separately constructed).

As outlined in 7.5.3, the base type is asphalt treated which results in an intermediate erodibility index of 3 (Erosion Resistant). Friction contact at the PCC-Base interface is assumed to be not applicable (zero friction contact).

7.6. Analytical Parameters

The above sums up the entire input data necessary to successfully analyze rigid pavement (JPCP) using the Design Guide Software. Based on this information, accumulative distresses and smoothness can be predicted using the Mechanistic-Empirical approach. It is important to remember that M-E design is not a thickness design; rather, it is considered to be an analytical procedure comparing predicted distresses and smoothness to target values provided by the user. Limiting numbers may differ from agency to agency and usual data ranges can be found in Appendix A, section A.5.

M-E JPCP analytical design is based on transverse cracking, transverse joint faulting, and pavement smoothness (IRI). To properly evaluate these pavement behaviors over the design life, target values and reliability factors were defined based on typical Florida conditions. Initial smoothness (IRI) for the virtual paving project was predefined at 58 inches per mile. The maximum value is referred to as terminal IRI which was limited to 160 inches per mile. Maximum transverse cracking was found to be adequate at less than 10 % slabs cracked while mean joint faulting has to maintain values below 0.12 inches. The reliability factor for all three performance criteria was fixed at 90.

In addition to Appendix A which summarizes general information for all input values and presents the M-E Design Guide Interfaces, Appendix B was created to provide a comprehensive overview of all parameters used in this research. While Appendix A exclusively deals with MIX-01, Appendix B captures all input data necessary for each mix design and all hierarchy levels in a convenient list view.

7.7. Analysis Approach

The M-E PDG research will be analytically conducted due to the diagnostic concept introduced by the M-E PDG. The first goal is to strive for the minimum PCC layer thickness while conformity of Florida distress and smoothness criteria (analytical parameters) is still guaranteed (including reliability). Thickness increments will be raised per quarter inch until any predicted performance criterion exceeds its limit. This strategy will be pursued for all mix designs under each hierarchy level.

After the ideal thickness has been determined for all scenarios, CTE sensitivity analysis will be initiated. The nine established pavement models will form the basic framework for the analysis matrix. Moreover, to properly evaluate the sensitivity of pavement performance and the mechanistic-empirical analysis method to CTE, the only control variable will be CTE while all other parameters will be held fixed. Although in reality it is very unlikely for one single concrete property to change its magnitude without causing differences in other characteristics, it was determined to vary CTE only as it is believed to preeminently show M-E PDG susceptibility to CTE. Values will ascend/descend by 0.10 μin/in/°F increments within a ± 10 % array. This will cause an analysis matrix of 15 (CTE values) by 6 (analysis criteria) per mix design and hierarchy level, resulting in a total sensitivity matrix of 135 by 6.

CHAPTER 8: M-E PDG RESEARCH - TEST RESULTS

8.1. Introduction

This section summarizes the results obtained from the experimental program which was conducted using the new M-E PDG Software. The following tables and figures are the product of significant findings. They were created for comparison and analysis of individual mix designs and hierarchy levels.

8.2. Results of Thickness Analysis

The thickness analysis was conducted by means of quarter inch increments. First, the starting PCC layer depth was fixed at 7.5 inches for all mixtures and hierarchy levels. Then, the thickness parameter was increased until the first pavement performance criterion was exceeded. The ideal thickness was determined through the measurement satisfactorily fulfilling all criteria. The following table outlines the numerical results of the thickness analysis.

Table 8.1: PCC layer thickness

	Unit	MIX-01	MIX-02	MIX-03
Level-1 thickness (h)	in	8.75	8.25	9.00
Level-2 thickness (h)	in	10.25	10.75	13.50
Level-3 thickness (h)	in	10.50	7.50	12.00

The numbers in Table 8.1 are the result of an extensive computer modeling process and iterative analyses. As opposed to MIX-02 and MIX-03, MIX-01 follows an expected pattern increasing its thickness with raised hierarchy level. Due to the 28-day modulus of rupture input, this pattern is broken for MIX-02. The 28-day flexural strength is unexpectedly high and even higher than the 90-day strength. However, the 28-day value (and the 28-day Young's modulus) is the only strength input for level three, whereas level two relays on compressive strength for all maturity levels (7, 14, 28, and 90-day). Notice that level three thickness even undercuts level one thickness. A similar approach

explains the behavior of MIX-03: the modulus of rupture is higher than expected when deriving from compressive strength input under level two.

The following compares the different mix designs due to their hierarchy levels for individual performance criteria. The graphs were created to visually depict the predicted pavement behavior over the entire design life for each of the nine structure models.

8.2.1. Results of Load Transfer Efficiency

Load transfer is a term used to describe the transfer (or distribution) load across discontinuities such as joints or cracks (AASHTO, 1993) [W 11]. When a wheel load is applied at a joint or crack, both the loaded slab and adjacent unloaded slab deflect. If a joint is performing perfectly, both the loaded and unloaded slabs deflect equally (LTE = 100 %).

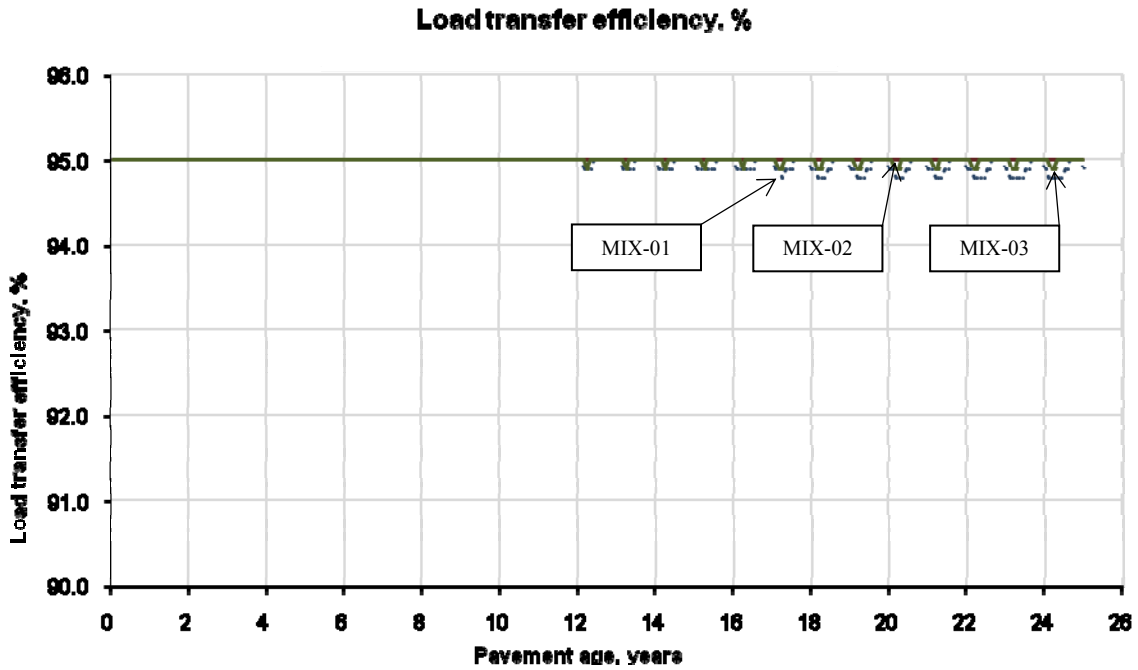

Figure 8.1: Level-1 load transfer efficiency

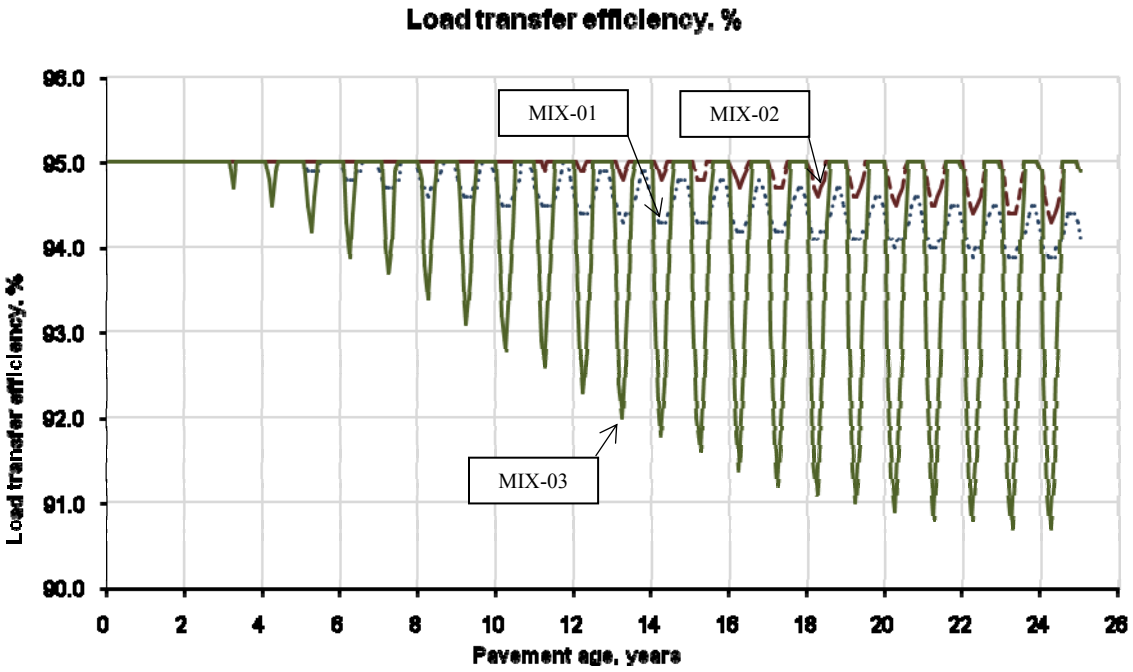

Figure 8.2: Level-2 load transfer efficiency

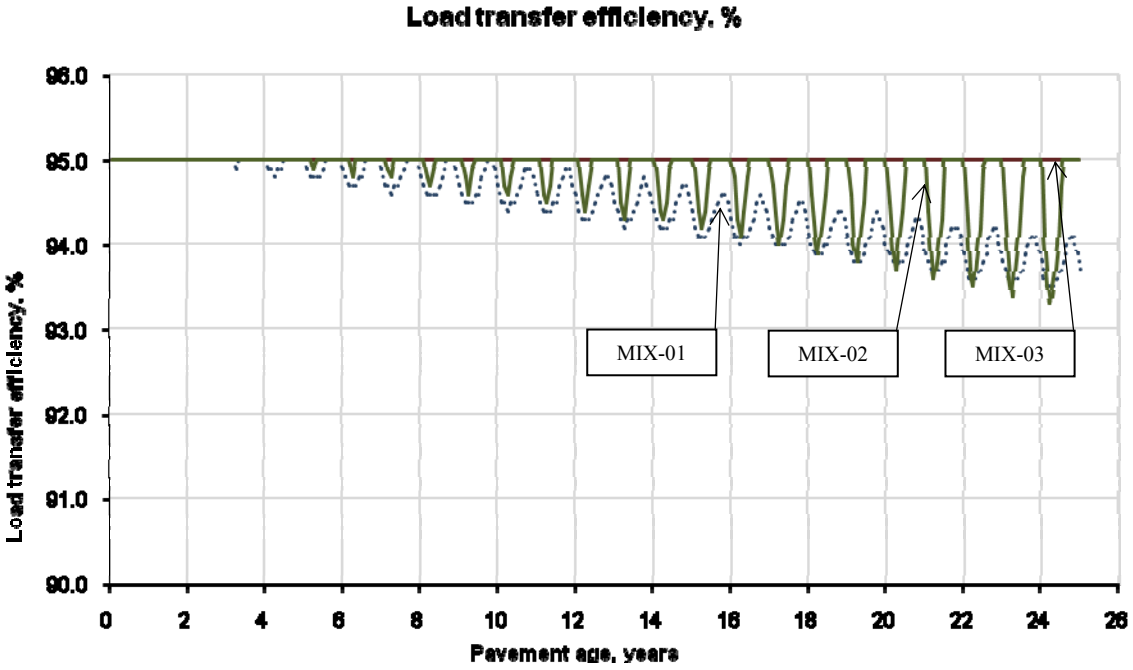

Figure 8.3: Level-3 load transfer efficiency

In this research, load transfer efficiency is not governing. In fact, LTE reduction is very small for all mix designs and all hierarchy levels until the end of the design life. However, the ordinate scale was overdrawn to emphasize affecting aspects.

In general, level one is least susceptible to LTE change and level two shows the highest response. MIX-02 exclusively loses LTE under level two consideration (thickest MIX-02 structure) and stays constant for levels one and three. MIX-01 loses LTE with increasing hierarchy level (increasing thickness). MIX-03 shows moderate LTE decrease under level one (thinnest PCC layer) and the most significant LTE change under level two (thickest PCC layer) MIX-03 layer.

Most performance problems with concrete pavement are a result of poorly performing joints [W 11]. Poor load transfer creates high slab stresses, which contribute heavily to distresses such as pumping, corner breaks, and faulting. Thus, adequate load transfer is vital to rigid pavement performance. Therefore, it is important to emphasize the frequency pattern of the LTE response. This mode is a resultant of weather fluctuation throughout each year and other resulting factors. The best visualization results from MIX-03 at level two. Notice that LTE drops as much as 4.2 % but not more than 0.5 % at the end of the pavement design life.

The load transfer efficiency depends on several factors including temperature, joint spacing, number and magnitude of load applications, base support, aggregate interlocking, the presence of dowel bars, and others. LTE reduction shows only minor effects here because those factors were beneficially chosen. A more explicit explanation will be provided in the following section as transverse joint faulting is the actual performance criteria and it ties closely into LTE.

8.2.2. Results of Transverse Joint Faulting

Transverse joint faulting is the differential elevation across the joint measured approximately one foot from the slab edge, or from the rightmost lane paint stripe for a widened slab [W 11]. Since joint faulting varies significantly from joint to joint, the mean faulting of all transverse joints in a pavement section is the predicted parameter in the M-E Pavement Design Guide. Faulting is a direct resultant of LTE decrease and an

important deterioration mechanism of JPCP because of its impact on ride quality (IRI, smoothness).

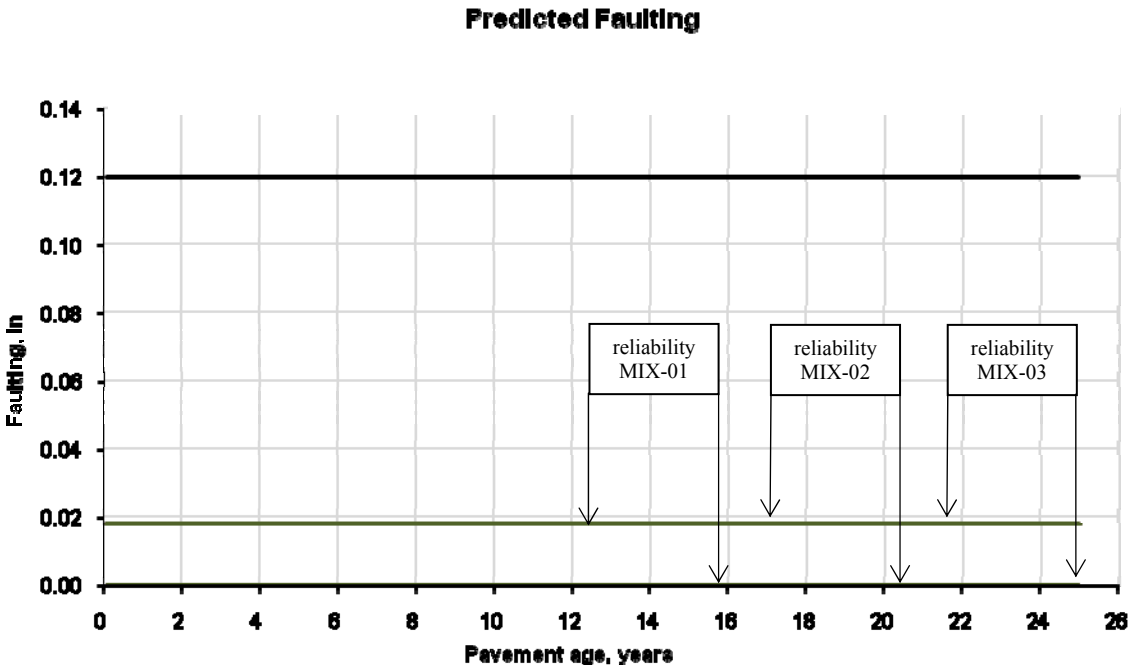

Figure 8.4: Level-1 predicted faulting

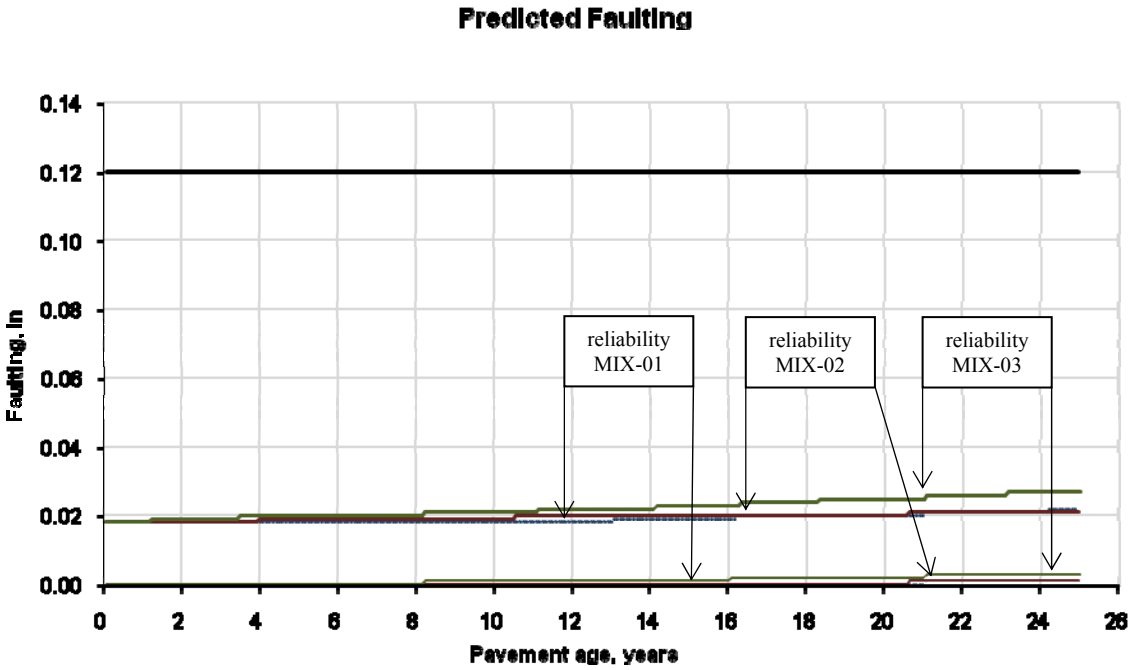

Figure 8.5: Level-2 predicted faulting

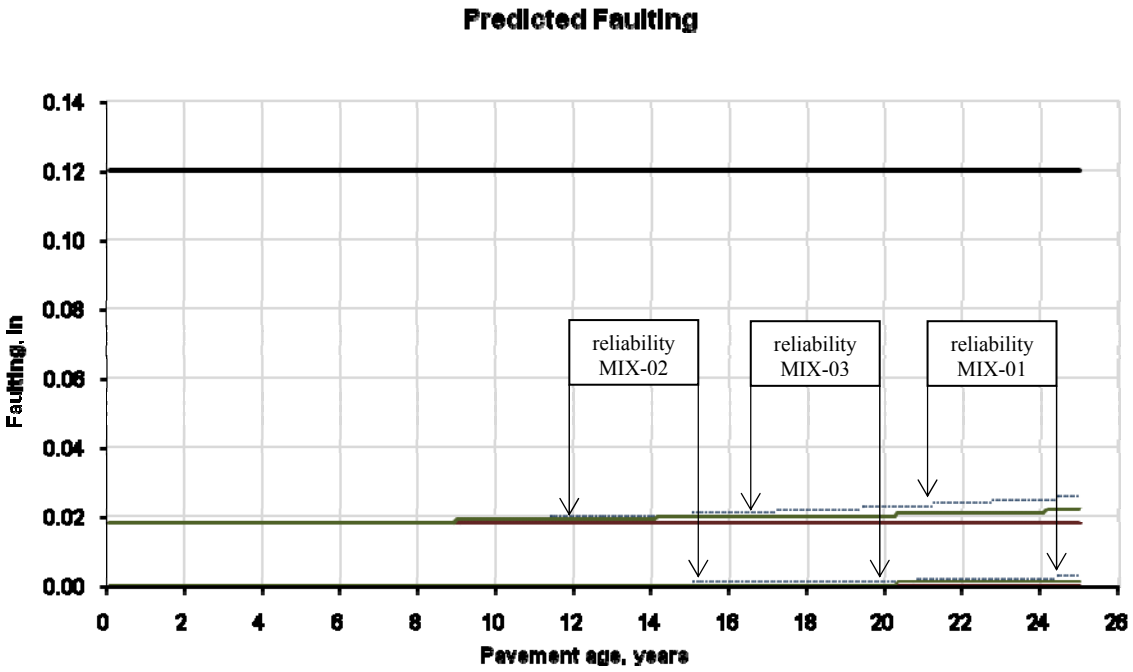

Figure 8.6: Level-3 predicted faulting

Faulting is not a concern for all scenarios; the predicted faulting performance stays constantly (far) below its limit of 0.12 inches (resultant of LTE). For level one consideration, faulting does not occur in any mix design causing a constant reliability faulting of 0.018. Under level two and three, MIX-02 experiences the smallest faulting throughout the design life while MIX-03 shows the highest faulting. The better performance of MIX-02 is founded on superior strength. However, it is emphasized that MIX-03 possesses the lowest and MIX-01 the highest PCC zero-stress temperature. Furthermore, notice that faulting begins early (8 years) at level two and later (15 years) for level three.

In general, faulting is not the thickness-determining criteria in this research for several reasons. A small but meaningful factor is the permanent curl/warp effective temperature difference. In this research the national calibration value of -10°F was used, a mid-ranging value which is beneficial under Florida weather conditions. Further, lower faulting is a resultant of less erodible base material and a small P_{200} value. Here, all PCC layers are supported by an asphalt-treated base with an erodibility index of 3 and 5.7 % passing through sieve #200. Also, shorter joint spacing results in smaller joint openings.

Thus, aggregate interlocking has a more useful effect on maintaining higher LTE. Additionally, the predicted mean joint faulting is smaller for shorter joint spacing (e.g., 13 foot). Moreover, a central feature is the edge support and the load location. The widened slab (13 foot) effectively moves the wheel away from the slab corner, greatly reducing the deflection of the slab and the potential for erosion and pumping. However, the most dominant properties reducing faulting are the doweled transverse joints and the massive diameter of 1.5 inches. A slight increase of dowel diameter significantly increases joint shear stiffness and reduces the mean steel-to-PCC bearing stress and, thus, the joint faulting [X 15].

8.2.3. Results of Cumulative Damage

Transverse cracking of PCC slabs can initiate either at the top surface of the PCC slab and propagate downward (top-down cracking) or vice versa (bottom-up cracking). The potential for either mode of cracking is present in all slabs. Damage accumulates differently for each of these different distresses and hence needs to be considered separately.

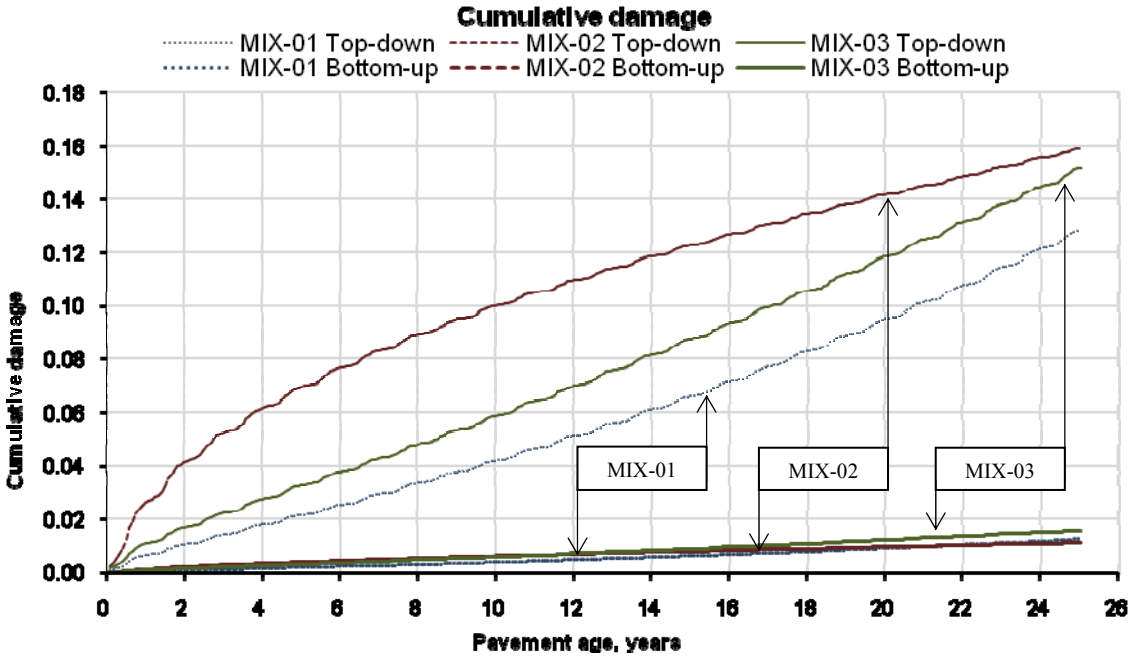

Figure 8.7: Level-1 cumulative damage

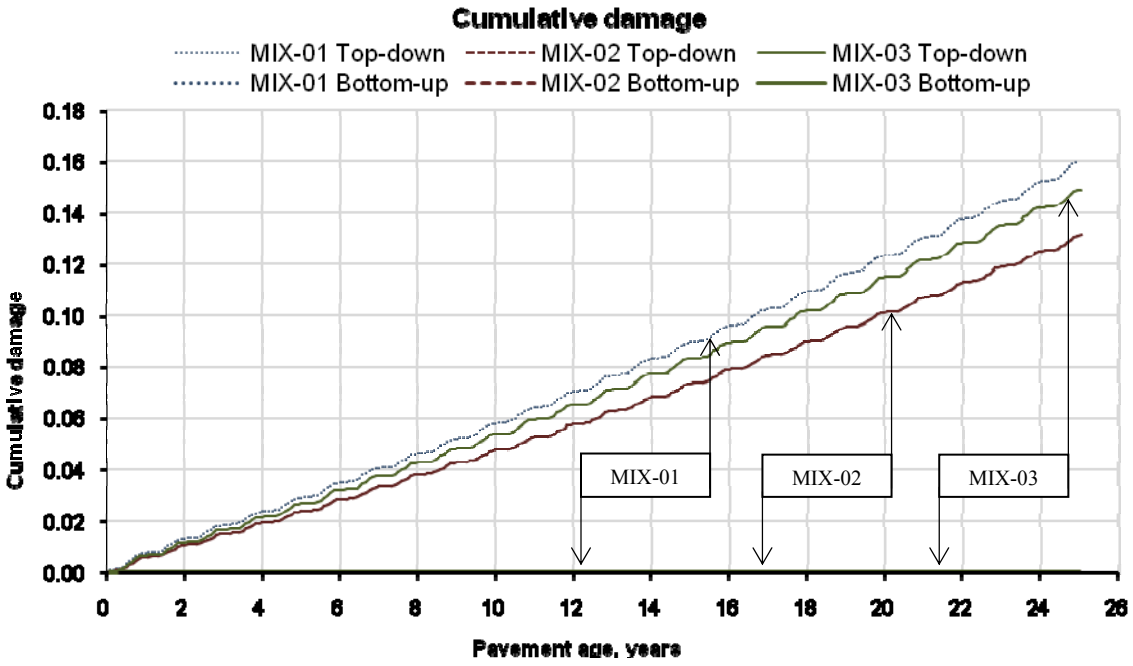

Figure 8.8: Level-2 cumulative damage

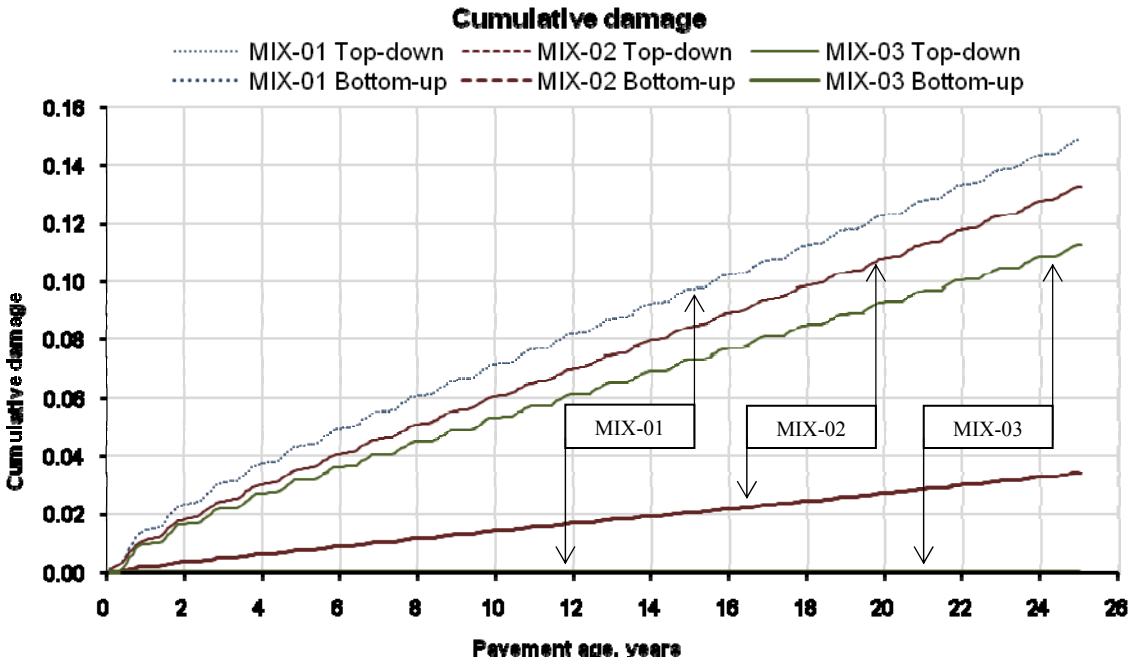

Figure 8.9: Level-3 cumulative damage

The same factors that affect bottom-up transverse cracking affect top-down cracking. However, different design parameters have a dissimilar impact on different performance measures.

Bottom-up damage shows only minor effects (if any) for the structural pavement models studied in this evaluation. It exists for all three mix designs under level one consideration, for none mix design at level two, and only for MIX-02 at level three where it experiences its highest magnitude with 0.034 (fraction). Bottom-up cracking is a bending problem most critical at the outermost edge and the insusceptibility in this research is a consequence of tied PCC shoulders and widened slabs. However, the minor occurrences in this study are simply due to different thicknesses. At level one, all PCC layers are very thin (relative to this study), and therefore susceptible to bottom-up damage. The same applies to MIX-02 under level three consideration. Because of its high 28-day flexural strength, the layer obtains the smallest thickness and is mostly affected by bottom-up damage.

Top-down damage is more prominent and widely exceeds bottom-up cracking for all scenarios. MIX-01 show highest fractions at level two and three but the smallest at level one. MIX-02 shows the (absolute) highest value for level one consideration and the lowest for level three. MIX-03 experiences its highest values at levels one and two but the overall lowest value under level three. Notice that in Figure 8.7, the convex character of the graph for MIX-02 at level one is the only constellation where top-down damage follows such a path; for all other scenarios the graph takes a concave shape.

Any given slab may crack either from the bottom up or from the top down, but not both. Therefore, the predicted bottom-up and top-down cracking are not particularly meaningful by themselves, and combined cracking must be determined, excluding the possibility of both modes of cracking occurring on the same slab.

8.2.4. Results of Predicted Cracking

The percentage of slabs with transverse cracks in a given traffic lane is used as the measure of transverse cracking. Throughout the design life, predicted cracking indicates the percentage of total slabs that shows transverse cracking.

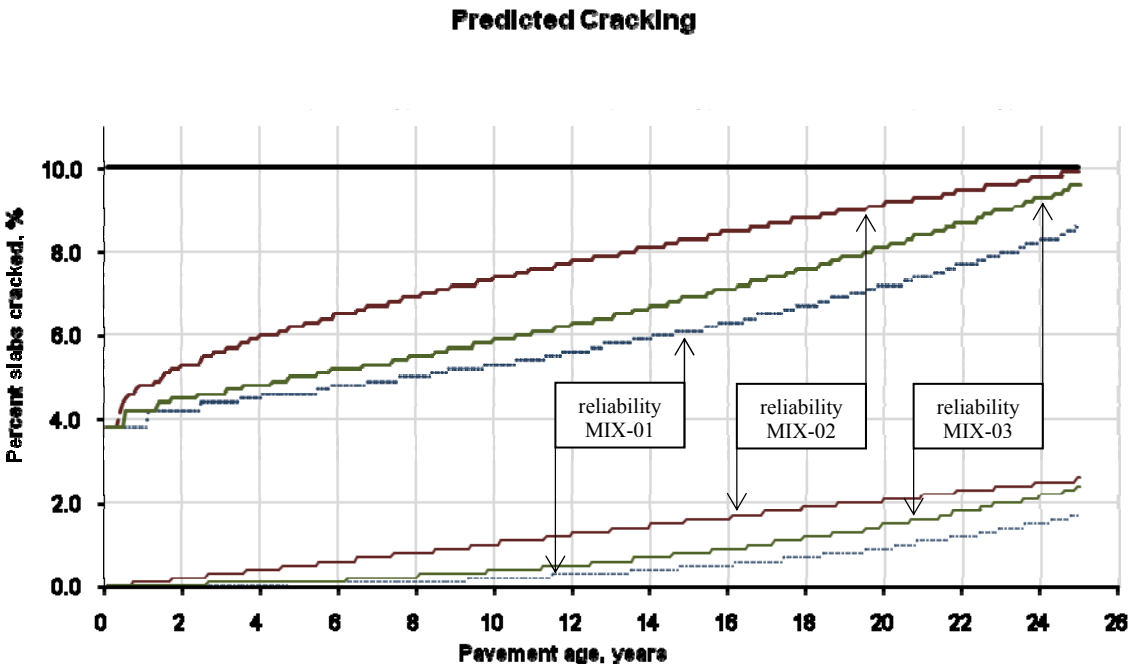

Figure 8.10: Level-1 predicted cracking

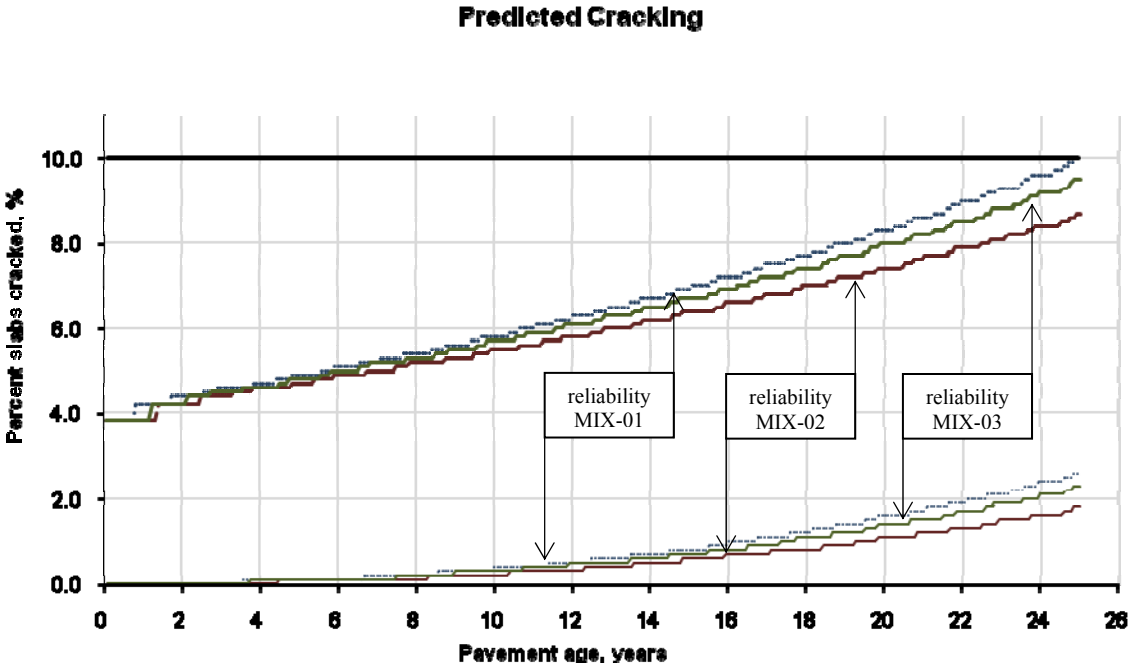

Figure 8.11: Level-2 predicted cracking

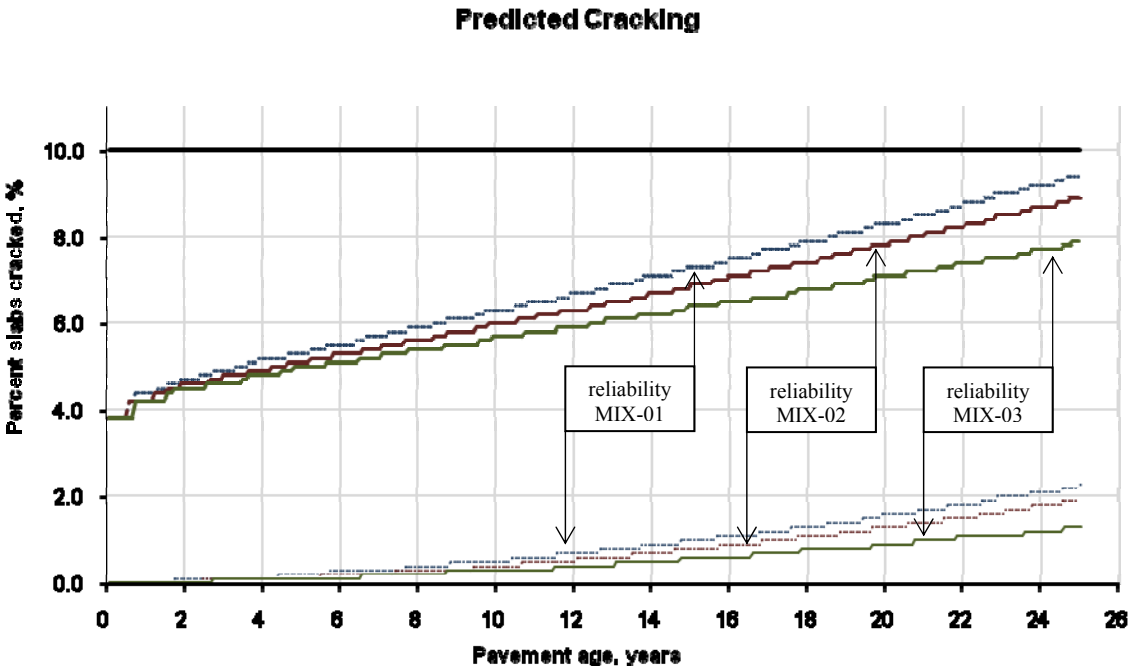

Figure 8.12: Level-3 predicted cracking

Predicted cracking is the thickness determining pavement performance criterion for the nine evaluated PCC layer. All models have been taken to the limit of 10 % slabs cracked as close as possible considering depth increments of 0.25 inches. Predicted cracking is the most critical performance in this research because of the eminent top-down fatigue damage behavior.

Notice that the percentage slabs cracked graphs follow the behavior of the top-down fatigue damage for all mix designs and hierarchy levels constantly; therefore, it also returns the convex shape of MIX-01 at level 1. It must be emphasized that any slab may experience either bottom-up or top-down cracking, but not both simultaneously which is accounted for by the M-E PDG cracking model:

$$TCRACK = \left(CRK_{Bottom-up} + CRK_{Top-down} - CRK_{Bottom-up} * CRK_{Top-down}\right)100\% \qquad (8.1)$$

Where: TCRACK = total cracking (%)

$CRK_{Bottom-up}$ = predicted amount of bottom-up cracking (fraction)

$CRK_{Top-down}$ = predicted amount of top-down cracking (fraction)

Equation 8.1 turns the top-down damage into the central failure criterion for this research because bottom-up damage is constantly overshadowed.

8.2.5. Results of Predicted Smoothness (IRI)

The international roughness index is used to define the characteristic of the longitudinal profile of a traveled wheel track and constitutes a standardized roughness measurement [W 11]. It is based on the average rectified slope (ARS), which is a filtered ratio of a standard vehicle's accumulated suspension motion divided by the distance traveled by the vehicle during the measurement. The M-E PDG approach predicts the change in IRI as a function of pavement distresses, site conditions, and maintenance. Smoothness is the most important pavement characteristic as rated by the highway user [X 15].

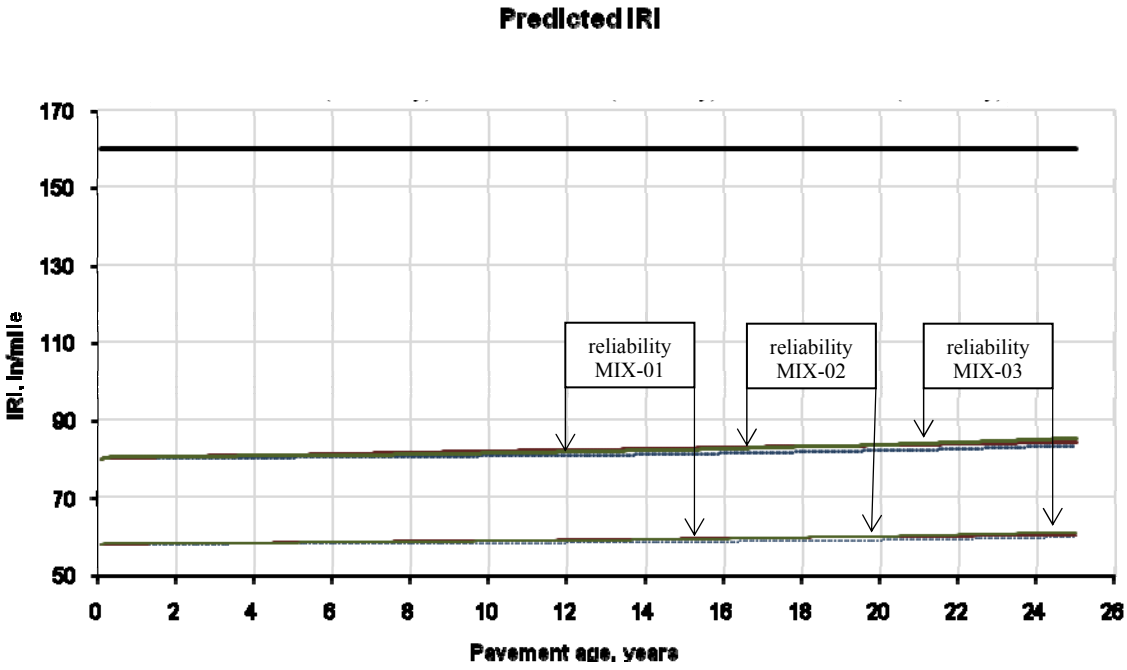

Figure 8.13: Level-1 predicted IRI

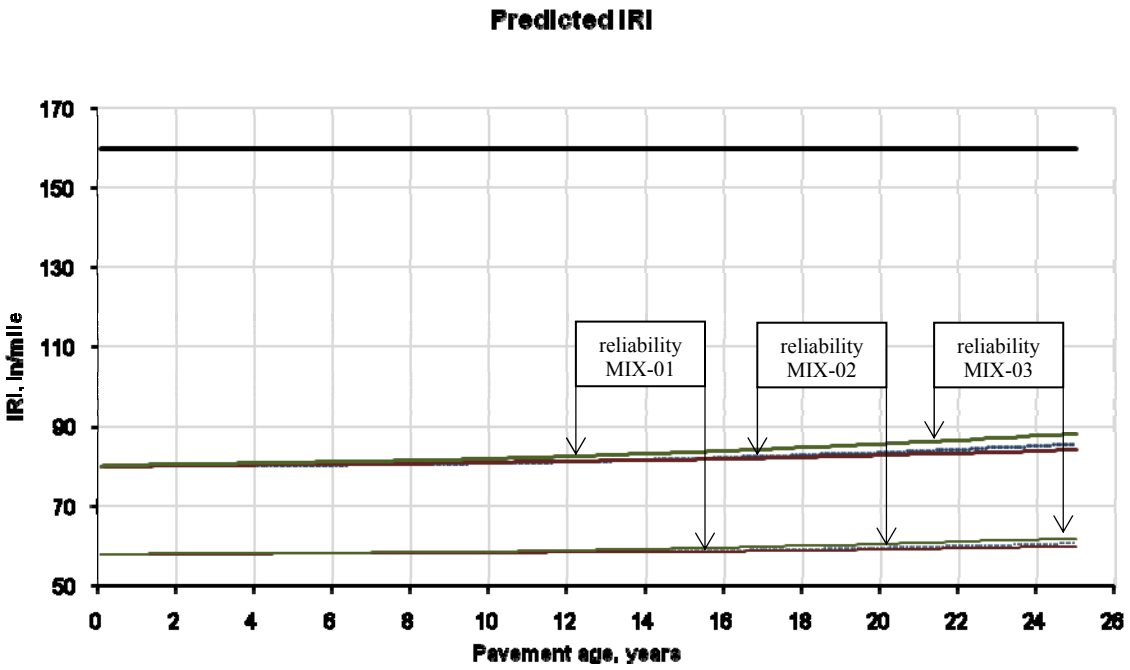

Figure 8.14: Level-2 predicted IRI

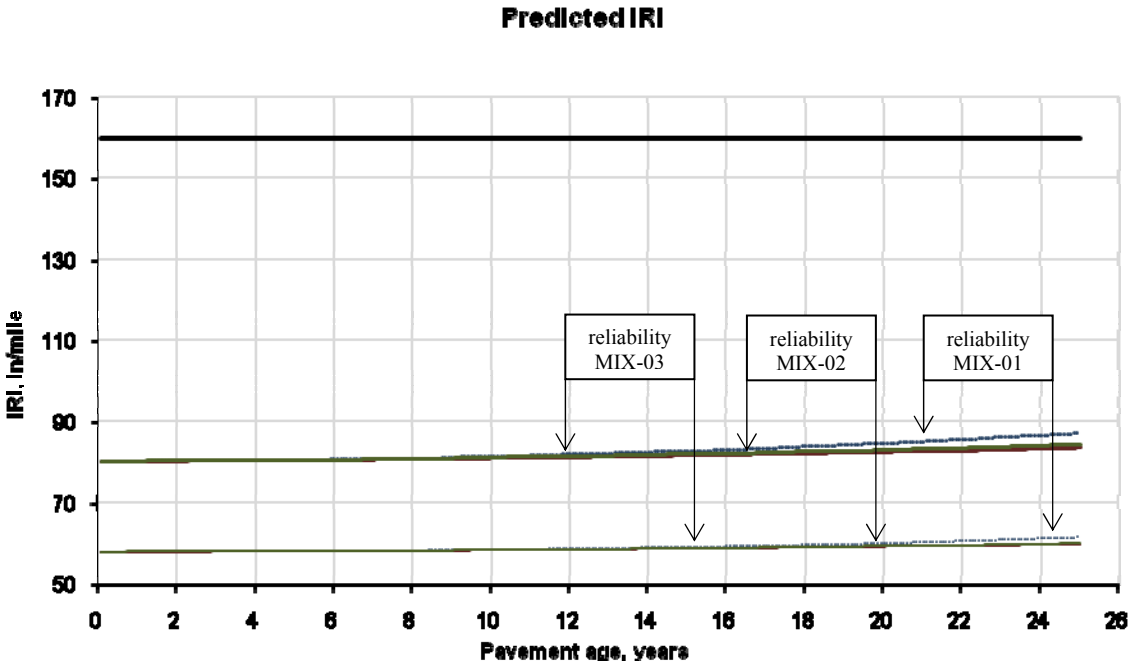

Figure 8.15: Level-3 predicted IRI

International roughness index is not a critical performance criterion for all scenarios under evaluation; the smoothness maintains values far below its limit of 160 inches per mile – even for reliability consideration. Moreover, it shows only marginal growth rates.

Due to smoothness-affecting factors, the predicted roughness index may almost be disregarded for the thickness analysis.

Notice that all mix designs within each hierarchy level approximately follow their faulting mode, meaning higher faulting results in more roughness. This is attributed to the mechanistic-empirical smoothness model, which remits the lion's share to faulting. According to M-E PDG prediction model, IRI is calculated as follows:

$$IRI = IRI_i + C1 * CRK + C2 * SPALL + C3 * TFAULT + C4 * SF \qquad (8.2)$$

where:

	IRI	= predicted IRI, in/mi
	IRI_i	= initial smoothness measured as IRI, in/mi
	CRK	= % slabs with transverse cracks (all severities)
	SPALL	= % of joints with spalling
	TFAULT	= total joint faulting cumulated per mi, in
	C1	= 0.8203
	C2	= 0.4417
	C3	= 1.4929
	C4	= 25.24
	SF	= site factor

The values C1, C2, C3, and C4 are empirical factors, their numerical values are nationally calibrated through the long-term pavement performance (LLTP) data. At a later point those values need to be adjusted for proper application of the M-E PDG in Florida. However, this research utilized the above mentioned (national) values turning faulting (and to a minor extent cracking) into the governing factor. Therefore, the observations for faulting apply.

8.2.6. Summary of Pavement Performance Results

It can be stated that cracking is the most critical performance criterion in Florida. All evaluated mix designs attain the "% slabs cracked limit" of 10 % before any other performance criteria tends to be problematic according to the chosen (Florida) analysis parameters. However, the results are highly dependent on the selected JPCP design features. The widened slabs with tied PCC shoulders and doweled transverse joints supported by an asphalt-treated base maintain faulting values in moderate ranges, far below the designated Florida limit of 0.12 inches. Of course, less faulting results in better driving quality and smoother pavement surface causing almost negligible IRI augmentation throughout the design life. Furthermore, because of its failure mechanism, bottom-up cracking benefits from widened slabs and tied PCC shoulders as well. When truck axles are near the longitudinal edge of the slab, midway between the transverse joints, the critical tensile bending stress occurs at the bottom of the slab, which is greatly reduced by those two JPCP design features. In essence, top-down fatigue damage can be isolated to be the controlling failure mechanism in this research; the percentage of cracked slabs is directly proportional to top-down damage for all scenarios turning the predicted cracking into the most critical pavement performance.

8.3. Results of CTE Sensitivity

The above assigned pavement thicknesses and performance analyses are the designated substructures for the CTE sensitivity matrices. In general, the above evaluation outlines the center values for each mix design and hierarchy level. Each 6 by 15 matrix will be stipulated through its CTE array (± 10 %) and the five consequential performance criteria at the end of the design life. The following tables outline the resultant total CTE sensitivity matrix.

Table 8.2: CTE sensitivity matrix for MIX-01

MIX-01												
Level	h	CTE		IRI		Faulting		LTE	Cum. Fatigue Damage		Cracking	
	in	μin/in/F	%	in/mile		in		%	(fraction)		% slabs cracked	
					at Spec. Reliability		at Spec. Reliability		Bottom-up	Top-down		at Spec. Reliability
		6.09	87.1	58.7	81.3	0.000	0.018	94.9	0.0084	0.0464	0.2	5.5
		6.19	88.6	58.8	81.4	0.000	0.018	94.9	0.0089	0.0543	0.3	5.7
		6.29	90.0	58.9	81.6	0.000	0.018	94.9	0.0094	0.0634	0.4	6.0
		6.39	91.4	59.0	81.8	0.000	0.018	94.9	0.0100	0.0736	0.6	6.4
		6.49	92.8	59.1	82.1	0.000	0.018	94.9	0.0105	0.0853	0.8	6.8
		6.59	94.3	59.3	82.5	0.000	0.018	94.9	0.0111	0.0984	1.0	7.3
		6.69	95.7	59.6	82.9	0.000	0.018	94.9	0.0118	0.1127	1.3	7.9
		6.79•	97.1	59.9	83.4	0.000	0.018	94.9	0.0124	0.1285	1.7	8.6
1	8.75	6.89	98.6	60.3	84.1	0.000	0.018	94.9	0.0131	0.1461	2.2	9.4
		6.99	**100.0**	**60.8**	**84.9**	**0.000**	**0.018**	**94.9**	**0.0138**	**0.1662**	**2.8**	**10.3**
		7.09	101.4	61.5	86.0	0.000	0.018	94.9	0.0145	0.1893	3.6	11.5
		7.19	102.9	62.2	87.2	0.000	0.018	94.9	0.0153	0.2144	4.5	12.8
		7.29	104.3	63.2	88.8	0.000	0.018	94.9	0.0161	0.2421	5.7	14.4
		7.39	105.7	64.3	90.5	0.000	0.018	94.9	0.0169	0.2723	7.1	16.2
		7.49	107.2	65.8	92.8	0.000	0.018	94.9	0.0177	0.3078	8.9	18.5
		7.59	108.6	67.4	95.3	0.000	0.018	94.9	0.0186	0.3452	10.9	21.0
		7.69	110.0	69.4	98.3	0.000	0.018	94.9	0.0196	0.3861	13.2	23.8
		5.74	89.1	58.7	81.7	0.000	0.020	94.2	0.0002	0.0481	0.3	5.5
		5.84	90.7	58.8	81.9	0.000	0.020	94.2	0.0002	0.0577	0.3	5.8
		5.94	92.2	59.0	82.3	0.000	0.020	94.2	0.0002	0.0694	0.5	6.2
		6.04	93.8	59.2	82.7	0.001	0.021	94.2	0.0003	0.0825	0.7	6.7
		6.14	95.3	59.4	83.1	0.001	0.021	94.1	0.0003	0.0986	1.0	7.3
		6.24	96.9	59.8	83.8	0.001	0.021	94.1	0.0003	0.1160	1.4	8.0
		6.34	98.4	60.3	84.6	0.001	0.021	94.1	0.0003	0.1374	1.9	8.9
2	10.25	**6.44•**	**100.0**	**60.9**	**85.6**	**0.001**	**0.022**	**94.1**	**0.0003**	**0.1599**	**2.6**	**10.0**
		6.54	101.6	61.5	86.7	0.001	0.022	94.1	0.0003	0.1819	3.3	11.1
		6.64	103.1	62.4	88.2	0.001	0.022	94.0	0.0003	0.2085	4.3	12.5
		6.74	104.7	63.3	89.6	0.001	0.023	94.0	0.0003	0.2319	5.3	13.8
		6.84	106.2	64.5	91.6	0.001	0.023	94.0	0.0003	0.2635	6.7	15.6
		6.94	107.8	66.0	93.9	0.002	0.024	94.0	0.0004	0.2969	8.3	17.7
		7.04	109.3	67.3	95.9	0.002	0.024	93.9	0.0004	0.3254	9.8	19.6
		7.14	110.9	69.0	98.6	0.002	0.025	93.9	0.0004	0.3607	11.7	22.0
		6.30	88.7	59.2	82.9	0.001	0.022	94.0	0.0002	0.0547	0.3	5.7
		6.40	90.1	59.3	83.2	0.001	0.023	93.9	0.0002	0.0643	0.4	6.0
		6.50	91.5	59.6	83.6	0.001	0.023	93.9	0.0002	0.0752	0.6	6.4
		6.60	93.0	59.8	84.1	0.002	0.024	93.9	0.0002	0.0860	0.8	6.8
		6.70	94.4	60.1	84.6	0.002	0.024	93.8	0.0002	0.0960	1.0	7.2
		6.80	95.8	60.5	85.3	0.002	0.025	93.8	0.0002	0.1141	1.3	7.9
		6.90	97.2	60.9	86.0	0.002	0.025	93.7	0.0002	0.1242	1.6	8.4
		7.00•	98.6	61.6	87.2	0.003	0.026	93.7	0.0002	0.1489	2.3	9.5
3	10.50	**7.10**	**100.0**	**62.0**	**87.9**	**0.003**	**0.026**	**93.7**	**0.0002**	**0.1597**	**2.6**	**10.0**
		7.20	101.4	62.6	88.9	0.003	0.027	93.6	0.0002	0.1738	3.0	10.7
		7.30	102.8	63.3	90.2	0.004	0.028	93.6	0.0002	0.1947	3.8	11.7
		7.40	104.2	64.3	91.8	0.004	0.029	93.6	0.0002	0.2174	4.6	12.9
		7.50	105.6	65.2	93.2	0.005	0.030	93.5	0.0003	0.2362	5.4	14.0
		7.60	107.0	66.6	95.4	0.005	0.031	93.5	0.0003	0.2672	6.8	15.9
		7.70	108.5	67.5	97.0	0.006	0.031	93.5	0.0003	0.2833	7.6	16.9
		7.80	109.9	68.8	98.9	0.006	0.033	93.4	0.0003	0.3052	8.7	18.3
		7.90	111.3	70.0	100.9	0.007	0.034	93.4	0.0003	0.3277	9.9	19.7

• CTE value used for thickness analysis

Table 8.3: CTE sensitivity matrix for MIX-02

MIX-02												
Level	h	CTE		IRI		Faulting		LTE	Cum. Fatigue Damage		Cracking	
	in	μin/in/F	%	in/mile		in		%	(fraction)		% slabs cracked	
					at Spec. Reliability		at Spec. Reliability		Bottom-up	Top-down		at Spec. Reliability
		6.14	89.8	58.6	81.3	0.000	0.018	95.0	0.0077	0.0587	0.4	5.9
		6.24	91.2	58.7	81.5	0.000	0.018	95.0	0.0081	0.0685	0.5	6.2
		6.34	92.7	58.9	81.7	0.000	0.018	95.0	0.0086	0.0796	0.7	6.6
		6.44	94.2	59.1	82.0	0.000	0.018	95.0	0.0090	0.0921	0.9	7.1
		6.54	95.6	59.3	82.4	0.000	0.018	95.0	0.0095	0.1061	1.2	7.6
		6.64	97.1	59.6	82.9	0.000	0.018	95.0	0.0100	0.1216	1.5	8.3
		6.74	98.5	60.0	83.5	0.000	0.018	95.0	0.0106	0.1389	2.0	9.0
1	8.25	**6.84•**	**100.0**	**60.4**	**84.3**	**0.000**	**0.018**	**95.0**	**0.0110**	**0.1587**	**2.6**	**9.9**
		6.94	101.5	61.0	85.3	0.000	0.018	95.0	0.0116	0.1808	3.3	11.0
		7.04	102.9	61.8	86.5	0.000	0.018	95.0	0.0122	0.2055	4.2	12.3
		7.14	104.4	62.7	88.0	0.000	0.018	95.0	0.0128	0.2327	5.3	13.8
		7.24	105.8	63.8	89.7	0.000	0.018	95.0	0.0135	0.2633	6.7	15.7
		7.34	107.3	65.3	92.0	0.000	0.018	95.0	0.0142	0.2994	8.4	17.9
		7.44	108.8	66.7	94.2	0.000	0.018	95.0	0.0149	0.3330	10.2	20.1
		7.54	110.2	68.5	97.1	0.000	0.018	95.0	0.0156	0.3730	12.4	22.9
		5.97	86.9	58.7	81.7	0.000	0.020	95.0	0.0000	0.0582	0.4	5.8
		6.07	88.4	58.9	82.1	0.000	0.020	95.0	0.0000	0.0702	0.5	6.3
		6.17	89.8	59.1	82.6	0.000	0.020	95.0	0.0000	0.0906	0.8	7.0
		6.27	91.3	59.3	82.9	0.000	0.020	95.0	0.0000	0.1029	1.1	7.5
		6.37	92.7	59.7	83.6	0.001	0.021	95.0	0.0000	0.1194	1.5	8.2
		6.47	94.2	60.1	84.3	0.001	0.021	95.0	0.0000	0.1376	1.9	8.9
		6.57	95.6	59.9	83.9	0.001	0.021	94.9	0.0000	0.1262	1.6	8.4
		6.67•	97.1	60.0	84.2	0.001	0.021	94.9	0.0000	0.1314	1.8	8.7
2	10.75	6.77	98.5	60.4	84.9	0.001	0.022	94.8	0.0000	0.1473	2.2	9.4
		6.87	**100.0**	**60.9**	**85.7**	**0.001**	**0.022**	**94.8**	**0.0000**	**0.1622**	**2.7**	**10.1**
		6.97	101.5	61.2	86.2	0.001	0.022	94.7	0.0001	0.1691	2.9	10.4
		7.07	102.9	61.6	87.0	0.001	0.023	94.7	0.0001	0.1842	3.4	11.2
		7.17	104.4	61.9	87.5	0.001	0.023	94.6	0.0001	0.1904	3.6	11.5
		7.27	105.8	62.3	88.1	0.002	0.024	94.5	0.0001	0.1983	3.9	11.9
		7.37	107.3	62.7	88.9	0.002	0.024	94.4	0.0001	0.2096	4.3	12.5
		7.47	108.7	63.2	89.8	0.002	0.025	94.4	0.0001	0.2208	4.8	13.1
		7.57	110.2	63.7	90.6	0.002	0.025	94.3	0.0001	0.2300	5.2	13.7
		6.30	88.7	58.6	81.3	0.000	0.018	95.0	0.0233	0.0490	0.3	5.7
		6.40	90.1	58.7	81.4	0.000	0.018	95.0	0.0247	0.0572	0.4	6.0
		6.50	91.5	58.8	81.6	0.000	0.018	95.0	0.0260	0.0667	0.5	6.3
		6.60	93.0	59.0	81.8	0.000	0.018	95.0	0.0275	0.0772	0.7	6.7
		6.70	94.4	59.1	82.1	0.000	0.018	95.0	0.0290	0.0888	0.9	7.1
		6.80	95.8	59.4	82.5	0.000	0.018	95.0	0.0306	0.1017	1.2	7.6
		6.90	97.2	59.6	83.0	0.000	0.018	95.0	0.0323	0.1162	1.5	8.2
		7.00•	98.6	60.0	83.6	0.000	0.018	95.0	0.0341	0.1327	1.9	8.9
3	7.50	**7.10**	**100.0**	**60.4**	**84.3**	**0.000**	**0.018**	**95.0**	**0.0359**	**0.1508**	**2.4**	**9.8**
		7.20	101.4	60.9	85.1	0.000	0.018	95.0	0.0378	0.1712	3.1	10.8
		7.30	102.8	61.6	86.2	0.000	0.018	95.0	0.0399	0.1937	3.9	11.9
		7.40	104.2	62.4	87.5	0.000	0.018	95.0	0.0420	0.2186	4.9	13.3
		7.50	105.6	63.4	89.0	0.000	0.018	95.0	0.0442	0.2462	6.1	14.9
		7.60	107.0	64.5	90.9	0.000	0.018	95.0	0.0465	0.2765	7.5	16.7
		7.70	108.5	65.9	93.0	0.000	0.018	95.0	0.0490	0.3099	9.2	18.9
		7.80	109.9	67.6	95.5	0.000	0.018	95.0	0.0515	0.3465	11.2	21.3
		7.90	111.3	69.5	98.4	0.000	0.018	95.0	0.0541	0.3867	13.5	24.1

• CTE value used for thickness analysis

Table 8.4: CTE sensitivity matrix for MIX-03

MIX-03												
Level	h	CTE		IRI		Faulting		LTE	Cum. Fatigue Damage		Cracking	
	in	μin/in/F	%	in/mile		in		%	(fraction)		% slabs cracked	
					at Spec. Reliability		at Spec. Reliability		Bottom-up	Top-down		at Spec. Reliability
		5.29	88.3	59.3	82.3	0.000	0.018	95.0	0.0108	0.0408	0.2	5.3
		5.39	90.0	59.4	82.4	0.000	0.018	95.0	0.0114	0.0501	0.3	5.6
		5.49	91.7	59.5	82.6	0.000	0.018	95.0	0.0119	0.0610	0.4	6.0
		5.59	93.3	59.7	82.9	0.000	0.018	95.0	0.0126	0.0740	0.6	6.4
		5.69	95.0	59.9	83.3	0.000	0.018	95.0	0.0133	0.0895	0.8	7.0
		5.79	96.7	60.2	83.8	0.000	0.018	95.0	0.0140	0.1073	1.2	7.7
		5.89	98.3	60.6	84.4	0.000	0.018	95.0	0.0148	0.1278	1.7	8.6
1	9.00	**5.99•**	**100.0**	**61.1**	**85.3**	**0.000**	**0.018**	**95.0**	**0.0156**	**0.1517**	**2.4**	**9.6**
		6.09	101.7	61.8	86.5	0.000	0.018	95.0	0.0165	0.1789	3.2	10.9
		6.19	103.3	62.8	88.0	0.000	0.018	95.0	0.0174	0.2100	4.4	12.6
		6.29	105.0	64.1	90.1	0.000	0.018	95.0	0.0183	0.2481	6.0	14.8
		6.39	106.7	65.7	92.6	0.000	0.018	95.0	0.0192	0.2884	7.9	17.2
		6.49	108.3	67.7	95.6	0.000	0.018	95.0	0.0203	0.3350	10.3	20.3
		6.59	110.0	70.1	99.3	0.000	0.018	95.0	0.0213	0.3866	13.3	23.8
		6.69	111.7	72.9	103.6	0.000	0.018	95.0	0.0224	0.4440	16.7	28.0
		6.22	89.9	59.6	83.6	0.002	0.024	95.0	0.0000	0.0420	0.2	5.3
		6.32	91.3	59.7	84.0	0.002	0.025	95.0	0.0000	0.0502	0.3	5.6
		6.42	92.8	59.9	84.4	0.002	0.025	95.0	0.0000	0.0626	0.4	6.0
		6.52	94.2	60.2	84.9	0.002	0.025	95.0	0.0000	0.0771	0.6	6.5
		6.62	95.7	60.5	85.5	0.003	0.026	95.0	0.0000	0.0905	0.8	7.0
		6.72	97.1	60.9	86.1	0.003	0.026	95.0	0.0000	0.1075	1.2	7.7
		6.82	98.6	61.4	87.1	0.003	0.027	95.0	0.0000	0.1261	1.6	8.4
2	13.50	**6.92•**	**100.0**	**62.0**	**88.1**	**0.003**	**0.027**	**94.9**	**0.0000**	**0.1492**	**2.3**	**9.5**
		7.02	101.4	62.9	89.5	0.004	0.028	94.8	0.0000	0.1748	3.1	10.7
		7.12	102.9	63.6	90.7	0.004	0.029	94.6	0.0000	0.1930	3.7	11.6
		7.22	104.3	64.9	92.7	0.004	0.029	94.5	0.0000	0.2281	5.1	13.6
		7.32	105.8	66.2	94.7	0.005	0.030	94.4	0.0000	0.2591	6.5	15.4
		7.42	107.2	67.6	97.0	0.005	0.030	94.3	0.0000	0.2896	7.9	17.3
		7.52	108.7	69.2	99.5	0.005	0.031	94.2	0.0000	0.3232	9.7	19.4
		7.62	110.1	70.9	102.0	0.006	0.032	94.1	0.0000	0.3552	11.4	21.6
		6.30	87.5	59.2	82.5	0.000	0.020	95.0	0.0000	0.0656	0.5	6.1
		6.40	88.9	59.4	82.9	0.000	0.020	95.0	0.0000	0.0786	0.7	6.6
		6.50	90.3	59.6	83.3	0.000	0.020	95.0	0.0000	0.0926	0.9	7.1
		6.60	91.7	59.9	83.8	0.001	0.021	95.0	0.0000	0.1075	1.2	7.7
		6.70	93.1	60.1	84.3	0.001	0.021	95.0	0.0000	0.1210	1.5	8.2
		6.80	94.4	60.5	84.8	0.001	0.021	95.0	0.0000	0.1340	1.8	8.8
		6.90	95.8	60.5	84.9	0.001	0.021	95.0	0.0000	0.1333	1.8	8.8
		7.00•	97.2	60.1	84.4	0.001	0.022	95.0	0.0000	0.1127	1.3	7.9
3	12.00	7.10	98.6	60.6	85.2	0.001	0.022	95.0	0.0000	0.1306	1.8	8.6
		7.20	**100.0**	**61.1**	**86.0**	**0.001**	**0.022**	**94.9**	**0.0000**	**0.1490**	**2.3**	**9.5**
		7.30	101.4	62.0	87.6	0.001	0.023	94.8	0.0000	0.1811	3.3	11.0
		7.40	102.8	63.5	89.9	0.002	0.023	94.7	0.0000	0.2243	4.9	13.3
		7.50	104.2	64.0	90.8	0.002	0.024	94.6	0.0000	0.2366	5.5	14.0
		7.60	105.6	65.8	93.7	0.002	0.024	94.5	0.0000	0.2824	7.6	16.8
		7.70	106.9	68.5	97.8	0.002	0.025	94.4	0.0000	0.3400	10.6	20.6
		7.80	108.3	71.5	102.4	0.003	0.026	94.3	0.0000	0.4008	14.1	24.8
		7.90	109.7	73.2	105.0	0.003	0.026	94.2	0.0000	0.4321	16.0	27.0
		8.00	111.1	77.3	111.0	0.003	0.027	94.1	0.0000	0.5071	20.7	32.5

• CTE value used for thickness analysis

CHAPTER 9: M-E PDG RESEARCH - ANALYSIS OF TEST RESULTS

9.1. Introduction

The new M-E PDG is the first pavement analysis tool that utilizes PCC CTE for distress and smoothness computations to predict accumulated faulting, cracking, and roughness. It describes a new approach, and therefore draws curiosity. The effect of CTE has been a major attraction and interesting studies have been conducted by different groups of researchers [2], [3], [4], [6], [13], [and others], and they revealed important findings mostly derived from comparison between field measurements and M-E PDG analytics. However, as those studies depend on numerous variables and dissimilar sample sections (problematic to compare), the actual M-E PDG CTE sensitivity is difficult to describe. Hence, a different approach was desired which isolates CTE as the control variable while proper comparison can be guaranteed. It seems to be problematic due to the nine different pavement models and their diverse characteristics. Although traffic loads, weather conditions, and substructures are identical, they differ considerably in strength properties, PCC thickness, and particularly CTE. Therefore, to ensure adequate comparison, the initial step had to express CTE as a percentage value. In general, 100 % CTE was defined by the nine different pavement models and their original CTE values but small modifications had to be made. It is especially noted that predicted cracking was the thickness-defining performance criterion for each pavement model. However, the quarter inch increments occasionally caused predicted cracking values far below the Florida performance limit (7.9 for MIX-03 at level 3). In such cases, the 100 % mark was adjusted to the CTE values resulting cracking closest to 10 % slabs cracked.

The following graphs are the result of the CTE sensitivity analysis; they were created to visualize the CTE effect on every performance criteria separately. For each graph, the abscissa is defined by CTE percentage while the ordinate represents the numerical results of the parameter in question.

9.2. Analysis of Load Transfer Efficiency Sensitivity

Load transfer efficiency was identified earlier (by thickness analyses) to be a minor response due to the PCC design features and base support. However, elevated CTE values may cause a different reaction and more pronounced LTE drop throughout the design life.

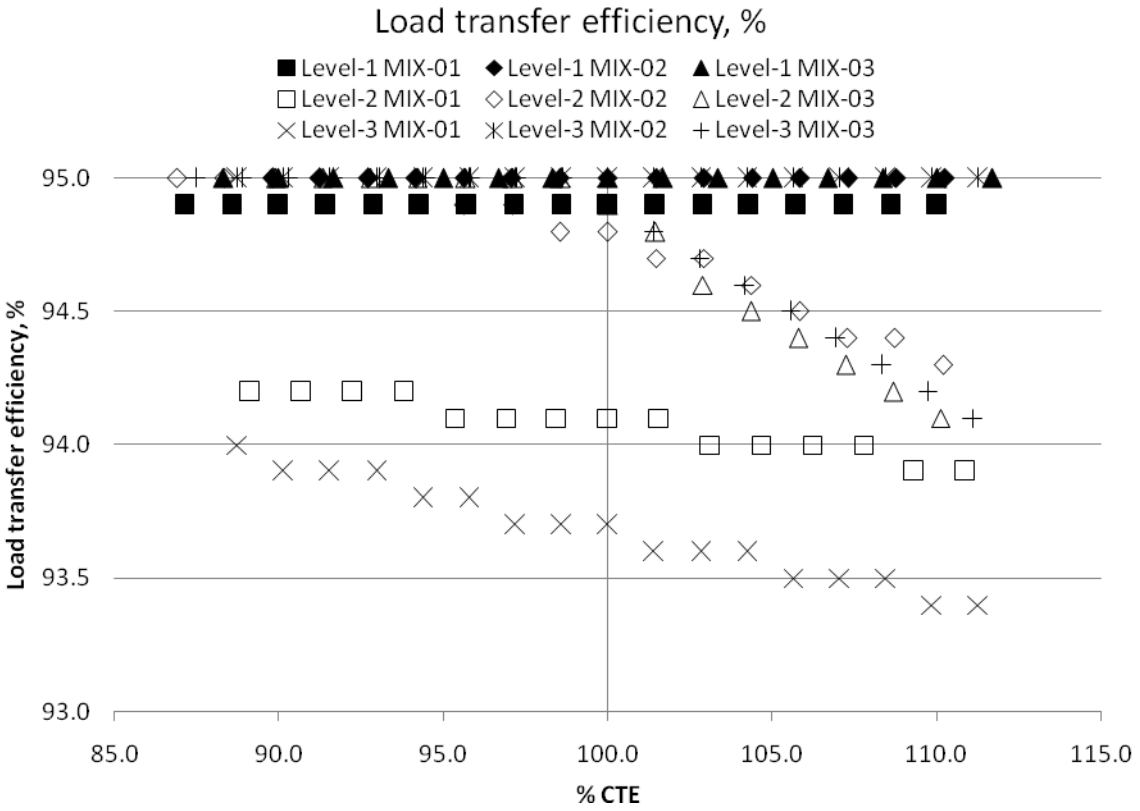

Figure 9.1: LTE sensitivity

In General, LTE is not problematic within the evaluated CTE array as abscissa values only range over 3 %. In fact, no response can be observed for any mix designs in level one and MIX-02 in level three, or more specifically the pavement models featuring thin PCC layers (less than 9 in) in respect to this study. Although LTE decreases moderately in acceptable ranges, it declines with CTE elevation for all thicker PCC layers. Therefore, it can be noted that CTE affects the load transfer efficiency in thicker slabs but only to a minor extent. In this research, LTE sensitivity can be disregarded.

9.3. Analysis of Predicted Faulting Sensitivity

Pavement faulting is a direct resultant of LTE, and therefore shows a similar response in this research. Nevertheless, increased CTE values may amplify the effect and turn faulting into a more dominant factor.

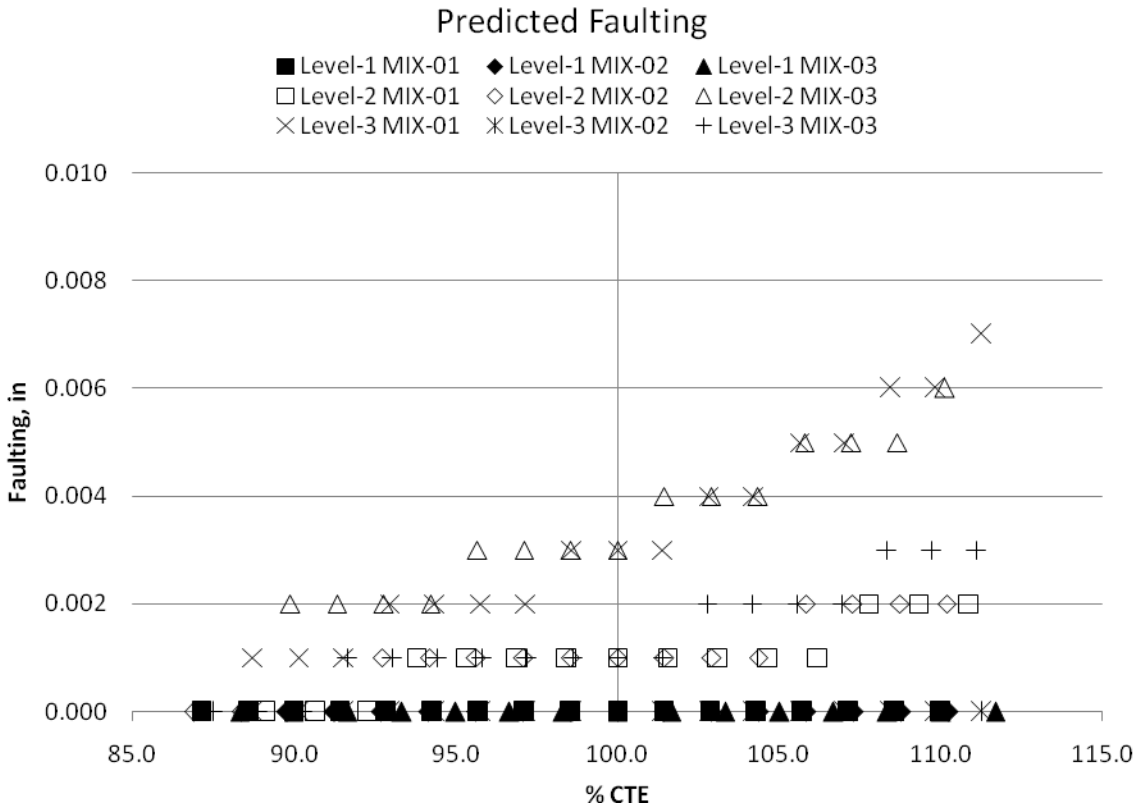

Figure 9.2: Faulting sensitivity

Figure 9.2 proves faulting to be insensitive to CTE magnification for the thin concrete slabs (less than 9 inch); all mix designs under hierarchy level one and MIX-02 under level three consideration maintain constant values throughout the CTE array. All other pavement models show slightly increased faulting results for amplified CTE values. Due to the chosen JPCP design features, in general the consequence is very little. However, the pattern becomes more apparent when predicted faulting at its specified reliability is analyzed. Figure 9.3 graphs the CTE percentage range versus faulting at specific reliability.

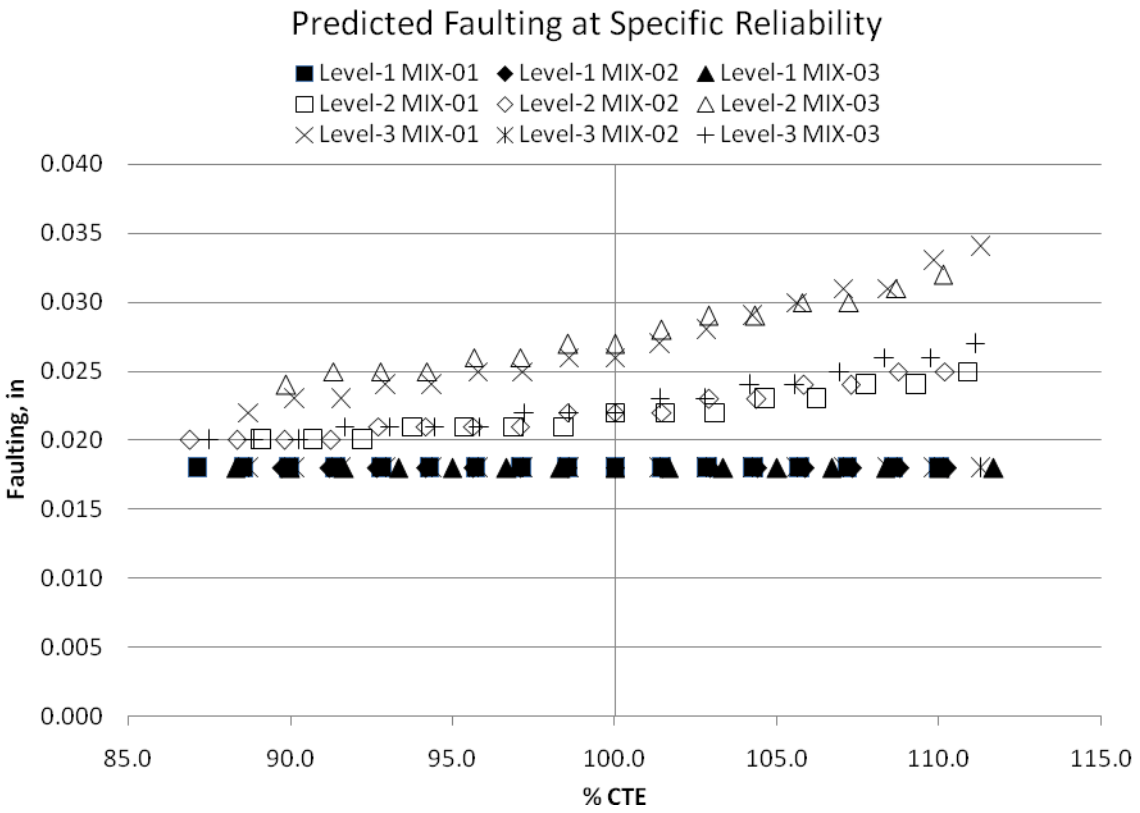

Figure 9.3: Faulting at specific reliability sensitivity

Notice that in Figure 9.3 the faulting growth rate due to CTE intensification is more pronounced following a linear path for the thicker slabs. They show analogous gradients ($\Delta_{faulting}$) ranging from 0.006 inches for MIX-01 at level two to 0.014 inches for MIX-01 at level three over the 20 % CTE range.

In general, predicted faulting has neither been an issue throughout the above outlined thickness analysis, nor during CTE sensitivity study. Even 10 % amplification of CTE could not challenge the predicted faulting (at specific reliability); the results fell consistently below the Florida analysis limit of 0.12 inches. It can be stated that pavement faulting is slightly affected by CTE intensification; its sensitivity can be neglected for the thin slabs (less than 9 inch) but a minor growth tendency has to be expected for thicker PCC layers.

9.4. Analysis of Cumulative Damage Sensitivity

During thickness analysis, bottom-up cracking was discovered to be present only for the thiner PCC layers which included all mix designs in hierarchy level one and MIX-02 under hierarchy level three. Therefore, it can be stated that cumulative bottom-up damage performs contrary to faulting in this research. The following graph was created to analyze the resistance of bottom-up cracking to CTE variation.

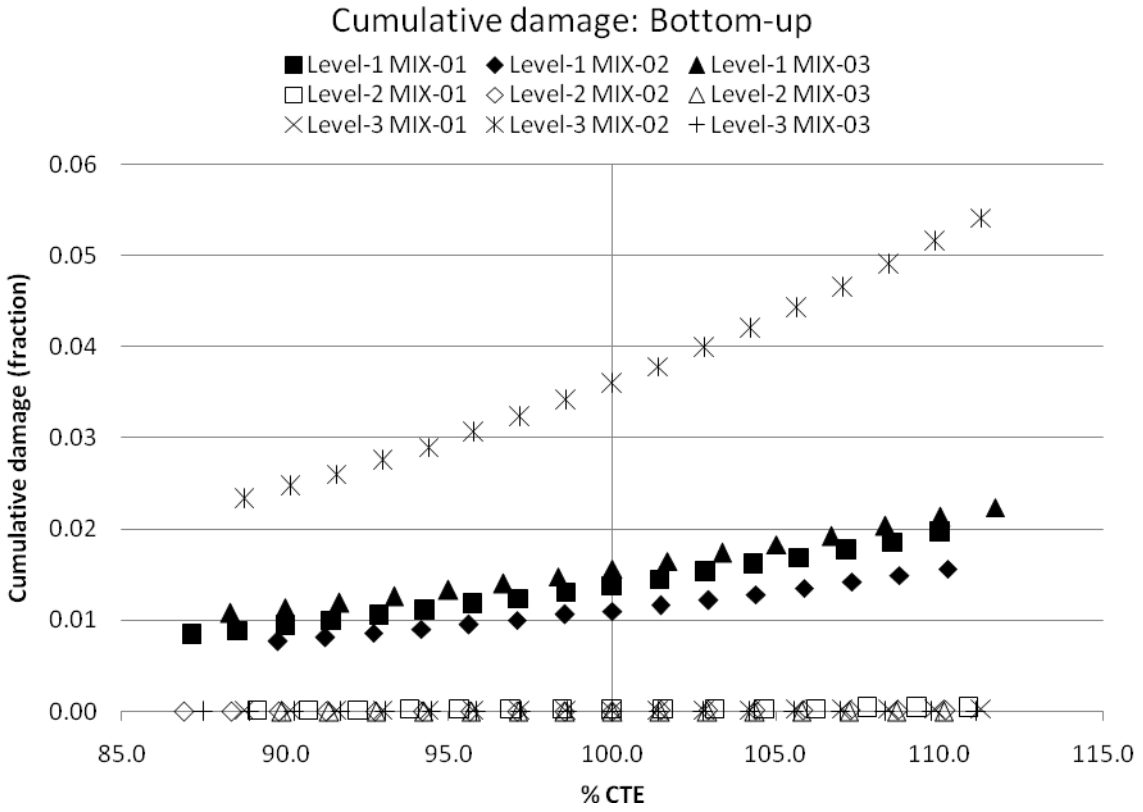

Figure 9.4: Bottom-up cracking sensitivity

Figure 9.4 proves once more that bottom-up cracking is not problematic in thick PCC layers as no response can be observed for any mix design at level two and MIX-01 and MIX-03 at level three, even for higher CTE values. However, the graph clearly shows a linear response to CTE if bottom-up cracking is present. Notice the comparable slope of the three mix designs under level one consideration. Though they possess dissimilar strength and CTE properties, they show parallel bottom-up cracking reactions throughout the CTE array. It is emphasized that MIX-02 under hierarchy level three features the

thinnest PCC slab and shows the steepest slope ($\Delta_{Bottom\text{-}up}$ = 0.03). The increased slope may be a result of the very thin (relative to this study) PCC layer but also might be caused by the different hierarchy level. Follow up studies should be conducted to further discover the behavior of thinner slabs at different hierarchy levels, especially since M-E PDG implies the use of low CTE PCC mixes to reduce bottom-up cracking – a methodology that could not be verified for all circumstances in this research.

During thickness analysis, cumulative top-down damage was more prominent than bottom-up damage. Consequently, the CTE sensitivity study is initially more pronounced at its 100 % value. However, as diverse conditions affect accumulated bottom-up and top-down damage differently, the following diagram is necessary to evaluate top-down sensitivity.

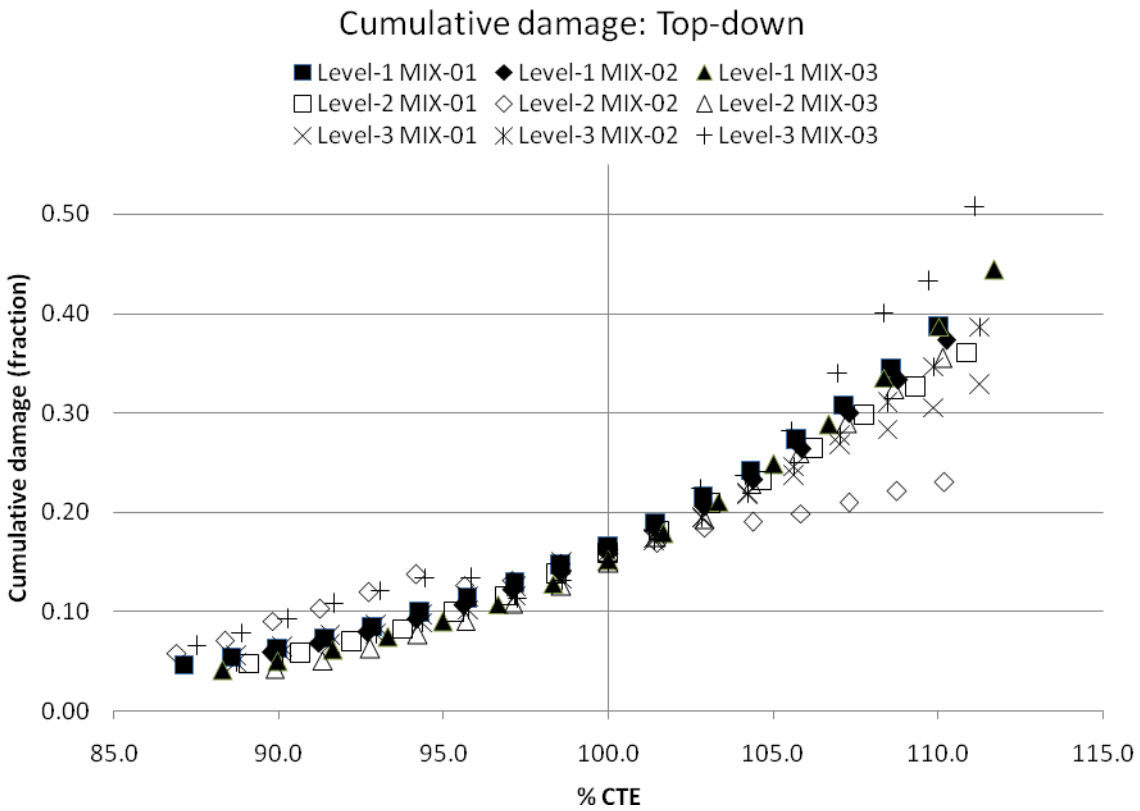

Figure 9.5: Top-down cracking sensitivity

From the graph above, it can be seen that all pavement models follow a similar response to top-down damage. Regardless of thickness or any other factor, the cumulative damage pattern is consistently described by a quadratic function. The only envelope-breaking pavement model is derived from MIX-02 at level two; note the spice to the right side of the abscissa caused by less accented slope. Nevertheless, it can be stated that top-down-damage shows quadratic responses for all scenarios and is therefore very sensitive to CTE changes.

9.5. Analysis of Predicted Cracking Sensitivity

Since it was the thickness-determining condition, predicted percentage of slabs cracked was identified to be the most critical pavement performance criterion in this research. Therefore, it is the central consideration as higher responses, caused by interchanged CTE values, would impact the mechanistic-empirical analysis tremendously.

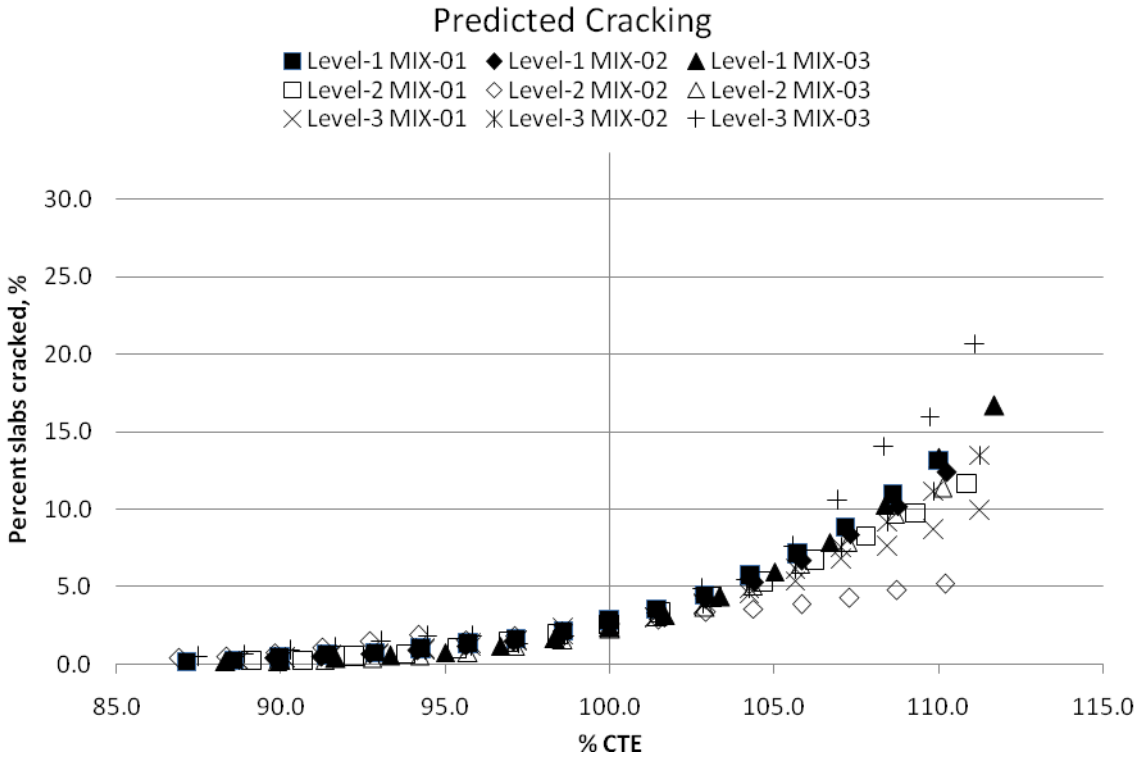

Figure 9.6: Total cracking sensitivity

Comparing Figure 9.5 to Figure 9.6, the predicted cracking is interrelated with top-down damage, with a more enhanced quadratic coefficient causing a rapid response for pavement structures among increased thermal behavior. As explained earlier, top-down cracking is the most dominant factor for cracking computations according to the new M-E PDG concept. Hence, the two graphs are congruent to one another reflecting any distinguishing mark. Consequently, the harmonized pattern (CTE sensitivity envelope) is again out of order for MIX-02 at hierarchy level two. However, it is emphasized that a 10 % CTE boost may cause an additional 15 % slabs cracked, but an underestimation of equal magnitude reduces the response by no more than 2.3 %.

Certainly, similar observations will be made for the predicted cracking at specific reliability. Nevertheless, predicted cracking for the specified reliability factor is the most significant property in this research as it predetermined the thickness, and therefore was turned into the reference mark for this CTE sensitivity study.

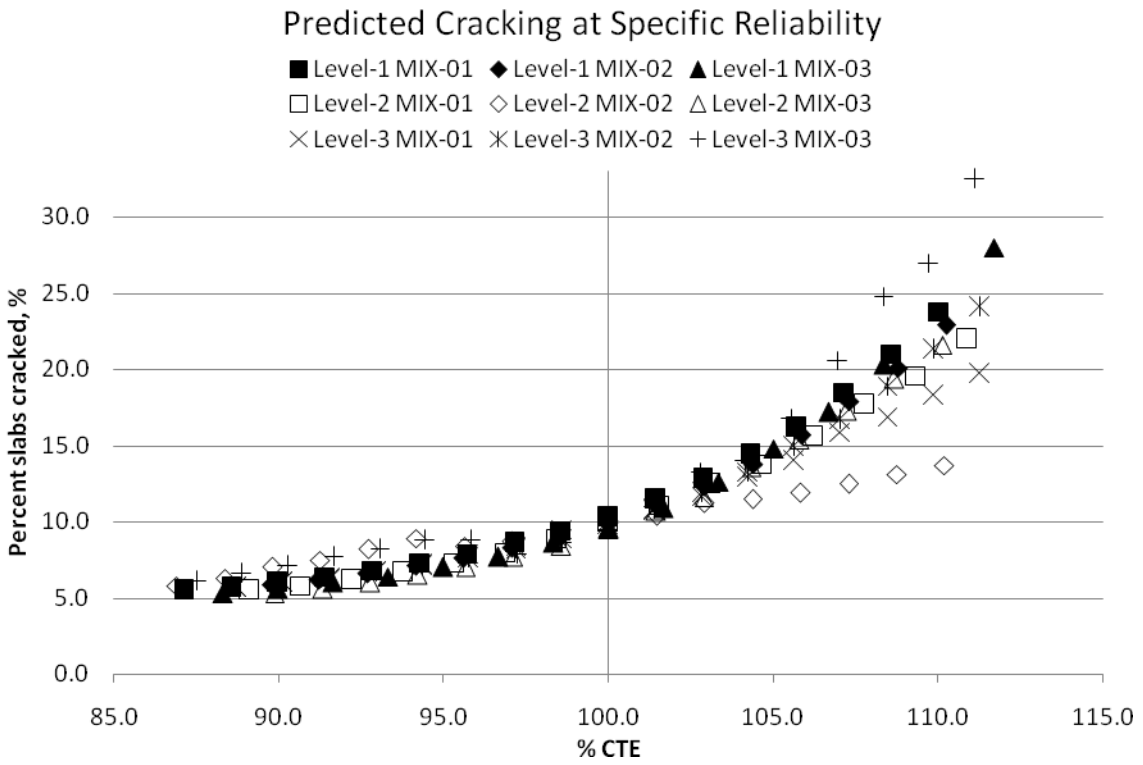

Figure 9.7: Cracking at specific reliability sensitivity

Due to the observations made above, it is not surprising that any CTE value exceeding the 100 % mark causes the resulting pavement model not to fulfill the desired Florida analysis parameter. Of course, all data points to the left of the abscissa underutilize the evolved pavement structure but because of the quadratic nature only minor effects have to be anticipated. In general, predicted transverse cracking (% slabs cracked) shows a high sensitivity to CTE. An overestimation of CTE or a concrete mixture with high thermal properties quickly causes augmented pavement cracking for the evaluated structure type.

9.6. Analysis of Smoothness (IRI) Sensitivity

During thickness analysis, predicted smoothness demonstrated an almost insignificant response. However, it is the most important performance to the end-user, and therefore its CTE sensitivity is an essential behavior in question.

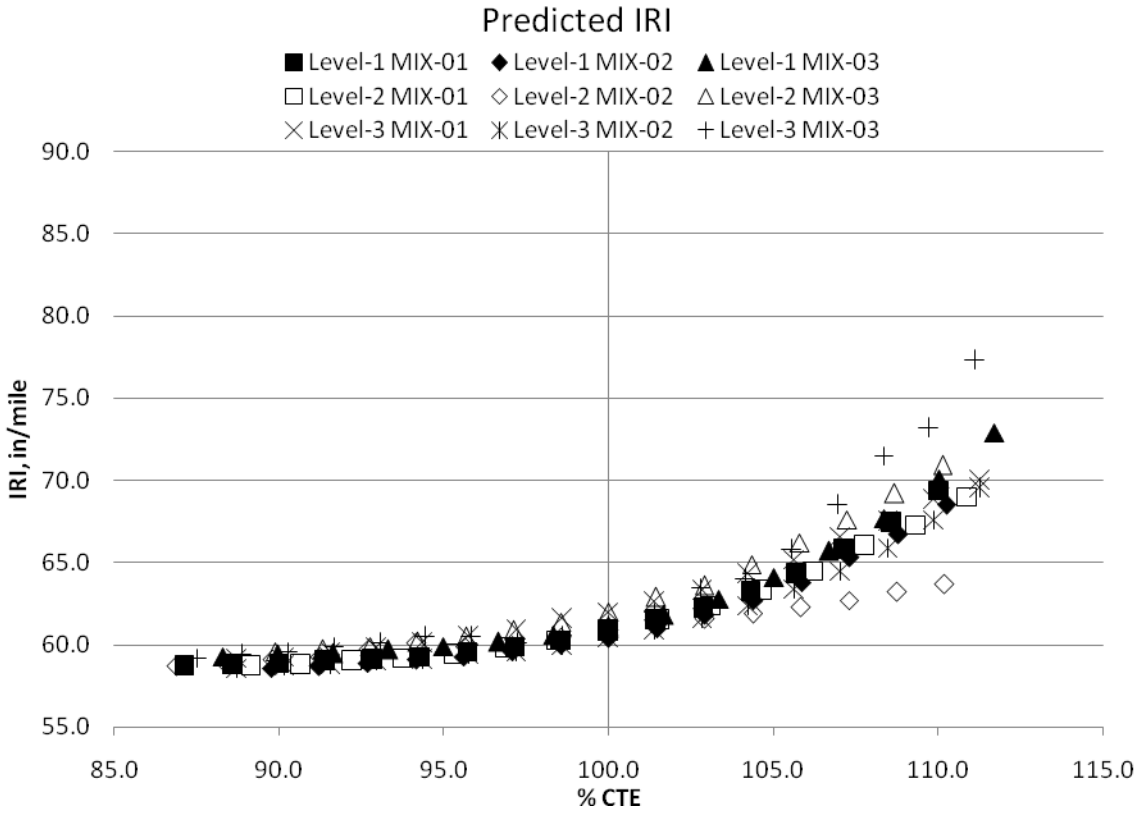

Figure 9.8: IRI sensitivity

In general, the graph in Figure 9.8 mirrors the cracking behavior which in turn is a consequence of top-down damage. This is assumed to be caused by the small faulting response due to the chosen structure type; it is not known if the graph would illustrate comparable CTE sensitivity for JPCP models among different design features. Nevertheless, it can be stated that the international roughness index is a direct consequence of cracking and is similarly sensitive to PCC's CTE.

The proposed reliability concept included in the new M-E PDG is usually the critical consideration which determines the approval of the pavement model. Consequently, the next graph plots the predicted IRI at specific reliability versus CTE percentage values to study the acceptance based on the prescribed Florida IRI limitation.

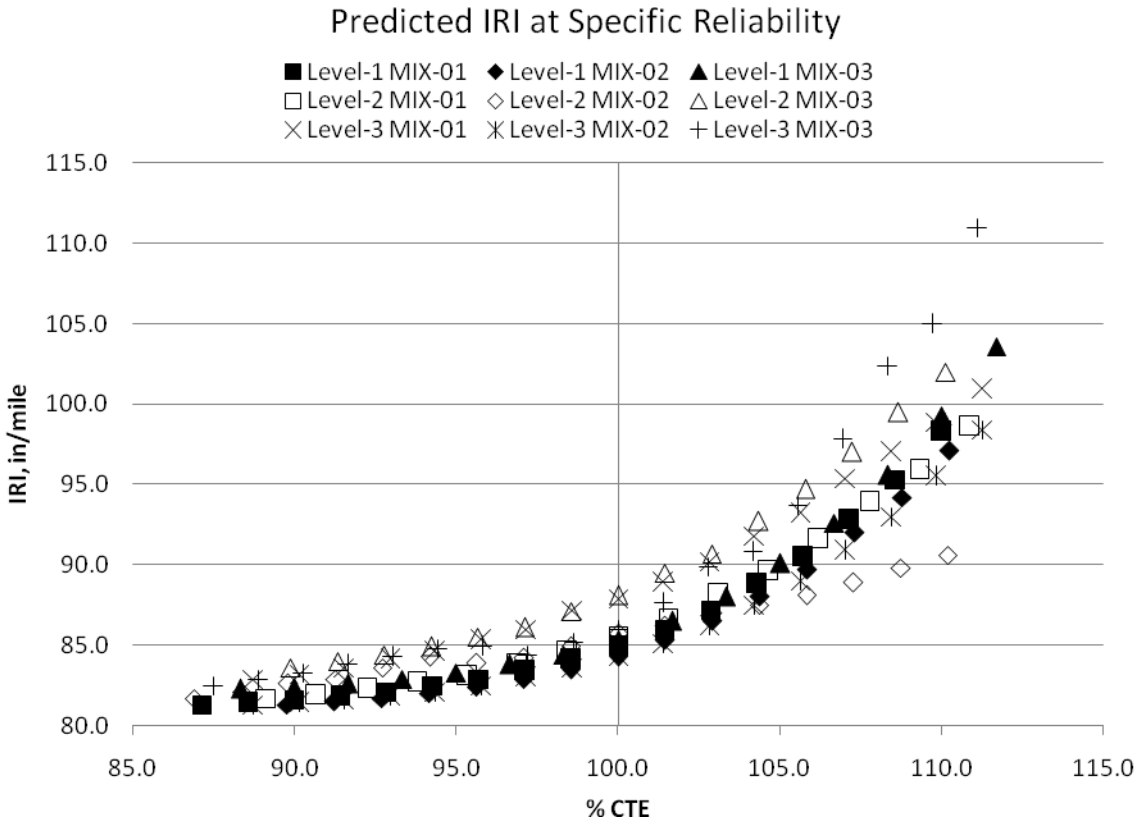

Figure 9.9: IRI at specific reliability sensitivity

It is emphasized that the abscissas in Figure 9.8 and Figure 9.9 are divided but numerically demonstrate the same IRI array of 35 inches per mile. Therefore, notice the

more pronounced separation of the pavement models and the consequential amplified growth rate in Figure 9.9. Naturally, this is a result of the reliability factor but it enlarges IRI sensitivity for higher CTE values tremendously. Nevertheless, the predicted smoothness throughout the 20 % CTE range maintains values constantly (far) below the Florida analysis limit of 160 inches per mile. In fact, the roughest roadway is predicted for MIX-03 at level three with 111 inches per mile for 11.1 % CTE. Consequently, IRI is not a concern but in general, its CTE sensitivity should not be underestimated.

9.7. Summary of Pavement Performance Sensitivity

The M-E PDG CTE sensitivity study was carried out for nine diverse pavement models, each differing in strength, PCC layer thickness, and CTE magnitude. Despite the dissimilar properties, a method was determined to properly compare the predicted performance criteria for alternating CTE values. Although different hierarchy levels were evaluated, clear resemblances were exposed and distinctive performance envelopes arose for certain criteria.

Load transfer efficiency showed minor reduction for the thicker concrete slabs but no response for the thinner oness. However, the LTE decrease did not demonstrate sufficient response to be considered CTE sensitive. Predicted faulting performance was illustrated to be slightly affected by CTE intensification; its sensitivity to CTE was determined to be negligible for thinner slabs but minor growth rates occurred for thicker PCC layers. Opposite findings were made for bottom-up cracking as only thin (less than 9 inch) concrete slabs were affected by interchanged CTE values. The study clearly revealed a linear response to CTE when bottom-up cracking was present initially. The most important finding, by far, was made when top-down damage was evaluated – all pavement models, regardless of their CTE or thickness values, performed identically and returned a quadratic behavior for amplified thermal expansion. It was the most important observation because predicted cracking and IRI could be retrieved from it; those two

pavement performance criteria executed proportional to top-down damage and mirrored each other's behavior.

Over all, ±10 % is a very generous CTE range as it captures approximately a difference of 1.5 µin/in/°F for the PCC mix designs evaluated here. Moreover, the data field varied from 5.29 to 8.00 µin/in/°F, values that most likely encompass thermal expansion properties for common Florida concrete mixtures. It is very unlikely that any follow-up study would estimate values outranging the given CTE array. Therefore, this study provides reference for Florida pavement analysis according to M-E PDG and emphasizes the importance of proper CTE measurement as an over-assessment may quickly cause amplified top-down damage, cracking, or IRI.

It can be stated that the new Mechanistic-Empirical Pavement Design Guide (considering the given design features) is not CTE-sensitive to load transfer efficiency, minimally sensitive to faulting, sensitive to bottom-up damage (for thin PCC layers with thicknesses less than 9 inch), and extremely sensitive to top-down damage, cracking, and smoothness. Overall, two out of three pavement performance criteria are highly susceptible to CTE.

CHAPTER 10: SUMMARY, CONCLUSION AND RECOMMENDATIONS

10.1. Research Summary

Three typical Florida pavement PCC mix designs have been thoroughly evaluated throughout research phase one. To encompass a certain range of local concrete mixtures, attention was paid to the constituents and their proportions, with special focus on coarse aggregates. Two mixes contained dissimilar quantities of limestone while one mixture was based on granite. Considering the input parameters required for the mechanistic-empirical analysis procedure according to the new M-E PDG, the concrete engineering properties were laboratory-measured for all essential maturity levels (7, 14, 28, and 90 days). To account for all three hierarchy levels, the characteristics under empirical evaluation included compressive strength, flexural strength, splitting tensile strength, Young's modulus, Poisson's ratio, (unit weight, air content, cement type, cement content, water-to-cement ratio), and coefficient of thermal expansion with an emphasis on concrete's thermal behavior. One sample per day was tested over a period of 130 days in accordance with AASHTO TP-60. Attributed to the proportions of constituents, the mix designs demonstrated distinctive results for all engineering properties with superior strength characteristics for one of the limestone mixes and beneficial thermal properties for the granite mixture. The two limestone mix designs showed comparable CTE values constantly increasing the granite mix by more than 1 μm/m/°C. However, the test results revealed that PCC CTE rises over time. It was shown that the thermal behavior increases rapidly within the first week and stabilizes subsequently. After 28 days, the CTE swell was considered insignificant as the change in CTE was less than 1/10 μm/m/°C.

To accurately analyze the three typical Florida mix designs by means of the new M-E PDG, research phase two was initiated through proper generation of computer analysis models. Traffic loads, environmental conditions, structural parameters, and analysis criteria were defined on account of local requirements. Due to the introduced data input quality concept (three different hierarchy levels), nine diverse JPCP models were established, each reflecting a certain range of numerical results derived from research

phase one to capture typical Florida PCC material properties. The remaining variable, PCC layer thickness, was iteratively idealized and the outcomes demonstrated favorable use of hierarchy level one and a high sensitivity to input parameters for level two and three. However, the resultant pavement structures were evaluated based on the predicted distresses (faulting and cracking) and smoothness (IRI). It was found that cracking is the critical performance criterion for Florida JPCP according to M-E PDG as the "% slabs cracked limit" was consistently attained before any other pavement performance became critical. Moreover, top-down fatigue damage was isolated to be the controlling failure mechanism because of insignificant faulting response and minor smoothness reduction.

The ensuing CTE sensitivity study was founded on the nine evaluated Florida pavement models (idealized for PCC layer thickness) and their original CTE values. A sensitivity matrix was developed to account for PCC's thermal behavior as a control variable over a ± 10 % CTE array comprising magnitudes typically expected in Florida. Although the sub-matrices differed considerably, a method was established to adequately compare the predicted performance criteria throughout alternating CTE values. Despite wide-ranging PCC, CTE, and thickness properties, clear resemblances were exposed for all scenarios under evaluation and distinctive performance envelopes arose for certain criteria. It was verified that the new Mechanistic-Empirical Rigid Pavement Design Guide is not CTE sensitive to load transfer efficiency, minimally CTE sensitive to faulting, CTE-sensitive to bottom-up damage (for the thinner PCC layers with thicknesses less than 9 inch), and extremely CTE-sensitive to top-down damage, cracking, and smoothness. Overall, two out of three pavement performance criteria are highly susceptible to CTE in Florida JPCP structures.

10.2. Conclusions

This report at hand summarizes a two year research project accomplished to promote the adoption of the new Mechanistic-Empirical Rigid Pavement Design Guide in Florida through proper implementation of local Portland cement concrete engineering properties.

The study required a comprehensive literature review, thoroughly conducted experiments, substantial computer modeling, and proper analysis of test results to successfully strive for the research goals. Each element of the evaluation was accompanied by essential findings that led to the following conclusions:

10.2.1. Measurement of PCC Input Properties for M-E PDG

The concrete strength properties required for rigid pavement analysis according to M-E PDG follow straight forward test setups. Established ASTM and AASHTO test standards or protocols are separately available for each destructive test method. Laboratories and material agencies will be capable to evaluate each PCC engineering property.

Similar to strength properties, test standards or protocols are available for Young's modulus and Poisson's Ratio. However, unlike strength properties, the proper assessment of PCC elasticity characteristics is still under debate [14] and heed must be taken when measuring these properties. However, laboratories and material agencies will be able to derive elasticity properties following the designated test protocol [X 8].

10.2.2. Local PCC Properties

All evaluated FDOT approved concrete mixtures tremendously increased their predicted target strength resulting in favorable PCC layer thickness when analyzed according to M-E PDG. This emphasizes the significance of PCC property measurement and consequential use of hierarchy level one for important and large-scale projects as the resultant pavement structure differed up to three inches in thickness for the same concrete mixture.

High CTE magnitudes have to be anticipated for typical Florida PCC mixtures. The here measured local CTE values ranged from 5.99 to 6.84 µin/in/°F – a relatively high CTE array. However, values reaching the upper limit for concrete (7 µin/in/°F) may be

encountered as thermal properties of PCC mixtures are highly influenced by the proportion and the characteristics of constituents.

10.2.3. Mechanistic-Empirical Pavement Design Guide

The new M-E PDG is a powerful tool which may or may not accurately predict pavement distresses and smoothness over the specified design life. However, this research outlines the design considerations that have to be accounted for before the actual JPCP analysis can be conducted and therefore, it concisely demonstrates the complexity of the proposed Design Guide. The daily use in pavement design offices will require well trained personnel properly familiarized with any material type to be included in the projected layer assembly. Suddenly thermal characteristics, among others, are critical to pavement design, properties that have not been taken into consideration by roadway and pavement designers before. The introduced complexity delays the adoption of the Design Guide and will result in numerous research projects before the mechanistic-empirical analysis design will be accepted.

The acceptance of the proposed roadway structure is highly dependent on the prescribed performance criteria and their limitations. It is emphasized that the M-E Design Guide Software follows an analytical process that ultimately compares the predicted distresses and smoothness throughout the design life to the limitations specified by the local agency. Although the new concept is assumed to prevent uneconomical pavement structures, carefree acceptance of analysis results may cause the contrary. This was demonstrated by a few pavement models with most of the emphasis on MIX-03 at hierarchy level two. The thickness was established throughout an iterative process that was controlled by predicted cracking (9.5 %) only. To fall below the "10 % slabs cracked limitation," the thickness was successively adjusted by quarter-inch increments. The next thinner PCC layer depth exceeded the limitation after 24.5 years resulting in 10.2 % terminal cracking and therefore, did not find acceptance for this research. However, in pavement application, the same thickness would perform satisfactorily and provide a

more economical design. Depending on the section length, material resources could be reduced significantly as 0.25 inches pavement thickness requires 49 cubic yards of PCC material per lane-mile.

Top-down damage is the activator for the critical pavement distresses in Florida JPCP (15 feet joint spacing) and therefore the problematic failure mechanism. Bottom-up damage has to be expected in thinner (less than 9 inch) PCC slabs only. For this study, this amounts to PCC layer thicknesses less than 9 inch, but it is emphasized that this threshold will vary with different design criteria and analysis parameter. However, top-down damage is the governing factor since the two failure mechanisms do not occur simultaneously in the same slab.

The M-E PDG analysis method for Florida JPCP is susceptible to PCC CTE magnitudes. Two out of three pavement performances react sensitively to interchanging thermal behaviors. Only minimal (negligible) reactions have to be anticipated for faulting but extreme responses will be seen for predicted cracking and smoothness (IRI).

10.3. Recommendations

The measurement of thermal expansion in Portland cement concrete represents a new test method and test configuration. Although, standardized by AASHTO and now described through standard test protocol TP-60, certain problems arose throughout PCC CTE acquisition using a commercially available test apparatus. For this research, it was indispensable to fathom the dilemma and to enclose any difficulty attributed either to the test protocol, test method, or test apparatus. An in-depth study was initiated which led to important findings and the recommendation to improve AASHTO TP-60 – separately outlined in Section 6.9.

Thermal properties of PCC mixtures are highly influenced by characteristics of constituents *and* their proportions. Although, typically presented in literature [1], [6], [8],

[W 6], [X 16], [and others], generalized CTE magnitudes exclusively attributed to the nature of coarse aggregates should be avoided. For important projects it is advisable to measure the CTE range experimentally.

The pavement performance criteria dictating the PCC layer thickness in Florida JPCP structures can be reduced to percentage slabs cracked. The limitation of 10 % may be reconsidered for the structure type under evaluation and its design features since faulting and particularly smoothness did not show problematic responses. A more generous (numerically higher) cracking restriction would close the gap between the different performance criteria and still guarantee adequate ride quality to the roadway user. Side analyses have shown that a hypothetical limit of 18 % slabs cracked may reduce the PCC layer thickness up to one inch while the terminal international roughness index remains below 100 inches per mile. In essence, this adds up to 195 cubic yard PCC material savings per lane-mile.

Attributed to the "CTE sensitivity performance envelopes," it is advised to act with caution during CTE measurement, calculation, or database estimation to truly assign CTE at its "100 % value." An overestimation of CTE's magnitude quickly results in excessive cracking accumulation and consequently more roughness.

10.4. Future Research

The above sections concluded the research at hand; nevertheless, to conduct proper implementation of the new Mechanistic-Empirical Rigid Pavement Design Guide, follow-up studies are indispensable. Only a small M-E PDG portion has been empirically captured by this research and the following affiliated studies are suggested:

The CTE measurement according to AASTHO TP-60 is not flawless and contains incorrect assumptions. The need for improvement is undeniable; however, it is questionable if the current test arrangement will be able to return the true CTE magnitude rather than an index value. Research should be conducted to find advanced methods for

correct data acquisition. An adequate test setup has to be discovered that properly disengages the LVDT mounting point from the temperature gradient.

The numerical mechanistic-empirical prediction models are currently calibrated to pavement performance data taken from the Long-term Pavement Performance (LTPP) program, but only few Florida PCC sections were included. The spread of data points across the United States may adulterate the true local PCC efficiency and calls for performance data exclusively taken from in-situ PCC pavement structures throughout Florida to properly calibrate the M-E models to local needs.

The pavement performances predicted throughout this research are highly attributed to the beneficially chosen design features. At this point, it is not known how/if other structural parameters (increased joint spacing, random joint spacing, un-doweled transverse joints, reduced dowel bar diameters, increased dowel bar spacing, and un-widened slabs) affect the pavement performance and if a change would reduce the dominance of percentage slabs cracked. Of course, it is assumed that faulting increases and roughness is reduced for unfavorable JPCP structural elements but research should be conducted to identify the significance of most affecting components.

The pavement performance controlling this research was traced back to the failure mechanism of top-down damage. Field studies should evaluate top-down damage affecting elements in Florida PCC pavements and compare the findings to M-E PDG analysis results. Methods to properly reduce top-down damage have to be determined.

Distinctive behaviors have been observed throughout different PCC layer thicknesses; in particular, thinner slabs (less than 9 inch) were demonstrating advanced responses where no reaction for thicker layers was noted. The size-effect should be evaluated as reduction of PCC layer depth is a major intention of the newly developed M-E Rigid Pavement Design Guide for guaranteeing economical design.

During side analysis, it was discovered that Poisson's Ratio may have a significant effect on the predicted pavement performances. Sensitivity matrices should be established on account of Poisson's ratio to properly evaluate the importance of lateral strain for M-E PDG analysis of Florida PCC mixtures.

REFERENCES

[X 1] ASTM Standard C 143: *Standard Test Methods for Slump of Hydraulic-Cement Concrete*, Published September 2003.

[X 2] ASTM Standard C 173: *Standard Test Method for Air Content of Freshly Mixed Concrete by the Volumetric Method*, Published 2001.

[X 3] ASTM Standard C 494: *Standard Specification for Chemical Admixtures for Concrete*, Published February 2004.

[X 4] ASTM Standard C 192: *Standard Practice for Making and Curing Concrete Test Specimen in the Laboratory*, Published October 2002.

[X 5] ASTM Standard C 39: *Standard Test Methods Compressive Strength of Cylindrical Concrete Specimens*, Published November 2004.

[X 6] ASTM Standard C 78: *Standard Test Method for Flexural Strength of Concrete (Using Simple Beam with Third-Point Loading)*, Published March 2002.

[X 7] ASTM Standard C 496: *Standard Specification for Splitting tensile Strength of Cylindrical Concrete Specimens*, Published March 2004.

[X 8] ASTM Standard C 469: *Standard Test Method for Static Modulus of Elasticity and Poisson's Ratio of Concrete in Compression*, Published October 2002.

[X 9] AASHTO T 196: *Standard Test Method for Air Content of Freshly Mixed Concrete by the Volumetric Method*, Published 2001.

[X 10] AASHTO T 126: *Standard Practice for Making and Curing Concrete Test Specimen in the Laboratory*, Published 2001.

[X 11] AASHTO T 22: *Standard Test Methods Compressive Strength of Cylindrical Concrete Specimens*, Published November 2006.

[X 12] AASHTO T 97: *Standard Test Method for Flexural Strength of Concrete (Using Simple Beam with Third-Point Loading)*, Published March 2003.

[X 13] AASHTO 198: *Standard Specification for Splitting tensile Strength of Cylindrical Concrete Specimens*, Published 2002.

[X 14] AASHTO TP 60: *Coefficient of Thermal Expansion of Hydraulic Cement Concrete*, Published 2005.

[X 15] "Guide for Mechanistic-Empirical Design of New and Rehabilitated Pavement Structures," National Cooperative Highway Research Program Transportation Research Board National Research Council, 2002.

[X 16] *"Building Movements and Joints*," Portland Cement Association, 1982.

[X 17] *"Rigid Pavement Design Manual,"* Published by Florida Department of Transportation, Document No. 625-010-006-c, July 2004.

[X 18] SHRP-C/FR-92-101. "*A Guide to Evaluating Thermal Effects in Concrete Pavements*," Strategic Highway Research Program, National Research Council, Washington, D.C., 1992.

[X 19] Florida Department of Transportation (2005) 2004 Florida Traffic Information, (CD-ROM).

[1] Coree, B., Ceylan, H., Harrington, D.; *"Implementing the Mechanistic-Empirical Pavement Design Guide: Implementation Plan*," Report No. IHRB Project TR-509: May 2005.

[2] Guclu, A., Ceylan, H.: *"Sensitivity Analysis of Rigid Pavement Systems Using Mechanistic-Empirical Pavement Design Guide*," Proceedings of the 2005 Mid-Continent Transportation Research Symposium, Ames, Iowa, August 2005.

[3] Hall, K. D., Beam, St.; "*Estimation of the Sensitivity of Design Input Variables for Rigid Pavement Analysis Using the Mechanistic-Empirical Design Guide,*" Preprint CD-ROM of the 83rd Annual Meeting of the Transportation Research Board, Washington, D.C., January 2004.

[4] Hossain, M., T. Khanum, J. Tanesi, and G. Schieber; "*The PCC Coefficient of Thermal Expansion Input for the Mechanistic-Empirical Pavement Design Guide,*" Published in the 85th Transportation Research Board Annual Meeting, Preperint CD-ROM, National Academy of Science, January 2006.

[5] Kim, S-M., Nam, J-H., Dossey T., Suh, Y-Ch., Claros, G., and McCullough, B.F., "*A New Methodology for Concrete Pavement Quality Control using Temperature and Moisture Measurement Techniques,*" a paper prepared for the 84th Annual Meeting of the Transportation Research Board, Washington, D.C., January 2005.

[6] Mallela, J., Abbas, A., Harman, T., Rao, C., Liu, R., and M. I. Darter; "*Measurement and Significance of Coefficient of Thermal Expansion of Concrete in Rigid Pavement Design,*" Paper No. 05-2671, Preprint CD-ROM of the 84th Annual Meeting of the Transportation Research Board, Washington, D.C., January 2005.

[7] Mindess, S., Joung, J.F.; *"Concrete,"* II Title, 1981, ISBN 0-13-167106-5.

[8] Mukhopadhyay, A. K., Neekhra, S., and D. Zollinger; "*New Mineralogical Approach to Predict Aggregate and Concrete Coefficient of Thermal Expansion (CoTE),*" Preprint CD-ROM of the 83rd Annual Meeting of the Transportation Research Board, Washington, D.C., January 2004.

[9] Nantung, T., Chehab, G., Newbolds, S., Galal, K., Li, K. and, D. H. Kim.; "*Implementation initiatives of the Mechanistic-Empirical Pavement Design Guide in Indiana,*" Preprint CD-ROM of the 84th Annual Meeting of the Transportation Research Board, Washington, D.C., January 2005.

[10] Popovics, S.; *"Strength and Related Properties of Concrete, A Quantitative Approach,"* J. Wiley & Sons, Inc., New York, NY, 1998, ISBN 0-471-14903-9.

[11] Salman, H.K., Buck, N., Chatti, K.; *"Significant M-E PDG Design Inputs for Joined Plain Concrete Pavements in Michigan,"* Proceedings of the Fifth International Conference on Maintenance and Rehabilitation of Pavements and Technological Control, Park City, Utah, August 2007.

[12] Trevino, M., and McCullough, B.F., "*Identifying Significant Basic Properties for Portland Cement Concrete Pavement,*" Preprint CD-ROM of the 83rd Annual Meeting of the Transportation Research Board, Washington, D.C., January 2004.

[13] Won, M., "*Improvements of Testing Procedures for Concrete Coefficient of Thermal Expansion*," Preprint CD-ROM of the 84th Annual Meeting of the Transportation Research Board, Washington, D.C., January 2005.

[14] Yazdani, N., McKinnie, B., and Haroon, S., "*Time Dependent Compressive Strength and Elasticity Development in Florida Concrete*," Final Report Submitted to the Florida Department of Transportation, March 2004.

[15] Yu, H. T., Kahazanovich, L., Dater, M. I., *"Consideration of JPCP Curling and Warping in the 2002 Design Guide,"* Preprint CD-ROM of the 83rd Annual Meeting of the Transportation Research Board, Washington, D.C., January 2004.

[W 1] http://en.wikipedia.org/wiki/Coefficient_of_thermal_expansion [25/10/2006]

[W 2] http://emtoolbox.nist.gov/Temperature/Tutorial.asp [30/10/2006]

[W 3] http://hyperphysics.phy-astr.gsu.edu/hbase/thermo/thexp.html [23/10/2006]

[W 4] http://irc.swan.ac.uk/ThExpansion.htm [12/12/2006]

[W 5] http://www.ndt-ed.org/EducationResources/CommunityCollege/Materials/Physical_Chemical/ThermalExpansion.htm [15/12/2006]

[W 6] http://www.fhwa.dot.gov/Pavement/pccp/thermal.cfm [22/01/2007]

[W 7] http://www.trb.org/mepdg/ [08/03/2007]

[W 8] https://www.ltrc.lsu.edu/lpc_presentations/pdf/Overview%20and%20Implementation%20Issues.pdf [27/04/2007]

[W 9] http://www.trb.org/ [11/10/2007]

[W 10] http://www.matweb.com/ [15/01/2008]

[W 11] http://training.ce.washington.edu/wsdot/modules/02_pavement_types/02-1_body.htm [20/04/2008]

[W 12] http://www.transportation.org/sites/design/docs/Reliability%20in%20the%20MEPDG%20one%20states%20perspective%20(Pierce)%20(1-2007).pdf [15/06/2008]

APPENDIX A: M-E PDG SOFTWARE

A.1. Design Process for Rigid Pavement:

1) Assemble a trial design for a specific site conditions including traffic, climate, and foundation - define layer arrangement, Portland cement concrete (PCC) and other paving material properties, and design and construction features.
2) Establish criteria for acceptable pavement performance at the end of the design period (i.e., acceptable levels of faulting and cracking for JPCP, punchouts for CRCP, and IRI for both).
3) Select the desired level of reliability for each of the applicable performance indicators (e.g., select design reliability levels for cracking, faulting, and IRI for JPCP).
4) Utilize Design Guide Software to accomplish the following:
    a) Process input to obtain monthly values of traffic, material, and climatic inputs needed in the design evaluations for the entire design period.
    b) Compute structural responses (stresses and deflections) using finite element based rapid solution models for each axle type and load and for each damage-calculation increment throughout the design period.
    c) Calculate accumulated damage at each month of the entire design period.
    d) Predict key distresses (joint faulting, slab cracking, CRCP punchouts) month-by-month throughout the design period using the calibrated mechanistic-empirical performance models provided in the Guide.
    e) Predict smoothness (IRI) as a function of initial IRI, distresses that occur over time, and site factors at the end of each time increment.
    f) Evaluate the expected performance of the trial design at the given reliability level for adequacy.
    g) Modify the design and repeat until the design does meet the established criteria.

The overall iterative design processes for JPCP and CRCP are illustrated in Figure A**.1** and Figure A**.2**, respectively.

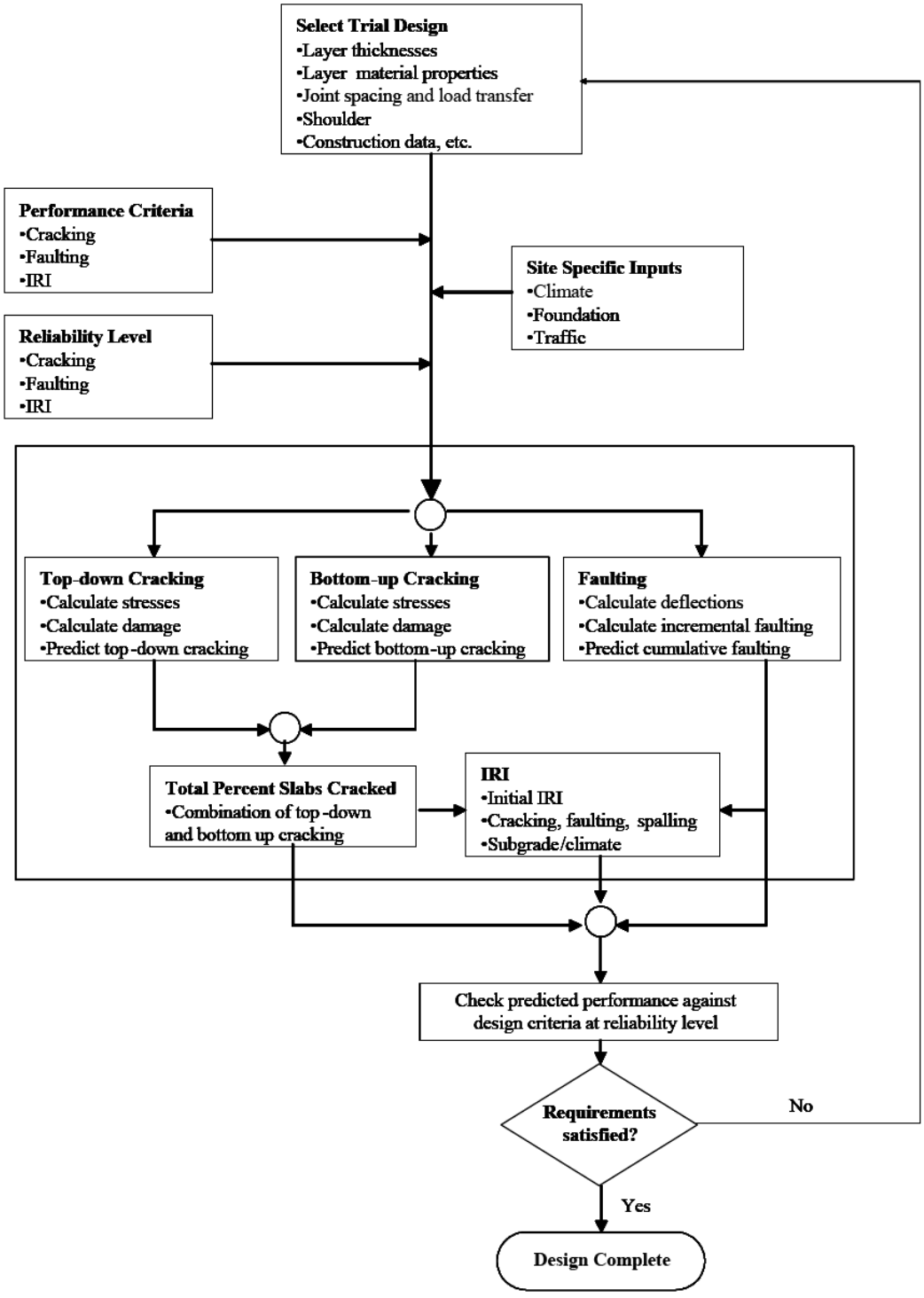

Figure A.1: Design process for JPCP

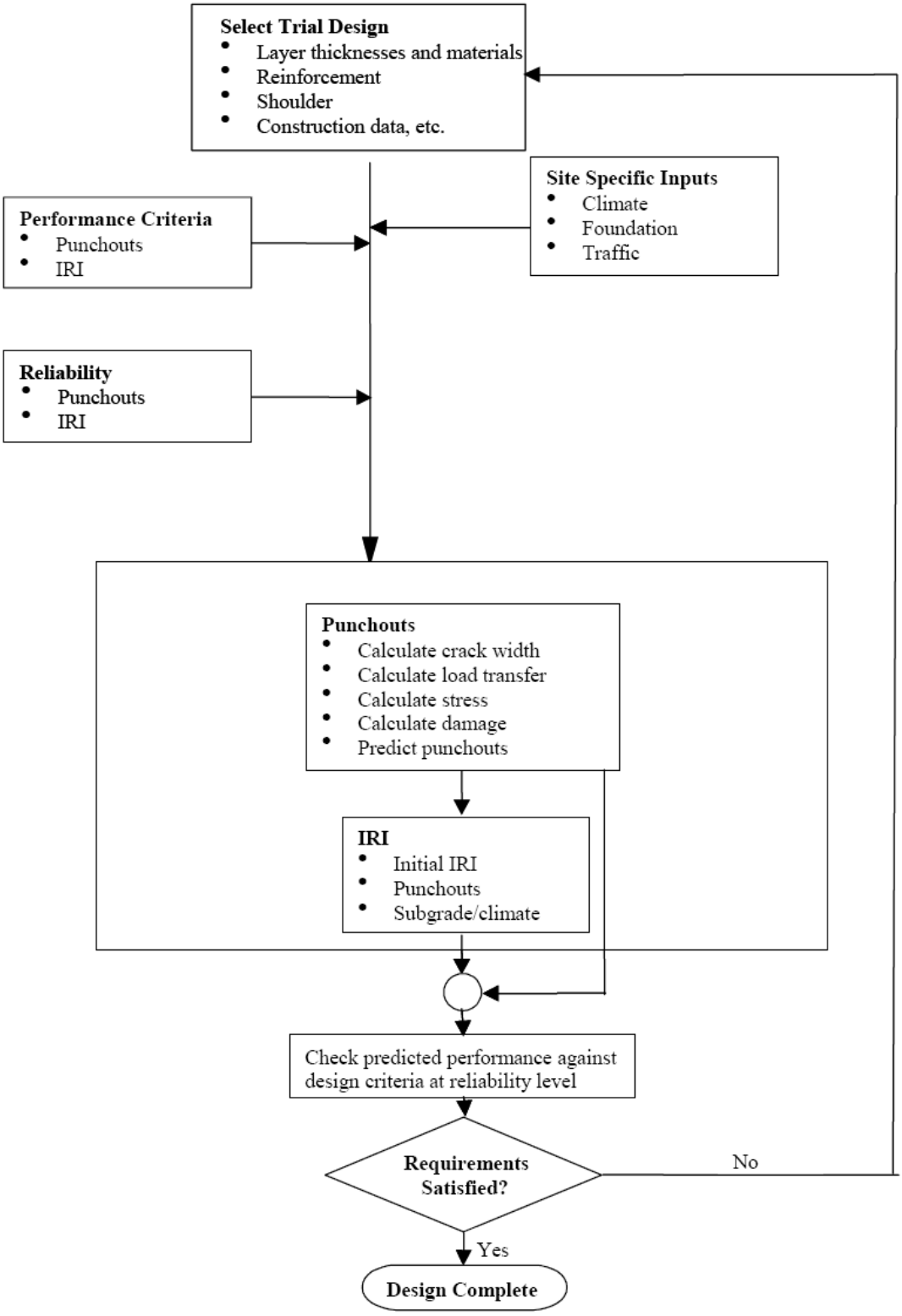

Figure A.2: Design process for CRCP

A.2. Software Design Guide Interface

The new Mechanistic-Empirical Pavement Design Guide requires numerous detailed calculations. Depending on the specified design life of the structure, the amount of computational effort increases. For example, the temperature profile inside the concrete slap results in 8,760 profiles per design year (365 days * 24 hours). Therefore, the design of (ridged) pavement structures according to ME-PDG is only practicable using the newly developed software. In this section the interface and input data used for the design are briefly explained. They may be summarized as:

- General information.
- Site/project identification.
- Analysis parameters.
- Traffic.
- Climate.
- Drainage and surface properties.
- Pavement structure.
- Design features.

Several of these inputs (e.g., traffic, climate) are identical to those used for flexible pavement design. However, there are variations in how some of these inputs are processed for use in JPCP and CRCP design. The focus of this section is to summarize all the inputs required for the design of rigid pavements.

Detailed descriptions for several of these inputs are beyond this text, but may be found in:

- [X 15] PART 2 – Design Inputs, Chapter 1: Subgrade/Foundation Design Inputs.
- [X 15] PART 2 – Design Inputs, Chapter 2: Material Characterization.
- [X 15] PART 2 – Design Inputs, Chapter 3: Environmental Effects.
- [X 15] PART 2 – Design Inputs, Chapter 4: Traffic.
- [X 15] PART 3 – Design Analysis, Chapter 1: Drainage.

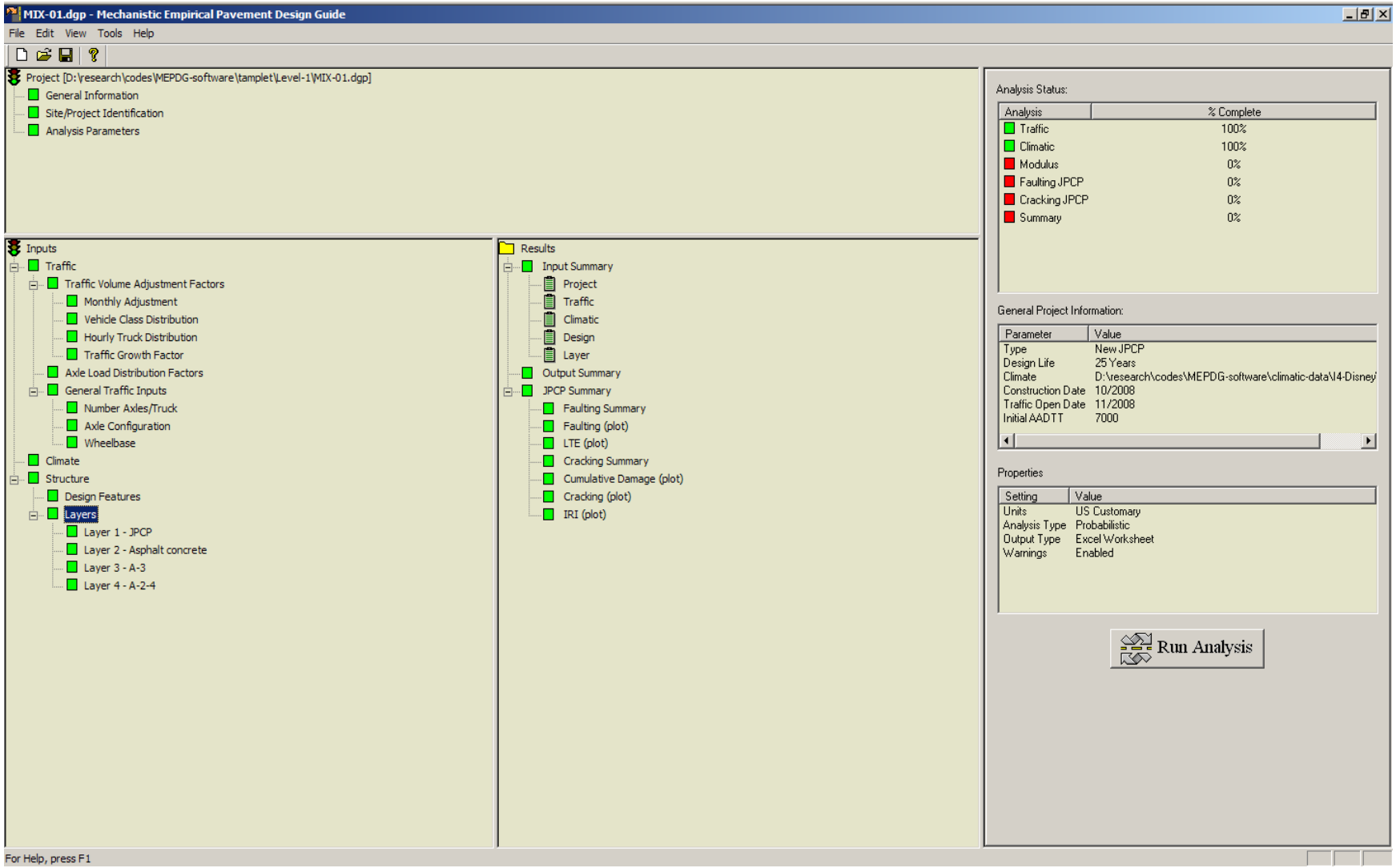

Figure A.3: ME-PDG software

A.3. General Information

The following inputs define the analysis period and type of design:

- Design life. Expected pavement design life (years).
- Construction month. Selecting June means construction occurs on June 1 and all aging is keyed to this date. Selecting hot months results in higher "zero-stress" temperatures and wider crack openings. By avoiding construction during the most adverse months (the months that will result in the PCC achieving the highest "zero-stress" temperatures), the risk of early pavement failures may be significantly reduced.
- Traffic opening month. This can be a sensitive input because it determines the PCC strength at which traffic is applied to the pavement.
- Pavement type – JPCP or CRCP. This input determines the method of design evaluations and the applicable performance models.

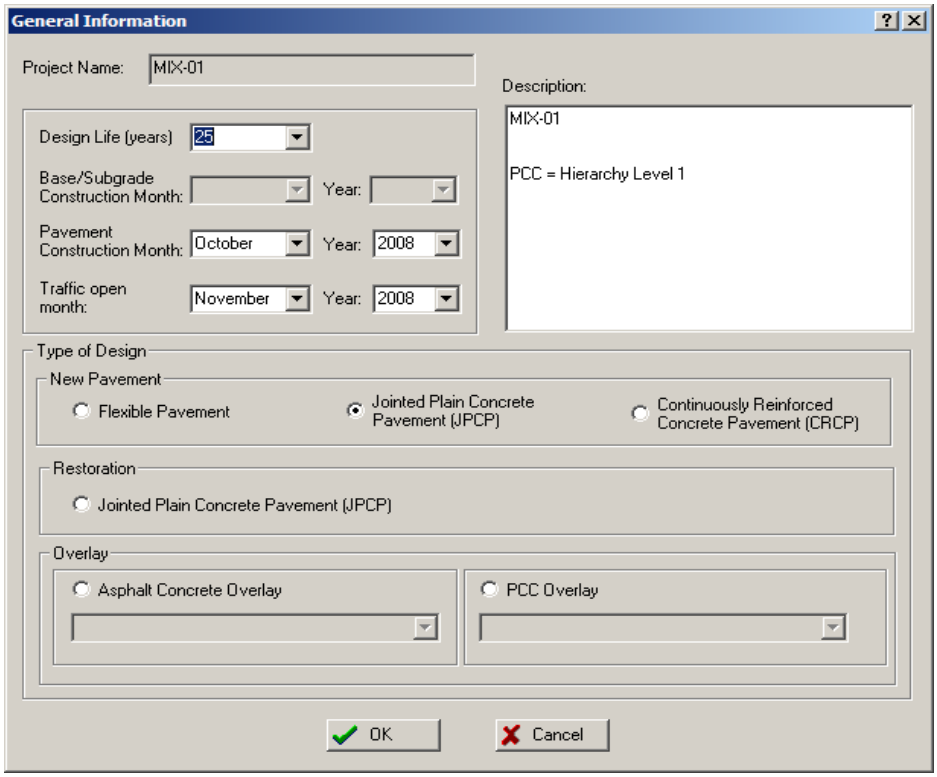

Figure A.4: Interface: General Information

A.4. Site/Project Identification

This group of inputs includes:

- Project location.
- Project identification – Project ID, Section ID, beginning and ending mile posts, and traffic direction.

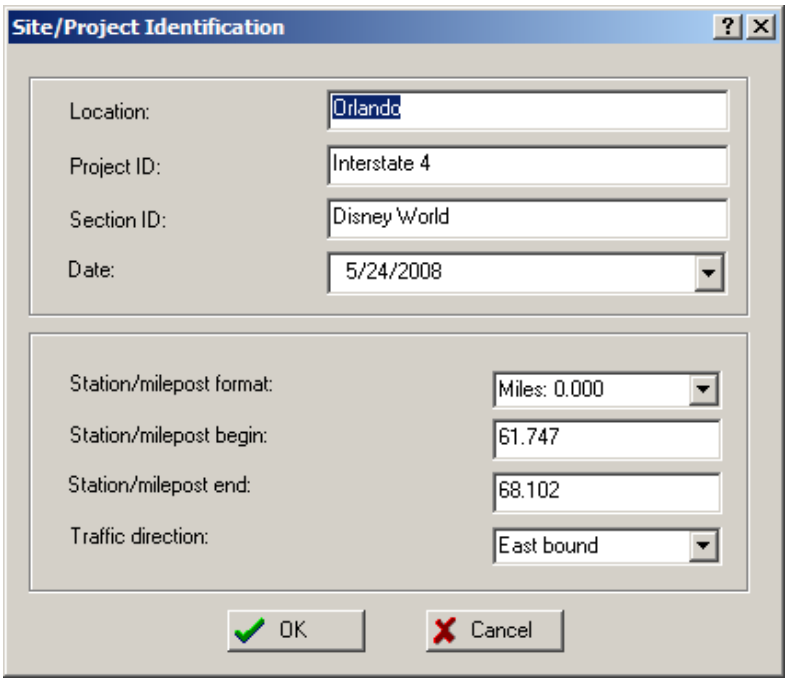

Figure A.5: Interface: Site/Project identification

A.5. Analysis Parameters

The initial IRI defines the as-constructed smoothness of the pavement. This parameter is highly dependent on the project smoothness specifications and has a significant impact on the long-term ride quality of the pavement.

The JPCP design is based on transverse cracking, transverse joint faulting, and pavement smoothness (IRI). For CRCP design, crack width and LTE, punchouts and smoothness

are the key performance indicators. For example, specifying a high reliability level and low distress level will result in a very conservative design.

The performance criterion for transverse cracking defines the maximum allowable percentage of cracked slabs at the end of design life and determines the level of slab cracking that may occur over the design period. Typical values of allowable cracking range from 10 to 45 %, depending on the functional class of the roadway and design reliability.

The performance criterion for joint faulting defines the allowable amount of mean joint faulting at the end of the design life and determines the level of joint faulting over the design period. Typical values of allowable JPCP mean faulting range from 0.1 in to 0.2 in, depending on the functional class of the roadway and design reliability.

Crack width in the cold weather is the most critical design parameter. The wider the crack the greater the probability it will lose load transfer efficiency. The Design Guide Software calculates the crack width at the depth of reinforcement. This should be limited to 0.02 inches or less. The crack LTE is the ultimate strength parameter and depends on crack width and number of heavy axles applied.

Punchouts are a major cause of loss of smoothness in CRCP. The performance criterion for punchouts defines the acceptable number of punchouts per mile at the end of design life and also determines the number of punchouts that may develop over the design period. Typical values of allowable CRCP punchouts (all severities) range from 10 to 20 per mile.

Functional adequacy is quantified most often by pavement smoothness. Simplistically, smoothness can be defined as “the variation in surface elevation that induces vibrations in traversing vehicles.” The IRI is the most common way of measuring smoothness in managing pavements. As with the structural distresses, the performance criterion for smoothness defines the acceptable IRI at the end of design life. Typically, values in the

range of 150 to 250 in/mile are used for terminal IRI, depending on the functional class of the roadway and design reliability.

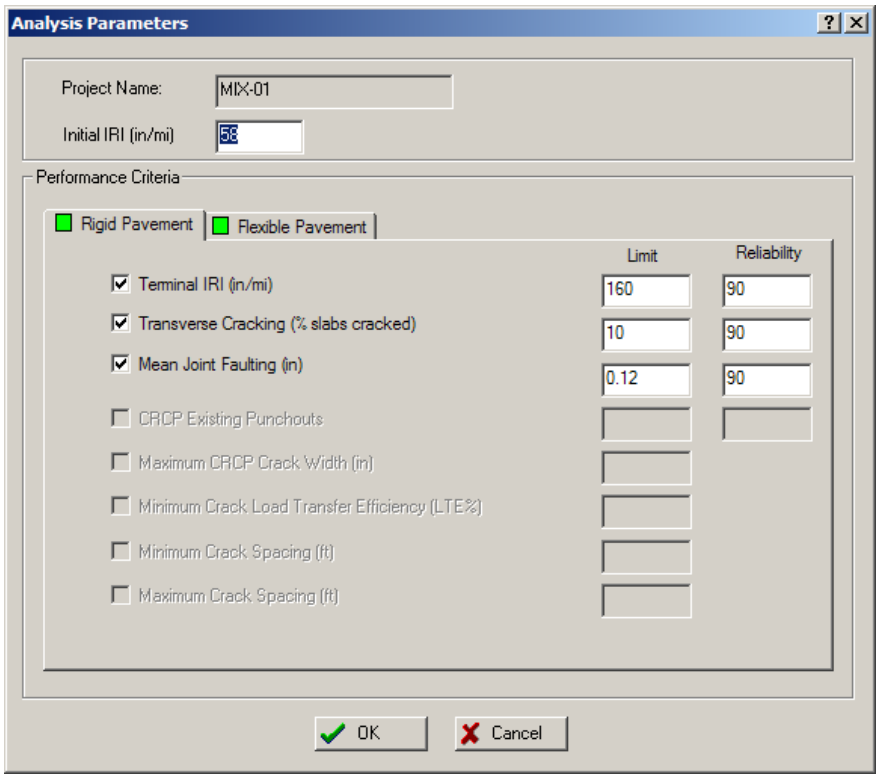

Figure A.6: Interface: Analysis Parameter (Rigid pavement)

A.6. Traffic

Traffic data is one of the key data elements required for the analysis and design of pavement structures. The Design Guide considers truck traffic loadings in terms of axle load spectra. The Design Guide Software puts out monthly based cumulative numbers of heavy trucks in the design lane as an overall indicator of the magnitude of truck traffic loadings (FHWA class 4 and above).

A.6.1. Basic Information

- Annual Average Daily Truck Traffic (AADTT) for base year – the total number of heavy vehicles (classes 4 to 13) in the traffic stream.
- Percent trucks in the design direction (directional distribution factor).
- Percent trucks in the design lane (lane distribution factor).
- Operational speed of vehicles – this input is used in the calculation of moduli of asphalt bound layers.

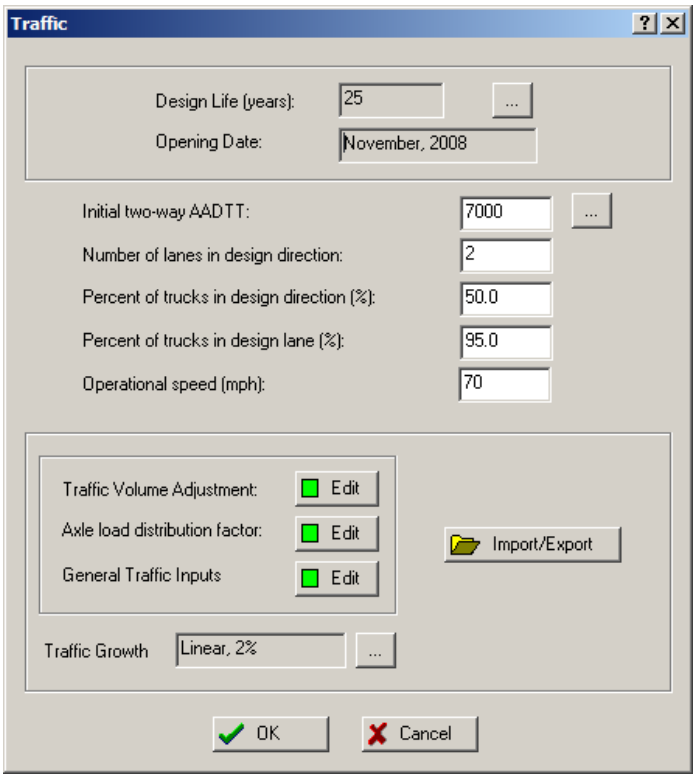

Figure A.7: Interface: Traffic

A.6.2. Traffic Volume Adjustment, Monthly Adjustment Factors

The truck monthly distribution factors are used to determine the monthly variation in truck traffic within the base year. These values are simply the ratio of the monthly truck traffic to the AADTT.

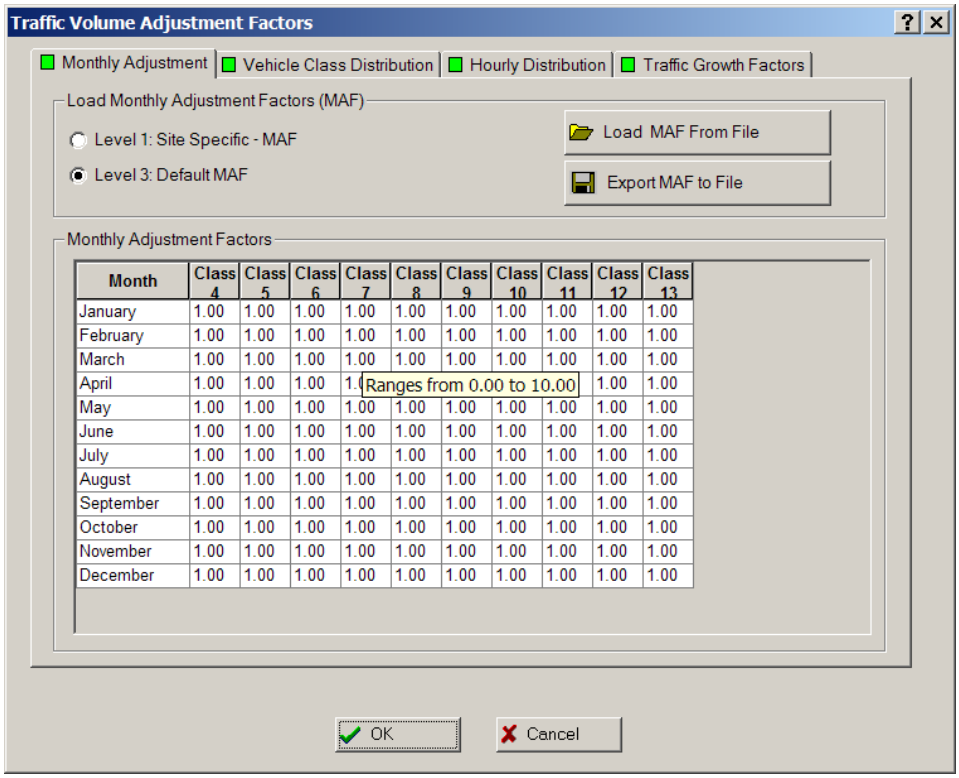

Figure A.8: Interface: Traffic Volume Adjustment Factors, Monthly Adjustment

A.6.3. Traffic Volume Adjustment, Vehicle Class Distribution

The normalized vehicle class distribution represents the percentage of each truck class (classes 4 through 13) within the AADTT for the base year. The sum of the % AADTT of all truck classes should equal 100. Each TTC represents a traffic stream with unique truck traffic characteristics. The default values are provided in [X 15] PART 2, Chapter 4 and Appendix AA. They are also a part of the Design Guide Software.

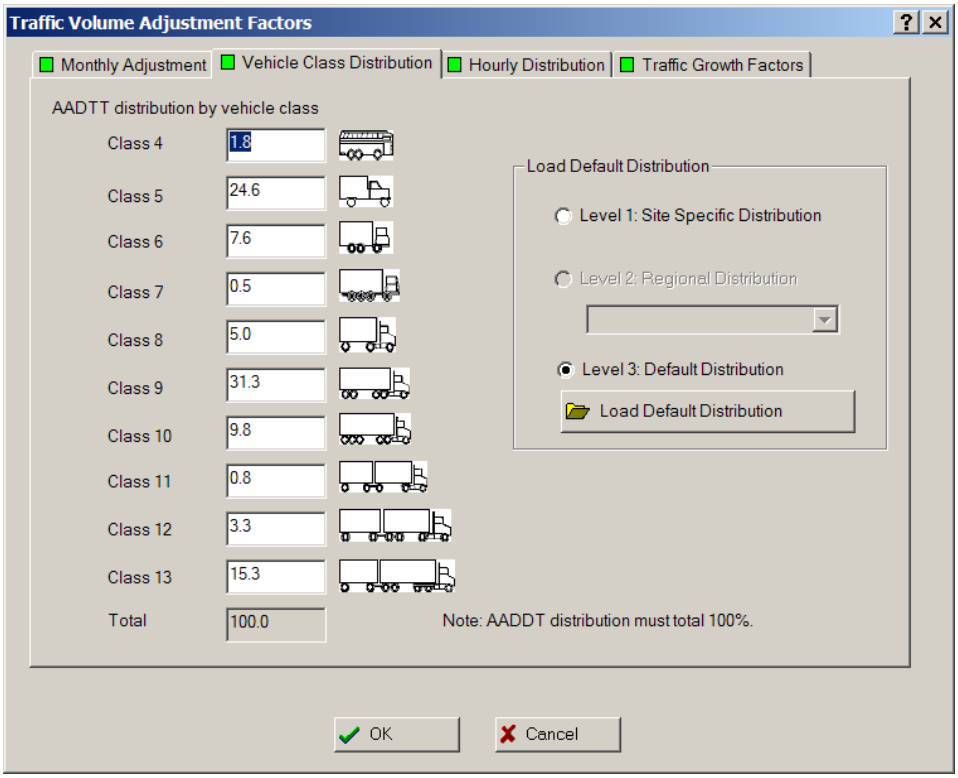

Figure A.9: Interface: Traffic Volume Adjustment Factors, Vehicle Class Distribution

A.6.4. Hourly Truck Traffic Distribution

The hourly distribution factors represent the percentage of the AADTT within each hour of the day. These factors are important in the prediction of JPCP cracking, JPCP faulting, and CRCP punchouts. They help accurately account for daytime and nighttime traffic streams required for performance prediction.

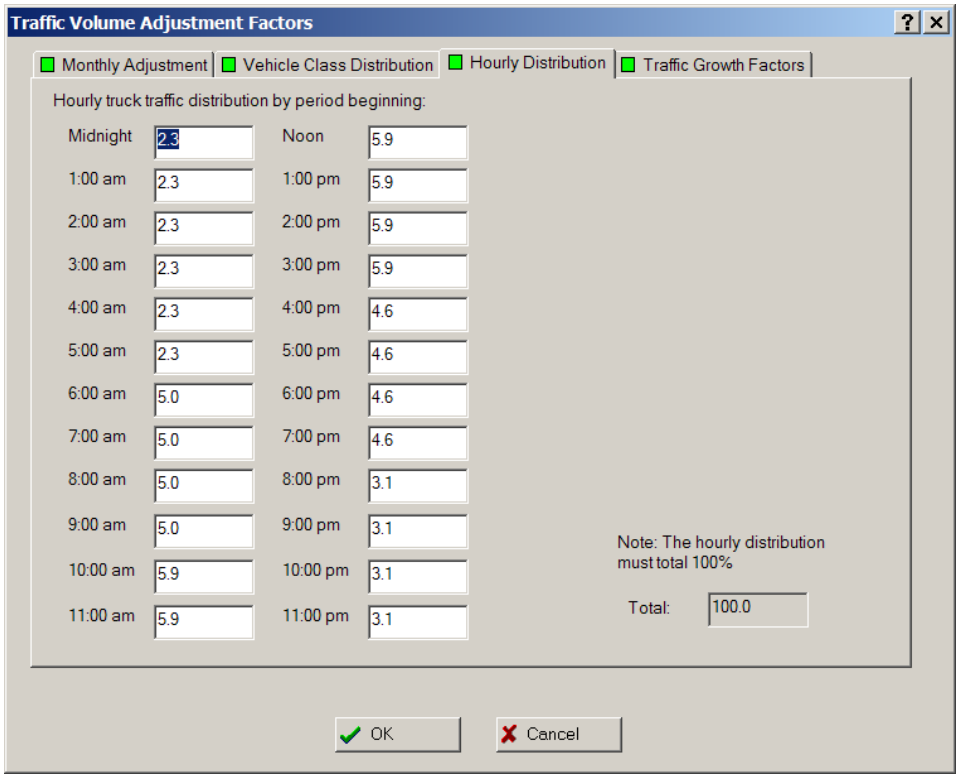

Figure A.10: Interface: Traffic Volume Adjustment Factors, Hourly Distribution

A.6.5. Traffic Growth Factors

The traffic growth function allows for the growth or decay in truck traffic over time (forecasting or backcasting truck traffic). Three functions are available to estimate future truck traffic volumes:

- No growth.
- Linear growth.
- Compound growth.

Based on the function chosen, the opening date of the roadway to traffic (excluding construction traffic), and the design life, the traffic is projected into the future.

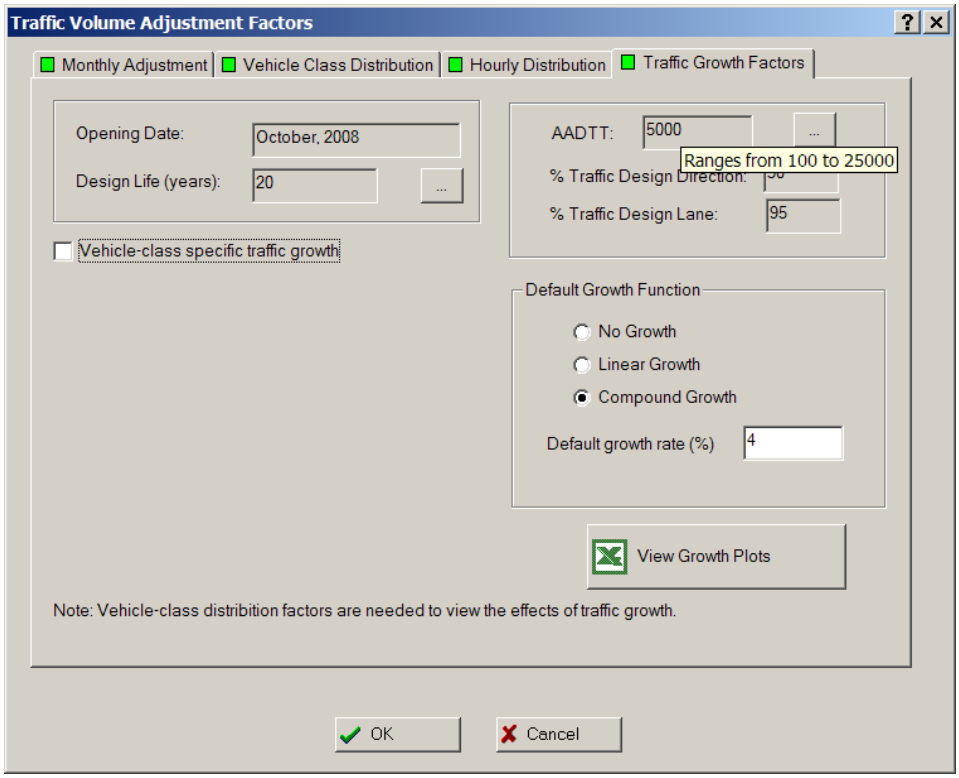

Figure A.11: Interface: Traffic Volume Adjustment Factors, Traffic Growth Factor

A.6.6. Axle Load Distribution Factors

The axle load distribution factors simply represent the percentage of the total axle applications within each load interval for a specific axle type and vehicle class (classes 4 through 13). This data needs to be provided for each month for each vehicle class. The definitions of load intervals for each axle type are:

- Single axles 3,000 lb to 41,000 lb at 1,000 lb intervals.
- Tandem axles 6,000 lb to 82,000 lb at 2,000 lb intervals.
- Tridem and quad axles 12,000 lb to 102,000 lb at 3,000 lb intervals.

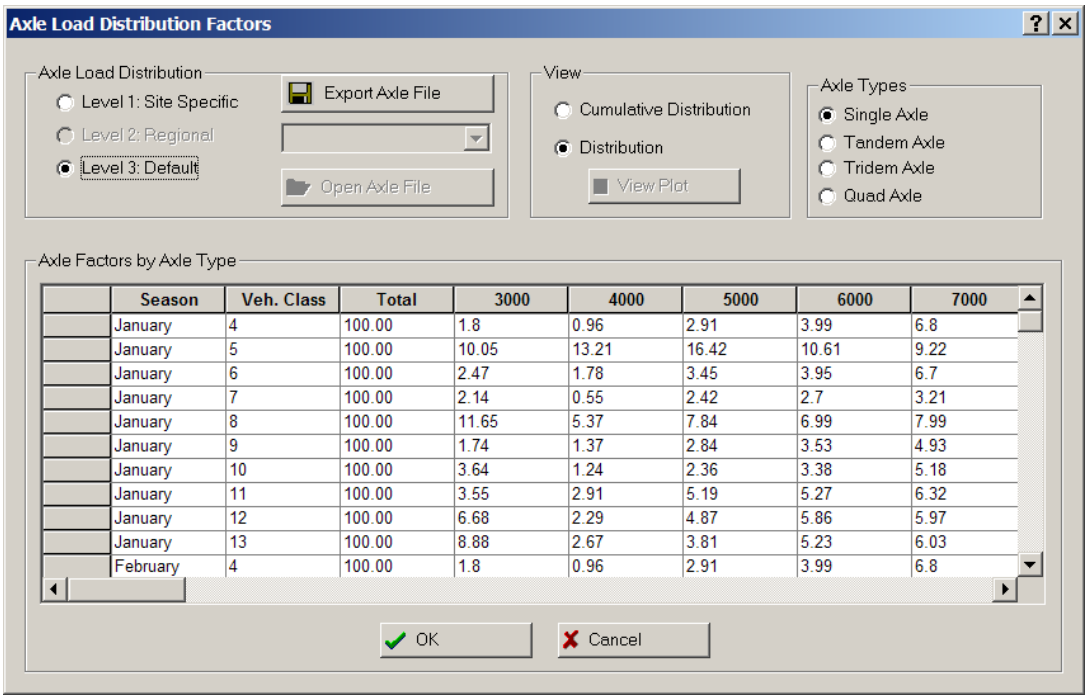

	Season	Veh. Class	Total	3000	4000	5000	6000	7000
	January	4	100.00	1.8	0.96	2.91	3.99	6.8
	January	5	100.00	10.05	13.21	16.42	10.61	9.22
	January	6	100.00	2.47	1.78	3.45	3.95	6.7
	January	7	100.00	2.14	0.55	2.42	2.7	3.21
	January	8	100.00	11.65	5.37	7.84	6.99	7.99
	January	9	100.00	1.74	1.37	2.84	3.53	4.93
	January	10	100.00	3.64	1.24	2.36	3.38	5.18
	January	11	100.00	3.55	2.91	5.19	5.27	6.32
	January	12	100.00	6.68	2.29	4.87	5.86	5.97
	January	13	100.00	8.88	2.67	3.81	5.23	6.03
	February	4	100.00	1.8	0.96	2.91	3.99	6.8

Figure A.12: Interface: Axle Load Distribution Factors

A.6.7. General Traffic Inputs

Most of the inputs under this category define the axle load configuration and loading details for calculating pavement responses. The exceptions are "Number of Axle Types per Truck Class" and "Wheelbase" inputs, which are used in the traffic volume calculations. Although these inputs have been described in PART 2, Chapter 4, additional discussion specific to JPCP and CRCP design is presented below.

The distance from the outer edge of the wheel to the pavement marking is termed mean wheel location. This input is very important in computing fatigue damage for both JPCP cracking and CRCP punchout predictions. The mean wheel location is a very sensitive factor that affects JPCP cracking and CRCP punchouts. If a typical-width (8.5-ft) truck were perfectly centered in a standard-width (12-ft) lane, the mean wheelpath would be 21 inches. At level 3, 18 inches may be used for this input unless more accurate information is available.

The wander is used to determine the number of axle load applications over a point for predicting distress and performance. This parameter affects prediction of all pavement distresses, but it is a relatively insensitive factor.

The distance between the lane markings on either side of the design lane is the design lane width. This input may or may not equal the slab width. The default value for standard-width lanes is 12 ft. It should be emphasized that this parameter refers to the actual traffic lane width, and not the "slab width," which has a very significant effect on both faulting and cracking performance of JPCP.

The number of axle types per truck class represents the average number of axles for each truck class (class 4 to 13) for each axle type (single, tandem, tridem, and quad).

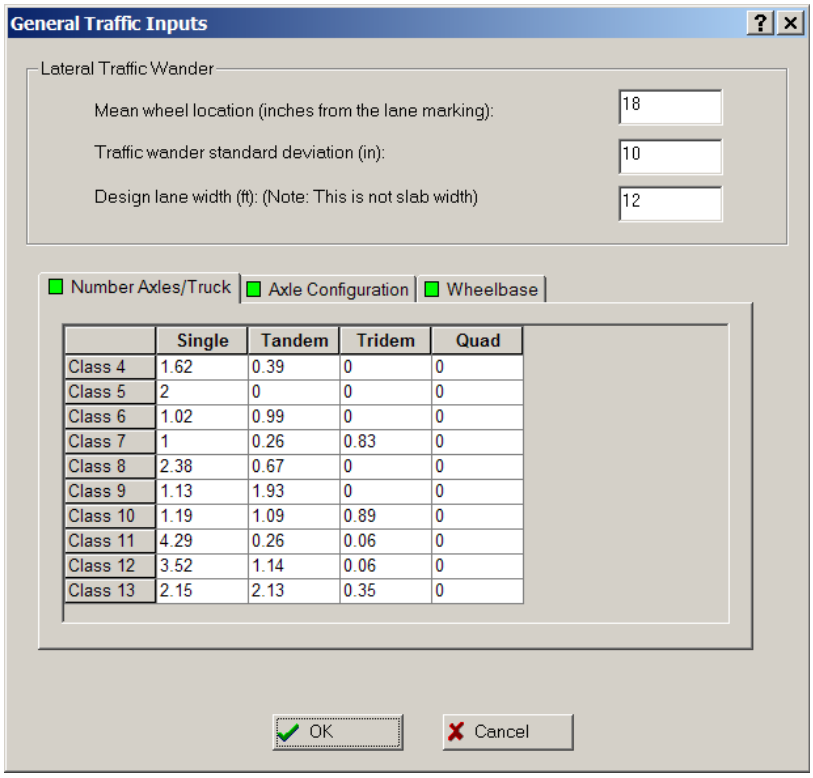

	Single	Tandem	Tridem	Quad
Class 4	1.62	0.39	0	0
Class 5	2	0	0	0
Class 6	1.02	0.99	0	0
Class 7	1	0.26	0.83	0
Class 8	2.38	0.67	0	0
Class 9	1.13	1.93	0	0
Class 10	1.19	1.09	0.89	0
Class 11	4.29	0.26	0.06	0
Class 12	3.52	1.14	0.06	0
Class 13	2.15	2.13	0.35	0

Figure A.13: Interface: General Traffic Inputs, Number Axles/Trucks

A series of data elements are needed to describe the details of the tire and axle loads for use in the pavement response module. Typical values are provided for each of the following elements:

- Average Axle-Width – the distance between two outside edges of an axle. (typical trucks, 8.5 ft)
- Dual Tire Spacing – the distance between centers of a dual tire. (typical dual tire spacing, 12 in)
- Tire Pressure – the hot inflation pressure or the contact pressure of a single tire or a dual tire. (For heavy trucks, typical hot inflation pressure is 120 psi)
- Axle Spacing – the distance between the two consecutive axles of a tandem, tridem, or quad (The average axle spacing is 51.6 in for tandem and 49.2 in for tridem axles).

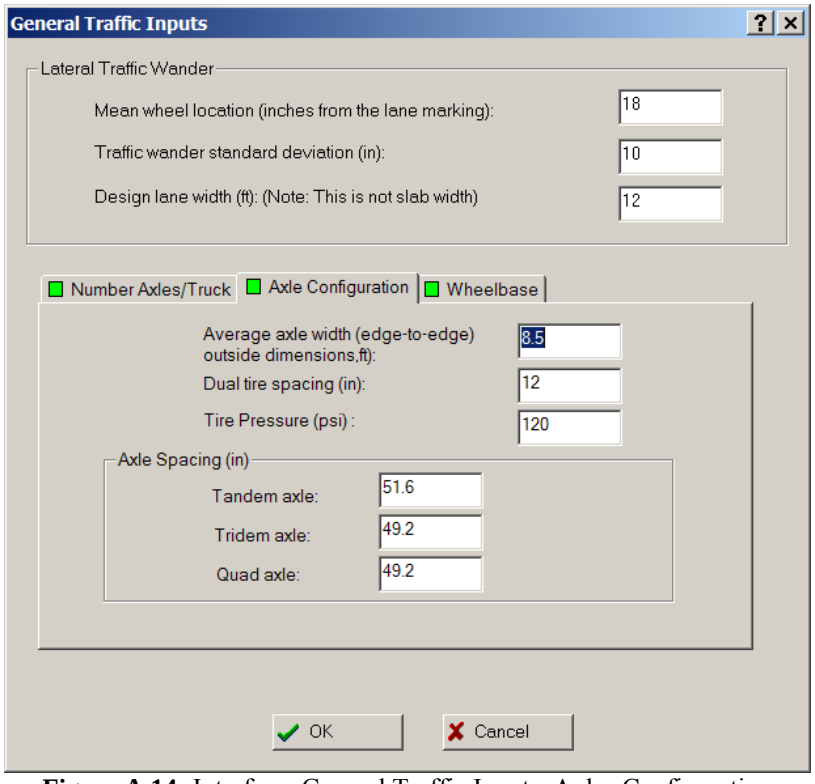

Figure A.14: Interface: General Traffic Inputs, Axles Configuration

Wheelbase information is used in determining the number of load applications for JPCP top-down cracking. For top-down cracking, the critical loading is caused by a combination of axles that places an axle load close to both ends of a slab at the same time. The inputs in this category include the following:

- Average axle spacing (ft) – short, medium, or long (The recommended values are 12, 15, and 18 ft for short, medium, and long axle spacing, respectively).
- Percent of trucks – the % of trucks with the short, medium, and long axle spacing. Usually, evenly distributed. The % of trucks is the axle spacing distribution of truck tractors (Class 8 and above).

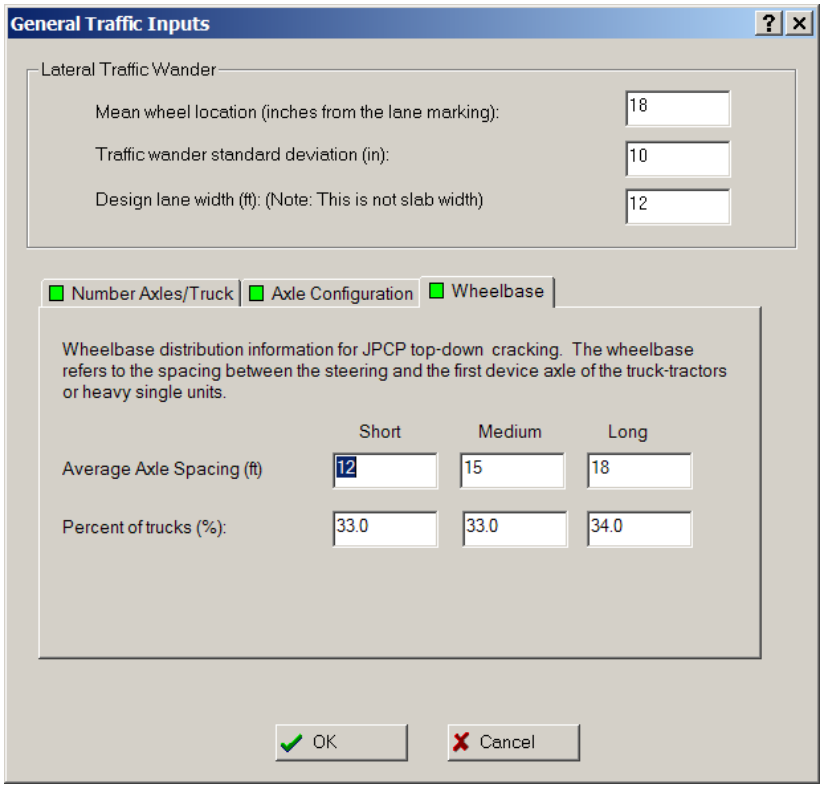

Figure A.15: Interface: General Traffic Inputs, Wheelbase

The traffic inputs are further processed to produce the following "processed input" for every month over the entire design period:

- Number of single axles under each load category
- Number of tandem axles under each load category
- Number of tridem axles under each load category
- Number of quad axles under each load category
- Number of truck tractors (Class 8 and above) under each load category (for top-down cracking)

The hourly traffic distribution factors are applied to the processed traffic input (the traffic counts by axle type for every month of the design period) to obtain hourly traffic at the time of damage calculation for each distress.

A.7. Climate

Environmental conditions have a significant effect on the performance of rigid pavements. The interaction of the climatic factors with pavement materials and loading is complex. Factors such as precipitation, temperature, freeze-thaw cycles, and depth to water table affect pavement and subgrade temperature and moisture content, which, in turn, directly affects the load-carrying capacity of the pavement layers and ultimately pavement performance. This section provides a summary of the climatic inputs required for rigid pavement:

The following weather related information is required to perform rigid pavement design:

1) Hourly air temperature over the design period.
2) Hourly precipitation over the design period.
3) Hourly wind speed over the design period.
4) Hourly percentage of sunshine over the design period.
5) Hourly ambient relative humidity values.
6) Seasonal or constant water table depth at the project site.

The first five inputs are obtained from weather station data for a given site, if available. For locations within the United States, they can be obtained from the National Climatic Data Center (NCDC) database. The Design Guide Software includes an extensive climatic database for over 800 cities in the U.S. and a capability to interpolate between the available sites.

The climatic inputs are combined with the pavement material properties, layer thicknesses, and drainage-related inputs by the EICM to yield the following information for use in the design analysis:

- Hourly profiles of temperature distribution through PCC slab – temperatures at 11 evenly spaced points through slab thickness for JPCP analysis.
- Hourly temperature and moisture profiles (including frost depth calculations) through other pavement layers.
- Temperature at the time of PCC zero-stress temperature for JPCP and CRCP design.
- Monthly or semi-monthly (during frozen or recently frozen periods) predictions of layer moduli for asphalt, unbound base/subbase, and subgrade layers.
- Annual freezing index values.
- Mean annual number of wet days.
- Number of ambient freeze-thaw cycles.
- Monthly relative humidity values.

Due to the extreme sensitivity of critical stresses in rigid pavements to temperature gradients, consideration of hourly variation in temperature conditions is necessary. This is accomplished automatically in the Design Guide Software. Based on the hourly historical climatic data, pavement structure, and material properties, the EICM produces a file that includes historical hourly temperature profiles in the PCC slab for every year of the design period (8,760 profiles per design year [365 days * 24 hours]).

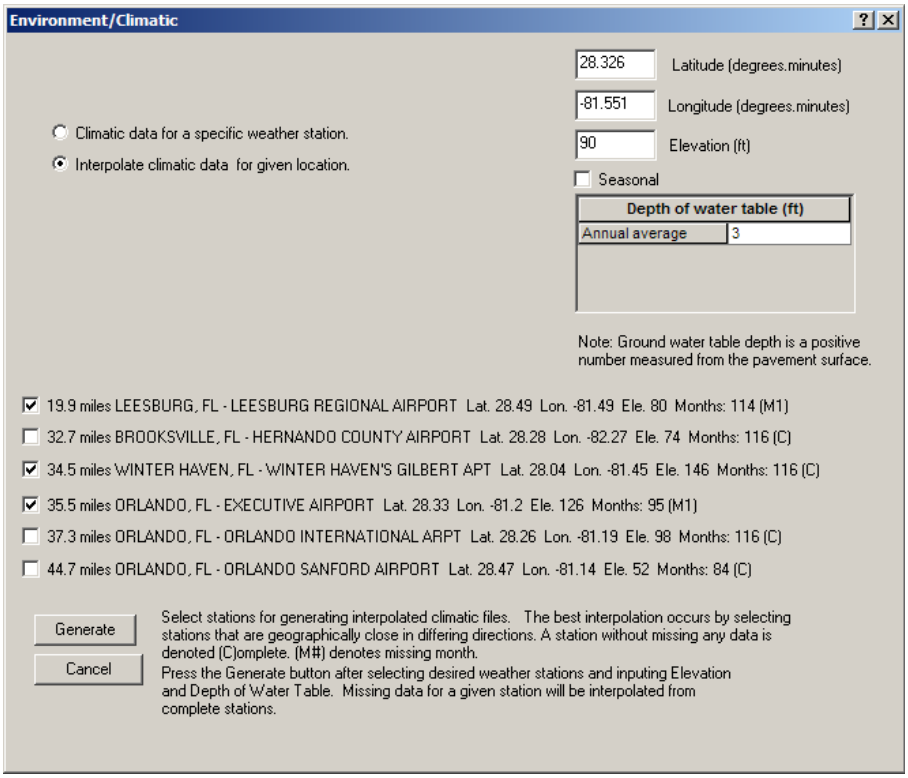

Figure A.16: Interface: Environment Climatic

A.8. Pavement Structure

The rigid pavement design procedure allows a wide variety of PCC, base (layer directly underneath the PCC slab), and subbase material properties and layer thicknesses. For example, a rigid pavement structure could consist of a PCC slab, an asphalt treated base, an aggregate subbase, compacted subgrade, natural subgrade, and bedrock. The Design Guide Software can be used to analyze a maximum of 20 layers (10 actual input layers are recommended) comprising the pavement structure and subgrade (or bedrock). The following rules or constraints need to be satisfied in defining a rigid pavement structure for design:

- The surface layer in rigid pavement design is always a PCC layer.
- Slab-on-grade (two layers) is the minimum structure that can be analyzed.
- Only one unbound granular layer can be placed between two stabilized layers.
- The last two layers in the pavement structure must be unbound layers.

A.8.1. Bedrock

The presence of bedrock within 10 ft of the pavement surface influences the structural response of pavement layers. The inputs for this layer include the following:

- Unit weight
- Poisson's ratio
- Layer modulus

Input Levels 1 and 2 do not apply for bedrock. Typical modulus values for bedrock in various conditions (e.g., solid, or highly fractured and weathered) are provided in [X 15] part 2, Chapter 2.

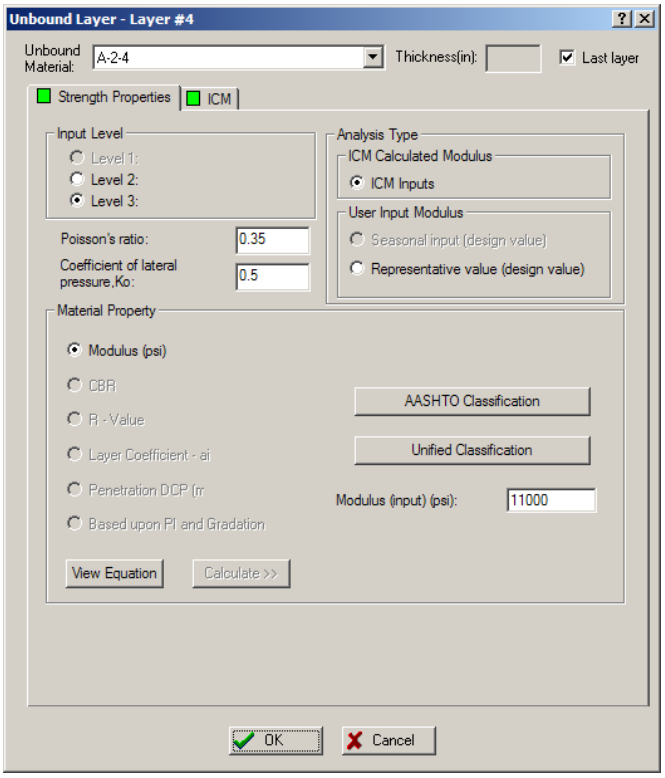

Figure A.17: Interface: Layer #4 (Bedrock), Strength Properties

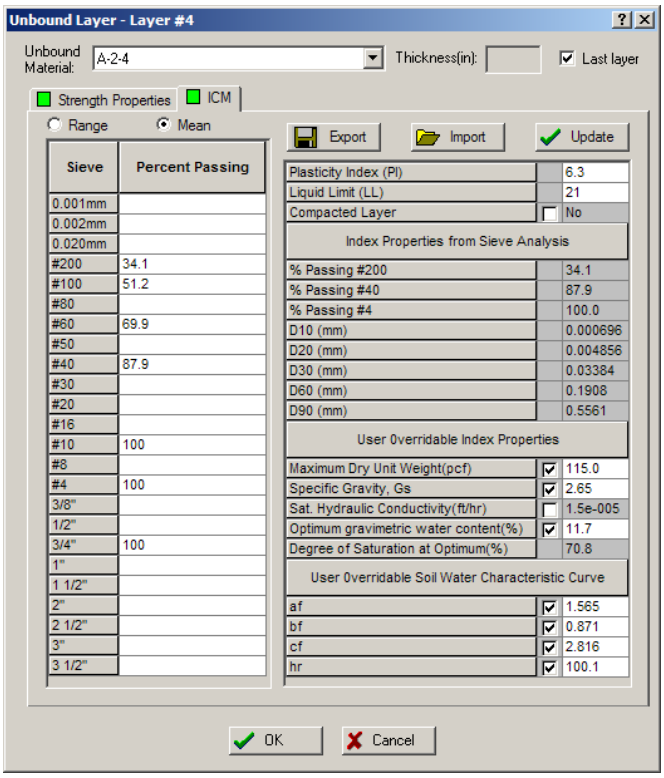

Figure A.18: Interface: Layer #4 (Bedrock), ICM

A.8.2. Unbound Base/Subbase/Subgrade

The major inputs required for unbound base/subbase and subgrade layers are:

- Layer thickness (only for base and subbase layers) – for subgrade layers if the lime modified or compacted subgrades need to be considered separately from the natural subgrade, they can be defined as a structural layer.
- Layer resilient modulus.
- Poisson's ratio.
- Coefficient of lateral earth pressure, K_o – a typical value for unbound compacted materials is 0.5.

The layer moduli for unbound layers and subgrade can be estimated at two levels – level 2 and level 3. For rigid pavement analysis, level 1 inputs are not available ([X 15] part 2, chapter 2). Level 2 requires testing of a soil sample using some test such as CBR or R-value and then estimating the layer resilient modulus using a prediction equation. Level 3

requires estimation using a correlation from soil classification such as AASHTO or UCS. The designer also has the choice of including or not including seasonal analysis for the unbound base materials and soils.

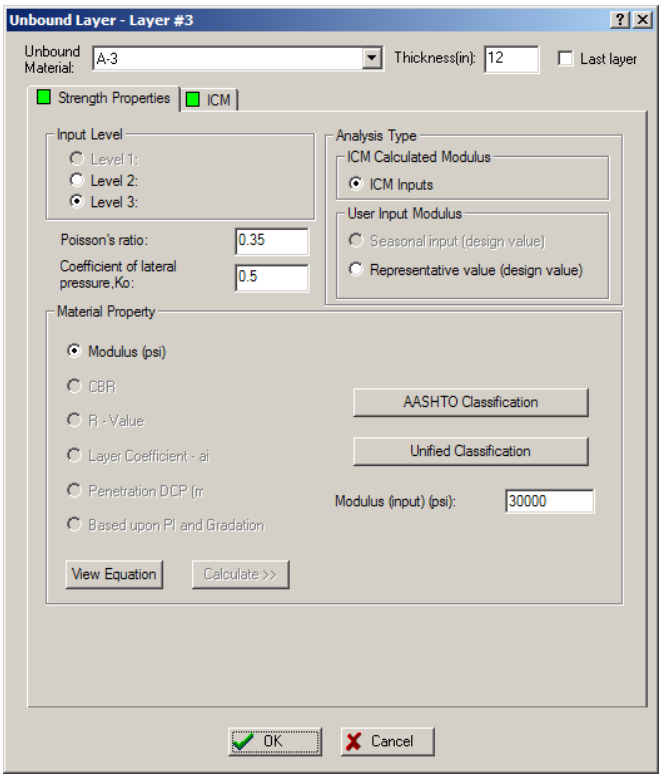

Figure A.19: Interface: Layer #3 (Subgrade), Strength Properties

[X 15] part 2, chapter 3 should be consulted for a more comprehensive coverage of the materials inputs required for climatic analysis.

The following options are available for Level 2:

1. Enter a representative design resilient modulus (at the optimum moisture content) or other allowable soil strength/stiffness parameters (CBR, R-value, AASHTO structural layer coefficient, or PI and gradation) and use the EICM module linked to the Design Guide Software to estimate seasonal variations based on changing moisture and temperature profiles through the pavement structure. The additional inputs for EICM include plasticity index, % passing No. 4 and No. 200 sieves, and the effective grain size corresponding to 60 % passing by weight (D_{60}) for the layer under consideration. Using these inputs, EICM estimates the unit weight, the specific gravity of solids, saturated

hydraulic conductivity of the pavement layer, optimum gravimetric moisture content, degree of layer saturation, and the soil water characteristic curve parameters. These computed quantities can be substituted with direct inputs.

2. In lieu of using EICM, the seasonal moduli, CBR, R-value, or other values may be entered directly. For direct input, 12 laboratory-estimated pavement resilient moduli (or other allowable soil tests) are required.

3. Finally at input Level 2, seasonal variation in modulus of unbound materials may be ignored. In this case, a representative design modulus value (or other test value) is required.

For Level 3, the required input is the layer resilient modulus at optimum water content, and the EICM will do the seasonal adjustment. If seasonal analysis is not desired, a single resilient modulus is entered that the designer wishes to hold constant throughout the entire year (no moisture content is entered).

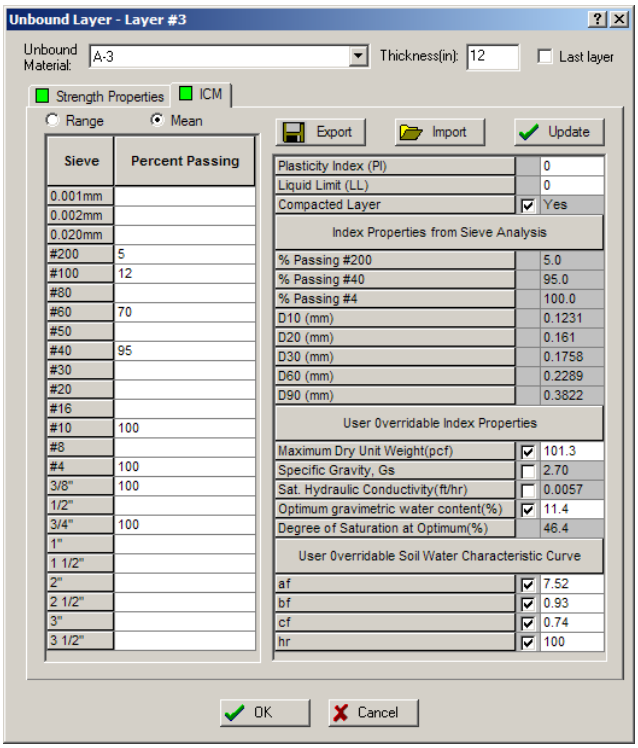

Figure A.20: Interface: Layer #3 (Subgrade), ICM

The Design Guide Software may internally subdivide the pavement structure into 12 to 15 sublayers for the modeling of temperature and moisture variations. Only the unbound base layers thicker than 6 inches and unbound subbase layer thicker than 8 inches are sublayered. For the base layer (first unbound layer), the first sublayer is always 2 inches. The remaining thickness of the base layer and any subbase layers that are sublayered are divided into sublayers with a minimum thickness of 4 inches. For compacted and natural subgrades, the minimum sublayer thickness is 12 inches. A pavement structure is sublayered only to a depth of 8 feet from the surface. Any remaining subgrade is treated as an infinite layer. If bedrock is present, the remaining subgrade is treated as one layer beyond 8 feet. Bedrock is not sublayered and is always treated as an infinite layer.

A.8.3. Asphalt-Stabilized Base Layer

No sublayering is done within the asphalt-stabilized base layer for rigid design and analysis purposes within the Design Guide Software. The material inputs required for this layer are grouped under two broad categories – general material inputs and inputs required to construct E^* master curve.

General Layer Property Inputs:

- Layer thickness
- Poisson's ratio
- Thermal conductivity – the quantity of heat that flows normally across a surface of unit area per unit of time of temperature gradient normal to the surface. The typical value for asphalt-stabilized base material is 0.67 BTU/hr-ft-°F
- Heat capacity – the heat required to raise the temperature of a unit mass of material by a unit temperature. A typical value for asphalt-stabilized base is 0.23 BTU/lb-°F
- Total unit weight – typical range for dense-graded hot-mix asphalt is 134 to 148 lb/ft^3

The primary material property of interest for asphalt stabilized layers is its dynamic modulus, E^*. For Level 1 input, the dynamic modulus, E*, is determined in the laboratory using standard test protocols for various frequencies and rates of loading. A master curve of E* versus reduced time is then derived from this data that defines the behavior of this layer under loading and at various climatic conditions. The master curve is constructed from the following information:

- % retained on ¾ in sieve – a typical value is 5 to 16 % for dense graded and 30% for permeable
- % retained on 3/8 in sieve – a typical value is 27 to 49 % for dense graded and 70% for permeable
- % retained on #4 sieve – a typical value is 38 to 61 % for dense graded and 95% for permeable
- % passing the #200 sieve – a typical value is 3 to 8% for dense graded and 1% for permeable

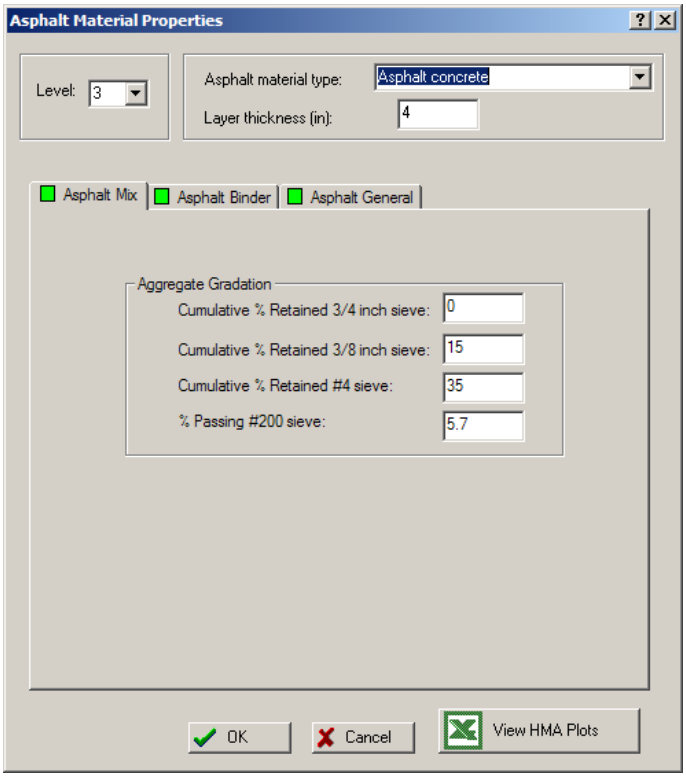

Figure A.21: Interface: Layer #2 (Base), Asphalt Mix

Asphalt binder:

- Level 1 input is generally not needed for rigid design
- For input Level 2 – specify PG grade or Viscosity grade
- For input Level 3 – specify PG grade, Viscosity grade, or Penetration Grade
- Volumetric effective binder content (%)
- Air voids (%)
- Reference temperature for master curve development (70 °F typical)

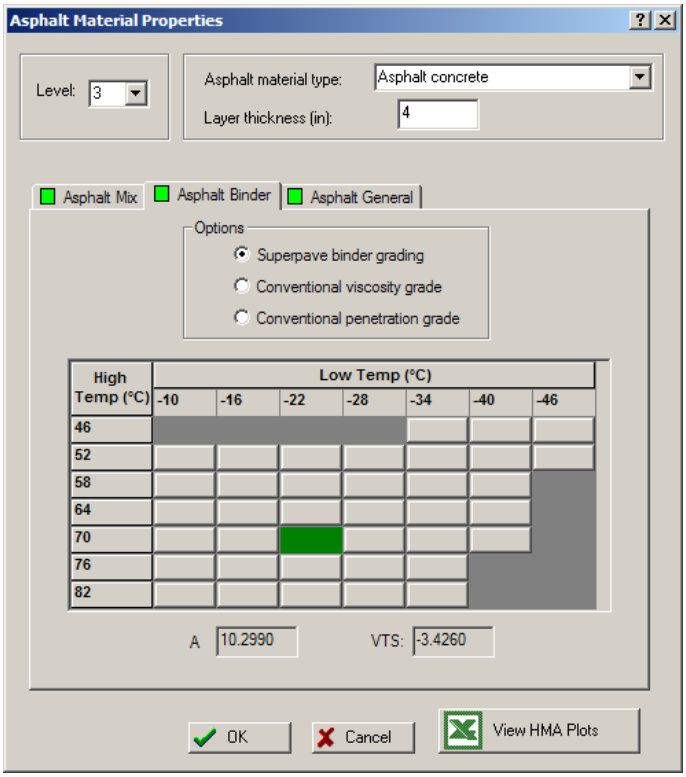

Figure A.22: Interface: Layer #2 (Base), Asphalt Binder

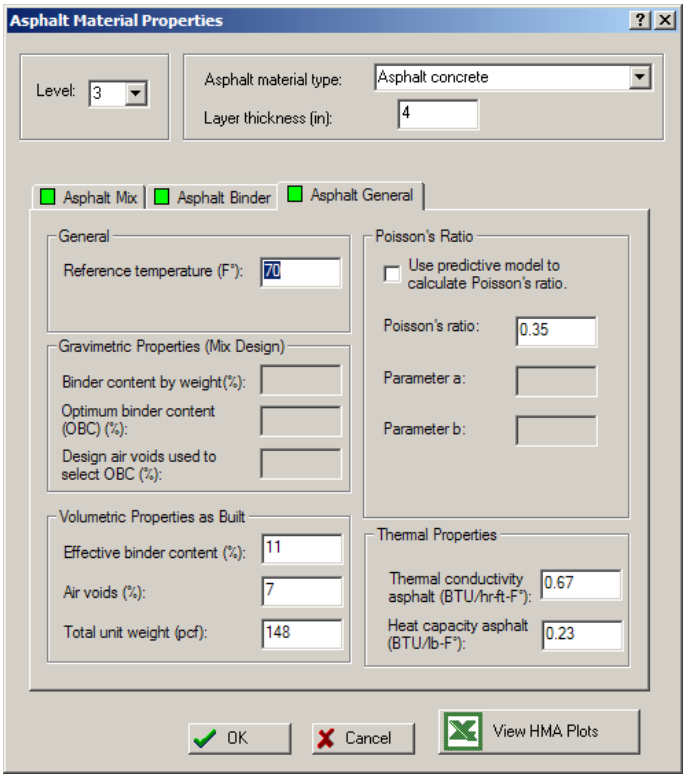

Figure A.23: Interface: Layer #2 (Base), Asphalt General

A.8.4. Portland Cement Concrete Layer

The properties required for the PCC layer are divided into three categories—general and thermal properties, PCC mixture properties, and strength and stiffness properties.

The input requirements for general and thermal properties are:

- Layer thickness. The range for design thickness for new pavement design is approximately 6 to 17 inches.
- Poisson's ratio, μ – typical values for PCC range from 0.15 to 0.25.
- Coefficient of thermal expansion, determining this value through direct testing of the project mix (Level 1 input) is recommended since this parameter is extremely significant.
- Thermal conductivity – the quantity of heat that flows normally across a surface of unit area per unit of time of temperature gradient normal to the surface.

- Heat capacity – the heat required to raise the temperature of a unit mass of material by a unit temperature.

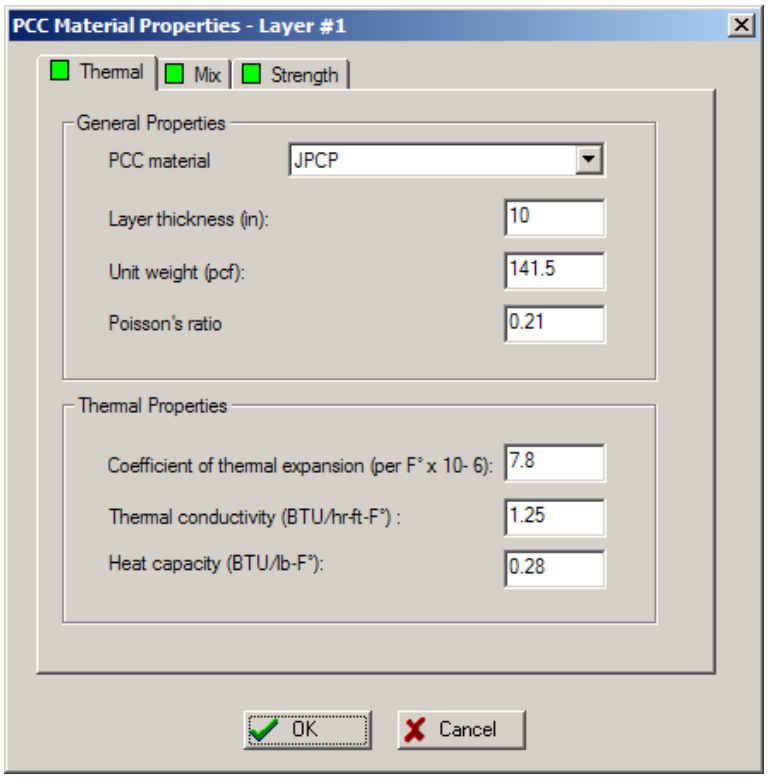

Figure A.24: Interface: Layer #1 **(**PCC) General and Thermal Properties

The design procedure requires the following PCC mix-related inputs for modeling material behavior, including shrinkage, PCC zero-stress temperature, and load-transfer deterioration:

- Cement type (Types I, II, or III)
- Cement content
- Water/cement (or w/c) ratio
- Aggregate type
- PCC zero-stress temperature
- Ultimate shrinkage at 40 % relative humidity
- Reversible shrinkage – % of ultimate drying shrinkage that is reversible upon rewetting
- Curing method – curing compound or wet curing (affects ultimate shrinkage)

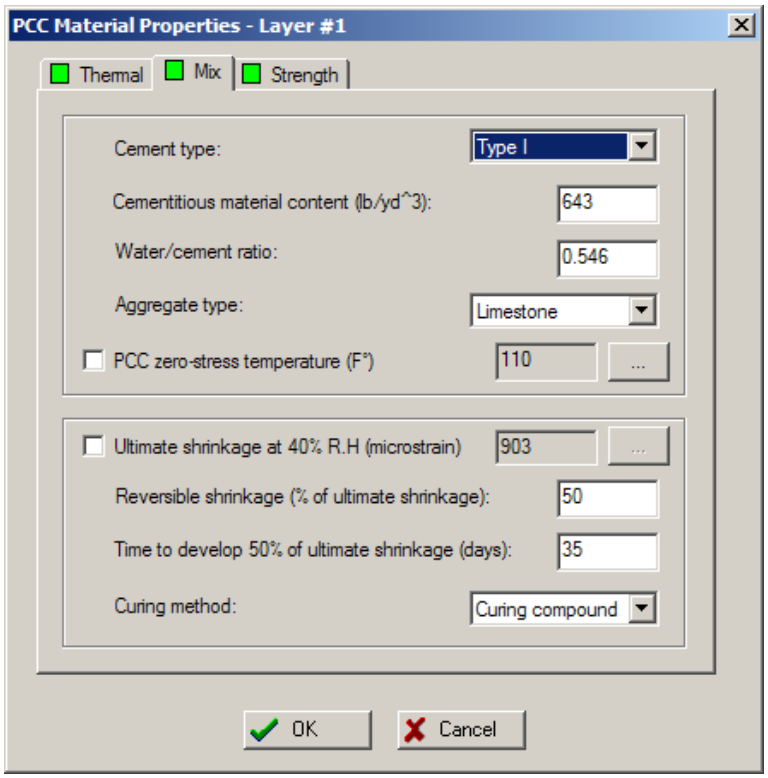

Figure A.25: Interface: Layer #1 (PCC), Mixture Properties

The long-term strength gain of PCC, and corresponding change in PCC stiffness, are considered in the Software Guide. The PCC strength and stiffness inputs consist of the following:

- Modulus of rupture (flexural strength), MR
- Static modulus of elasticity, E_{PCC}
- Compressive strength, f'_c
- Split tensile strength, f_t

Depending on the input level, different amounts of information are required as follows:

- Level 1 – Laboratory values of MR, f'_c, f_t, and E_c at 7, 14, 28, and 90 days determined using appropriate testing procedures.

- Level 2 – Laboratory-determined values of compressive strength f'_c at 7, 14, 28, and 90 days and the 20-yr to 28-day strength ratio. The strength at each damage increment is determined using a best-fit regression line fit through these data points, and the remaining strength parameters (MR, f_t, and E_c) are estimated using well established strength-to-strength and strength-to-stiffness correlations.
- Level 3 – Estimated 28-day compressive strength or modulus of rupture from historical data or other information. The PCC strength over time is estimated using the default strength model, and the other inputs are calculated based on the projected strength using the appropriate correlations. The PCC elastic modulus can also be entered at level 3 if desired

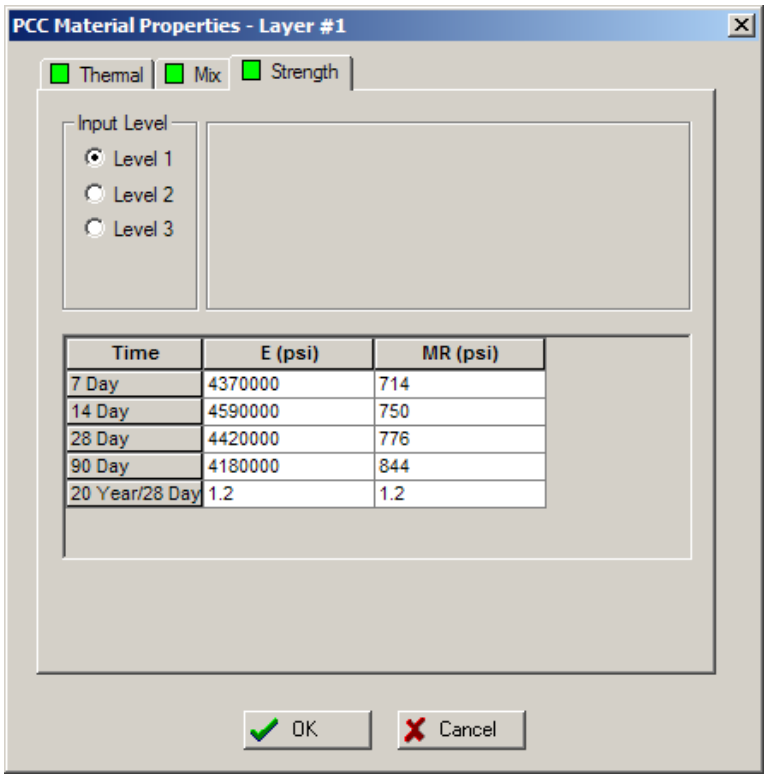

Figure A.26: Interface: Layer #1 (PCC), Strength Properties

A.8.5. Pavement Design Features

Various design features have significant effect on performance of both JPCP and CRCP. Examples of these include joint spacing and edge support (tied PCC shoulder or widened slab) for JPCP and steel content and base type for CRCP.

The magnitude of permanent curl/warp is a sensitive factor that affects all rigid pavement performance. Some of the factors that affect the permanent effective permanent curl/warp include the following:

- Climate (air temperature, solar radiation, relative humidity, wind speed) during PCC placement
- Construction time and curing procedure
- PCC mix properties including cement type, water-cement ratio, water content, cement quantity, and aggregate type
- Creep of the PCC slab from its own weight and edge constraints
- Base type and properties

The recommended value for permanent curl/warp is -10 °F for all new and reconstructed rigid pavements for all climatic regions. This is an equivalent linear temperature difference from top to bottom of the slab.

Joint spacing must be selected within the context of design features such as slab thickness, slab width, PCC materials properties, base type, and subgrade stiffness. In general, a short joint spacing (15 ft) is recommended. The average cracking from the two designs is the expected cracking in the random jointed section. The Design Guide Software uses the average joint spacing for faulting analysis and the maximum joint spacing for cracking analysis when random joint spacing is entered.

Dowel spacing is simply the spacing between dowels. Typical dowel spacing is 12 inches. Normally, as the required slab thickness increases (due to heavier traffic to control slab cracking), an increase in dowel diameter is required to control joint faulting.

Sealant type is an input to the empirical model used to predict spalling. Spalling is used in smoothness predictions, but it is not considered directly as a measure of performance in this Guide. The sealant options are liquid, silicone, and preformed.

Tied PCC shoulders and widened slabs can significantly improve JPCP performance by reducing critical deflections and stresses along the edge. The shoulder type also affects the amount of moisture infiltration into the pavement structure. The effects of moisture infiltration are considered in the determination of seasonal moduli values of unbound layers. The structural effects of the edge support features are directly considered in the design process, for cracking and for faulting. The design inputs for these design features are as follows:

- Tied PCC Shoulder – for tied concrete shoulders the long-term LTE between the lane and shoulder must be provided. The LTE is defined as the ratio of deflections of the unloaded and loaded slabs. The higher the LTE, the greater the support provided by the shoulder to reduce critical responses of the mainline slabs. Typical long-term deflection LTE are:
    - 50 to 70 % for monolithically constructed and tied PCC shoulder
    - 30 to 50 % for separately constructed tied PCC shoulder
        - Untied concrete shoulders or other shoulder types do not provide significant support; therefore, a low LTE value should be used
- Widened Slab – The design input for widened slab is the slab width

The potential for base or subbase erosion (layer directly beneath the PCC layer) has a significant impact on the initiation and propagation of pavement distress. Different base types are classified based on long-term erodibility behavior as follows:

- Class 1 – Extremely erosion resistant materials

- Class 2 – Very erosion resistant materials
- Class 3 – Erosion resistant materials
- Class 4 – Fairly erodible materials
- Class 5 – Very erodible materials

The interface between a stabilized base and PCC slab is modeled either completely bonded or unbonded for JPCP design.

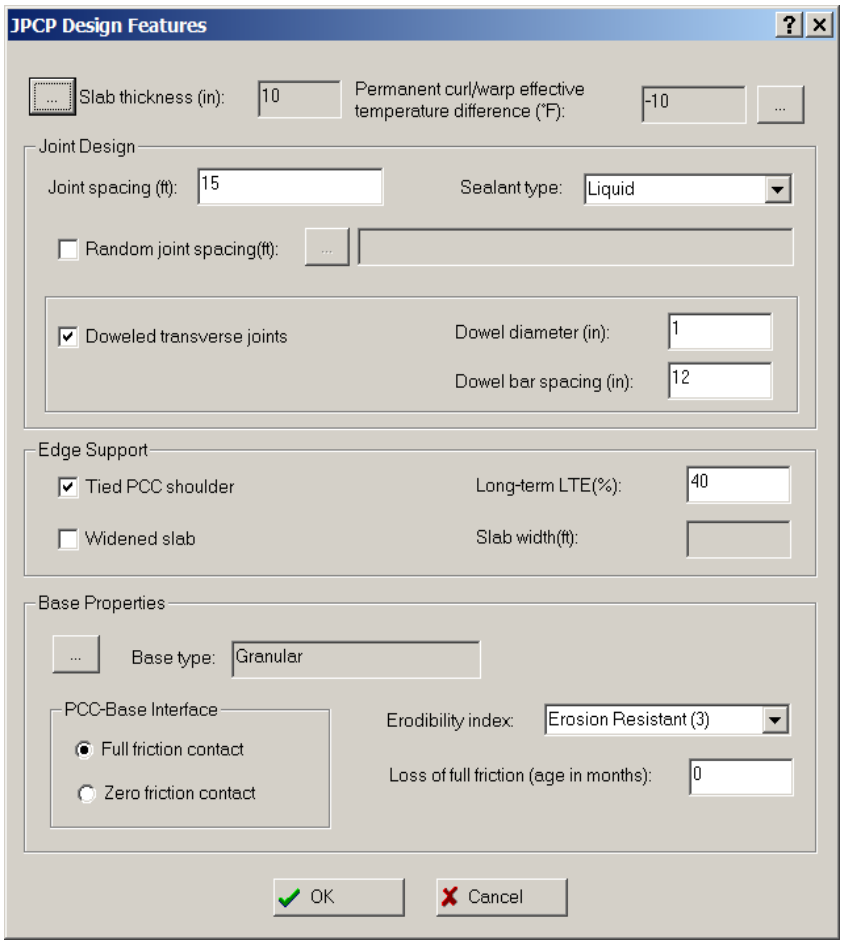

Figure A.27: Interface: JPCP Design Features

APPENDIX B: M-E PDG INPUT DATA

B.1. General Information

Design Life	25 years
Pavement construction month	October 2008
Traffic open month	November 2008
Type of design	New-JPCP

B.2. Site/Project Identification

Location	Orlando
Project ID	Interstate 4
Section ID	Disney World
Date	4/6/2008
Milepost begin	61.747
Milepost end	68.102
Traffic direction	Eastbound

B.3. Analysis Parameter

Initial IRI	58 in/mi
Terminal IRI limit	160 in/mi
Transverse cracking limit	10 % of slab
Mean joint faulting limit	0.12 in
Terminal IRI reliability	90 (95 - 35)
Transverse cracking reliability	90 (95 - 35)
Mean joint faulting reliability in	90 (95 - 35)

B.4. Traffic

Initial two-way AADTT	7000
Number of lanes in design direction	2
Percent of trucks in design direction	50 %
Percent of trucks in design lane	95 %
Operational speed	70 mph
Monthly adjustment factor	Default MAF
Vehicle class distribution	Principal Arterials – TTC=11
Hourly distribution	Default distribution
Traffic growth factors	Default linear growth rate 2%
Axle load distribution factor	Default distribution
Mean wheel location	18 in
Traffic wander standard deviation	10 in
Design lane width	12 ft
Number axle/truck	Default values
Average axle width	8.5 ft
Dual tire spacing	12 in
Tire pressure	120 psi
Tandem axle spacing	51.6 in
Tridem axle spacing	49.2 in
Quad axle spacing	49.2 in
Average axle spacing (short)	12 ft
Average axle spacing (medium)	15 ft
Average axle spacing (long)	18 ft
Percent of Truck (short)	33 %
Percent of Truck (medium)	33 %
Percent of Truck (long)	34 %

B.5. Climatic

Weather station 1	Leesburg Regional Airport
Weather station 2	Winter Haven's Gilsberg APT
Weather station 3	Executive Airport

B.6. Structure

Short-wave absorptivity	0.85

B.6.1. Layer 4 – Bedrock

Thickness	semi-infinite
Material	A-2-4
Poisson's Ratio	0.35
K_o	0.5
#200	34.1
#100	51.2
#60	69.9
#40	87.9
#10	100
#4	100
¾	100
Plasticity Index (PI)	6.3
Liquid Limit (LL)	21
D10	0.000696 mm
D20	0.004856 mm
D30	0.03384 mm
D60	0.1908 mm
D90	0.5561 mm

Maximum dry unit weight	115 pcf
Specific gravity	2.65
Optimum gravimetric water content	11.7 %
a_f	1.565
b_f	0.871
c_f	2.816
h_r	100.1

B.6.2. Layer 3 – Subgrade

Thickness	12 inches
Material	A-3
Poisson's Ratio	0.35
K_o	0.5
#200	5
#100	12
#60	70
#40	95
#10	100
#4	100
¾	100
Compacted layer	yes
D10	0.1231 mm
D20	0.161 mm
D30	0.1758 mm
D60	0.2289 mm
D90	0.3822 mm
Maximum dry unit weight	101.3 pcf
Optimum gravimetric water content	11.4 %
a_f	7.52

b_f	0.93
c_f	0.74
h_r	100.0

B.6.3. Layer 2 – Base layer

Material	Asphalt concrete
Thickness	4.0 inches
Retaining on 3/4 inch sieve	0 %
Retaining on 3/8 inch sieve	15 %
Retaining on #4 sieve	35 %
Passing #200 sieve	5.7 %
Method	Superpave binder grading
High Temperature	70°C
Low Temperature	-28°C
A	10.2990
VTS	-3.426
Reference Temperature	70°F
Poisson's ratio	0.35
Effective binder content	11 %
Air Voids	7 %
Total unit weight	148 pcf
Thermal conductivity	0.67 BTU/hr-ft-°F
Heat capacity	0.23 BTU/lb-°F

B.6.4. Layer #1 – Surface layer

Thickness	variable
Material	PCC
Properties	see table next page

Table B.1: PCC material input parameters

	Unit	MIX-01	MIX-02	MIX-03
General and Thermal				
Layer thickness	in	variable		
Unit weight	pcf	143.1	146.6	144.2
Poisson's ratio	-	0.23	0.266	0.21
Coefficient of thermal expansion	μin/in/°F	6.79	6.84	5.99
Thermal conductivity •	BTU/hr-ft-°F	1.25		
Heat capacity •	BTU/lb-°F	0.28		
Mix				
Cement Type	-	Type I		
Cementitious material content	lb/yd3	643	520	470
Water/cement ratio	-	0.546	0.622	0.568
Aggregate type	-	limestone		granite
zero-stress temperature •	F	109	103	100
Ultimate shrinkage at 40% R.H. •	μin/in	957	812	629
Reversible shrinkage	%	50		
Time to develop 50% shrinkage	days	35		
Curing method	-	Curing compound		
Strength (level 1)				
E-modulus (7-day)	psi	4370000	4530000	3290000
E-modulus (14-day)	psi	4590000*	4590000*	3470000
E-modulus (28-day)	psi	4420000*	4360000*	3680000
E-modulus (90-day)	psi	4180000*	4905000	4020000
20 year/28 day ratio •	-	1.2		
Modulus of rupture (7-day)	psi	714	777	545
Modulus of rupture (14-day)	psi	745♦	825♦	603.5♦
Modulus of rupture (28-day)	psi	776	873	662
Modulus of rupture (90-day)	psi	844	831	707
20 year/28 day ratio •	-	1.2		
Strength (level 2)				
Compressive Strength (7-day)	psi	4832	6183	3489
Compressive Strength (14-day)	psi	6067	7442	4225
Compressive Strength (28-day)	psi	6908	8256	4883
Compressive Strength (90-day)	psi	7856	9188	5794
20 year/28 day ratio •	-	1.2		
Strength (level 3)				
Modulus of rupture (28-day)	psi	776	873	662
E-Modulus (28-day)	psi	4420000*	4360000*	3680000

• non empirical value (suggested by ME-PDG)

* measured values not increasing as expected by theory

♦ non empirical value (linearly interpolated)

B.6.5. JPCP Design Features

Curl/Warp temperature difference	-10 °F
Joint spacing	15 ft
Sealant type	liquid
Type	Tied PCC shoulder
Widened Slab (Slab width)	13 ft
Dowel diameter	1.5 in
Dowel bar spacing	12 in
Tied PCC shoulder Long-term LTE	40 %
PCC-Base interface	Zero friction contact
Erodibilty index	Erosion Resistant (3)